A STUDY OF INERTIAL EFFECT IN THE WELLBORE

IN PRESSURE TRANSIENT WELL TESTING

A DISSERTATION

SUBMITTED TO THE DEPARTMENT OF PETROLEUM ENGINEERING

AND THE COMMITTEE ON GRADUATE STUDIES

OF STANFORD UNIVERSITY

IN PARTIAL FULFILLMENT OF THE REQUIREMENTS

FOR THE DEGREE OF

DOCTOR OF PHILOSOPHY

by

KIYOSHI SHINOHARA

April 1980

I certify that I have read this thesis and that in my opinion it is fully adequate, in scope and quality, as a dissertation for the degree of Doctor of Philosophy.

(Principal Advisor)

I certify that I have read this thesis and that in my opinion it is fully adequate, in scope and quality, as a dissertation for the degree of Doctor of Philosophy.

I certify that I have read this thesis and that in my opinion it is fully adequate, in scope and quality, as a dissertation for the degree of Doctor of Philosophy.

Approved for the University Committee on Graduate Studies:

Dean of Graduate Studies

Dedicated to my parents, Kisaburo and Maki,
to my son, Daisuke,
and to my wife, Kiyomi

ACKNOWLEDGEMENT

The author wishes to express his sincere appreciation to Professor H. J. Ramey, Jr., Department of Petroleum Engineering, for his guidance, understanding, encouragement, and critical review of the manuscript as a research advisor. The author is grateful to Professors W. E. Brigham, S. K. Sanyal, and R. N. Horne, Department of Petroleum Engineering, for serving on his reading committee.

The author is also indebted to the Nippon Steel Corporation, Stanford Geothermal Program at Stanford University, and the Halliburton Oil Well Services Company for financial support.

In addition, thanks are due to Dr. M. Sengul, Marathon Oil Company, for assistance with numerical Laplace inversion. The scrupulous help in editing and typing of the manuscript by Ms. Elizabeth S. Luntzel and the drafting of the figures by Ms. Terri Ramey are gratefully acknowledged.

Finally, the author wishes to express his sincere appreciation to his wife, Kiyomi, for her constant support, encouragement, and understanding during this work.

ABSTRACT

In a "slug test," a finite amount of liquid is removed suddenly from a static well, causing a perturbation which can be used to obtain information on the reservoir. Ideally, the wellbore liquid would start to move up the well to replace the removed liquid, reach a maximum velocity, then begin to decelerate as the liquid level approaches the initial static liquid level. This is a useful method as a short-time well test. The solution for this problem is old, and the problem has been investigated by many people. However, the solutions available thus far do not rigorously include the inertial effect of movement of the liquid in the wellbore, and do not explain pressure oscillations andliquid level fluctuations in the wellbore completely. Inertia delays the start of movement of the wellbore liquid, and momentum can cause it to eject above the final static level. Oscillations in pressure and liquid level may result.

Actually, this kind of problem can be involved in the start of liquid production for all wells, and in the shut-in of high-rate water injection wells. It is also important to drill stem testing of liquid producing formations.

In this study, a new and complete solution for this problem is obtained and the effects of important parameters are investigated. A finite difference solution was also prepared and used to study this class of problem. The available field data were interpreted and discussed. A new solution for flow period data analysis for a closed chamber test was prepared as an extension of the general slug test solution.

TABLE OF CONTENTS

LIST OF TABLES

LIST OF FIGURES

1. INTRODUCTION

Often in drill stem tests (hereinafter abbreviated as "DST"), flow period data are characterized by a pressure trace which increases with increasing time, showing the accumulation of liquid in the drill string. In some cases the pressure-time trace is linear at the beginning of the flow period, and then becomes concave to the time axis, showing an initial apparent constant flowrate and then a decreasing flowrate. In other cases the pressure-time trace is concave to the time axis from the beginning of the flow period, showing a decreasing rate throughout the flow period (see Figs. 1 and 2).

In cases where the formation pressure is too low to lift a column of the reservoir liquid to the surface, the well may actually stop flowing before the DST tester valve is closed. This results because the head of liquid in the drill string becomes equal to the initial formation pressure. In rare cases with high productivity formations, the liquid level in the wellbore may initially oscillate around the eventually stable static level.

In any event, the initial portion of a DST flow period may be viewed as a test in which a column of liquid whose head is equal to the initial formation pressure has been removed instantaneously. If there is a liquid cushion, the concept becomes more complicated, but is still valid. We consider that a head of liquid equivalent to the difference in pressure between initial formation pressure and the pressure above the tester valve has been removed.

This kind of test is similar to a well response test called a "slug test" by Ferris and Knowles[1] in 1954. The word "slug" refers to an

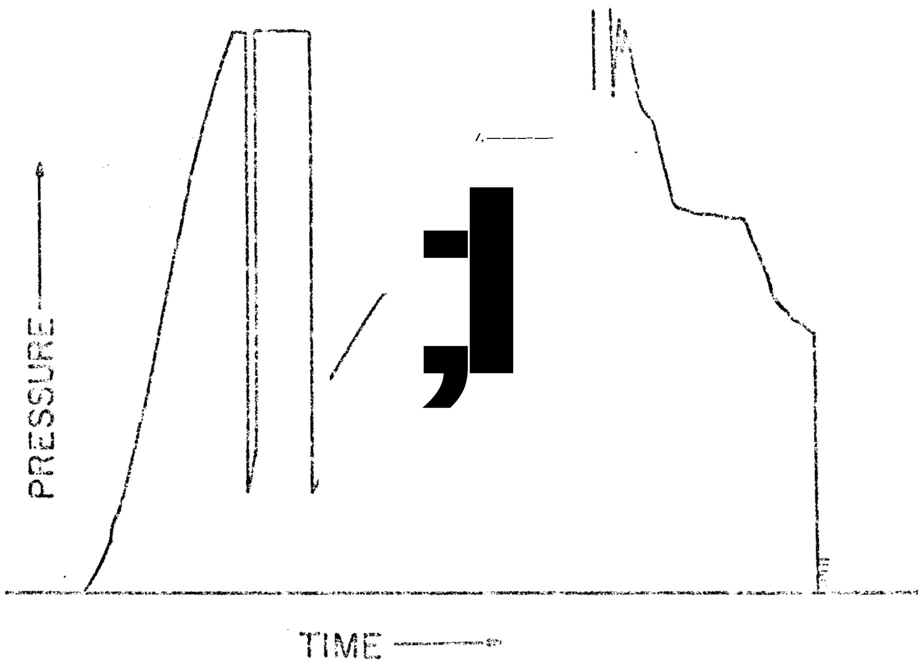

FIG. 1: TYPICAL DRILL STEM TEST DATA 1

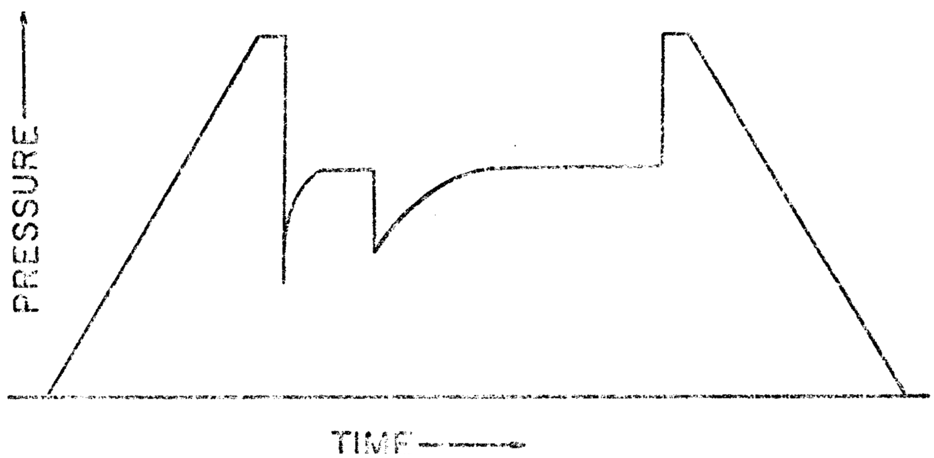

FIG. 2: TYPICAL DRILL STEM TEST DATA 2

initial volume of liquid removed from the wellbore to initiate flow. Cooper et al.,[3] in 1967, reported the results of a field test in a static water well from which a float was suddenly removed, giving the appearance of the instantaneous removal of a quantity of water equal to that displaced by the float. Actually, the Cooper et al. data interpretation method was based on studies by Jaeger[2,7] in 1956. A field application involving the cooling of a batch of hot water was reported by Beck, Jaeger, and Newstead[2] in 1956.

Maier[4] presented an approximate analysis of the equivalent DST problem in 1970. van Poollen and Weber,[5] in 1970, and Kohlhaas,‘ in 1972, applied the Cooper et al.[3] solution to DST flow period data analysis. Although most current studies refer to the study by Jaeger in 1956,[7] which included a surface resistance similar to the skin effect,"' most recent works do not include wellbore damage effects. A solution including the skin effect was presented by Agarwal et al.[10,11] in 1970 and 1972, although the use of the solutions was not demonstrated. Papadopulous et al.[12] presented extended results for the zero skin effect case in 1973.

The most complete discussion of DST applications of the slug test solutions was presented in 1975 by Ramey et al.[13] Three new slug test type-curves were developed for the analysis of flow period data. This study, which was reviewed in the Earlougher[14] monograph in 1977, did include the wellbore skin effect.

The solutions mentioned thus far did not consider the inertia of liquid moving in the wellbore. In deep, high productivity wells, the inertia of the liquid in the wellbore cannot be neglected. Sometimes this effect causes oscillations of the pressure and the liquid level in the wellbore about static positions.

The inertial effect of liquid in the wellbore was first investigated by Bredehoeft et al.[15] in 1966, using an analog computer. However, a general solution was not given. An approximate method to determine the permeability assuming an exponentially damped fluctuation was presented by van der Kamp[16] in 1976; however, he did not provide a general solution and did not include a skin effect. Thus far, no general solution including the case when the well behavior is affected by the inertial effect of the liquid in the wellbore with no oscillation has been presented, to our knowledge.

Another related well test is the closed chamber test,[17,18] which has become popular for pollution protection especially for offshore wells. It is a deviation from conventional drill stem testing. A solution useful for analysis of flow period data from closed chamber tests has never been offered, to our knowledge, and bottomhole pressure data for the flow period have been discarded or have not even been reported in many cases.

The purposes of this study are to derive a complete solution for the slug test, including the inertial effect of the liquid in the wellbore and the skin effect; to investigate the effects of parameters on the general solution; to advance the understanding of slug test data; and to study the analysis of flow period data from closed chamber tests as an extension of general slug test solutions.

2. SLUG TEST ANALYSIS

The slug test problem was stated by Ramey et al.[13] as that posed by a formation whose initial pressure, p_i, is at most less than the pressure to lift a column of reservoir liquid just to the surface of the earth. When a drill stem test packer is set just above the formation with the drill string empty except for the appropriate cushion liquid, all the elements for a slug test would be present. At zero time, the tester valve is opened to expose the formation suddenly to the cushion pressure, $(p_o - p_{atm})$, in the drill string above the valve (see Fig. 3). As the formation begins to produce, the produced liquid is stored within the drill string, and the liquid level begins to rise. The initial production rate will be high and will gradually decline as accumulating liquid in the drill string causes an increasing back pressure. Usually the liquid production ceases by itself, and in some cases the liquid level in the wellbore oscillates before it reaches equilibrium.

The mathematical formulation of the slug test problem is explained in Section 2-1. The solution for this problem is obtained and investigated in Section 2-2. Field data examples are discussed in Section 2-3.

2-1 Mathematical Formulation

In order to obtain a solution which includes the inertial effect of the liquid in the wellbore, a momentum balance is required. The linear momentum balance in the wellbore states that the rate of change of momentum is equal to the net force on the liquid:

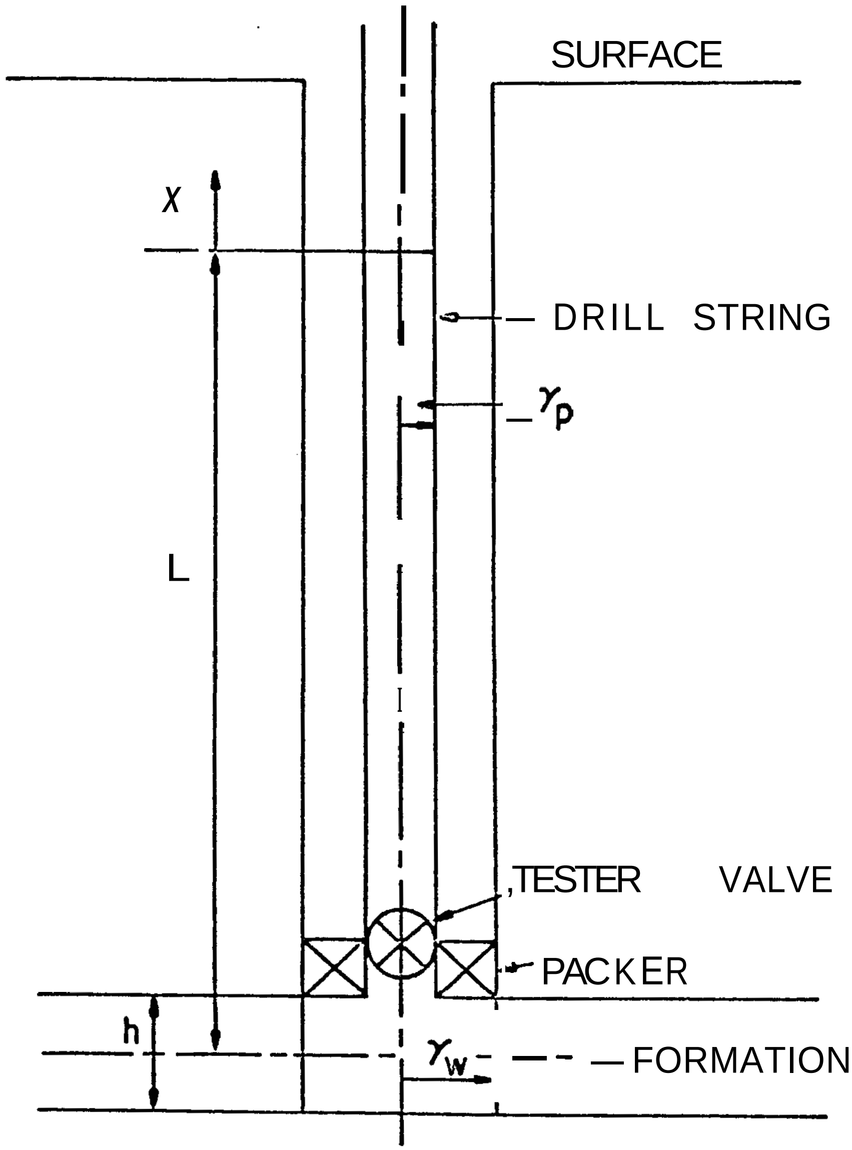

FIG. 3: SCHEMATIC DIAGRAM OF A SLUG TEST

$$\frac{d}{dt}\left[\rho_f \pi r_p^2 (L+x)\frac{dx}{dt}\right] = \pi r_p^2 \, p_w - \pi r_p^2 \, p_{atm} - \pi r_p^2 \, \rho_f (L+x)\, g$$

$$- \frac{f}{8}\rho_f \cdot \frac{dx}{dt}\left|\frac{dx}{dt}\right| \cdot 2\pi r_p (L+x) \qquad (1)$$

The term inside the parentheses in the left-hand side is the product of the mass of liquid in the wellbore and the velocity of the liquid level in the wellbore. The first term in the right-hand side is the force caused by the wellbore bottomhole pressure. The second term is the force caused by the atmospheric pressure. The third term is the gravity force, and the fourth term is the friction force.

ρ_f is the density of the liquid in the wellbore, r_p is the inside radius of the drill string, the tubing, or the casing pipe in which the produced liquid enters, L is the liquid length whose head is equivalent to the initial formation pressure, p_i, minus atmospheric pressure, p_{atm}, x is the liquid level in the wellbore measured from the stable point, p_w is the wellbore bottomhole pressure (we will call this the "wellbore pressure"), g is the gravitational acceleration, and f is the Moody friction factor.

Rearranging Eq. 1:

$$\rho_f (L+x)\frac{d^2x}{dt^2} + \rho_f \left(\frac{dx}{dt}\right)^2 + (L+x)\frac{dx}{dt}\frac{d\rho_f}{dt} = p_w - p_{atm} - \rho_f (L+x) g$$

$$- \frac{f}{4r_p}\rho_f \cdot \frac{dx}{dt}\left|\frac{dx}{dt}\right| (L+x) \qquad (2)$$

For a constant compressibility liquid, the following relation holds in the wellbore approximately:

$$\frac{d\rho_f}{dt} = \rho_f c_f \frac{\partial p}{\partial t} \cong \frac{\rho_f c_f}{2} \cdot \frac{\partial p_w}{\partial t} \qquad (3)$$

Then, Eq. 2 becomes as follows:

$$(L+x)\,\frac{d^2x}{dt^2} + xg + \left(\frac{dx}{dt}\right)^2 + \frac{f}{4r_p}\,(L+x)\,\frac{dx}{dt}\left|\frac{dx}{dt}\right| + \frac{c_f}{2}\,(L+x)\,\frac{\;}{\partial t}\,\frac{dx}{dt}$$

$$= \frac{p_w - p_{atm}}{\rho_f} - Lg \tag{4}$$

Since the head of the liquid length, L, is equivalent to the initial formation pressure, p_i, minus the atmospheric pressure, p_{atm}:

$$\frac{p_w - p_{atm}}{\rho_f} - Lg = \frac{p_w - p_i}{\rho_f} \tag{5}$$

So, Eq. 4 becomes:

$$(L+x)\,\frac{d^2x}{dt^2} + xg + \left(\frac{dx}{dt}\right)^2 + \frac{f}{4r_p}\,(L+x)\,\frac{dx}{dt}\left|\frac{dx}{dt}\right| + \frac{c_f}{2}\,(L+x)\,\frac{\;}{\partial t}\,\frac{dx}{dt}$$

$$= \frac{p_w - p_i}{\rho_f} \tag{6}$$

For the formation, if we adopt the following assumptions, the well-known diffusivity equation" derived from the continuity equation and Darcy's law can be used.

1) Horizontal, isotropic, homogeneous, isothermal, radial, infinite porous medium of constant thickness, h, porosity, ϕ, and permeability, k.

2) Constant liquid viscosity, μ, and small constant total system compressibility, c_t.

3) No fluid flow across the horizontal boundaries and negligible gravity effect.

4) The square of the pressure gradient with respect to radial distance is negligible.

These assumptions appear to be reasonable for slug tests. Then:

$$\frac{\partial^2 p}{\partial r^2} + \frac{1}{r} \cdot \frac{\partial p}{\partial r} = \frac{\phi \mu c_t}{k} \frac{\partial p}{\partial t} \tag{7}$$

p is the pressure inside the reservoir, r is the radial distance, t is the time, and c_t is the total system compressibility defined as the sum of the reservoir liquid compressibility and the formation compressibility.

In order to arrange the equations in dimensionless form, the following dimensionless variables are introduced:

$$p_D = \frac{p_i - p}{p_i - (p_o + p_{atm})} \tag{8}$$

$$t_D = \frac{kt}{\phi \mu c_t r_w^2} \tag{9}$$

$$r_D = \frac{r}{r_w} \tag{10}$$

$$x_D = \frac{\rho_f g x}{p_i - (p_o + p_{atm})} \left(- \frac{x}{x(t=0)} \right) \tag{11}$$

$$p_{wD} = \frac{p_i - p}{p_i - (p_o + p_{atm})} \tag{12}$$

p_D is the dimensionless pressure, t_D is the dimensionless time, r_w is the wellbore radius, r_D is the dimensionless radial distance, x_D is the dimensionless liquid level in the wellbore, $x(t=0)$ is the initial liquid level in the wellbore, and p_{wD} is the dimensionless wellbore bottomhole pressure (we will call this "dimensionless wellbore pressure").

Using these dimensionless variables, the following equations are derived:

From Eq. 7:

$$\frac{\partial^2 p_D}{\partial r_D^2} + \frac{1}{r_D}\frac{\partial p_D}{\partial r_D} = \frac{\partial p_D}{\partial t_D} \qquad (13)$$

From Eq. 6:

$$\frac{L}{g}\left(\frac{k}{\phi\mu c_t r_w^2}\right)^2\left(1+\frac{x_D}{L_D}\right)\frac{d^2x_D}{dt_D^2} + x_D + \frac{p_i-(p_o+p_{atm})}{\rho_f g^2}\left(\frac{k}{\phi\mu c_t r_w^2}\right)^2 \cdot$$

$$\left[\left(\frac{dx_D}{dt_D}\right)^2 + \frac{f(L+x)}{4r_p}\frac{dx_D}{dt_D}\frac{dx_D}{dt_D} - \frac{\rho_f c_f g}{2}(L+x)\frac{dp_{wD}}{dt_D}\frac{dx_D}{dt_D}\right]$$

$$= -p_{wD} \qquad (14)$$

In order to obtain an equation which we can handle analytically, the following assumptions are adopted:

5) The pressure drop caused by friction in the wellbore is negligible.

6) The compressibility of the liquid in the wellbore is negligible.

7) The $\left(\frac{dx}{dt}\right)^2$ term is negligible.

8) L is much greater than x.

Assumption 5 can be checked using available field case data. It was found that this assumption is reasonable, especially when there is cushion liquid in the wellbore. Examples of the pressure drop caused by friction in the wellbore are shown in Appendix C, and will be explained in Section 2-3. Assumption 6 is reasonable because we are considering liquid-filled reservoirs. To satisfy assumptions 7 and 8, the cushion liquid should exist in the wellbore before the test starts. It can be seen in Eq. 14 that the order of the $\left(\frac{dx}{dt}\right)^2$ term is the same as that of the pressure drop term caused by friction.

Applying these assumptions to Eq. 14, the following result is obtained:

$$\frac{L}{g}\left(\frac{k}{\phi\mu c_t r_w^2}\right)^2 \frac{d^2x_D}{dt_D^2} + x_D = -p_{wD} \tag{15}$$

The new group $\sqrt{\frac{L}{g}}\left(\frac{k}{\phi\mu c_t r_w^2}\right)$ is a dimensionless number and represents the effect of inertia of the liquid in the wellbore. In fact, this dimensionless number, a, is equivalent to Froude's number,[20] which represents the ratio between inertia force and gravity force. This number is defined as:

$$\alpha = \sqrt{\frac{L}{g}}\left(\frac{k}{\phi\mu c_t r_w^2}\right) \tag{16}$$

or:

$$\alpha = \sqrt{\frac{p_i - p_{atm}}{\rho_f g^2}}\left(\frac{k}{\phi\mu c_t r_w^2}\right) \tag{17}$$

Then, Eq. 15 becomes:

$$a^2 \cdot \frac{d^2x_D}{dt_D^2} + x_D = -p_{wD} \tag{18}$$

In order to determine the initial conditions, we assume that the initial reservoir pressure, p_i, is the same at any point in the reservoir. This condition is expressed as:

$$p_D(r_D, t_D=0) = 0 \tag{19}$$

The initial liquid level in the wellbore in dimensionless form is always -1, because:

$$x_D(t_D=0) = \frac{\rho_f g x(t=0)}{(p_{atm}+\rho_f Lg)-[\rho_f g\{L+x(t=0)\}+p_{atm}]}$$

$$= - \frac{x(t=0)}{x(t=0)}$$

$$= -1 \tag{20}$$

This is the second initial condition.

The initial velocity of the liquid level in the wellbore can be considered zero for the usual slug tests; however, to make the solution general, it is assumed that the initial velocity of liquid level in the wellbore is given as some value. This condition is the third initial condition:

$$\left.\frac{dx_D}{dt_D}\right|_{t_D=0} = x'_D(t_D=0) \tag{21}$$

Next we will consider the boundary conditions. Since we assumed that the reservoir is infinite:

$$\lim_{r_D\to\infty} p_D(r_D,t_D) = 0 \tag{22}$$

This is the first boundary condition.

From a material balance on the wellbore:

$$\pi r_p^2 \cdot \frac{dx}{dt} = \frac{2\pi r_w hk}{\mu} \left(\frac{\partial p}{\partial r}\right)_{r=r_w} \tag{23}$$

Using the dimensionless variables defined in Eqs. 8 to 11, the following equation is obtained:

$$\frac{dx_D}{dt_D} = - \frac{1}{C_D} \left(\frac{\partial p_D}{\partial r_D} \right)_{r_D=1} \tag{24}$$

C_D is the dimensionless wellbore storage constant,[21] and C is the wellbore storage constant defined as follows:

$$C_D = \frac{C}{2\pi r_w^2 h\phi c_t} \tag{25}$$

$$C = \frac{\pi r_p^2}{\rho_f g} \tag{26}$$

As the third boundary condition, we can use the following equation[10] obtained from a pressure balance at the sandface based on the definition of the steady-state skin factor.[8,9]

$$p_{wD} = \left[p_D - s \left(\frac{\partial p_D}{\partial r_D} \right) \right]_{r_D=1} \tag{27}$$

As a summary of this section, the following equations are obtained as the result of mathematical formulation of the slug test problem.

$$\frac{\partial^2 p_D}{\partial r_D^2} + \frac{1}{r_D} \cdot \frac{\partial p_D}{\partial r_D} = \frac{\partial p_D}{\partial t_D} \tag{13}$$

$$\alpha^2 \cdot \frac{d^2 x_D}{dt_D^2} + x_D = - p_{wD} \tag{18}$$

Initial Conditions:

$$p_D(r_D, t_D=0) = 0 \tag{19}$$

$$x_D(t_D-0) = - 1 \tag{20}$$

$$\left.\frac{dx_D}{dt_D}\right|_{t_D=0} = x_D'(t_D=0) \tag{21}$$

Boundary Conditions:

$$\lim_{r_D \to \infty} p_D(r_D, t_D) = 0 \tag{22}$$

$$\frac{dx_D}{dt_D} = - \frac{1}{C_D} \left(\frac{\partial p_D}{\partial r_D} \right)_{r_D=1} \tag{24}$$

$$p_{wD} = \left[p_D - s \left(\frac{\partial p_D}{\partial r_D} \right) \right]_{r_D=1} \tag{27}$$

2-2. Solutions

Since Eq. 13 and Eqs. 18 through *27* are linear equations, solutions **may** be obtained using the Laplace transformation. The solutions in Laplace space are given in Section *2-2-1.* The analytical Laplace transform inversions of these solutions are considered in Section *2-2-2;* however, the complete real space solutions could not be obtained. Numerical Laplace transform inversion methods considered in Section 2-2-3 were applied. The characteristics of the solutions are investigated in Section 2-2-4.

2-2-1. Solutions in Laplace Space

Applying the Laplace transformation with respect to time to Eq. 13:

$$\frac{\partial^2 \bar{p}_D}{\partial r_D^2} + \frac{1}{r_D} \cdot \frac{\partial \bar{p}_D}{\partial r_D} = \ell \cdot \bar{p}_D - p_D(t_D=0) \tag{28}$$

$\bar{p}_D$ is the Laplace transform of p_D with respect to time, and ℓ is the Laplace transform variable.

Substituting the initial condition Eq. 19, Eq. 28 becomes:

$$\frac{\partial^2 \bar{p}_D}{\partial r_D^2} + \frac{1}{r_D} \cdot \frac{\partial \bar{p}_D}{\partial r_D} = \ell \cdot \bar{p}_D \tag{29}$$

This is a modified Bessel equation of order zero, and the solution is:[44]

$$\bar{p}_D = AI_0(r_D\sqrt{\ell}) + BK_0(r_D\sqrt{\ell}) \tag{30}$$

I_0 is the modified Bessel function of the first kind of order zero, K_0 is the modified Bessel function of the second kind of order zero, and A and B are arbitrary constants.

To satisfy the boundary condition Eq. 22:

$$A = 0 \tag{31}$$

so:

$$\bar{p}_D = BK_0(r_D\sqrt{\ell}) \tag{32}$$

Then:

$$\frac{\partial \bar{p}_D}{\partial r_D} = - B\sqrt{\ell} \cdot K_1(r_D\sqrt{\ell}) \tag{33}$$

K_1 is the modified Bessel function of the second kind of order unity.
Applying the Laplace transformation with respect to time to Eq. 27:

$$p_{wD} = \left[\bar{p} - s \left(\frac{\partial \bar{p}_D}{\partial r_D} \right) \right]_{r_D=1} \tag{34}$$

Substituting Eqs. 32 and 33 into Eq. 34:

$$p_{wD} = B \{ K_0(\sqrt{\ell}) + s\sqrt{\ell} \cdot K_1(\sqrt{\ell}) \} \tag{35}$$

Applying the Laplace transformation with respect to time to Eq. 18:

$$a^2 \{ \ell^2\bar{x}_D - Rx_D(t_D-0) - x_D'(t_D=0) \} + \bar{x}_D = - \bar{p}_{wD} \tag{36}$$

$\bar{x}_D$ is the Laplace transform of x_D.
From Eqs. 35 and 36:

$$\bar{x}_D = \frac{-B \{ K_0(\sqrt{\ell}) + s\sqrt{\ell}\, K_1(\sqrt{\ell}) \} + \alpha^2\ell x_D(t_D=0) + \alpha^2 x_D'(t_D=0)}{(\alpha^2\ell^2+1)} \tag{37}$$

Applying the Laplace transformation with respect to time to Eq. 24:

$$R\bar{x}_, - x_D(t_D=0) = - \frac{1}{C_D}\left(\frac{\partial \bar{p}_D}{\partial r_D} \right)_{r_D=1} \tag{38}$$

From Eqs. 33 and 38:

$$B = \frac{C_D\{\ell\bar{x}_D - x_D(t_D=0)\}}{\sqrt{\ell}\cdot K_1(\sqrt{\ell})} \tag{39}$$

Substituting Eq. 39 into Eq. 37:

$$\bar{x}_D = \frac{\{(\alpha^2\ell+C_Ds)\sqrt{\ell}K_1(\sqrt{\ell}) + C_DK_0(\sqrt{\ell})\}\ x_D(t_D=0) + \alpha^2\sqrt{\ell}K_1(\sqrt{\ell})\ x_D'(t_D=0)}{(\alpha^2\ell^2+C_Ds\ell+1)\sqrt{\ell}K_1(\sqrt{\ell}) + C_D\ell K_0(\sqrt{\ell})} \tag{40}$$

From Eqs. 35, 39, and 40:

$$\bar{p}_{wD} = \frac{C_D\{s\sqrt{\ell}K_1(\sqrt{\ell}) + K_0(\sqrt{\ell})\}\{-x_D(t_D=0) + \alpha^2\ell x_D'(t_D=0)\}}{(\alpha^2\ell^2+C_Ds\ell+1)\sqrt{\ell}K_1(\sqrt{\ell}) + C_D\ell K_0(\sqrt{\ell})} \tag{41}$$

From Eqs. 32, 39, and 40:

$$\bar{p}_D = \frac{C_DK_0(r_D\sqrt{\ell})\{-x_D(t_D=0) + \alpha^2\ell x_D'(t_D=0)\}}{(\alpha^2\ell^2+C_Ds\ell+1)\sqrt{\ell}K_1(\sqrt{\ell}) + C_D\ell K_0(\sqrt{\ell})} \tag{42}$$

Equations 40, 41, and 42 are the solutions for x_D, p_{wD}, and p_D in the Laplace space, respectively. We seek the corresponding real space solutions. The procedure will be discussed in the following sections.

2-2-2 Analytical Approach to Laplace Transform Inversion

The complete analytical inversions of Eq. 40 through 42 could not be obtained. The reason is explained in this section and in Appendix A. As an approximation, the analytical solutions for early times and late times are obtained.

2-2-2.1 Trial for Analytical Inversion

Appendix A shows the mathematical treatment of this trial. As shown in Appendix A, it was not possible to find the poles of the function analytically except at the origin. In order to check whether the poles (except at the origin) exist or not (i.e., whether the values of β which satisfy Eqs. A-19 and A-20 exist or not), we assumed that the sum of residues $\sum Re$ is zero. Then, from Eq. A-21:

$$x_D = \frac{2}{\pi}\int_0^\infty \frac{\Delta_3(u)\Delta_2(u) - \Delta_4(u)\Delta_1(u)}{\Delta_1(u)^2 + \Delta_2(u)^2} e^{-u^2 t_D} du \tag{43}$$

where:

$$\Delta_1(u) = (\alpha^2 u^4 - C_D s u^2 + 1) J_1(u) - C_D u J_0(u) \tag{44}$$

$$\Delta_2(u) = (\alpha^2 u^4 - C_D s u^2 + 1) Y_1(u) - C_D u Y_0(u) \tag{45}$$

$$\Delta_3(u) = \{\alpha^2 u^2 x_D(t_D{=}0) - C_D s x_D(t_D{=}0) - \alpha^2 x'_D(t_D{=}0)\} u J_1(u) - C_D x_D(t_D{=}0) J_0(u) \tag{46}$$

$$\Delta_4(u) = \{\alpha^2 u^2 x_D(t_D{=}0) - C_D s x_D(t_D{=}0) - \alpha^2 x'_D(t_D{=}0)\} u Y_1(u) - C_D x_D(t_D{=}0) Y_0(u) \tag{47}$$

J_0 and J_1 are the Bessel functions of the first kind, order zero and unity. Y_0 and Y_1 are the Bessel functions of the second kind, order zero and unity. In order to check whether the assumption that there is no pole besides the origin is correct, Eq. 43 was integrated numerically using the Romberg method.[23] Figure 4 shows an example of the results. The solution behaves reasonably for a^2 values less than 10^5; however, the solution for a^2 values greater than 10^6 does not make sense for the example case when

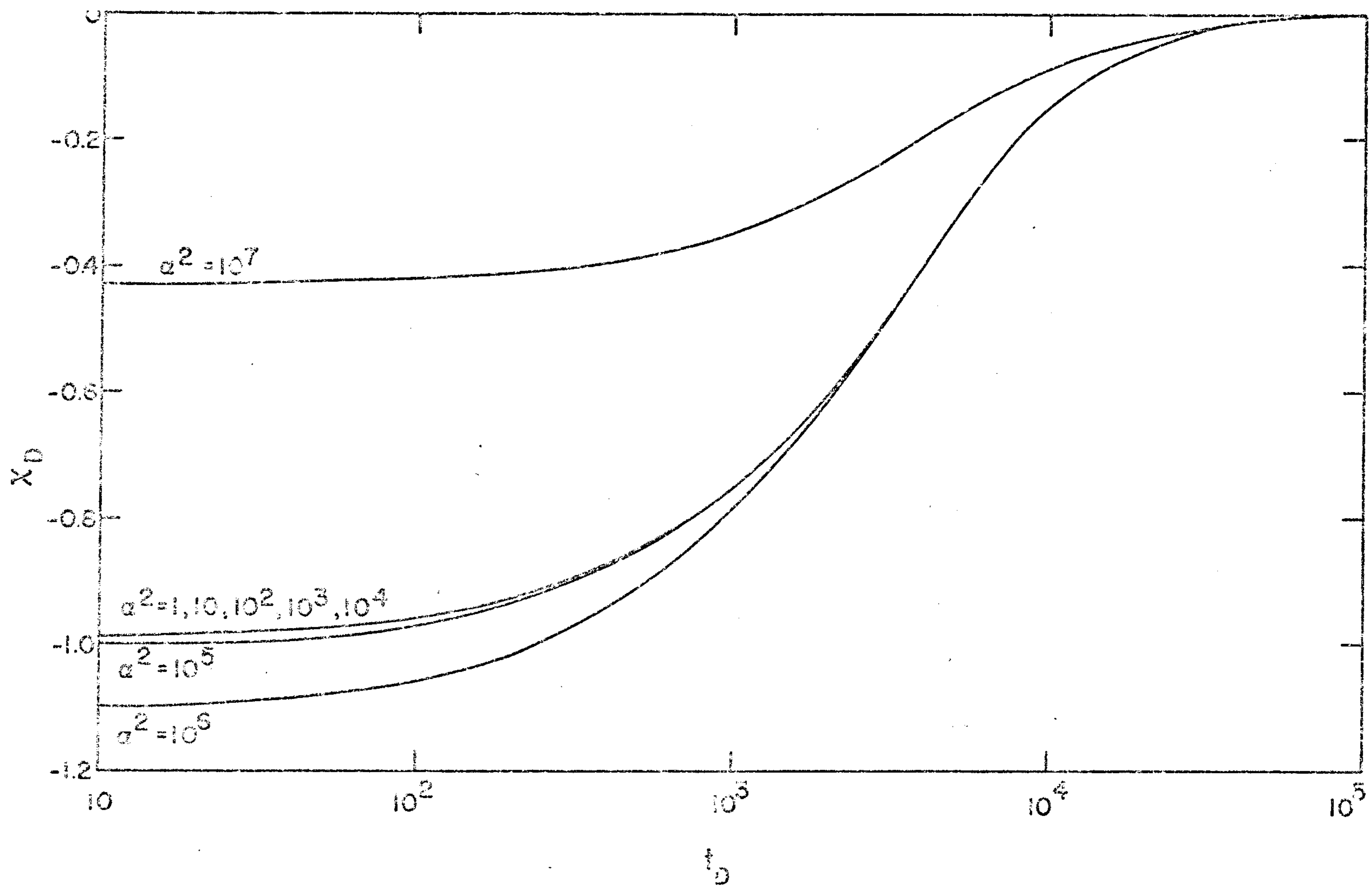

FIG. 4: DIMENSIONLESS LIQUID LEVEL IN THE WELLBORE VS DIMENSIONLESS TIME FOR $C_D = 10^3$ AND $s = 0$ BY NUMERICAL INTEGRATION OF EQ. 43

$C_D = 10^3$ and $s = 0$. This means that the sum of the residues, $\sum Re$, in Eq. A-21, plays an important role for α^2 values greater than 10^6 for this example case. Then, the assumption that other residues are negligible was wrong. This also can be guessed from the fact that the liquid level in the wellbore oscillates for some conditions. The pole must exist on the left-hand side of the Laplace plane to allow converging oscillation to happen.

In conclusion, it was not possible to obtain a complete real space solution. An alternative step is to use numerical Laplace transform inversion methods to obtain the entire solution. This procedure will be discussed in the following sections. The early time and late time approximate solutions can be obtained analytically, and will be discussed in the remaining part of this section. The same discussion is applicable to Eqs. 41 and 42, be+ cause their denominators are the same as that of Eq. 40, and it seems that there is no pole cancellation between denominator and numerator.

2-2-2.2 Early Time Solutions

Rearranging Eq. *40:*

$$\bar{x}_D = \frac{x_D(t_D=0)}{\ell} + \left\{\alpha^2 x_D'(t_D=0) - \frac{x_D(t_D=0)}{\ell}\right\} x \frac{1}{\alpha^2\ell^2 + C_D s\ell + 1 + C_D\sqrt{\ell} \cdot \frac{K_0}{K_1(\sqrt{\ell})}} \tag{48}$$

Similarly, from Eq. 41:

$$\bar{p}_{wD} = C_D \left\{\alpha^2 x_D'(t_D=0) - \frac{x_D(t_D=0)}{\ell}\right\} x \frac{s\ell + \sqrt{\ell} \cdot \frac{K_0(\sqrt{\ell})}{K_1(\sqrt{\ell})}}{\alpha^2\ell^2 + C_D s\ell + 1 + C_D\sqrt{\ell} \cdot \frac{K_0(\sqrt{\ell})}{K_1(\sqrt{\ell})}} \tag{49}$$

For early times, we can say that $\ell \to \infty$. Then, from the characteristics of modified Bessel functions:24

$$K_0(\sqrt{\ell}) = K_1(\sqrt{\ell}) \cong \sqrt{\frac{\pi}{2\sqrt{\ell}}}\ e^{-\sqrt{\ell}} \quad \text{for} \quad \ell \to \infty \tag{50}$$

Substituting Eq. 50 into Eqs. 48 and 49:

$$\bar{x}_D \cong \frac{x_D(t_D=0)}{\ell} + \left\{\alpha^2 x_D'(t_D=0) - \frac{x_D(t_D=0)}{\ell}\right\} x \frac{1}{\alpha^2\ell^2 + C_D s\ell + 1 + C_D\sqrt{\ell}} \tag{51}$$

$$\to \frac{x_D(t_D=0)}{\ell} - \frac{x_D(t_D=0)}{\alpha^2\ell^3} + \frac{x_D'(t_D=0)}{\ell^2} \quad \text{as } \ell \to \infty \tag{52}$$

$$\bar{p}_{wD} \cong C_D \left\{ a^2 x_D'(t_D=0) - \frac{x_D(t_D=0)}{\ell} \right\} \frac{s\ell + \sqrt{\ell}}{\alpha^2\ell^2 + C_D s\ell + 1 + C_D\sqrt{\ell}} \tag{53}$$

$$\to -\frac{C_D x_D(t_D=0)}{\alpha^2}\left\{\frac{s}{\ell^2} + \frac{1}{\ell^{5/2}}\right\} + C_D x_D'(t_D=0)\left\{\frac{s}{\ell} + \frac{1}{\ell^{3/2}}\right\} \text{as } \ell \to \infty \tag{54}$$

Applying the inverse Laplace transformation[25] directly:

$$x_D(t_D) = x_D(t_D=0)\left\{1 - \frac{t_D^{\,2}}{2\alpha^2}\right\} + x_D'(t_D=0) \cdot t_D \tag{55}$$

$$p_w(t_D) = -\frac{C_D x_D(t_D=0)}{a^2}\left\{ st_D + \frac{4}{3\sqrt{\pi}}\, t_D^{\,3/2}\right\} + C_D x_D'(t_D=0)\left\{ s + \frac{2}{\sqrt{\pi}}\, t_D^{\,1/2}\right\} \tag{56}$$

These early time solutions will be used to check the solutions obtained by the numerical Laplace transform inversion methods in the next section.

2-2-2.3 Late Time Solutions

Similarly as for early times, we can say that $\ell \to 0$ for late times. From the characteristics of modified Bessel functions,[26] for small arguments:

$$K_0(\sqrt{\ell}) \cong - \left\{ \ln \left(\frac{\sqrt{\ell}}{2} \right) + \gamma \right\} \quad (57)$$

$$K_1(\sqrt{\ell}) \cong \frac{1}{\sqrt{\ell}} \quad (58)$$

where γ is Euler's number.

Substituting Eqs. 57 and 58 into Eqs. 48 and 49:

$$\tilde{x}_D = \frac{x_D(t_D=0)}{\ell} + \left\{ \alpha^2 x_D'(t_D=0) - \frac{x_D(t_D=0)}{\ell} \right\}$$

$$\times \frac{1}{\alpha^2\ell^2 + C_D s\ell + 1 - C_D\ell \left[\ln \left\{ \frac{\sqrt{\ell}}{2} \right\} + \gamma \right]} \quad (59)$$

$$\to a^2 x_D'(t_D=0) \quad \text{as } \ell \to 0 \quad (60)$$

$$\overline{p}_{wD} \cong C_D \left\{ \alpha^2 x_D'(t_D=0) - \frac{x_D(t_D=0)}{\ell} \right\} \times \frac{s\ell - \ell \left[\ln \left\{ \frac{\sqrt{\ell}}{2} \right\} + \gamma \right]}{\alpha^2\ell^2 + C_D s\ell + 1 - C_D\ell \left[\ln \left\{ \frac{\sqrt{\ell}}{2} \right\} + \gamma \right]} \quad (61)$$

$$\to 0 \quad \text{as } \ell \to 0 \quad (62)$$

Then:

$$x_D(t_D) = a^2 x_D'(t_D=0) \cdot \delta(t_D) \quad (63)$$

$$p_{wD}(t_D) = 0 \quad (64)$$

$\delta(t_D)$ is the Dirac delta function.[45] Since we are now looking at the late time zone, $\delta(t_D) = 0$.

so:

$$x_D(t_D) = 0 \tag{65}$$

These results for late times agree with an understanding of the physical phenomena.

2-2-3 Numerical Laplace Transform Inversion

As shown in the previous section, we cannot obtain the real space solution analytically except for the approximate solutions at early times and late times. Therefore, three numerical Laplace transform inversion methods were used in this study. The results obtained by these methods were compared mutually, as well as to the result obtained from a finite difference solution. The finite difference solution was developed mainly for closed chamber test analysis and is explained in Section 3 and in Appendix D. The finite difference computer program is presented in Appendix E,

2-2-3.1 Stehfest Method

A simple and accurate numerical Laplace transform inversion method was presented by Stehfest[27] in 1970. This method is based on the following algorithm derived assuming a special probability density[28] with which the expectation of a function becomes similar to the Laplace transform of the function.

$$f(t) = \frac{\ln 2}{t} \sum_{i=1}^{N} V_i \cdot \overline{f}\left(\frac{\ln 2}{t} \cdot i\right) \tag{66}$$

$$V_i = (-1)^{[\frac{N}{2} + i]} \sum_{k = \frac{i+1}{2}}^{\min(i,\frac{N}{2})} \frac{k^{\frac{N}{2}}(2k)!}{(\frac{N}{2} - k)!k!(k-1)!(i-k)!(2k-i)!} \tag{67}$$

$\bar{f}$ is the Laplace transform of the function $f(t)$. A large value of N will cause a more accurate result theoretically; on the other hand, large N also causes a larger roundoff error. In this study, 16 was used for N. This value was selected from a comparison of the results obtained by this method with those from other methods. The function should not have discontinuities, salient points, or rapid oscillations (this depends on the ratio between the wavelength of the function and the peak of the probability density). The computer program for this method is presented in Appendix E.

2-2-3.2 Veillon Method

Another method was presented by Veillon[29] in 1972. This method is based on the following algorithm which is an approximation of the Fourier cosine transform inversion of the function assuming $f(t)$ is a real function.

$$f(t) = \frac{2e^{at}}{T} \left[\frac{1}{2} \operatorname{Re} \left\{ \bar{f}(a) \right\} + \sum_{k=1} \operatorname{Re}\left\{ \bar{f}\left(a + \frac{ik\pi}{T} \right)\right\} \cos\left(\frac{k\pi t}{T} \right) \right]$$

$$\text{for } 0 < t < T/2 \tag{68}$$

a is positive and greater than the real part of the singularities of $f(t)$. The function should be reasonably smooth. The program for this method was developed by Dr. M. Sengul of the Marathon Oil Company. In order to use this program, it was necessary to obtain the real part and the imaginary part of the function separately. The procedure used is explained in Appendix B. N was taken as 16.

2-2-3.3 Albrecht-Honig Method

The third method was presented by Albrecht and Honig[31] in 1977. This method is a variation of the Veillon method, and is based on the following algorithm.

$$f(t) = \frac{e^{at}}{T}\left[-\frac{1}{2}\,\mathrm{Re}\left\{ \bar{f}(a) \right\} + \sum_{k=1}^{N} \mathrm{Re}\left\{ \bar{f}\left(a + \frac{ik\pi}{T} \right) \right\} (-1)^k \right]$$

$$+ \frac{e^{-at}}{T} R(N) \qquad \text{far } 0 < t < T/2 \tag{69}$$

The definition of variables and constants are the same as those used in the previous two methods, and $R(N)$ is the correction term. The function should be reasonably smooth. N was taken as 16. The computer program for this method is presented in Appendix E.

2-2-3.4 Comparison of Results

Since these three numerical Laplace transform inversion methods have limitations on the function to which they can be applied (the function should be smooth, or should not have discontinuities or rapid oscillations), it is necessary to test the results obtained by these numerical Laplace transform inversion methods to assure reliability. In order to investigate the reliability of the solutions, the case of $C_D = 10^3$ and $s = 0$ was selected as a typical case. Solutions for this case for various a values were obtained by numerical Laplace transform inversion methods and the finite difference solution. The dimensionless wellbore pressures for this example case are shown in Fig. 5. One of the main differences between the previous slug test solutions which neglect inertial effect ($a = 0$) and the present problem can be seen on Fig. 5. The wellbore pressures drop instantly ($p_D = 1$)

for the inertia-less cases, but pass through a minimum (maximum in p_D) on Fig. 5. Furthermore, there is an "overshooting" for each value of α^2 shown on Fig. 5. Finally, the $\alpha^2 = 10^8$ case shows a distinct oscillation. This behavior causes computation difficulties.

To investigate the overshooting portion of the solution at early times, solutions for the $a^2 = 10^3$ case were calculated by the finite difference and Stehfest and Albrecht-Honig methods. It was necessary to apply early time or late time approximations for the modified Bessel functions in order to use the computer program developed by the Marathon Oil Company for the Veillon algorithm, and these approximations were not reasonable for this time range. Thus the Veillon method was not used for this test. Table 1 shows the results. The result by the Stehfest method and by the Albrecht-Honig method agree until $t_D = 0.9$; however, after this time, the result from the Albrecht-Honig method starts oscillating, and after $t_D = 20$, they agree again. The result by Stehfest for $t_D = 0.9 \sim 20$ agrees with the result from the finite difference method. From these results we infer that the Albrecht-Honig method is too sensitive to the oscillation of the function to apply to the subject problem, and the result by the Stehfest method is more reliable than that from the Albrecht-Honig method. The strange point at $t_D = 2$ for the Stehfest method with N = 16 happens for other combinations of C_D, s, and a values, but only at the special time of $t_D = 2$. This phenomena does not happen for the Stehfest method with N = 10. The reason for this odd result is not known; however, when N increases, the number of odd results increases. We suspect that this might be caused by roundoff error increased by the large N value. This phenomenon is the subject of continuing study. The result by the Stehfest method with N = 16 is closer to the result from the

TABLE 1: DIMENSIONLESS WELLBORE PRESSURE VERSUS DIMENSIONLESS TIME FOR $C_D = 10^3$, $s = 0$, and $\alpha^2 = 10^3$ BY VARIOUS METHODS

t_D	STEHFEST METHOD N = 10	STEHFEST METHOD N = 16	ALBRECHT-HONIG METHOD	FINITE DIFFERENCE SOLUTION
0.10000D 00	0.0214529976	0.0214507363	0.0214505620	0.0296930354
0.20000D 00	0.0578522690	0.0578439567	0.0578434726	0.0700351029
0.30000D 00	0.1019990041	0.1019870617	0.1019861843	0.1168018516
0.40000D 00	0.1510830739	0.1510840462	0.1510828088	0.1677057573
0.50000D 00	0.2033681582	0.2033970438	0.2033259769	0.2212252448
0.60000D 00	0.2575993243	0.2577032417	0.2576497229	0.2762451511
0.70000D 00	0.3126960014	0.3131997766	0.3130012126	0.3319048262
0.80000D 00	0.3682835860	0.3681005270	0.3686016063	0.3875206592
0.90000D 00	0.4239998059	0.4211825268	0.4238777015	0.4425412130
0.10000D 01	0.4782305760	0.4866216143	0.4753216573	0.4965186962
0.20000D 01	0.9210326406	(-1.6019925079)	1.4896993142	0.9267022871
0.30000D 01	1.1209044423	1.1239439997	1.0351876301	1.1258199853
0.40000D 01	1.1501383129	1.1592637356	1.2738960311	1.1618849632
0.50000D 01	1.1153425412	1.1193314975	1.2260014287	1.1259700598
0.60000D 01	1.0730757852	1.0679626756	0.9760606407	1.0774909751
0.70000D 01	1.0409903521	1.0308154293	1.1037051060	1.0415048465
0.80000D 01	1.0204467957	1.0106315690	1.0754371487	1.0218452864
0.90000D 01	1.0084321135	1.0021360619	0.9435804441	1.0138078186
0.10000D 02	1.0018058894	0.9996989531	1.0521378927	1.0116362626
0.20000D 02	0.9925003643	0.9933859569	0.9926207621	
0.30000D 02	0.9868769238	0.9863506528	0.9862765264	
0.40000D 02	0.9817682235	0.9815167752	0.9818258892	
0.50000D 02	0.9773025744	0.9772050251	0.9777967584	
0.60000D 02	0.9732328125	0.9731945947	0.9736910945	
0.70000D 02	0.9694145433	0.9694000645	0.9696838148	
0.80000D 02	0.9657707501	0.9657663945	0.9659079126	
0.90000D 02	0.9622576376	0.9622578679	0.9623413326	
0.10000D 03	0.9588482118	0.9588506142	0.9589228953	
0.20000D 03	0.9281217579	0.9281251965	0.9282446282	
0.30000D 03	0.9009117264	0.9009144810	0.8999731574	
0.40000D 03	0.8758621810	0.8758645594	0.8753262051	
0.50000D 03	0.8524251531	0.8524275719	0.8525508066	
0.60000D 03	0.8302951976	0.8302974954	0.8304213432	
0.70000D 03	0.8092746401	0.8092769553	0.8094012954	
0.80000D 03	0.7892235773	0.7892259629	0.7893507636	
0.90000D 03	0.7700368590	0.7700393313	0.7701646121	
0.10000D 04	0.7516319677	0.7516344375	0.7517603409	
0.20000D 04	0.5998270822	0.5998351744	0.5999662337	
0.30000D 04	0.4882504455	0.4882674117	0.4884032500	
0.40000D 04	0.4029095646	0.4029255755	0.4030656960	
0.50000D 04	0.3361799338	0.3361788777	0.3363229901	
0.60000D 04	0.2832016559	0.2831698941	0.2833177809	
0.70000D 04	0.2406405455	0.2405712959	0.2407225771	
0.80000D 04	0.2061099426	0.2060032650	0.2061577871	
0.90000D 04	0.1778534067	0.1777147562	0.1778724918	

finite difference solution in the overshooting portion of the solution than is the result by the Stehfest method with N = 10. The existence of the overshooting portion of the solution at early times was assured by the Veillon method for smaller a values. Table 2 presents the results. Although not shown, these results agree with the early time analytical solution expressed by Eq. 56.

Table 3 shows a comparison of the results by these four methods for the $\alpha^2 = 10^7$ case (see also Fig. 5). The results from these four methods agree quite well. The result by the Stehfest method with N = 16 and N = 10 are quite close, but the N = 16 value agrees best with other results.

Table 4 shows the comparison of the results by all four methods for $\alpha^2 = 10^8$, for which the solution has an oscillation. The results by the Albrecht-Honig method and by the Veillon method agree very well. This is probably because the algorithms for these two methods are similar. However, the results show a higher amplitude of the oscillation than do the results by the Stehfest method and by the finite difference solution. This might be caused by the higher sensitivity to the oscillation of the function of these methods, which appeared at the overshooting portion of the solution for the $\alpha^2 = 10^3$ case in the Albrecht-Honig method. The result by the Stehfest method with N = 16 is closer to the result by the finite difference solution than the result by the Stehfest method with N = 10.

From these comparisons of the results obtained by various methods for the example case, we conclude that solution by the Stehfest method with N = 16 gives the most reliable solution for present problems. The

TABLE 2: DIMENSIONLESS WELLBORE PRESSURE VERSUS DIMENSIONLESS TIME FOR SMALL a^2 VALUES WHEN $C_D = 10^3$ AND $s = 0$ BY THE VEILLON METHOD

$\alpha^2 = 10^{-4}$		$\alpha^2 = 10^{-7}$	
t_D	p_{wD}	t_D	p_{wD}
5.00000000D-06	8.20475719D-02	5.00000000D-08	8.20475740D-02
6.00000000D-06	1.07018134D-01	6.00000000D-08	1.07018138D-01
7.00000000D-06	1.33722237D-01	7.00000000D-08	1.33722244D-01
8.00000000D-06	1.61899765D-01	8.00000000D-08	1.61899776D-01
9.00000000D-06	1.91326994D-01	9.00000000D-08	1.91327010D-01
1.00000000D-05	2.21807005D-01	1.00000000D-07	2.21807028D-01
2.00000000D-05	5.52322567D-01	2.00000000D-07	5.52322800D-01
3.00000000D-05	8.61512986D-01	3.00000000D-07	8.61513818D-01
4.00000000D-05	1.09554509D+00	4.00000000D-07	1.09554701D+00
5.00000000D-05	1.23809928D+00	5.00000000D-07	1.23810272D+00
6.00000000D-05	1.29629459D+00	6.00000000D-07	1.29629985D+00
7.00000000D-05	1.28982849D+00	7.00000000D-07	1.28983565D+00
8.00000000D-05	1.24256281D+00	8.00000000D-07	1.24257175D+00
9.00000000D-05	1.17674162D+00	9.00000000D-07	1.17675205D+00
1.00000000D-04	1.10970029D+00	1.00000000D-06	1.10971184D+00
2.00000000D-04	1.01220135D+00	2.00000000D-06	1.01221536D+00
3.00000000D-04	1.00412114D+00	3.00000000D-06	1.00413878D+00
4.00000000D-04	1.00377037D+00	4.00000000D-06	1.00379068D+00
5.00000000D-04	1.00246443D+00	5.00000000D-06	1.00248714D+00
6.00000000D-04	1.00186191D+00	6.00000000D-06	1.00188678D+00
7.00000000D-04	1.00148557D+00	7.00000000D-06	1.00151244D+00
8.00000000D-04	1.00121204D+00	8.00000000D-06	1.00124077D+00
9.00000000D-04	1.00100964D+00	9.00000000D-06	1.00104010D+00
1.00000000D-03	1.00085534D+00	1.00000000D-05	1.00088745D+00
2.00000000D-03	1.00026381D+00	2.00000000D-05	1.00030922D+00
3.00000000D-03	1.00010884D+00	3.00000000D-05	1.00016446D+00
4.00000000D-03	1.00003922D+00	4.00000000D-05	1.00010345D+00
5.00000000D-03	9.99999204D-01	5.00000000D-05	1.00007101D+00
6.00000000D-03	9.99972619D-01	6.00000000D-05	1.00005128D+00
7.00000000D-03	9.99953199D-01	7.00000000D-05	1.00003816D+00
8.00000000D-03	9.99938042D-01	8.00000000D-05	1.00002887D+00
9.00000000D-03	9.99925627D-01	9.00000000D-05	1.00002196D+00

TABLE 3: DIMENSIONLESS WELLBORE PRESSURE VERSUS DIMENSIONLESS TIME FOR $C_D = 10^3$, $s = 0$, AND $\alpha^2 = 10^7$ BY VARIOUS METHODS

t_D	STEHFEST METHOD N = 10	STEHFEST METHOD N = 16	ALBRECHT-HONIG METHOD	VEILLON METHOD	FINITE DIFFERENCE SOLUTION
0.10000D 03	0.0223778916	0.0223765606	0.0223762625	0.021882596	0.0245780818
0.20000D 03	0.0505988964	0.0505956357	0.0505949324	0.050016660	0.0531373086
0.30000D 03	0.0804824477	0.0804773776	0.0804761081	0.079863019	0.0832152001
0.40000D 03	0.1110040701	0.1109981202	0.1109963113	0.110372235	0.1138818160
0.50000D 03	0.1416426133	0.1416381645	0.1416357895	0.141015091	0.1446383223
0.60000D 03	0.1720743841	0.1720752804	0.1720723203	0.171464604	0.1751697573
0.70000D 03	0.2020771873	0.2020884227	0.2020848556	0.201936894	0.2052584182
0.80000D 03	0.2314896540	0.2315167013	0.2315124990	0.230949196	0.2347453535
0.90000D 03	0.2601907467	0.2602386288	0.2602337732	0.259698709	0.2635104588
0.10000D 04	0.2880881088	0.2881604085	0.2881548782	0.287650663	0.2914610526
0.20000D 04	0.5132767362	0.5130881017	0.5130759062	0.512310180	0.5160905404
0.30000D 04	0.6347464599	0.6327883674	0.6327741735	0.632856109	0.6349898172
0.40000D 04	0.6628471056	0.6612853330	0.6612371121	0.661429619	0.6627444003
0.50000D 04	0.6205855407	0.6235327193	0.6234187696	0.623613973	0.6246125571
0.60000D 04	0.5368212663	0.5450850438	0.5450161095	0.545153844	0.5463469039
0.70000D 04	0.4376588198	0.447842524[illegible]	0.4480082656	0.448071545	0.4498229611
0.80000D 04	0.3412862295	0.3485067303	0.3489316364	0.348933341	0.3514027313
0.90000D 04	0.2575422502	0.2582809352	0.2587096699	0.258678013	0.2618323983

TABLE 4: DIMENSIONLESS WELLBORE PRESSURE VERSUS DIMENSIONLESS TIME FOR $C_D = 10^3$, $s = 0$, and $\alpha^2 = 10^8$ BY VARIOUS METHODS

t_a	STEHFEST METHOD N = 10	STEHFEST METHOD N = 16	ALBRECHT-HONIG METHOD	VEILLON METHOD	FINITE DIFFERENCE SOLUTION
0.10000D 04	0.0331531681	0.0331508357	0.0331502881	0.033061751	0.0353332677
0.20000D 04	0.0714577922	0.0714494608	0.0714482271	0.071353398	0.0736981727
0.30000D 04	0.1100515363	0.1100441630	0.1100422062	0.109948988	0.1120515168
0.40000D 04	0.1475228274	0.1475609739	0.1475582704	0.147470579	0.1491189184
0.50000D 04	0.1830199383	0.1831858564	0.1831822959	0.183102506	0.1841262055
0.60000D 04	0.2159845529	0.2163477470	0.2163429140	0.216272588	0.2165336690
0.70000D 04	0.2460808241	0.2466204373	0.2466135391	0.246553646	0.2459453589
0.80000D 04	0.2731346655	0.2736808964	0.2736712259	0.273622355	0.2720691200
0.90000D 04	0.2970584640	0.2972877975	0.2972758639	0.297238271	0.2946956618
0.10000D 05	0.3177776407	0.3172691443	0.3172580280	0.317231704	0.3136859575
0.20000D 05	0.3170374101	0.3190583109	0.3187469040	0.318800650	0.3099478714
0.30000D 05	0.0627842606	0.0903431607	0.0912518231	0.091308405	0.0920336270
0.40000D 05	-0.0743155008	-0.1091733563	-0.1048339191	-0.104796499	-0.0906861020
0.50000D 05	-0.0704809502	-0.1178743800	-0.1307250070	-0.130679147	-0.1160104786
0.60000D 05	-0.0309785203	-0.0253703940	-0.0344316984	-0.034358502	-0.0325873102
0.70000D 05	-0.0020176319	0.0387623852	0.0588906336	0.058981109	0.0482244032
0.80000D 05	0.0116317327	0.0487070007	0.0755005001	0.075588864	0.0641114439
0.90000D 05	0.0156387037	0.0321176409	0.0312333089	0.031315662	0.0291747739

Stehfest method with N = 16 was used to obtain the solutions cited in the following sections, although the solutions were checked by other methods consistently. The reliability of the solution should decrease as the solution has more oscillations. Bessel functions are calculated using the polynomial approximations,[32] as shown in the computer programs in Appendix E. The numerical Laplace transform inversion program should be run in double precision. Sometimes results show a slight oscillation around the correct answers if the program is run in single precision. This entire discussion is applicable not only to the function p_{wD} (see Eq. 41), but alto to the function x_D (see Eq. 39) and p_D (see Eq. 42).

2-2-4 Results and Discussion

The solutions were obtained by the Stehfest method with N = 16 for a range of parameters. These solutions were checked by the results obtained by other numerical Laplace transform inversion methods, and by the finite difference solution.

Based on these solutions, the effect of parameter values on the solution and the characteristics of the solution are investigated in this section.

2-2-4.1 Effect of α on Solutions

The dimensionless number α was defined in Eqs. 16 and 17:

$$\alpha = \sqrt{\frac{L}{g}}\left(\frac{k}{\phi\mu c_t r_w^2}\right) \tag{16}$$

or:

$$\alpha = \sqrt{\frac{(p_i - p_{atm})}{\rho_f g^2}}\left(\frac{k}{\phi\mu c_t r_w^2}\right) \tag{17}$$

The dimensionless number α represents the effect of inertia of the liquid in the wellbore on the solution. In order to investigate the characteristics of the solution including the inertial effect of the liquid in the wellbore, the case when $C_D = 10^3$ and $s = 0$ will be used as a typical example, and the solutions for various α values will be obtained for this case. Figure 5 shows the dimensionless wellbore pressure, p_{wD}, versus the dimensionless time, t_D, and Figure 6 shows the dimensionless liquid level in the wellbore, x_D, versus t_D, both in semilog coordinates. Figures 7 and 8 show the same results on Cartesian coordinates. The tabulated results obtained by the Stehfest method are given in Tables 5 and 6.

The solution for $\alpha = 0$ agrees with the previous slug test solution,[13] which neglects the inertial effect of the liquid in the wellbore. Considering the range of dimensionless times in which field data usually lie, it can be said that the inertial effect of the liquid in the wellbore is negligible when α^2 is less than about 10^4 for this example. On the other hand, when α^2 is greater than about 10^4, field data should not follow the available slug test solution. This can be seen by comparing the $\alpha = 0$ and $\alpha^2 > 10^4$ cases on Figs. 5 and 6. In these situations, the solutions including the inertial effect of the liquid in the wellbore presented herein should be used to analyze field data. This is true even though no oscillation in pressure or liquid level is evident. In fact, it is not rare for α^2 to take values greater than 10^4 for high initial formation pressure wells or high permeability reservoirs. When α^2 is greater than about 10^8 for this example case, the liquid level in the wellbore shows an oscillation.

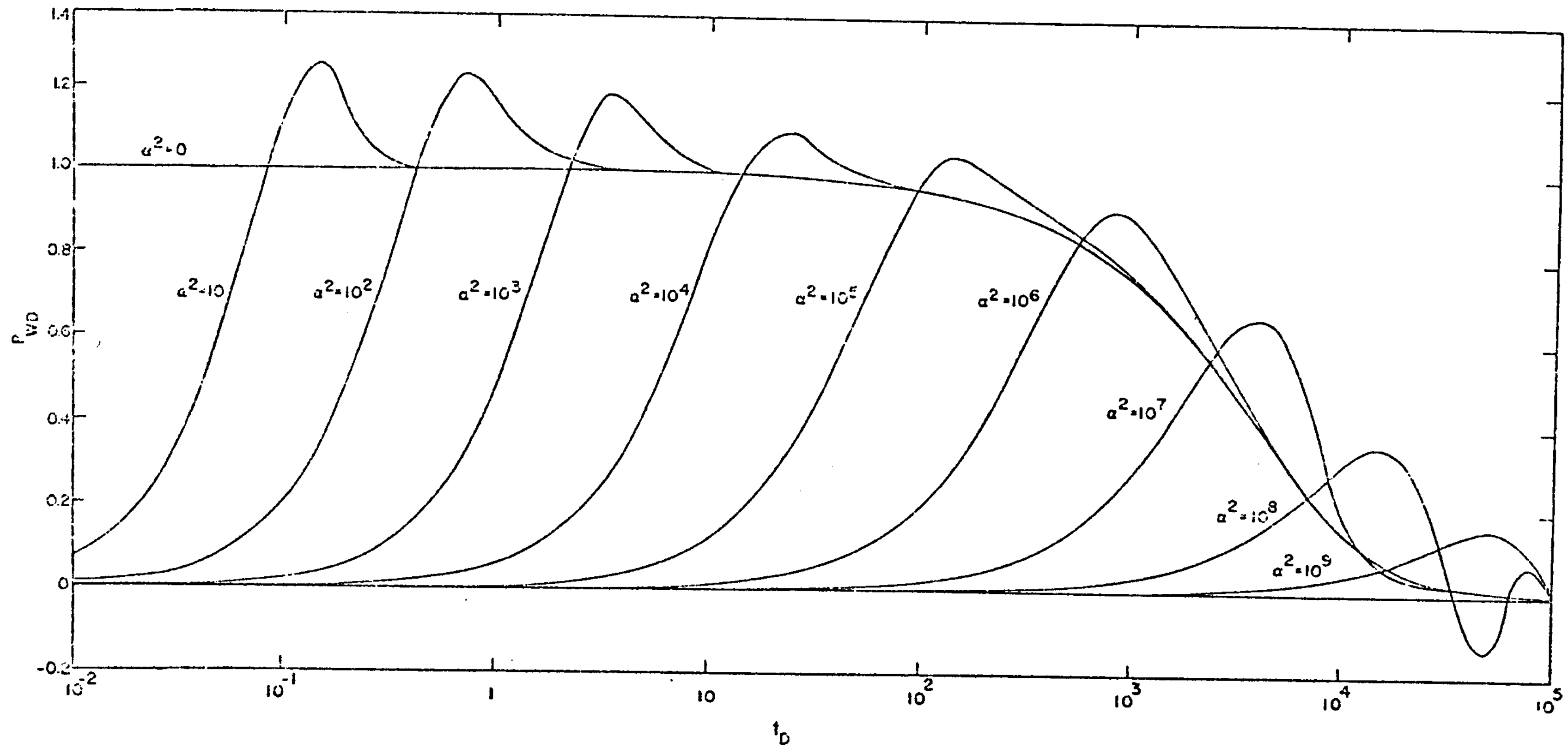

FIG. 5: DIMENSIONLESS WELLBORE PRESSURE VS DIMENSIONLESS TIME FOR $C_D = 10^3$ AND $s = 0$

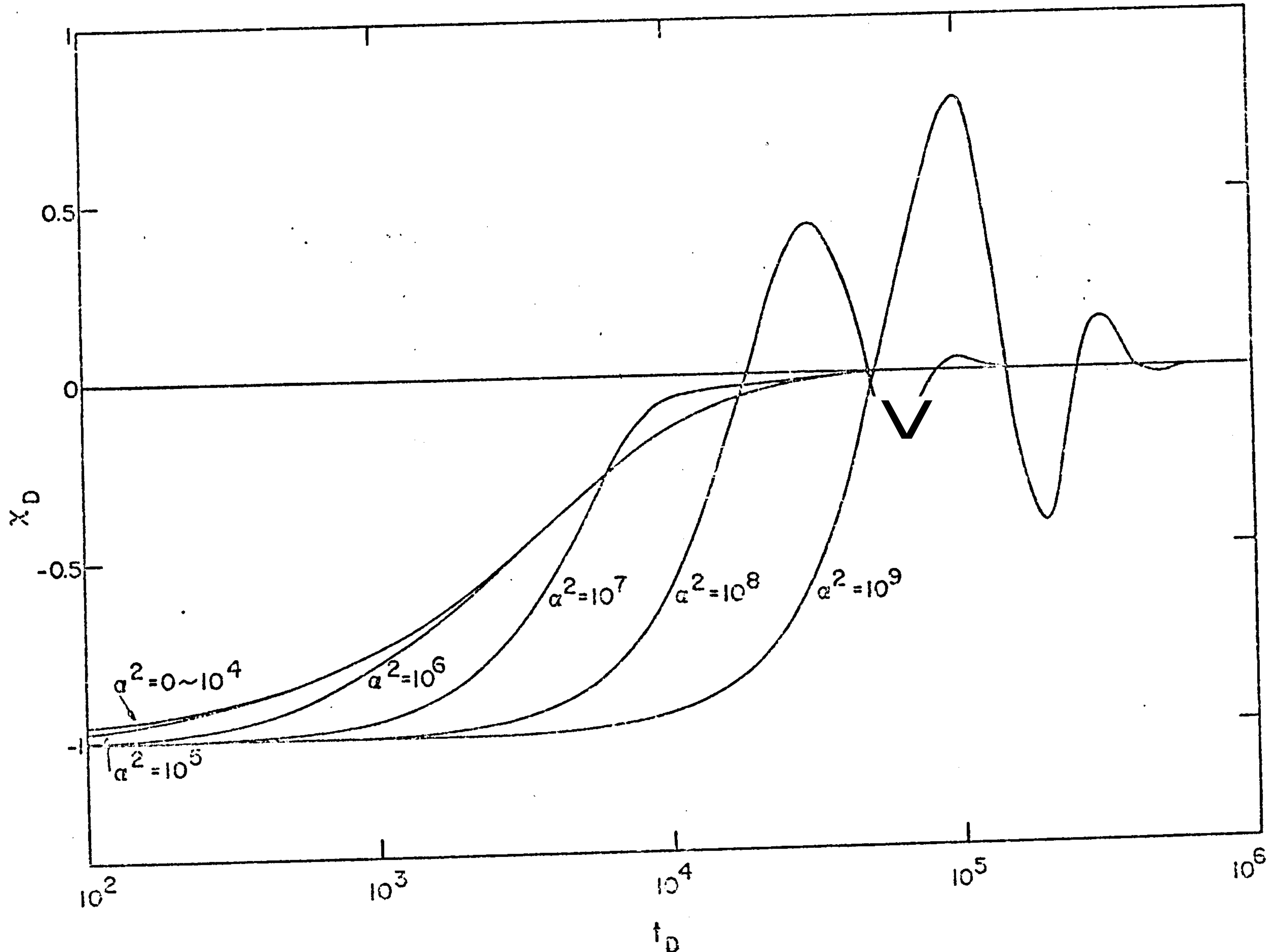

FIG. 6: DIMENSIONLESS LIQUID LEVEL IN THE WELLBORE VS DIMENSIONLESS TIME FOR $C_D = 10^3$ AND $s = 0$

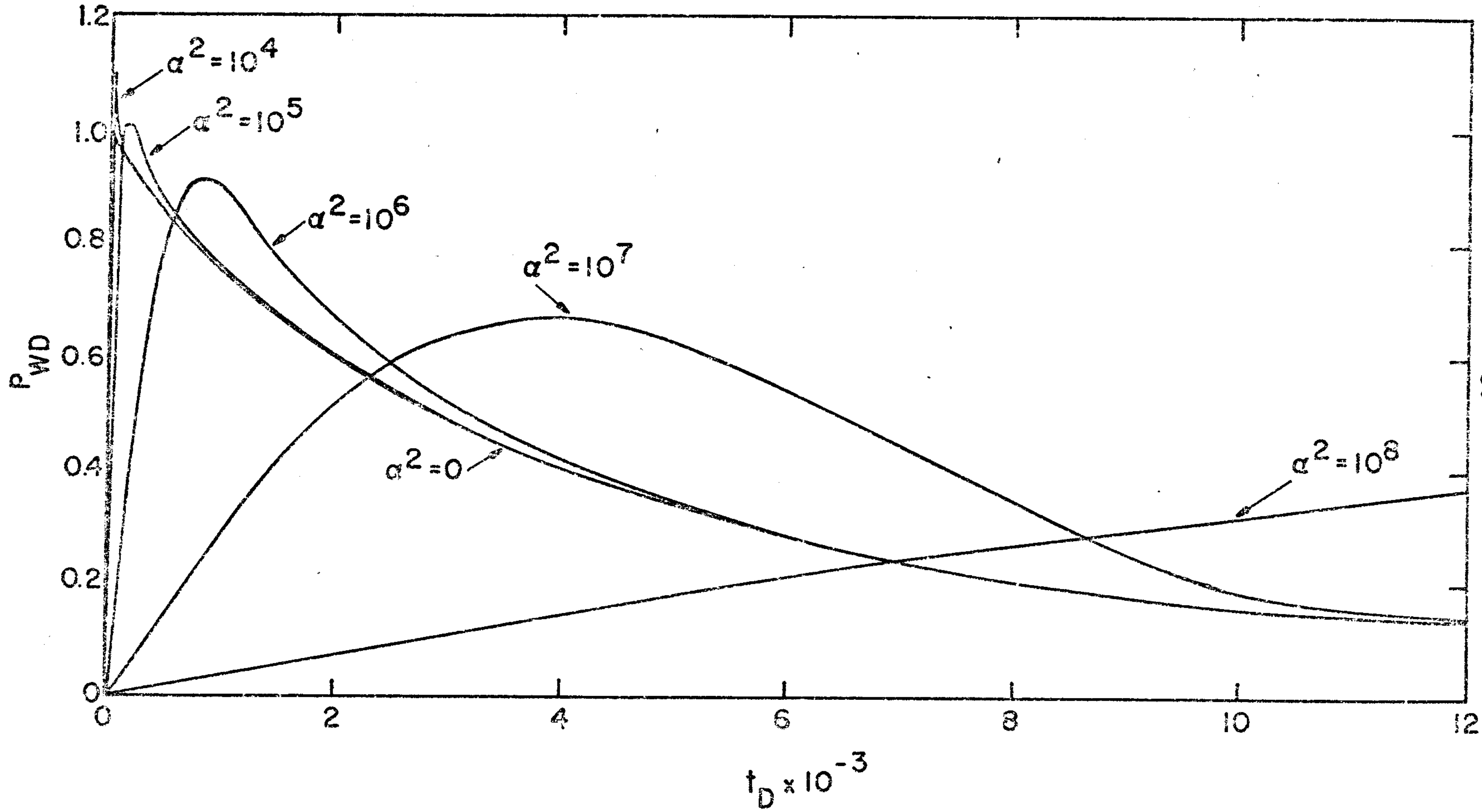

FIG. 7: DIMENSIONLESS WELLBORE PRESSURE VS DIMENSIONLESS TIME FOR $C_D = 10^3$ AND $s = 0$ IN CARTESIAN COORDINATES

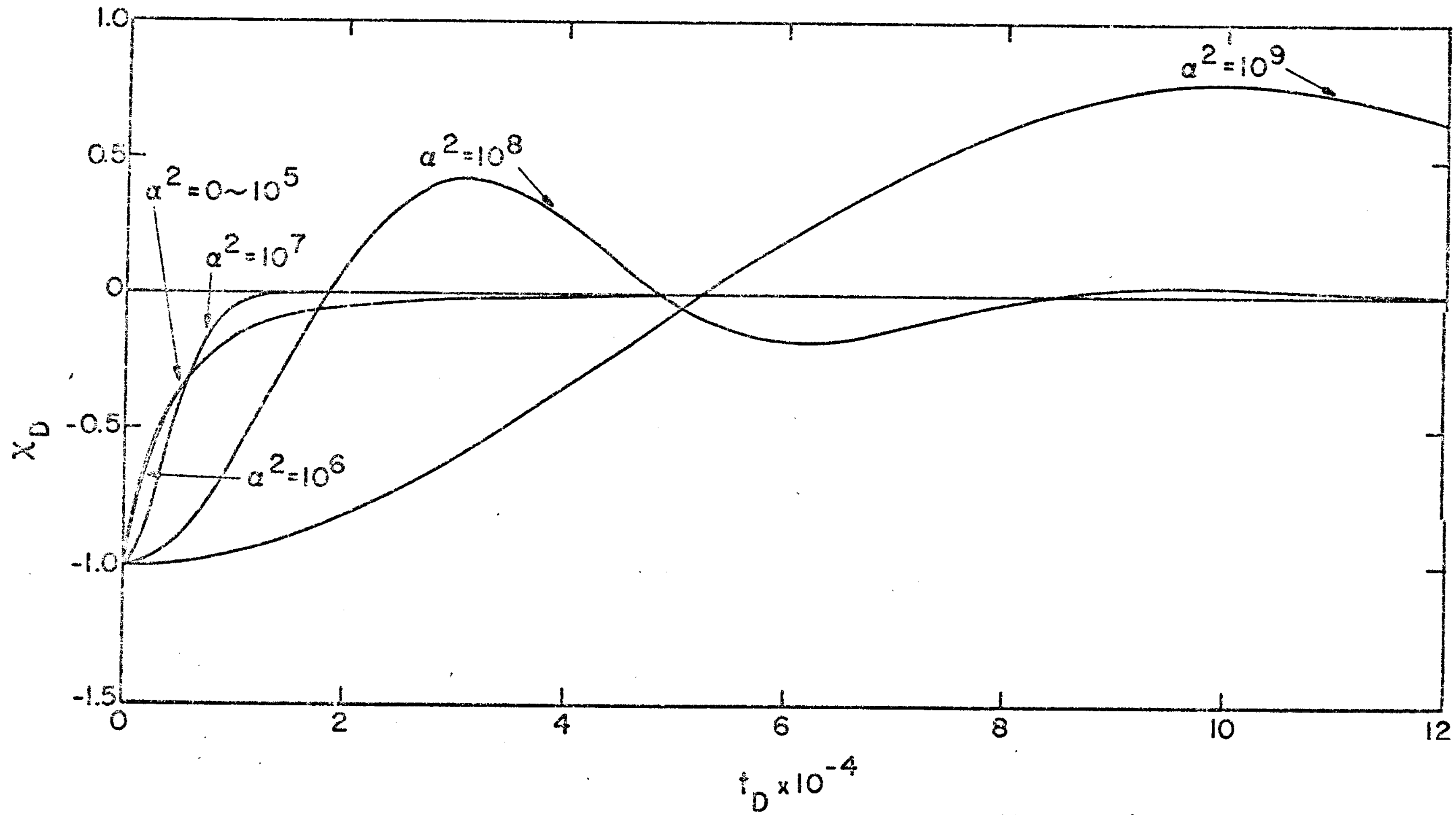

FIG. 8: DIMENSIONLESS LIQUID LEVEL IN THE WELLBORE VS DIMENSIONLESS TIME FOR $C_D = 10^3$ AND $s = 0$ IN CARTESIAN COORDINATES

TABLE 5: DIMENSIONLESS WELLBORE PRESSURE VERSUS DIMENSIONLESS TIME FOR $C_D = 10^3$ AND $s = 0$

t_D	$\alpha = 0$	$\alpha^2 = 10^4$	$\alpha^2 = 10^5$	$\alpha^2 = 10^6$	$\alpha^2 = 10^7$	$\alpha^2 = 10^8$
0.10000D 01	0.9998823183	0.0000728307	0.0000072832	0.0000007283	0 0000000728	0 0000000073
0.20000E 01	0.9998307354	0.0002033494	0.0000203361	0.0000020336	0 0000002034	0 0000000203
0.30000D 01	0.9997900406	0.0003699482	0.0000369985	0.0000036999	0 0000003700	0 0000000370
0.40000D 01	0.9997550835	0.0005649629	0.0000565050	0.0000056506	0 0000005651	0 0000000565
0.50000D 01	0.9997236210	0.0007839842	0.0000784152	0.0000078417	0 0000007842	0 0000000784
0.60000D 01	0.9996948746	0.0010240492	0.0001024337	0.0000102437	0 0000010244	0 0000001024
0.70000D 01	0.9996680492	0.0012829908	0.0001283443	0.0000128349	0 0000012835	0 0000001283
0.80000D 01	0.9996428011	0.0015591357	0.0001559805	0.0000155987	0 0000015595	0 0000001560
0.90000D 01	0.9996187166	0.0018511421	0.0001852088	0.0000185218	0 0000018522	0 0000001852
0.10000D 00	0.9995958091	0.0021579032	0.0002159191	0.0000215932	0 0000021593	0 0000002159
0.20000D 00	0.9994022030	0.0058806065	0.0005890320	0.0000589129	0 0000058914	0 0000005891
0.30000D 00	0.9992440358	0.0105072001	0.0010538588	0.0001054173	0 0000105420	0 0000010542
0.40000D 00	0.9991043189	0.0158075690	0.0015879352	0.0001588655	0 0000158873	0 0000015887
0.50000D 00	0.9989764521	0.0216502140	0.0021786128	0.0002179977	0 0000218011	0 0000021801
0.60000D 00	0.9988572261	0.0279492648	0.0028177747	0.0002820070	0 0000282030	0 0000028203
0.70000D 00	0.9987456216	0.0346585401	0.0035012830	0.0003504847	0 0000350520	0 0000035052
0.80000D 00	0.9986328998	0.0416042730	0.0042119362	0.0004217124	0 0000421764	0 0000042177
0.90000D 00	0.9985156885	0.0486564982	0.0049367694	0.0004943942	0.0000494466	0 0000049447
0.10000D 01	0.9984946696	0.0575578974	0.0058540047	0.0005863925	0.0000586492	0 0000058650
(0.20000D 01	0.9793847736	-0.1586018658	-0.0157700540	-0.0015760124	-0.0001575912	-0 0000157590
0.30000D 01	0.9968074569	0.2377397260	0.0257394155	0.0025945542	0.0002596625	0.0000259683
0.40000D 01	0.9961220661	0.3349903693	0.0376954784	0.0038146037	0.0003819142	0 0000381960
0.50000D 01	0.9954803550	0.4302220421	0.0504831207	0.0051304968	0.0005138796	0 0000513963
0.60000D 01	0.9948702784	0.5209325162	0.0639109536	0.0065248829	0 0006538431	0 0000653979
0.70000D 01	0.9942847666	0.6055644702	0.0778430657	0.0079857258	0 0008006184	0 0000800823
0.80000D 01	0.9937191355	0.6831957733	0.0921769217	0.0095041407	0 0009533326	0 0000953625
0.90000D 01	0.9931699527	0.7533539457	0.1068318661	0.0110732753	0 0011113151	0 0001111715
0.10000D 02	0.9926347789	0.8158921957	0.1217425066	0.0126876711	0 0012740332	0 0001274561
0 20000D 02	0.9877777956	1.0950296523	0.2760470517	0.0306048529	0 0030924790	0 0003095699
0 30000D 02	0.9834372289	1.0705985275	0.4248235216	0.0505504513	0 0051450457	0 0005154146

TABLE 5, CONTINUED

t_D	$\alpha = 0$	$\alpha^2 = 10^4$	$\alpha^2 = 10^5$	$\alpha^2 = 10^6$	$\alpha^2 = 10^7$	$\alpha^2 = 10^8$
0.40000D 02	0.9793895300	1.0196691366	0.5581597418	0.0716622415	0.0073518380	0.0007370702
0.50000D 02	0.9755425285	0.9947159026	0.6726687250	0.0934[illegible]9859	0.0096732672	0.0009706320
0.60000D 02	0.9718465096	0.9848174782	0.7678804413	0.1157826[illegible]51	0.0120854005	0.0012137518
0.70000D 02	0.9682714291	0.9795922613	0.8448100542	0.13832685[illegible]4	0.0145721176	0.0014648562
0.80000D 02	0.9647962782	0.9752181505	0.9052146[illegible]68	0.1609916905	0.0171217805	0.0017228154
0.90000D 02	0.9614063893	0.9708737291	0.9511738731	0.183670924[illegible]	0.0197255708	0.0019867781
0.10000D 03	0.9580908150	0.9665635697	0.9848386188	0.2062809047	0.0223765606	0.0022560791
0.20000D 03	0.9277433010	0.9316016001	1.0040797[illegible]6[illegible]	0.4182480054	0.0505956957	0.0051588070
0.30000D 03	0.9006483706	0.9033525094	0.9[illegible]69080[illegible]74	0.590756[illegible]672	0.0804773776	0.0083095151
0.40000D 03	0.8756560542	0.8777690733	0.89888052[illegible]9	0.720036[illegible]102	0.1109981202	0.0116172479
0.50000D 03	0.8522542619	0.8540038882	0.8710[illegible]64[illegible]7	0.8102194261	0.1416381645	0.0150379867
0.60000D 03	0.8301484637	0.8316494639	0.8463281344	0.8677978298	0.1720752804	0.0185453760
0.70000D 03	0.8091459223	0.8104635651	0.8232349143	0.899[illegible]62[illegible]417	0.2020884227	0.0221217174
0.80000D 03	0.7891089687	0.7902842034	0.8015232543	0.9117334974	0.2315167013	0.0257542209
0.90000D 03	0.7699336525	0.7709938508	0.7810101677	0.90[illegible]6230296	0.2602386288	0.0294331567
0.10000D 04	0.7515383201	0.7525029567	0.7615340293	0.8975576603	0.2881604085	0.0331508357
0.20000D 04	0.5997885700	0.6002551386	0.604[illegible]443917	0.6681923132	0.5130881017	0.0714494608
0.30000D 04	0.4882414686	0.4885009905	0.4908739160	0.518678[illegible][illegible]79	0.6327883674	0.1100441630
0.40000D 04	0.4029106734	0.4030590793	0.[illegible]044090038	0.4194812793	0.6612853330	0.1475609739
0.50000D 04	0.3361705516	0.3362536322	0.3370067796	0.3452067320	0.6235327193	0.1831858564
0.60000D 04	0.2831655867	0.2832089012	0.2835998990	0.2876584[illegible]51	0.5450850438	0.2163477470
0.70000D 04	0.2405694203	0.2405881449	0.24[illegible]7561424	0.2423229286	0.4478425242	0.2466204373
0.80000D 04	0.2060028972	0.2060065341	0.2060376030	0.2061313504	0.3485067303	0.2736808964
0.90000D 04	0.1777153104	0.1777098129	0.1776583970	0.176906[illegible]575	0.2582809352	0.2972877975
0.10000D 05	0.1543920066	0.1543812219	0.1542823058	0.1530714680	0.1833057040	0.3172691443
0.20000D 05	0.0522818770	0.0522731628	0.052194332[illegible]	0.0513891957	0.0335369286	0.3190583109
0.30000D 05	0.0270293108	0.0270265757	0.027001899[illegible]	0.0267575066	0.0274886325	0.0903431607
0.40000D 05	0.0176547464	0.0176538382	0.0176455789	0.017[illegible]643610	0.0165237652	-0.1091733563
0.50000D 05	0.0130516335	0.0130512741	0.0130479952	0.01301[illegible]6[illegible]68	0.0121828152	-0.1178743800
0.60000D 05	0.0103505939	0.0103504213	0.0103488850	0.0103336705	0.0100136998	-0.0253703940
0.70000D 05	0.0085774984	0.0085774164	0.0085765955	0.0085685414	0.0085102330	0.0387623852
0.80000D 05	0.0073242078	0.0073241620	0.0073236980	0.0073191274	0.0073491486	0.0487070007
0.90000D 05	0.0063911369	0.0063911131	0.0063908294	0.0063881058	0.0064333691	0.0321176409
0.10000D 06	0.0056694455	0.0056694302	0.0056692521	0.0056675785	0.0057046643	0.0134407376

TABLE 6: DIMENSIONLESS LIQUID LEVEL IN THE WELLBORE VERSUS DIMENSIONLESS TIME FOR $C_D = 10^3$ AND s = 0

t_D	$\alpha = 0$	$\alpha^2 = 10^4$	$\alpha^2 = 10^5$	$\alpha^2 = 10^6$	$\alpha^2 = 10^7$	$\alpha^2 = 10^8$
0.10000D-01	-0.9998822531	-0.9999999764	-1.0000000069	-0.9999999895	-1.0000000000	-1.0000000214
0.20000D-01	-0.9998306906	-0.9999999970	-1.0000000081	-1.0000000156	-1.0000000030	-1.0000000126
0.30000D-01	-0.9997900874	-0.9999999872	-1.0000000810	-1.0000000417	-1.0000000390	-1.0000000941
0.40000D-01	-0.9997550843	-0.9999999251	-1.0000000474	-1.0000000618	-1.0000000572	-1.0000001016
0.50000D-01	-0.9997236823	-0.9999998463	-0.9999999508	-1.0000000020	-0.9999999421	-0.9999999861
0.60000D-01	-0.9996948719	-0.9999998107	-0.9999999702	-1.0000000057	-0.9999999311	-0.9999999482
0.70000D-01	-0.9996680165	-0.9999997599	-0.9999999379	-1.0000000079	-1.0000000696	-1.0000000471
0.80000D-01	-0.9996427791	-0.9999996798	-0.9999999667	-1.0000000028	-0.9999999945	-0.9999999942
0.90000D-01	-0.9996187005	-0.9999995440	-0.9999999622	-0.9999999879	-0.9999999370	-0.9999999806
0.10000D 00	-0.9995958091	-0.9999994758	-0.9999999791	-1.0000000064	-0.9999999985	-0.9999999522
0.20000D 00	-0.9994022393	-0.9999979765	-0.9999997785	-0.9999999667	-0.9999999843	-0.9999999756
0.30000D 00	-0.9992440181	-0.9999955277	-0.9999995607	-0.9999999706	-0.9999999900	-1.0000000266
0.40000D 00	-0.9991042536	-0.9999920201	-0.9999991816	-0.9999999155	-0.9999999893	-0.9999999998
0.50000D 00	-0.9989763895	-0.9999875512	-0.9999987382	-0.9999998521	-1.0000000180	-1.0000000238
0.60000D 00	-0.9988572562	-0.9999821749	-0.9999982524	-0.9999998708	-1.0000000822	-1.0000000675
0.70000D 00	-0.9987455669	-0.9999756475	-0.9999975764	-0.9999997660	-1.0000000180	-0.9999999626
0.80000D 00	-0.9986329450	-0.9999683202	-0.9999967444	-0.9999996456	-1.0000000107	-0.9999999359
0.90000D 00	-0.9985156168	-0.9999599946	-0.9999960161	-0.9999995871	-0.9999999251	-0.9999999651
0.10000D 01	-0.9984946648	-0.9999506939	-0.9999949667	-0.9999994980	-0.9999999098	-0.9999999686
(0.20000D 01	-0.9793847897	-0.9998053690	-0.9999800518	-0.9999979857	-0.9999997877	-0.9999999741)
0.30000D 01	-0.9968074801	-0.9995781894	-0.9999552878	-0.9999954776	-0.9999995222	-0.9999999536
0.40000D 01	-0.9961220861	-0.9992729423	-0.9999207709	-0.9999920013	-0.9999992030	-0.9999999207
0.50000D 01	-0.9954803592	-0.9989012606	-0.9998766083	-0.9999875194	-0.9999987560	-0.9999998637
0.60000D 01	-0.9948702892	-0.9984726451	-0.9998229515	-0.9999819992	-0.9999981576	-0.9999998012
0.70000D 01	-0.9942847419	-0.9979961779	-0.9997599311	-0.9999754877	-0.9999974993	-0.9999996842
0.80000D 01	-0.9937191510	-0.9974805642	-0.9996877717	-0.9999680858	-0.9999967831	-0.9999996758
0.90000D 01	-0.9931699389	-0.9969333630	-0.9996064779	-0.9999596158	-0.9999959194	-0.9999995764
0.10000D 02	-0.9926347417	-0.9963617676	-0.9995162194	-0.9999501589	-0.9999949886	-0.9999994782
0.20000D 02	-0.9877777520	-0.9903476753	-0.9981568362	-0.9998016936	-0.9999800370	-0.9999980206
0.30000D 02	-0.9834372644	-0.9851413042	-0.9960747391	-0.9995562373	-0.9999550826	-0.9999955043
0.40000D 02	-0.9793895648	-0.9807727521	-0.9934202001	-0.9992159065	-0.9999201695	-0.9999920204
0.50000D 02	-0.9755425410	-0.9768107970	-0.9903288520	-0.9987828720	-0.9998753661	-0.9999875245
0.60000D 02	-0.9718465952	-0.9730447207	-0.9869182421	-0.9982592441	-0.9998205945	-0.9999819835

TABLE 6, CONTINUED

t_D	$\alpha = 0$	$\alpha^2 = 10^4$	$\alpha^2 = 10^5$	$\alpha^2 = 10^6$	$\alpha^2 = 10^7$	$\alpha^2 = 10^8$
0.70000D 02	-0 9682713724	-0.9694070853	-0.9832870858	-0.9976473926	-0.9997559744	-0.9999754917
0.80000D 02	-0.9647962023	-0.9658746010	-0.9795160402	-0.9963496623	-0.9996815622	-0.9999680147
0.90000D 02	-0.9614063443	-0.9624339332	-0.9756693153	-0.9961682794	-0.9995972312	-0.9999393119
0.10000D 03	-0 9580908493	-0.9590742164	-0.9717970255	-0 9953036889	-0.9995031982	-0 9999500424
0.20000D 03	-0 9277432220	-0.9284739095	-0.9361994127	-0.9827203641	-0.9980297043	-0 9998002910
0.30000D 03	-0 9006483312	-0.9012483144	-0.9069787589	-0.9644616150	-0.9956089970	-0.9995511777
0.40000D 03	-0.8756560542	-0.8761678283	-0.8809878934	-0 9424325108	-0.9922732039	-0.9992027674
0.50000D 03	-0.8522542831	-0.8526995589	-0.8568784579	-0.9181487157	-0.9880563704	-0.9987557030
0.60000D 03	-0 8301485011	-0.8305406175	-0.8342041873	-0.8927587627	-0.9829930637	-0 9982102723
0.70000D 03	-0 8091449336	-0.8094939143	-0.8127309491	-0.8670970756	-0.9771189375	-0 9973668795
0.80000D 03	-0 7891089585	-0.7894192384	-0.7922964736	-0.8417432298	-0.9704697883	-0.9968259507
0.90000D 03	-0 7639336339	-0.7702112922	-0.7727792683	-0.8170776507	-0.9630816909	-0.9959878919
0.10000D 04	-0 7515382891	-0.7517871553	-0.7540851310	-0.7933303004	-0.9549906776	-0 9950531609
0.20000D 04	-0.5997886173	-0.5998660894	-0.6005761383	-0.6096691567	-0.8431787892	-0 9804984092
0.30000D 04	-0.4882414863	-0.4882430192	-0.4882568159	-0.4883469313	-0.6977469405	-0.9568608065
0.40000D 04	-0.4029107335	-0.4028751632	-0.4025511141	-0.3989110866	-0.5451264870	-0.9247614852
0.50000D 04	-0 3361705833	-0.3361174127	-0.3356346917	-0 3303161047	-0.4034414894	-0.8848953000
0.60000D 04	-0 2831656319	-0.2831055804	-0.2825609021	-0.2766398302	-0.2831642514	-0 8380160555
0.70000D 04	-0 2405693782	-0.2405083383	-0.2399551686	-0.2340129943	-0.1887064110	-0 7849222700
0.80000D 04	-0.2060029040	-0.2059440759	-0.2054116541	-0 1997524363	-0.1200875349	-0.7264445669
0.90000D 04	-0.1777153777	-0.1776604442	-0.1771639728	-0 1719350746	-0.0744247942	-0.6634347225
0.10000D 05	-0 1543920048	-0.1543417733	-0.1538878992	-0 1491473760	-0.0472587860	-0.5967570031
0.20000D 05	-0.0522818765	-0.0522673163	-0.0521363579	-0.0508314153	-0.0431740058	0 0911140197
0.30000D 05	-0.0270292801	-0.0270252018	-0.0269885489	-0.0266292126	-0.0243305255	0 4273962656
0.40000D 05	-0.0176547602	-0.0176534072	-0.0176413057	-0 0175226864	-0.0158979611	0.2652499141
0.50000D 05	-0.0130516282	-0.0130510713	-0.0130461982	-0 0129982425	-0.0124615167	-0.0328637563
0.60000D 05	-0 0103506150	-0.0103503429	-0.0103479792	-0.0103250232	-0.0102165171	-0 1753614591
0.70000D 05	-0.0085775234	-0.0085773402	-0.0085761185	-0.0085637179	-0.0085581331	-0 1199122900
0.80000D 05	-0.0073241011	-0.0073240951	-0.0073233737	-0 0073161702	-0.0073180018	-0.0310042138
0.90000D 05	-0.0063911725	-0.0063911007	-0.0063906553	-0.0063862589	-0.0063782332	0.0201691939
0.10000D 06	-0 0056694925	-0.0056694436	-0.0056691684	-0 0056663002	-0.0056505186	0.0322004607
0.20000D 06	-0.0026640770	-0.0026640738	-0.0026640239	-0.0026636966	-0.0026577669	-0 0049332458
0.30000D 06	-0.0017400914	-0.0017401133	-0.0017400976	-0.0017399425	-0.0017387669	-0.0013221145
0.40000D 06	-0.0012916535	-0.0012916763	-0.0012916856	-0 0012915919	-0.0012913163	-0.0011742303

The α values for which the liquid level in the wellbore oscillates depend on the value of the dimensionless wellbore storage constant, C_D, and the skin factor, s.

In order to obtain general limits on the effect of α on the results, solutions for various C_D and s values were obtained. Figures 9 through 15 show the results. α_1 is defined as the value of α below which p_{wD} is essentially the same as the $\alpha = 0$ (inertia-less) case solution when p_{wD} is smaller than 0.9. This means that the effect of α can be neglected for practical purposes if $\alpha < \alpha_1$. α_2 is defined as the value beyond which oscillation of the liquid level in the wellbore occurs. This number α_2 corresponds to the critical damping condition discussed by van der Kamp.[16] "Critical damping" was used here to refer to a condition under which oscillations in liquid level could not happen and just beyond which oscillations in liquid level could happen. A linear relationship between log α_1 and log α_2 versus log C_D was found for the entire range of C_D investigated when s is greater than 5, and for C_D values greater than 10^{-2} when s is smaller than 5. Figures 16 and 17 show the coefficient of these straight lines in the log-log scale for different s values. Figure 18 shows how the actual curves deviate from straight lines for $C_D = 1$ when s is smaller than 5. Then, we conclude that the effect of α on the solution can be estimated from the following:

When $s \geq 5$:

$$\alpha_1 = 1.99\text{x}10^{-2}\ s^{1.25}\ C_D^{\ 1.077\ -\ 0.0385\ \log s} \tag{70}$$

$$\alpha_2 = s^{0.85}\ C_D^{\ 1.077\ -\ 0.0385\ \log s} \tag{71}$$

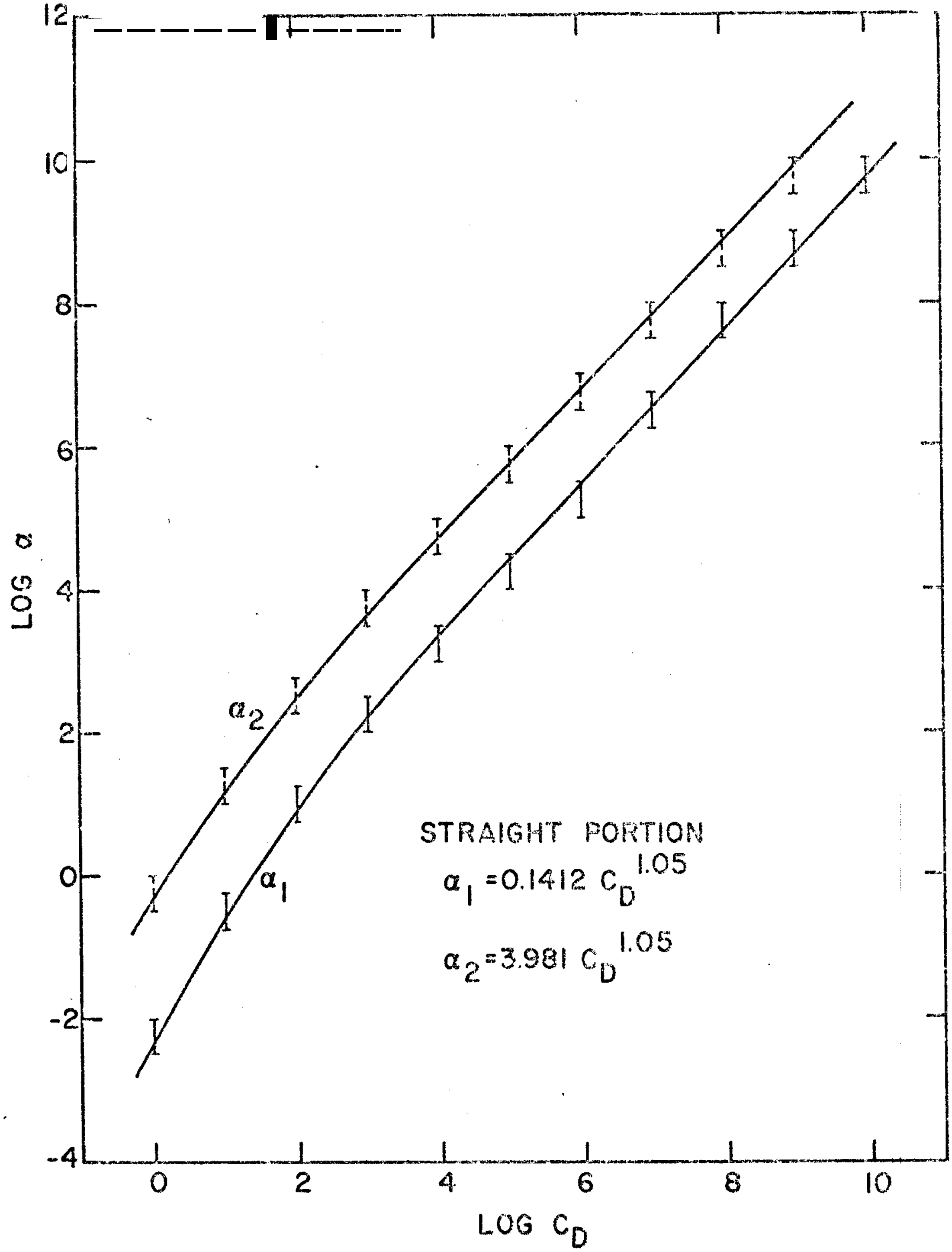

FIG. 9: LOG α_1 AND LOG α_2 VS LOGARITHM OF DIMENSIONLESS WELLBORE STORAGE CONSTANT FOR $s = 0$

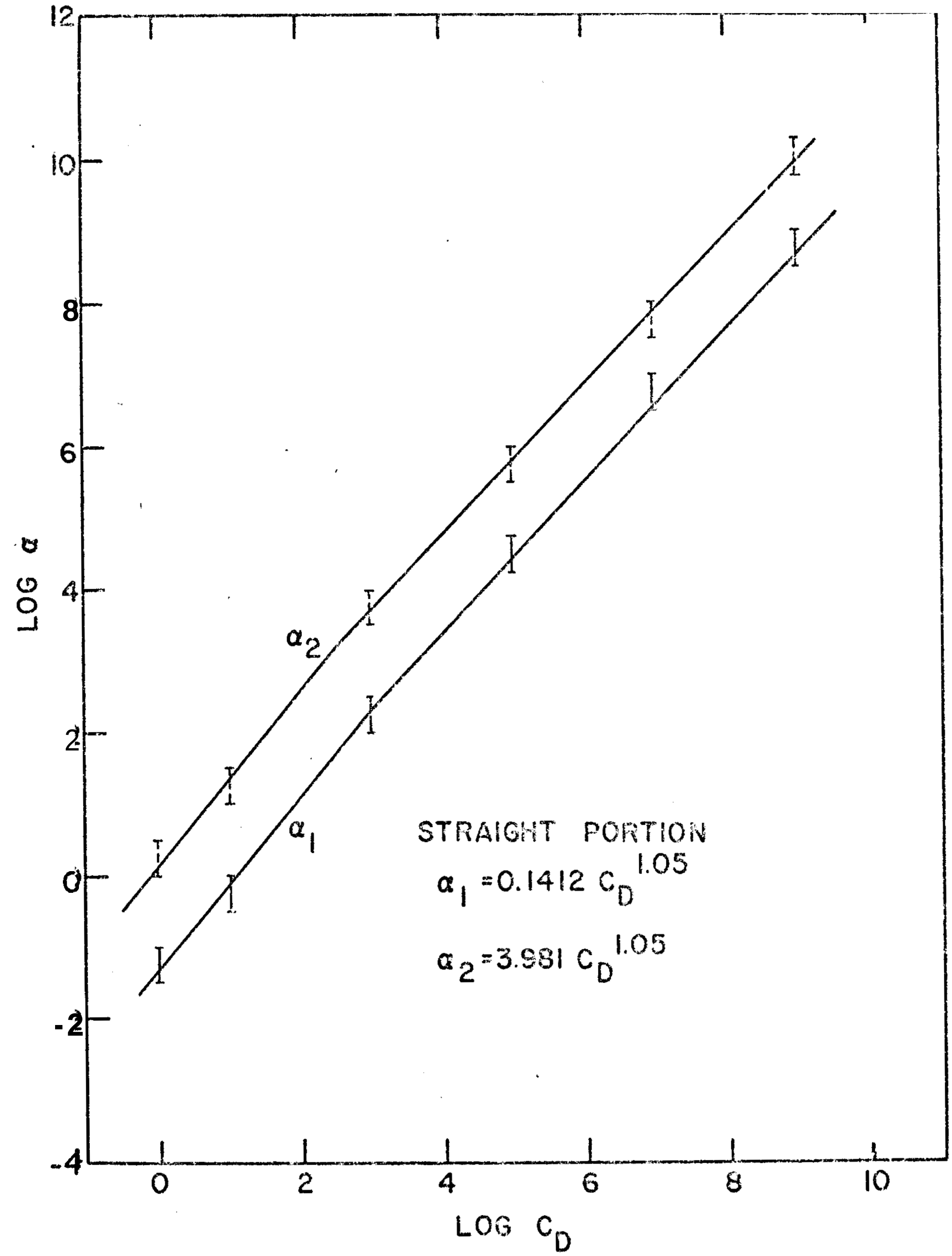

FIG. 10: LOG α_1 AND LOG α_2 VS LOGARITHM OF DIMENSIONLESS WELLBORE STORAGE CONSTANT FOR $s = 1$

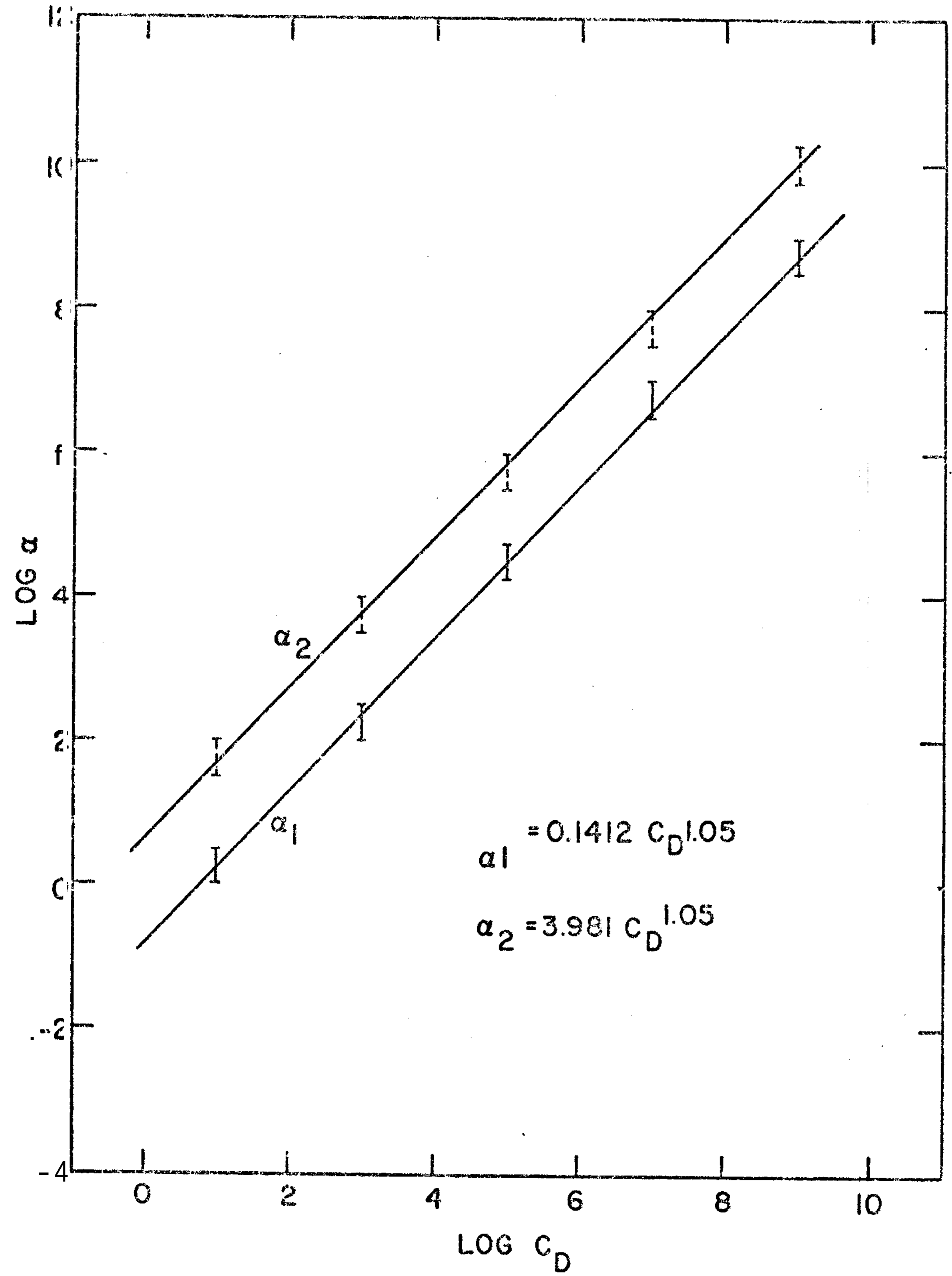

FIG. 11: LOG α_1 **AND** LOG α_2 **VS LOGARITHM OF DIMENSIONLESS WELLBORE STORAGE CONSTANT FOR** $s = 5$

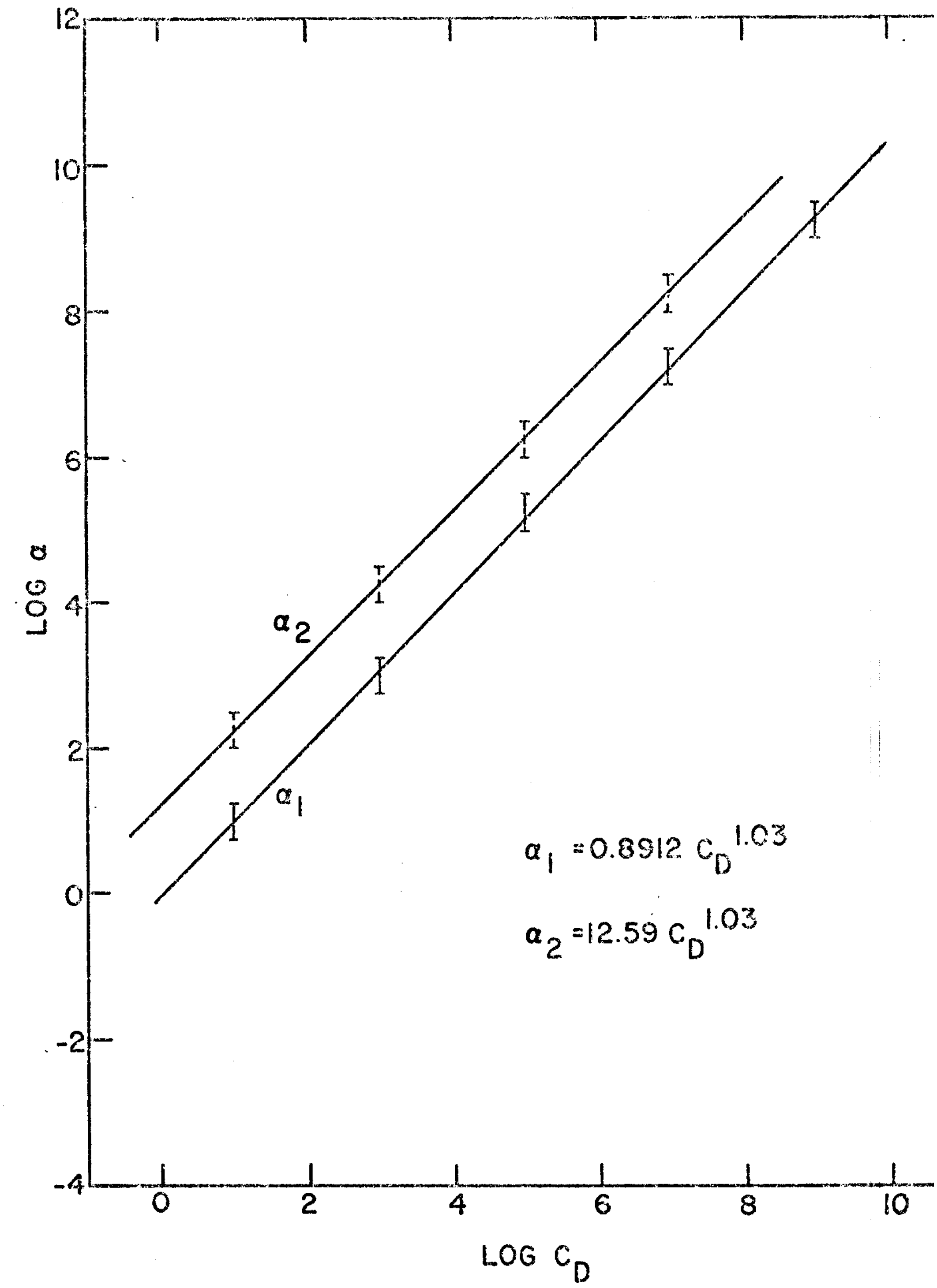

FIG. 12: LOG α_1 AND LOG α_2 VS LOGARITHM OF DIMENSIONLESS WELLBORE STORAGE CONSTANT FOR $s = 20$

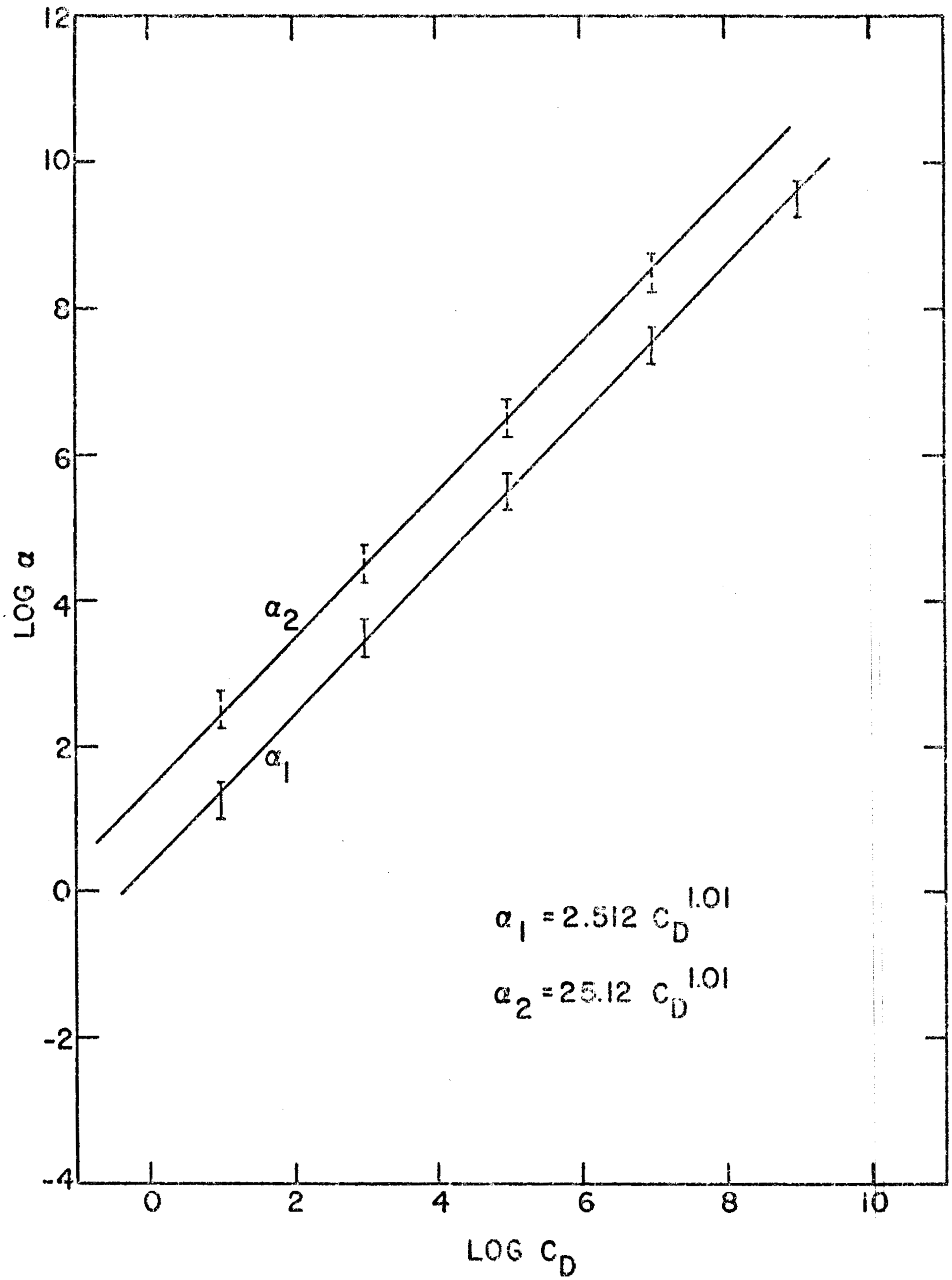

FIG. **13:** LOG α_1 AND LOG α_2 VS LOGARITHM OF DIMENSIONLESS WELLBORE STORAGE CONSTANT FOR $s = 50$

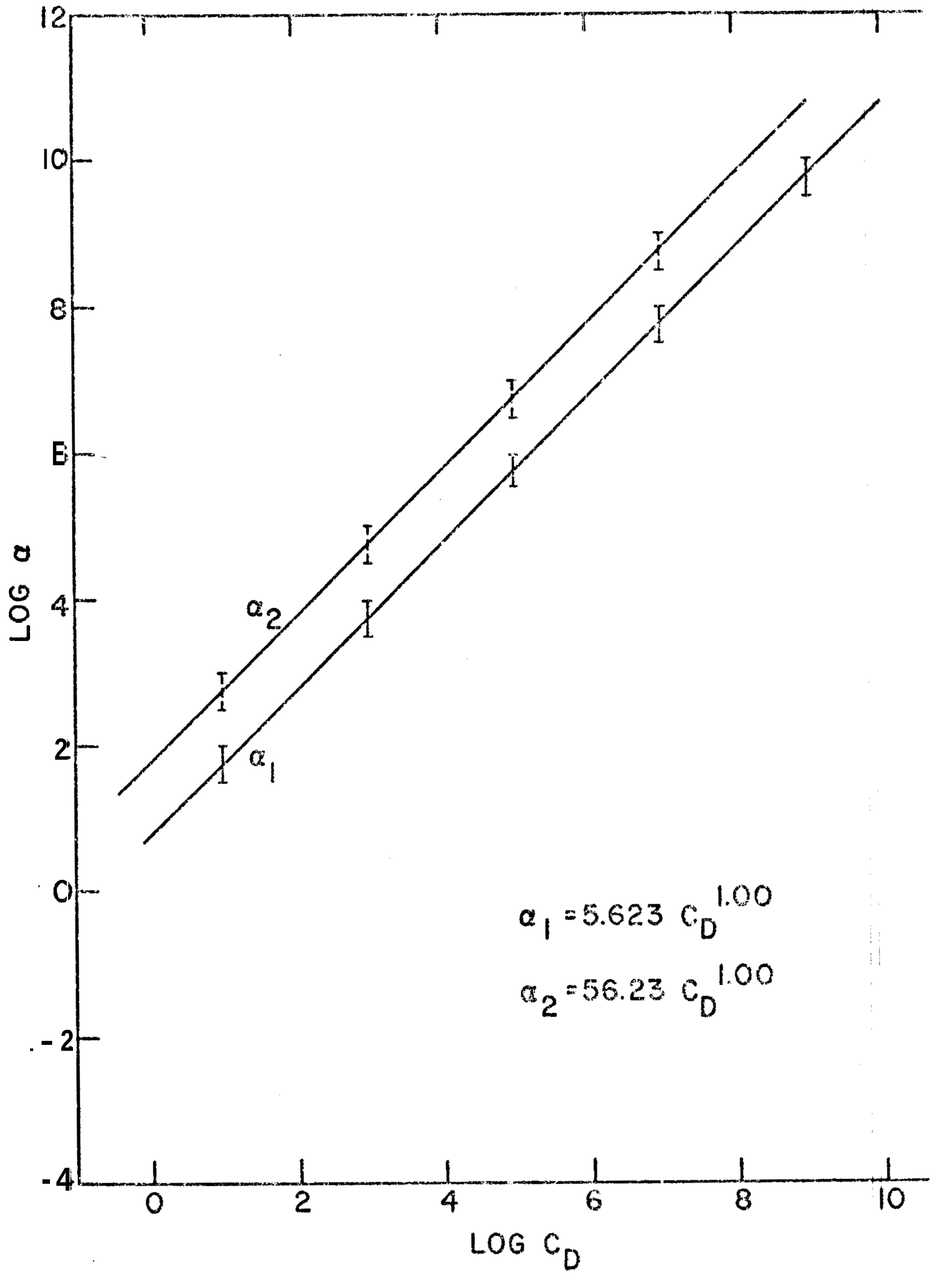

FIG. 14: LOG α_1 AND LOG α_2 VS LOGARITHM OF DIMENSIONLESS WELLBORE STORAGE CONSTANT FOR s = 100

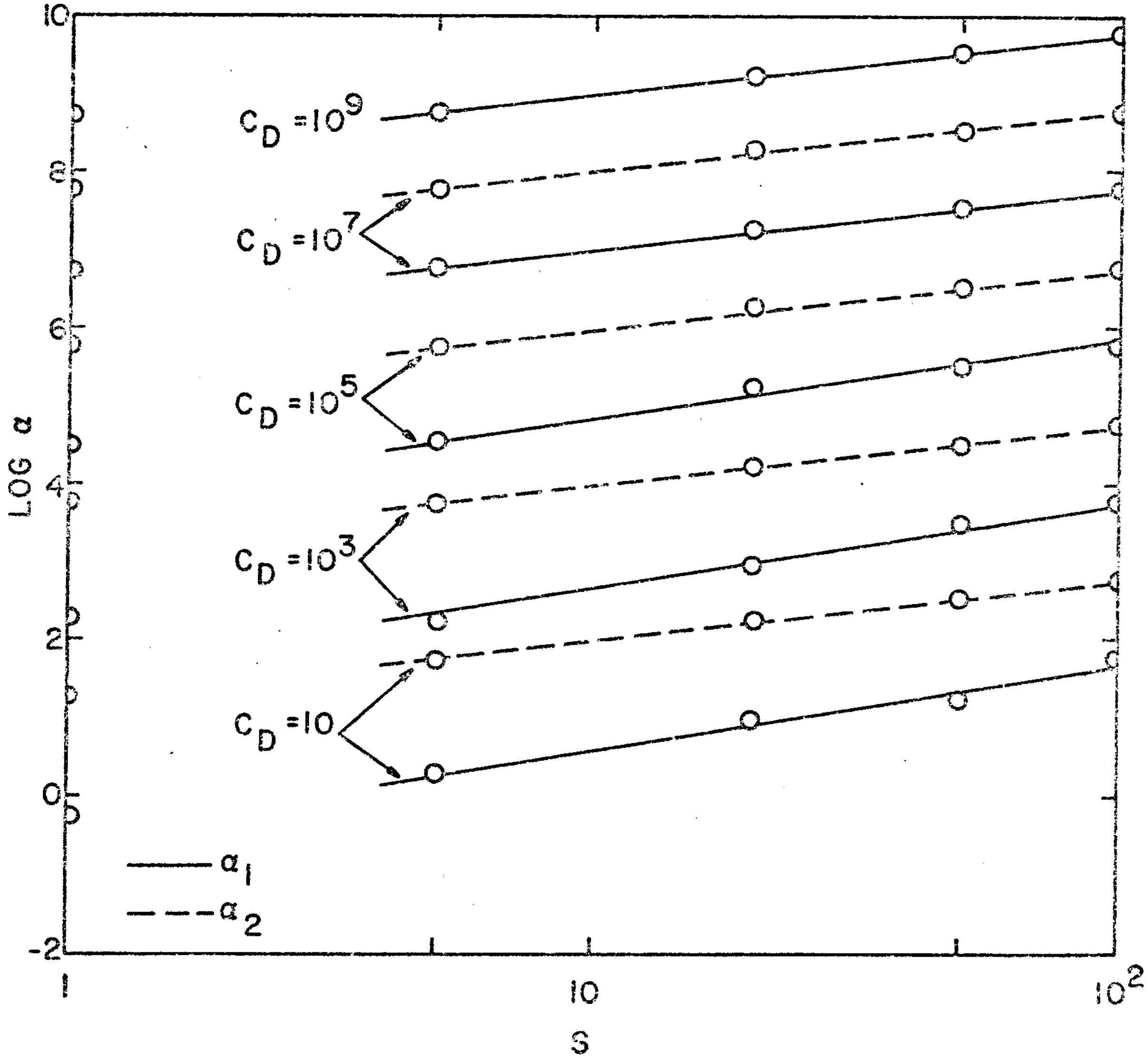

FIG. 15: LOG α_1 AND LOG α_2 VS SKIN FACTOR

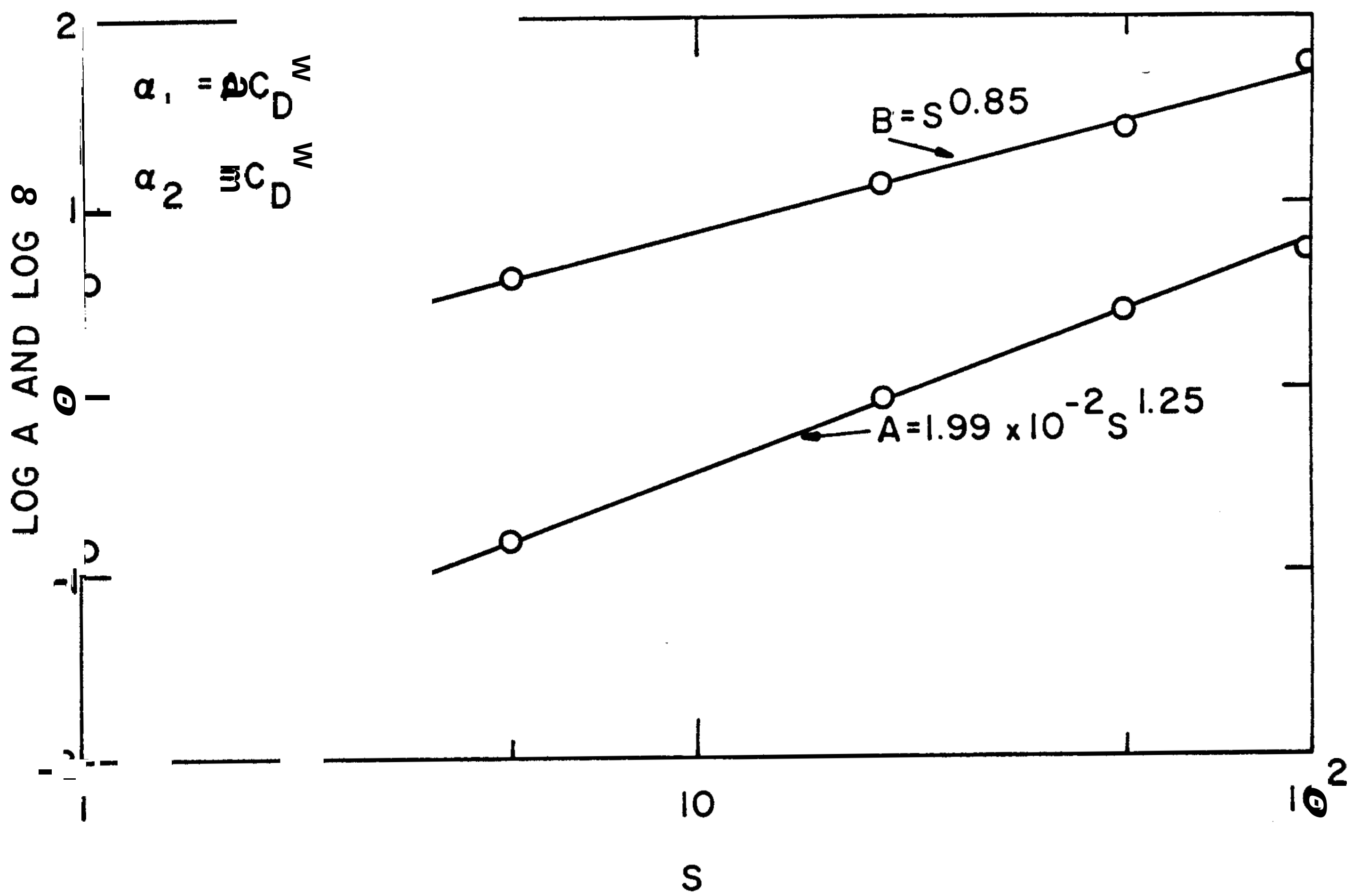

FIG. 16 LOG A AND LOG B VS SKIN FACTOR

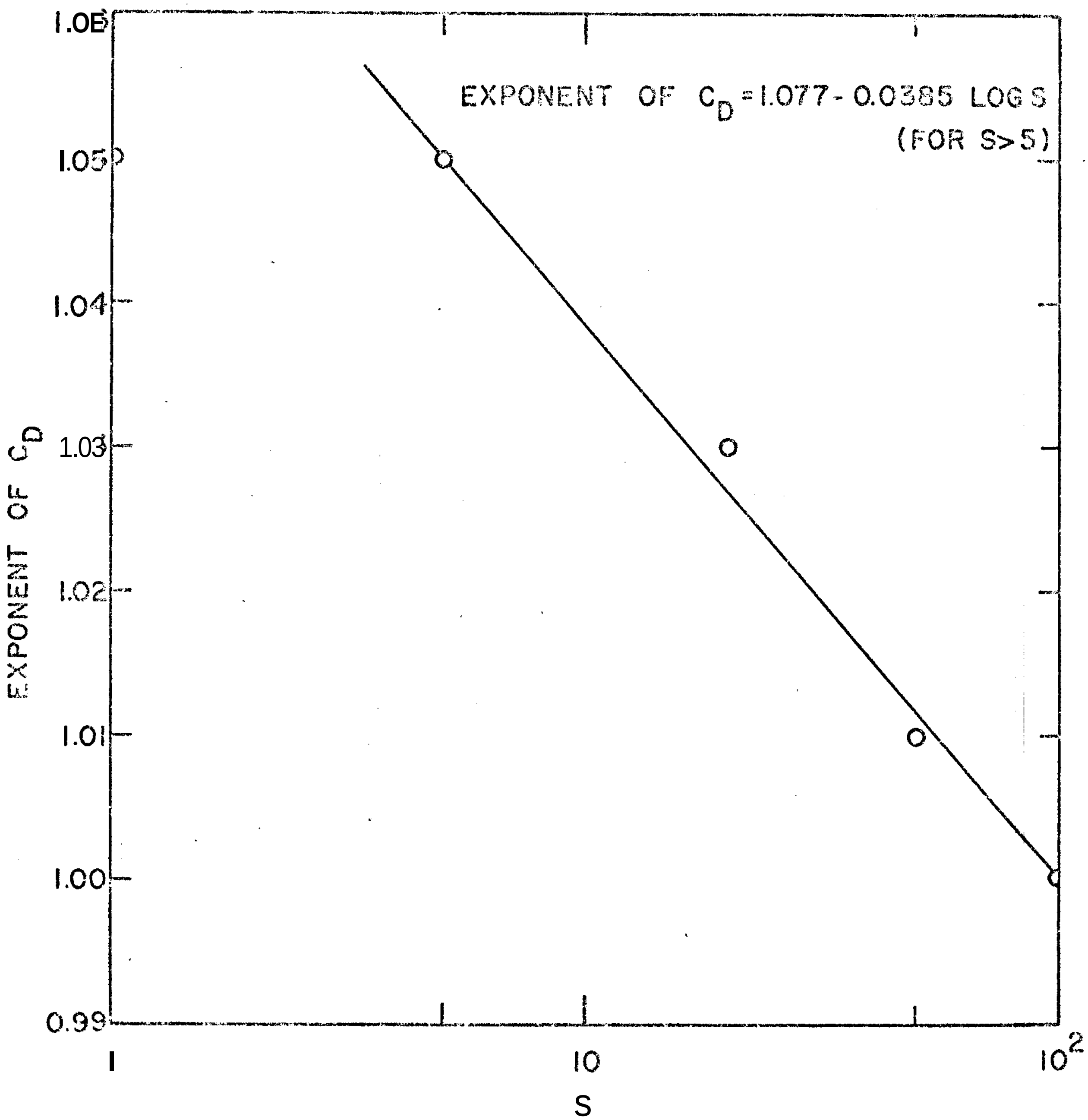

FIG. 17: EXPONENT OF DIMENSIONLESS WELLBORE STORAGE CONSTANT VS SKIN FACTOR

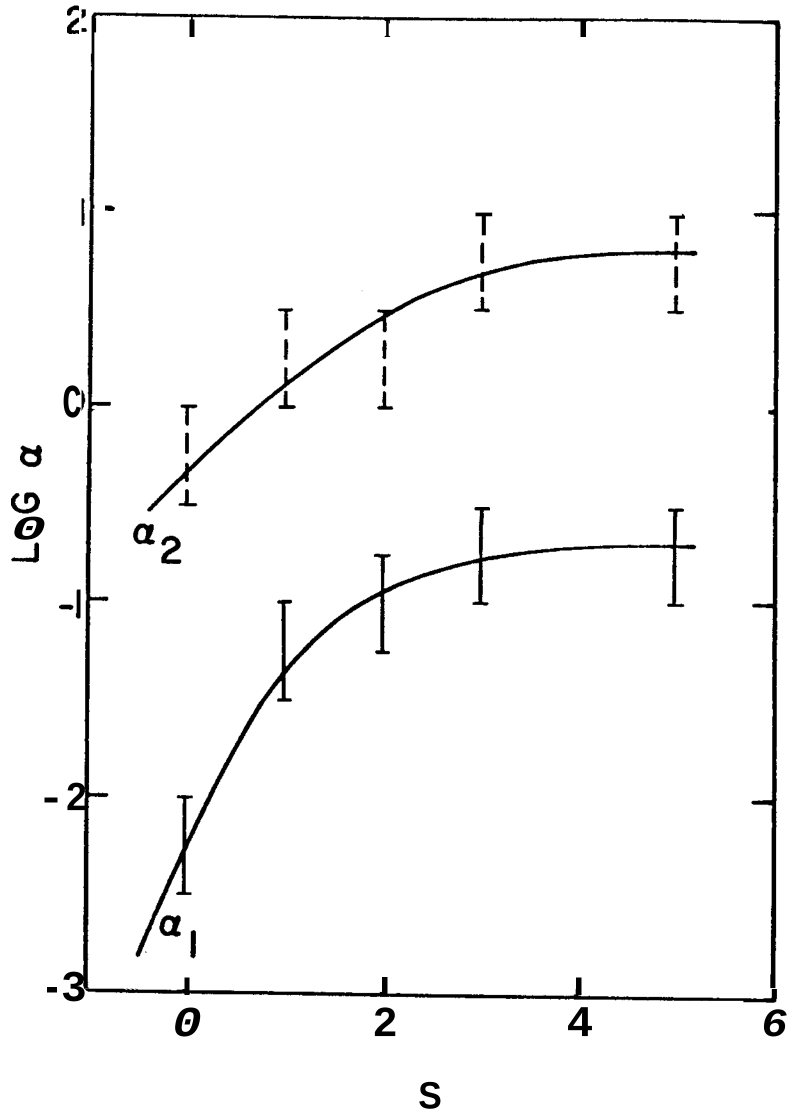

FIG. 18: LOG α_1 AND LOG α_2 VS SKIN FACTOR FOR C_D = 1

When $s < 5$, $C_D \geq 10^3$:

$$\alpha_1 = 0.141\ C_D^{1.05} \tag{72}$$

$$\alpha_2 = 3.98\ C_D^{1.05} \tag{73}$$

When $s < 5$, $C_D < 10^3$: use Figs. 9, 10, and 11.

In van der Kamp's paper,[16] the parameter which controlled the critical damping condition was presented as d.

$$d = \frac{-r_c^2 \left(\frac{g}{L}\right)^{\frac{1}{2}} \ln\left[0.79\ r_f^2 \left(\frac{S}{T}\right)\left(\frac{g}{L}\right)^{\frac{1}{2}}\right]}{8T} \tag{74}$$

This parameter d is expressed as follows in the nomenclature of this study (see the correspondence between the symbols used in petroleum engineering and those used in ground water hydrology in Table 10, Section 2-3-4).

$$d = \frac{C_D \ln\left[\frac{\alpha}{0.79}\right]}{4\alpha} \tag{75}$$

However, the value of d at which critical damping occurs could not be obtained in van der Kamp's analysis and was hypothesized as 0.7. The actual data presented showed d to be between about 0.4 and 1.2. This uncertainty is mainly due to the uncertainty in the value of transmissivity. Since the α_2 value which corresponds to the critical damping condition was obtained in this study, d can be calculated. Often the skin factor is negligible for water wells. Then, d may be obtained using Eq. 73 and Fig. 9. Table 7 shows the results. As a conclusion, critical damping should occur when d is between 0.45 and 0.52 for practical C_D values.

TABLE 7: THE VALUE OF d AT WHICH CRITICAL DAMPING OCCURS

C_D	d
10	0.47
10^2	0.47
10^3	0.46
10^4	0.45
10^5	0.48
10^6	0.51
10^7	0.52

For small α values, there is a time range wherein p_{wD} is greater than 1, as can be seen in Fig. 5. This happens for small α values at early times. This means that the wellbore pressure becomes less than the initial cushion head in the wellbore. This is caused by the increase in kinetic energy of the liquid by rapid movement of the liquid up the wellbore. This overshooting remains about 30% for all small α values studied. However, this phenomenon probably has no useful meaning for field data interpretation because the dimensionless time is usually large even for a minute of real time, and might not be seen in field data because of friction.

2-2-4.2 Effect of C_D on Solutions

Figure 19 shows the dimensionless wellbore pressure, p_{wD}, versus dimensionless time, t_D, and Fig. 20 shows the dimensionless liquid level, x_D, versus t_D for three different values of dimensionless wellbore storage constant, C_D, when the skin factor, s, is zero. When C_D increases, the corresponding solution shifts toward smaller t_D for the same α value. The increase in C_D decreases the effect of α. This phenomenon agrees with Eqs. 70 and 72. On the other hand, the solution for $\alpha = 0$ shifts toward increasing t_D when C_D increases. This is because the liquid takes a longer time to occupy the larger wellbore. Then, it can be said that the greater C_D is, for a wide range of α, the less important will be the inertial effect for the liquid in the wellbore. At a glance, this statement appears strange. However, it is true.

In order to evaluate the shift toward increasing t_D for $\alpha = 0$ solutions, the solutions for various C_D and s values were obtained. Figure 21 shows the dimensionless time, t_{D_1}, at which p_{wD} becomes 0.9. We

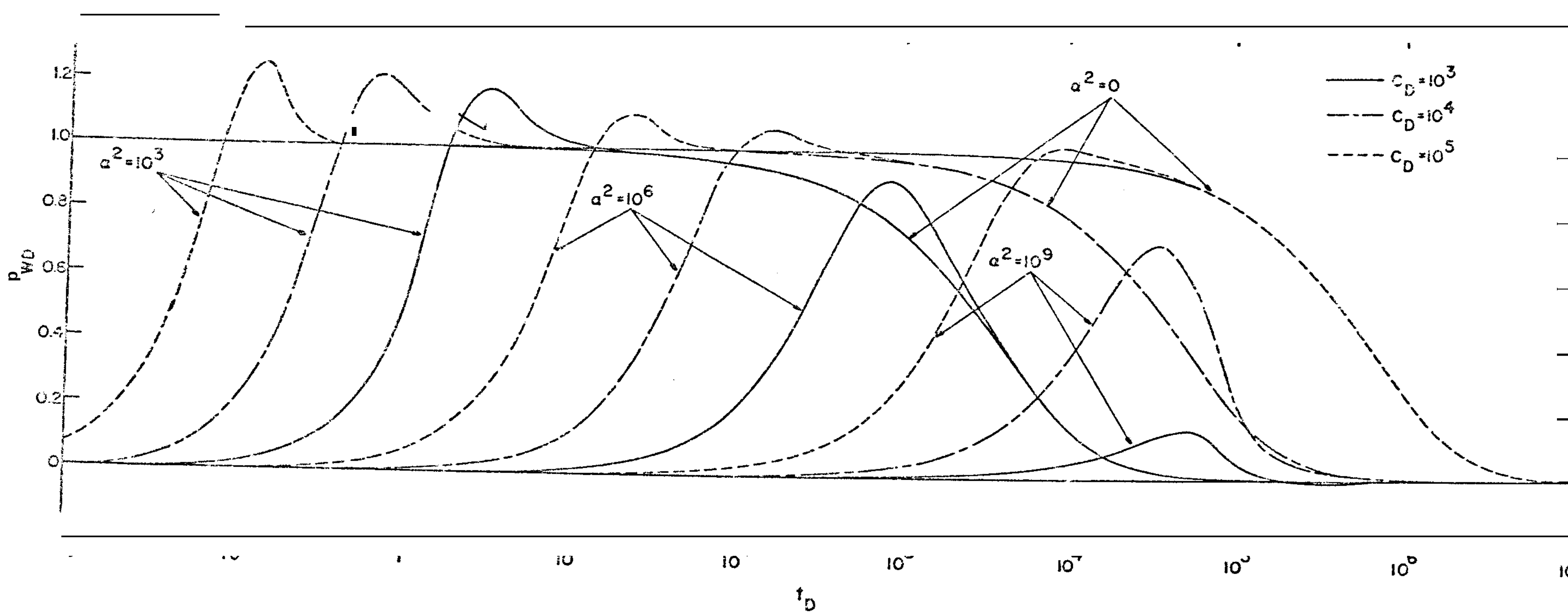

FIG. 19: EFFECT OF DIMENSIONLESS WELLBORE STORAGE CONSTANT ON DIMENSIONLESS WELLBORE PRESSURE FOR s = 0

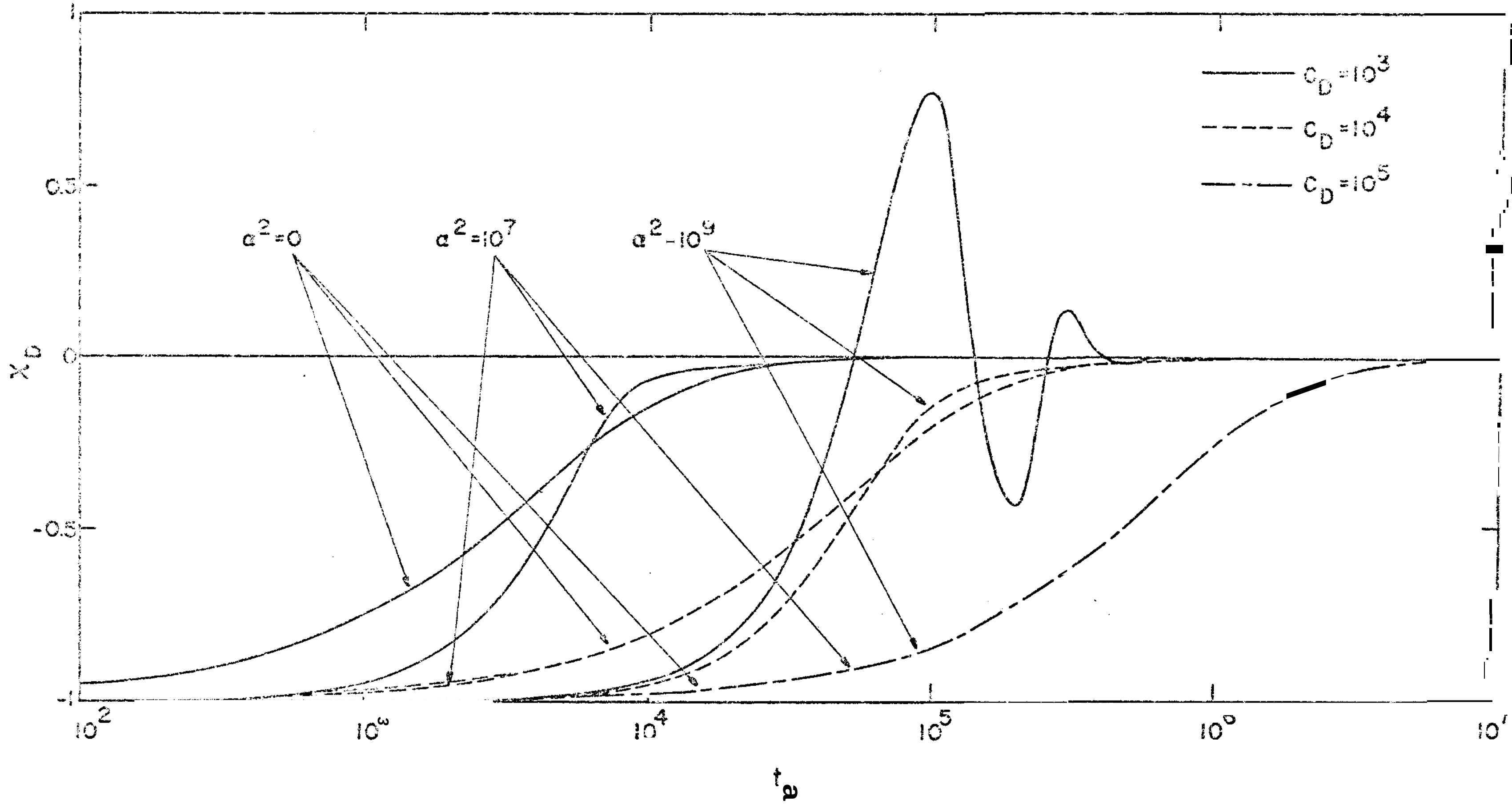

FIG. 20: EFFECT OF DIMENSIONLESS WELLBORE STORAGE CONSTANT ON DIMENSIONLESS LIQUID LEVEL IN THE WELLBORE FOR s = 0

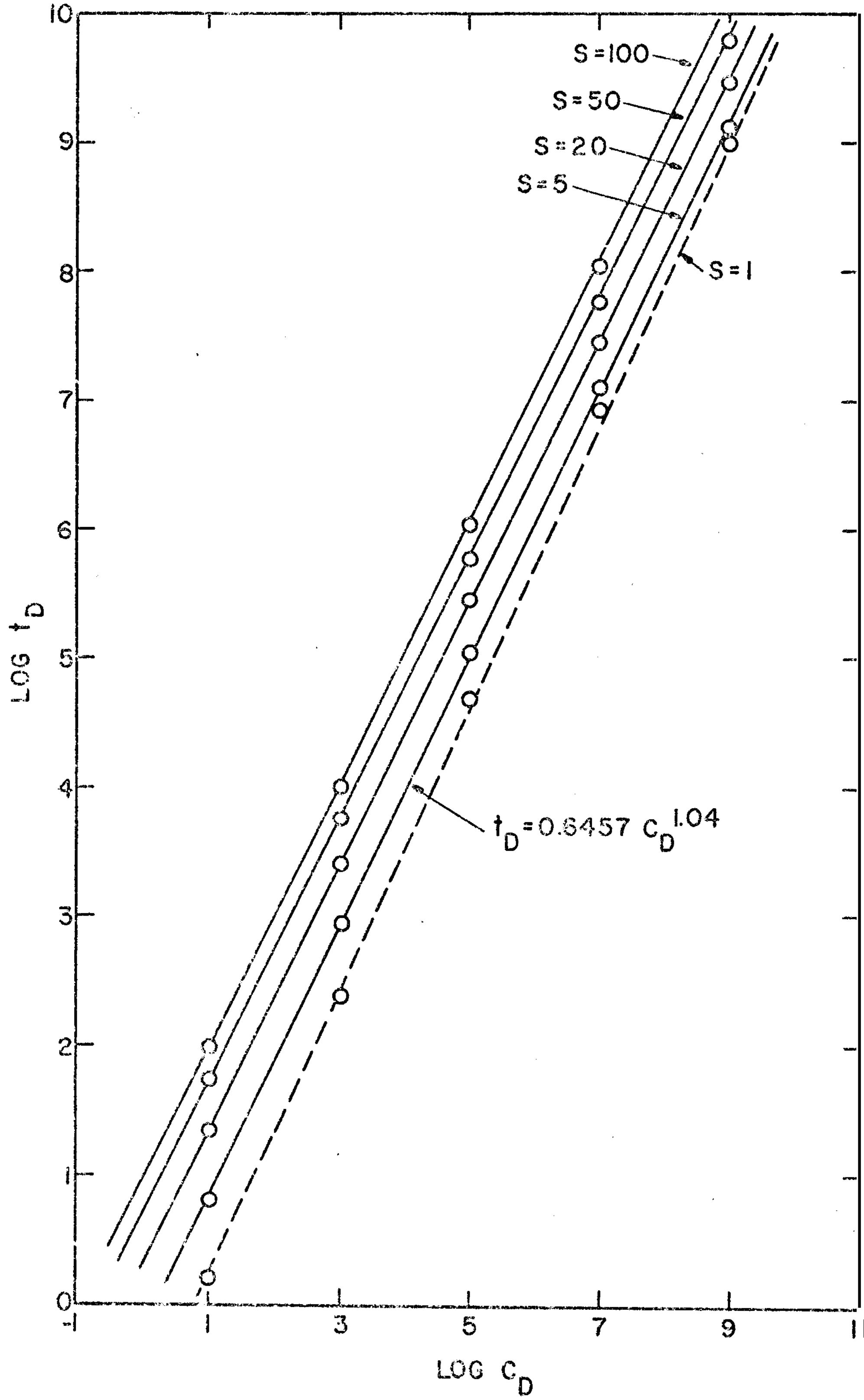

FIG. 21: LOG t_{D_1} VS LOGARITHM OF DIMENSIONLESS WELLBORE STORAGE CONSTANT

can say these lines are approximately parallel for $s \geq 5$. Figure 22 presents the logarithm of t_{D_1} versus s when $C_D = 10^3$. We obtain an exact straight line for $s > 5$. As a result, the following relation was obtained:

When $s \geq 5$:

$$t_{D_1} = 0.17 \; s^{0.83} \; C_D^{\;1.04} \tag{76}$$

When $s < 5$, it is necessary to obtain a solution for each case.

The a value, which is necessary for oscillations in liquid level, increases with increasing C_D as seen in Fig. 20. This phenomenon agrees with Eqs. 71 and 73. This means that when the C_D value is large, oscillation of the liquid level in the wellbore will not happen easily.

2-2-4.3 Effect of s on Solutions

Figure 23 shows the dimensionless wellbore pressure, p_{wD}, versus the dimensionless time, t_D, and Fig. 24 shows the dimensionless liquid level, x_D, versus t_D for three different values of skin factor, s. When the skin factor increases, the solution for a given value of a shifts toward smaller times. An increased skin factor decreases the effect of *a*. This phenomenon agrees with Eqs. 70 and 73. On the other hand, the solution for $a = 0$ shifts toward increased time when the skin factor increases. This agrees with Eq. 73. This is because it is more difficult for the liquid to flow into the wellbore because of the skin effect. Then, similarly to the effect of C_D, it can be said that the greater the skin factor, for a wide range of a values, the less the inertial effect of the liquid moving in the wellbore.

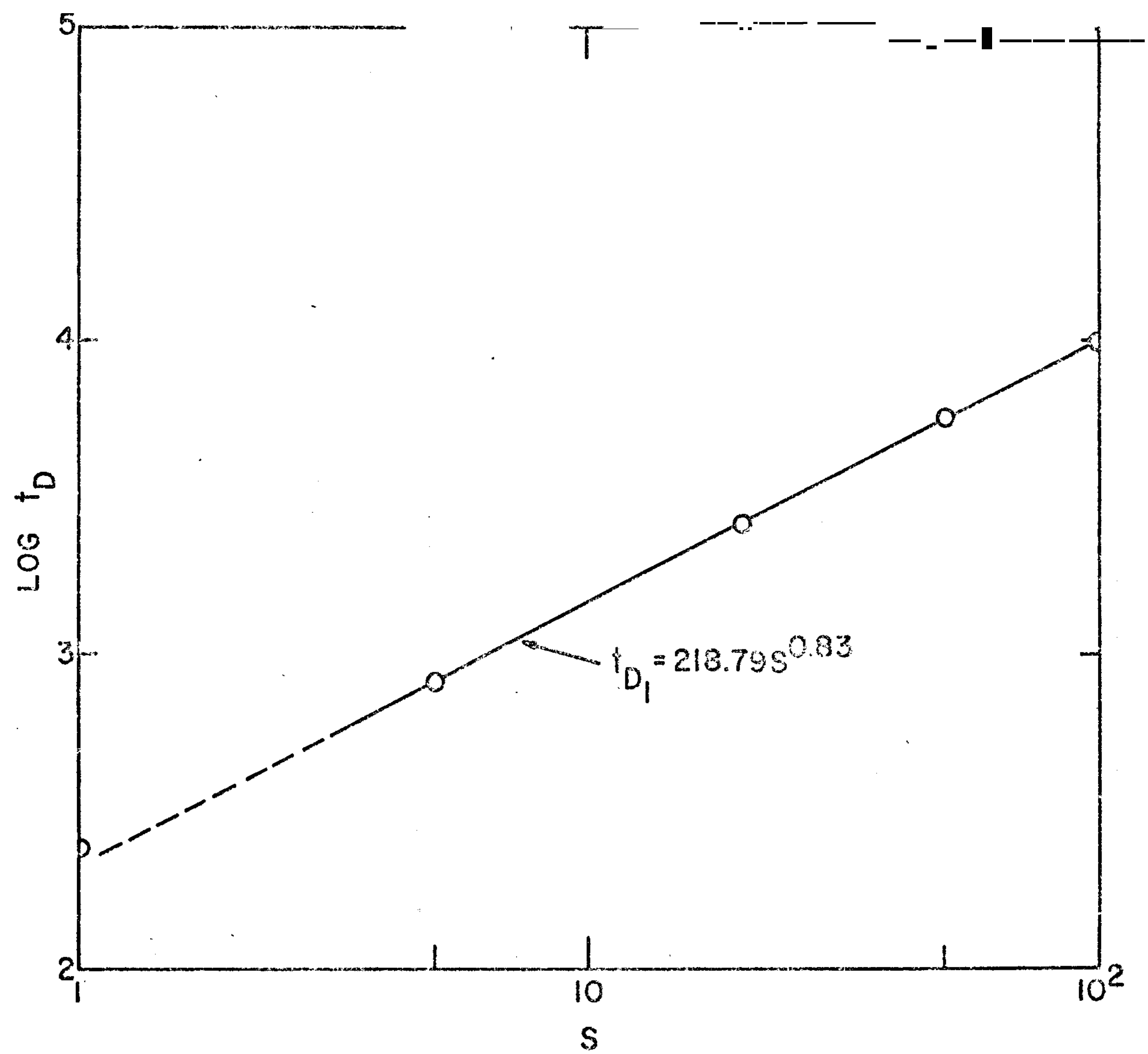

FIG. 22: LOG t_{D_1} VS SKIN FACTOR FOR $C_D = 10^3$

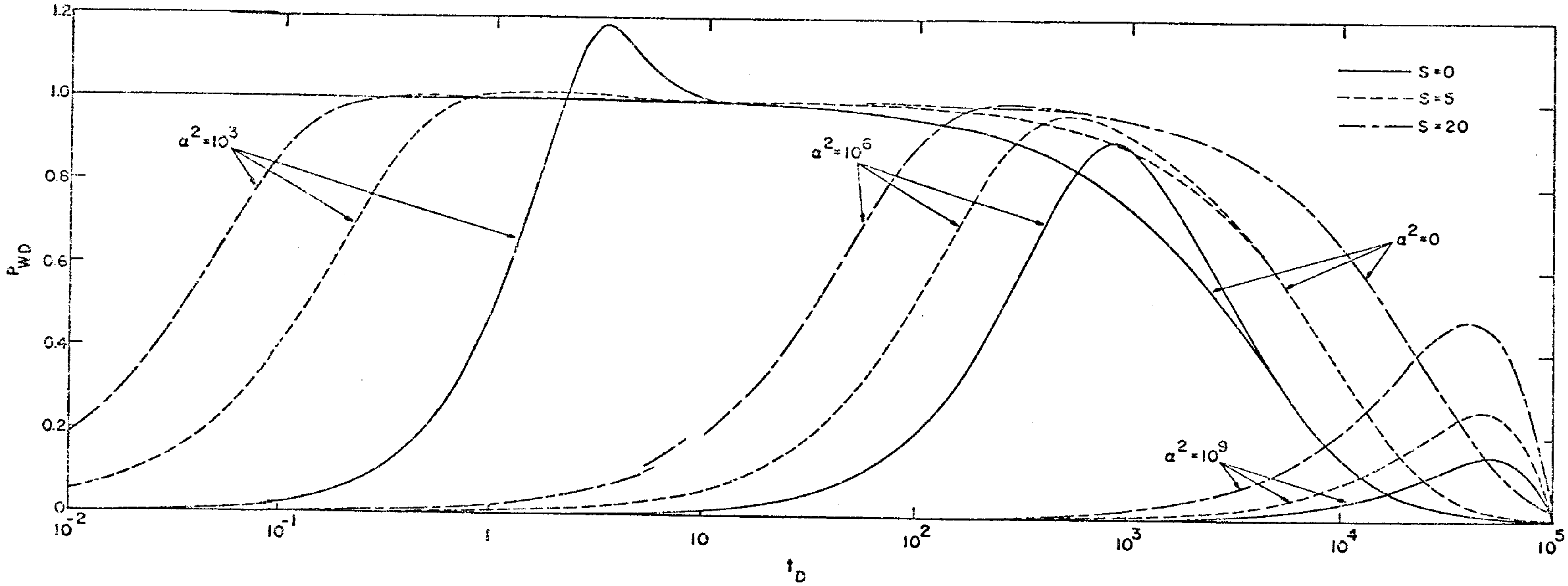

FIG. 23: EFFECT OF SKIN FACTOR ON DIMENSIONLESS WELLBORE PRESSURE FOR $<_D = 10^3$

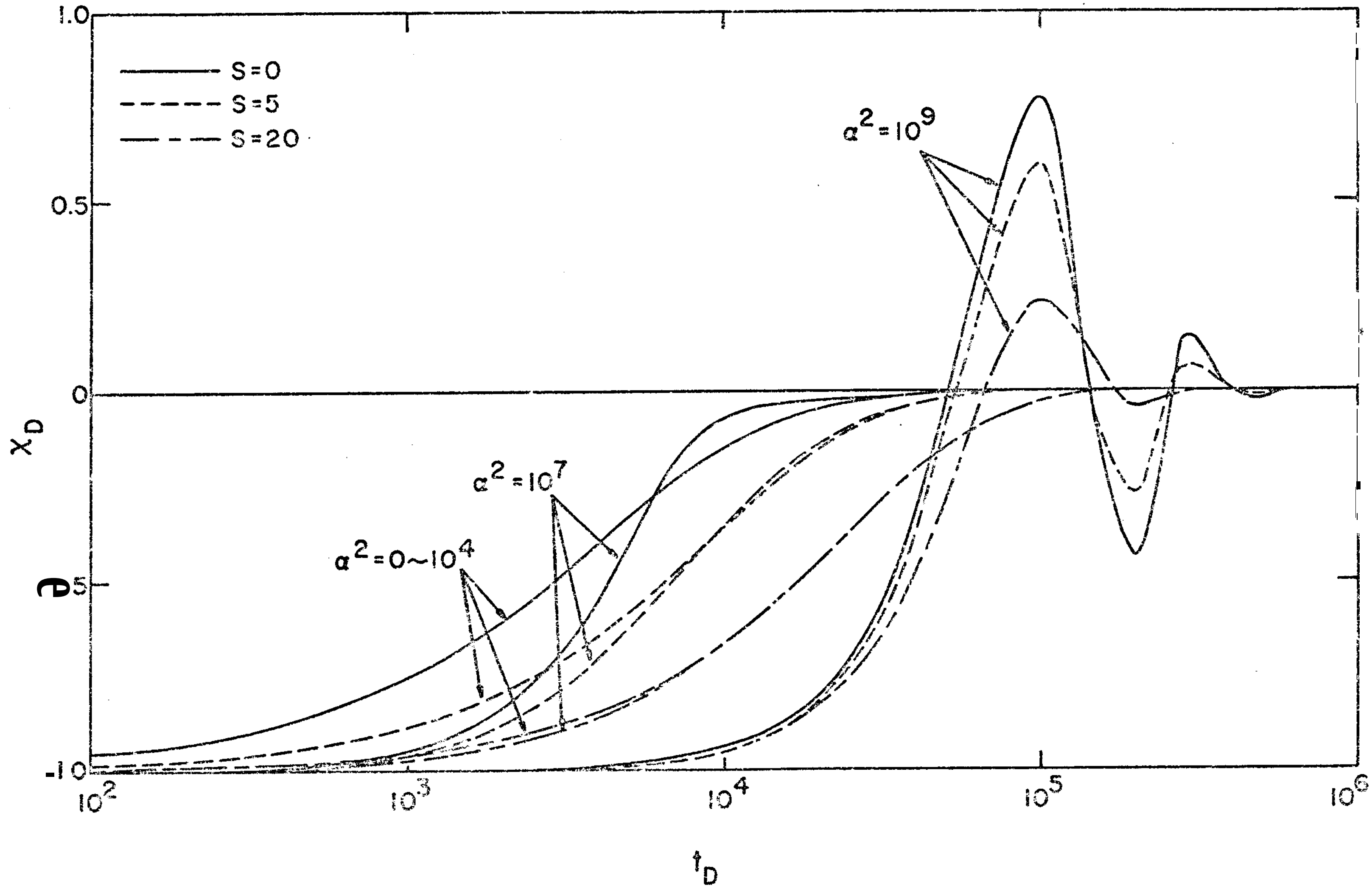

FIG. 24: EFFECT OF SKIN FACTOR ON DIMENSIONLESS LIQUID LEVEL IN THE WELLBORE FOR $C_D = 10^3$

Equation 76, reported in the previous section, shows how far the solutions shift, depending on the s values generally.

The overshooting of p_{wD} at early times for small α values decreases with increasing skin factor, s. This is because the liquid cannot flow into the wellbore freely because of the flow resistance caused by the skin factor, and cannot permit the liquid column in the wellbore to accelerate sufficiently to induce the overshooting.

For a negative skin factor or a fractured well, the opposite effect would be expected. But for negative values of the skin factor, the solution diverges in some cases. This may be caused by the definition of the steady-state skin factor (i.e., a sudden increase of pressure at the sandface for a negative skin factor). In order to avoid this problem, we can use the effective wellbore radius, $r_w' = r_w e^{-s}$, instead of the actual wellbore radius, r_w, as an approximation. Using this effective wellbore radius, C_D and α will be replaced by $C_D e^{2s}$ and αe^{2s}, respectively. Then, the values of α_1 and α_2 in Eqs. 72 and 73 will be multiplied by $e^{0.1s}$ when $C_D e^{2s}$ is greater than 10^3. A negative skin factor gives smaller values of α_1 and α_2 because of this multiplication. This means that a negative skin factor increases the inertial effect of the liquid in the wellbore on slug test solutions. If $C_D e^{2s}$ is less than 10^3, this tendency is more obvious from the characteristics of the curves in Fig. 18.

Another interesting result concerns an apparent constant flowrate phenomenon at early times in many drill stem tests. This phenomenon in DST flow period data has been discussed by several investigators.[13,33] It was suggested that critical flow choking might be the cause of this phenomenon. This explanation was also given in the Earlougher monograph.[14] Critical flow choking can happen for multiphase gas-liquid flow. Critical choking is not likely if only liquid flows, or if there is no orifice in the system. However, the same apparent constant flowrate phenomenon at early times is often observed for liquid flow. Judging from the solutions obtained in this study, a large skin factor may be one explanation of this phenomenon. Figure 25 shows a linear relation between the dimensionless wellbore pressure, p_{wD}, and the dimensionless time, t_D, at early times for a large skin factor case (s = 100). Since $p_W = p_i - p_{wD} \{ p_i - (p_o + p_{atm})\}$, this solution means a linear relationship between the wellbore pressure, p_w, and the time, t, for t_D from 0 to 10^4. This linearity would appear to be a constant flowrate period. The reason why the large skin factor might be a cause of this phenomenon is that the reservoir liquid cannot flow into the wellbore rapidly because of the large skin factor (i.e., the pressure drop occurs mainly at the sandface), then the back pressure caused by the accumulated liquid in the wellbore is relatively negligible compared to the pressure inside the formation, and the pressure gradient inside the formation remains almost constant for a time.

For the same reason, we can expect that this phenomenon happens for a large wellbore storage case because the fluid head in the wellbore does not increase as rapidly if the wellbore storage is large. Theoretically, this is true. Figure 26 shows the dimensionless wellbore pressure, p_{wD}, versus the dimensionless time, t_D, for the case when $C_D = 10^{30}$. A definitely straight portion of the solution can be seen at early times. However, such a large wellbore storage constant is impractical. For feasible dimensionless wellbore storage constants, C_D of $10^2 \sim 10^6$, this phenomenon cannot be seen. Figures 27 and 28 show the dimensionless wellbore pressure, p_{wD}, versus dimensionless time, t_D, for the cases when $C_D = 10^3$ and $C_D = 10^5$, respectively. There is no evident linear portion of the solutions for these cases.

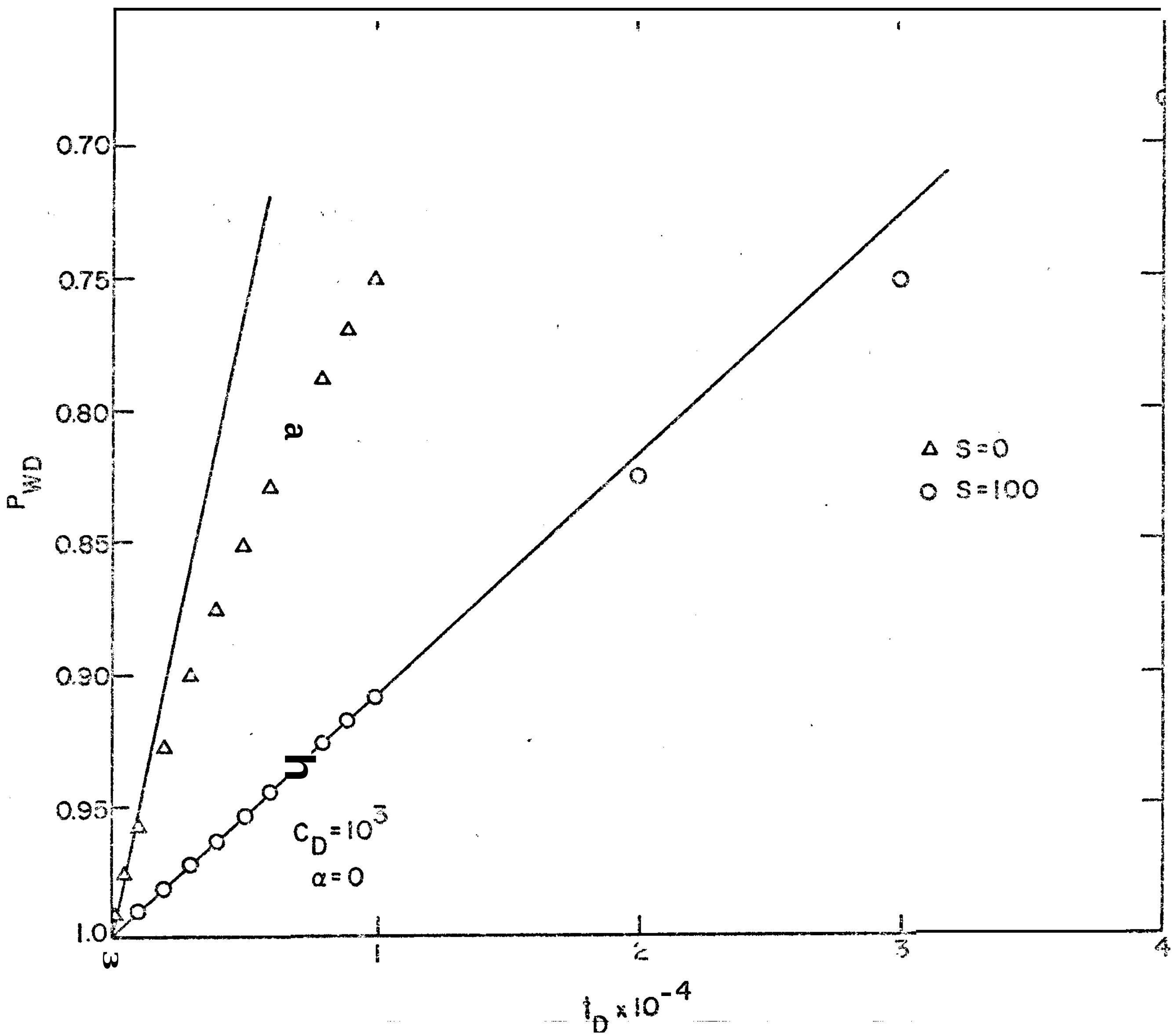

FIG. 25: DIMENSIONLESS WELLBORE PRESSURE VS DIMENSIONLESS TIME FOR A LARGE SKIN FACTOR (s = 100)

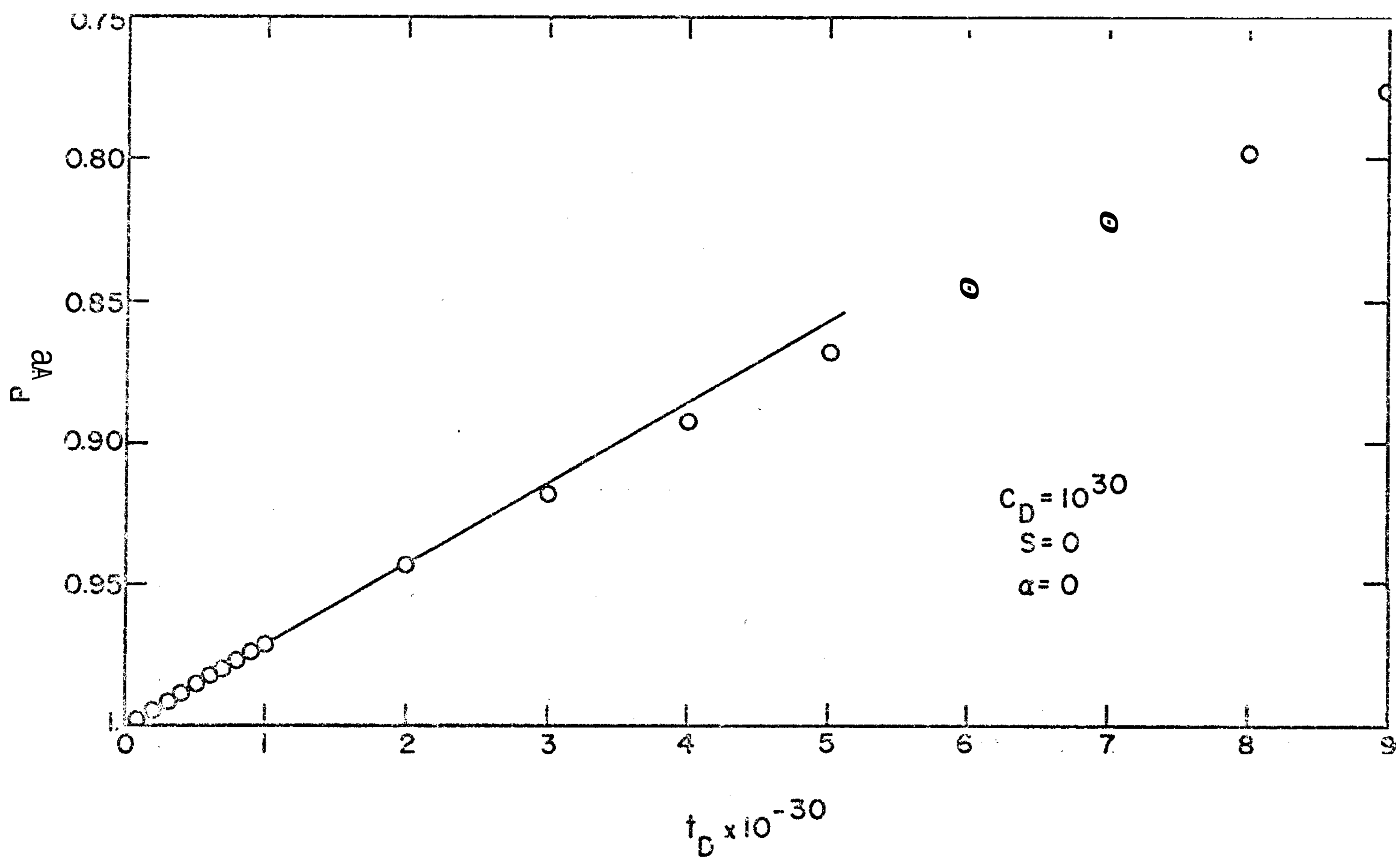

FIG 26: DIMENSIONLESS WELLBORE PRESSURE VS DIMENSIONLESS TIME FOR A LARGE DIMENSIONLESS WELLBORE STORAGE CONSTANT ($C_D = 10^{30}$)

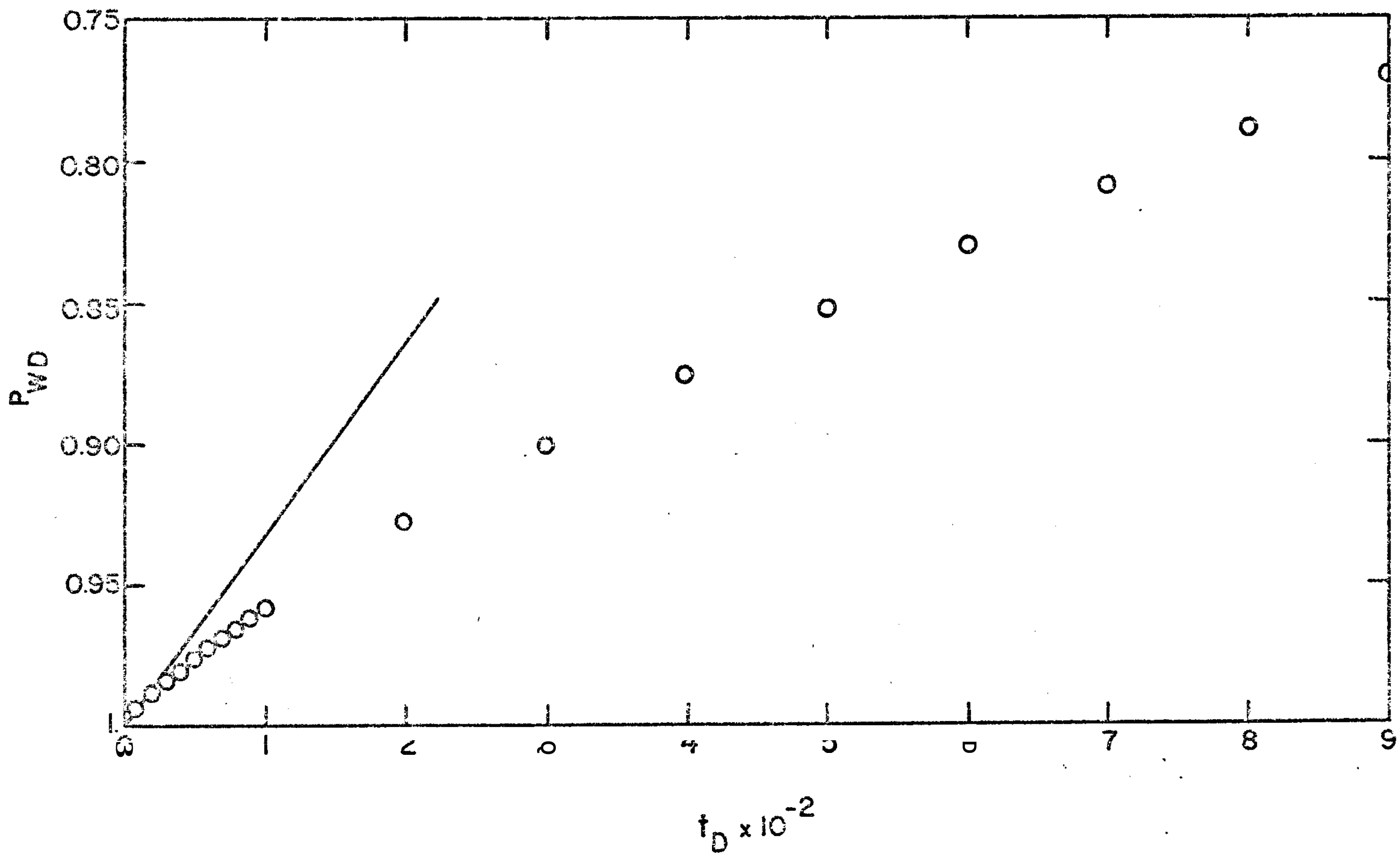

FIG. 27: DIMENSIONLESS WELLBORE PRESSURE VS DIMENSIONLESS TIME FOR $C_D = 10^3$ AND $s = \alpha = 0$ AT EARLY TIMES

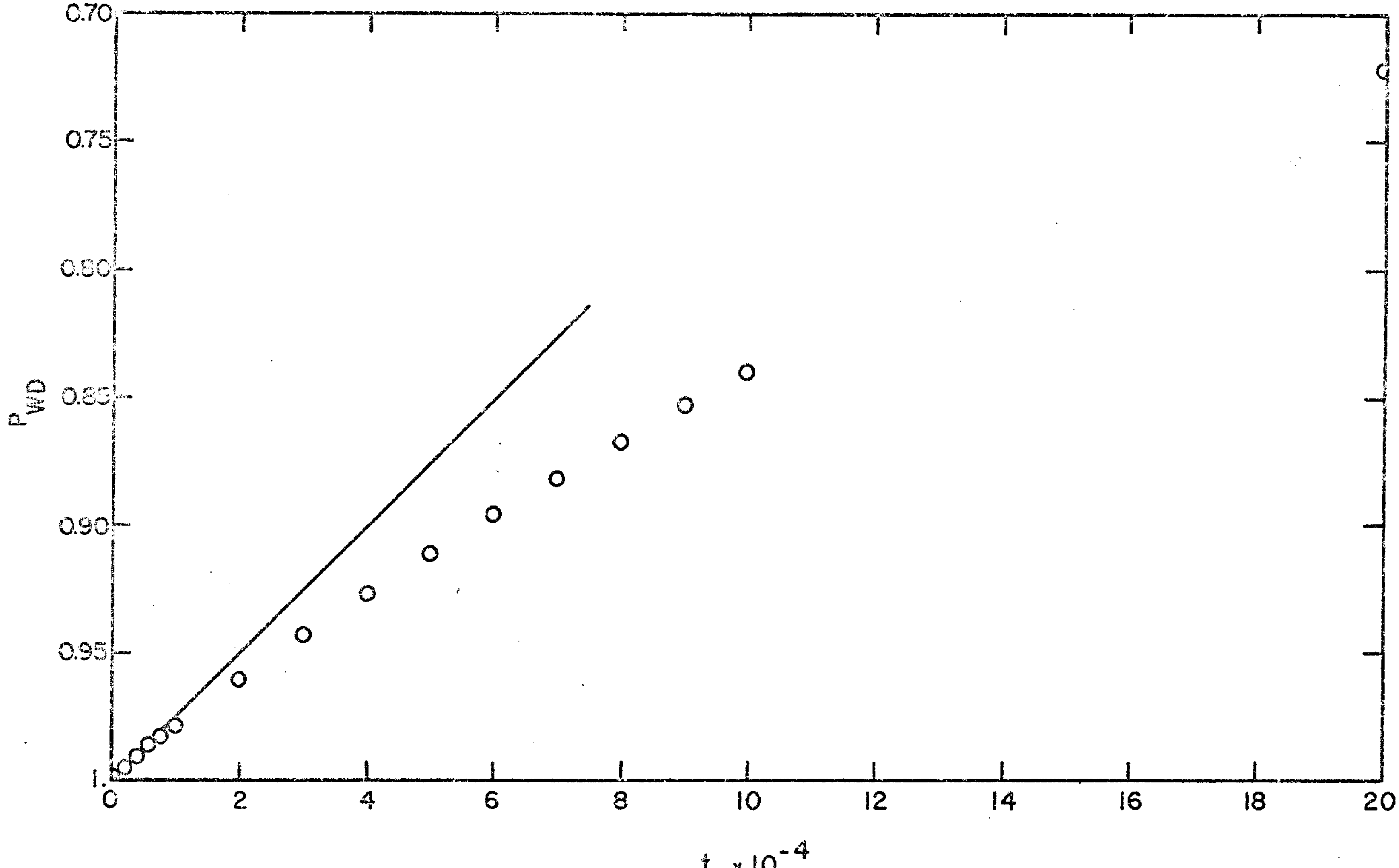

FIG 28: DIMENSIONLESS WELLBORE PRESSURE VS DIMENSIONLESS TIME FOR $C_D = 10^5$ AND $s = \alpha = 0$ AT EARLY TIMES

One more cause of apparent constant flowrates is the inertial effect of the liquid in the wellbore. Figure 29 shows the dimensionless wellbore pressure, p_{wD}, versus dimensionless time, t_D, for the case when $C_D = 10^3$, $s = 0$, and $\alpha^2 = 10^7$. A straight portion of the solution can be seen for t_D values from $6x10^3$ to $8.4x10^3$. However, the straight portion does not start from the zero time, and it does not continue for a long time. Therefore, although this may happen, we infer that this is not the main explanation for the apparent constant flowrate phenomenon at early times.

2-2-4.4 Radius of Investigation

The pressure distribution inside the reservoir for slug tests can be calculated by obtaining the real space solution of Eq. 42 for various parameter values. Figure 30 shows the pressure distribution inside the reservoir for a simple example case when $C_D = 10^3$ and $s = \alpha = 0$ at various times. The pressure gradient with respect to radial distance reaches a maximum value shortly after start of production and then the pressure gradient decreases gradually with time (i.e., the flowrate decreases) and the investigation radius increases with time. A graph of pressure versus radius is linear in the reservoir close to the well; however, far from the well pressure versus radius is convex to the coardinate of radial distance for early times. The graph of pressure versus radius becomes concave to the radial coordinate after the flowrate starts decreasing.

In order to investigate the effect of a on the pressure distribution inside the reservoir, the case of $C_D = 10^3$ and $s = 0$ was selected as a typical example, and the pressure distribution inside the reservoir

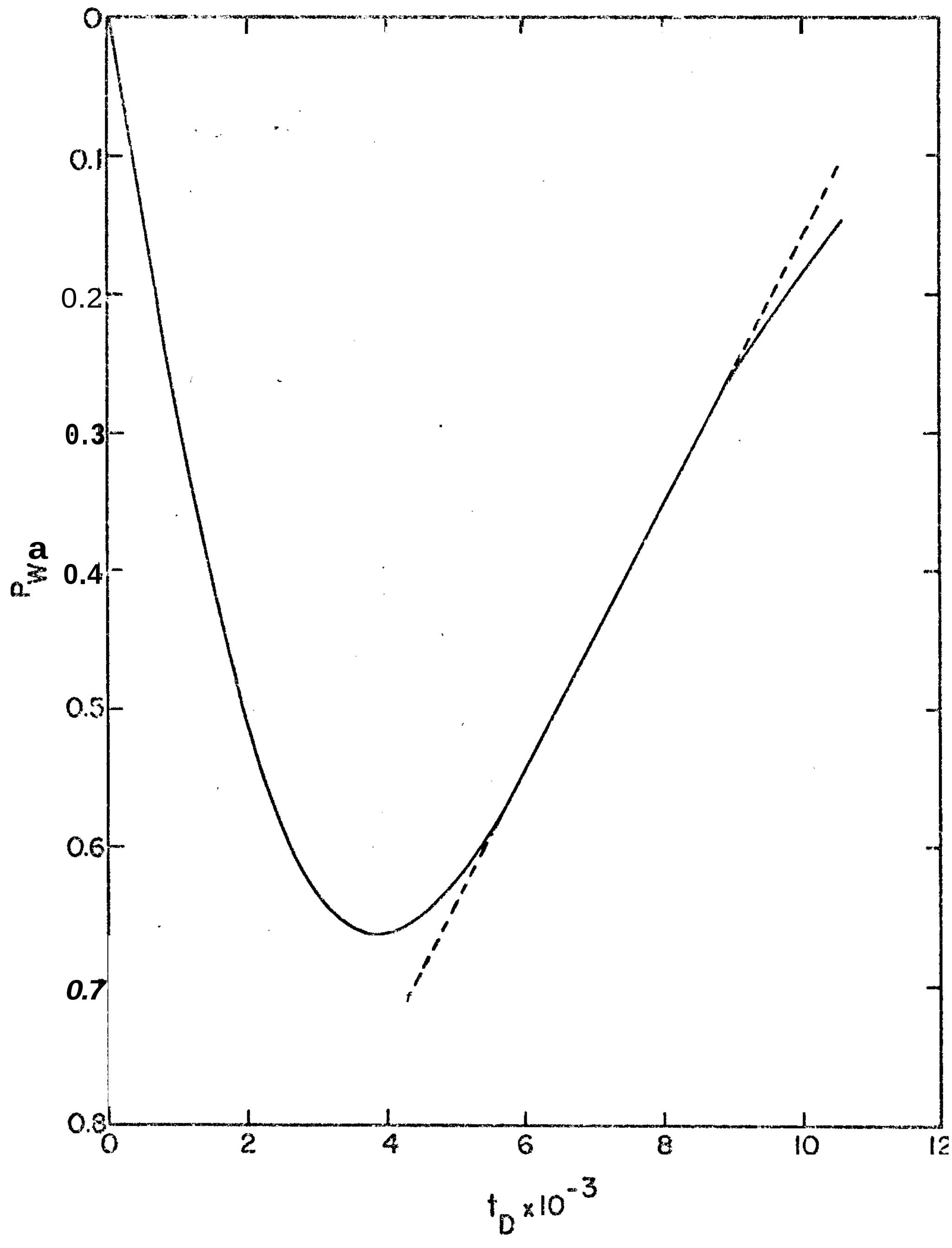

FIG. 29: DIMENSIONLESS WELLBORE PRESSURE VS DIMENSIONLESS TIME FOR $C_D = 10^3$, s = 0, AND $\alpha^2 = 10^7$ AT EARLY TIMES

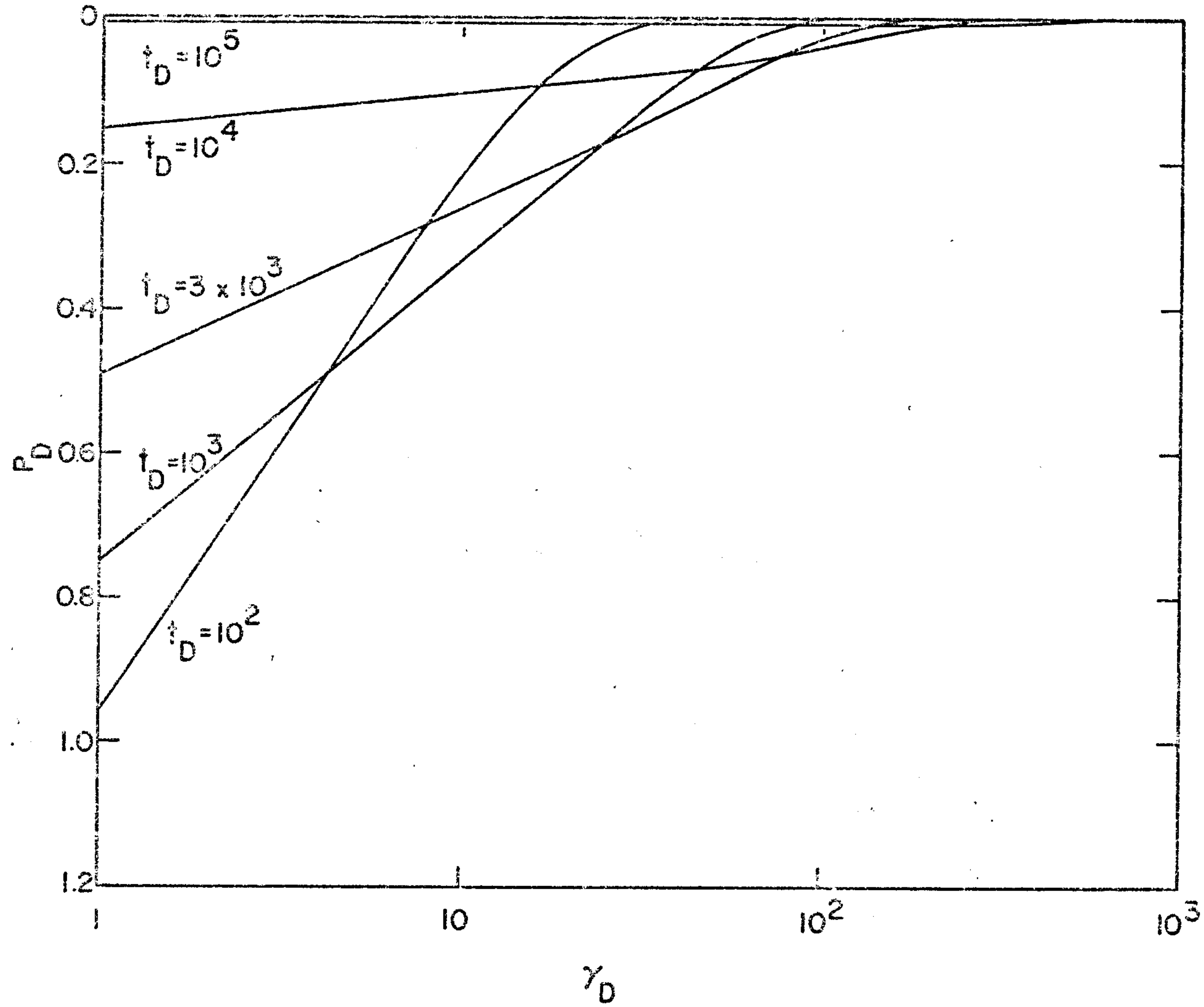

FIG. 30: PRESSURE DISTRIBUTION INSIDE THE RESERVOIR FOR $C_D = 10^3$ AND $s = \alpha = 0$ WITH DIMENSIONLESS TIME

was obtained for various α values at certain times. Figures 31 through 35 show the results. At early times, $t_D = 10^2$, a slight difference exists between the pressure distribution for $\alpha = 0$ and $\alpha^2 = 10^5$, and the pressure remains the same as the initial formation pressure for $\alpha^2 = 10^8$. The pressure distribution for $\alpha = 0$ and $\alpha^2 = 10^5$ remain the same, and the pressure for $\alpha^2 = 10^8$ starts showing some response at $t_D = 3x10^3$. The pressure gradient for $\alpha = 0$ and $\alpha^2 = 10^5$ are decreasing (i.e., the flowrate is decreasing and the wellbore pressure is recovering); however, the pressure gradient for $\alpha^2 = 10^8$ is still increasing at $t_D = 10^4$. The wellbore pressure for $\alpha^2 = 10^8$ becomes greater than the initial formation pressure, p_i; i.e., the liquid level in the wellbore oscillates. On the other hand, the wellbore pressure for $\alpha = 0$ and $\alpha^2 = 10^5$ become almost the same as the initial formation pressure, p_i, at $t_D = 5x10^4$. The wellbore pressure for all three α values are nearly the same as the initial formation pressure, p_i at $t_D = 10^5$. We conclude that the greater the α value, the later the pressure distribution starts changing and the longer it continues changing, and the smaller the pressure gradient will be. However, the investigation radius itself is almost the same for all α values. A significant pressure drop was found at values of r_D of 100 and less.

Figure 36 shows the effect of the skin factor, s, on the investigation radius. When the skin factor is large, the pressure drop occurs mainly at the sandface, and the pressure gradient inside the reservoir is small (i.e., the flowrate is small). However, the investigation radii are almost the same for all values of s. Then, we can say approximately that the skin factor does not affect the investigation radius greatly.

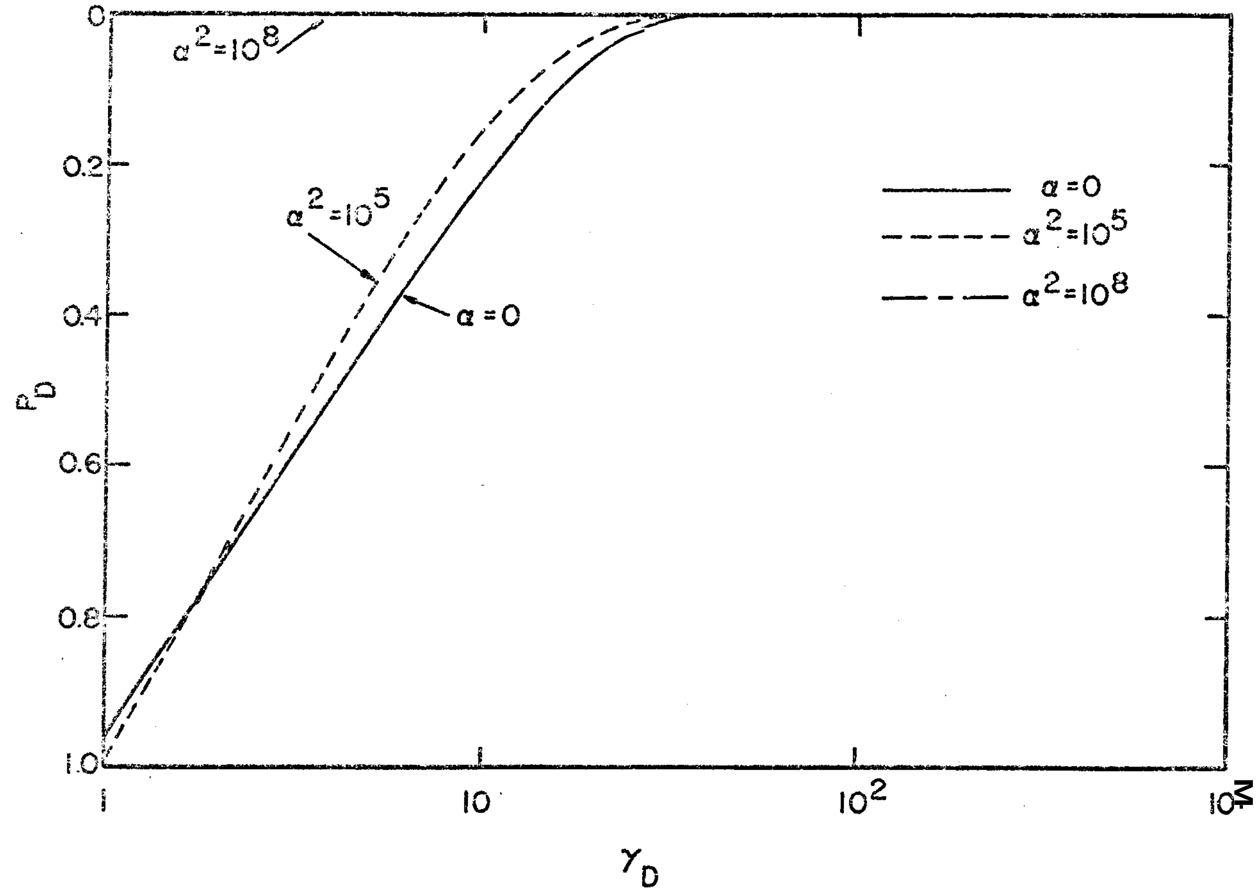

FIG. 31: EFFECT OF α ON PRESSURE DISTRIBUTION INSIDE THE RESERVOIR AT $t_D = 10^2$, FOR $C_D = 10^3$, AND $s = 0$

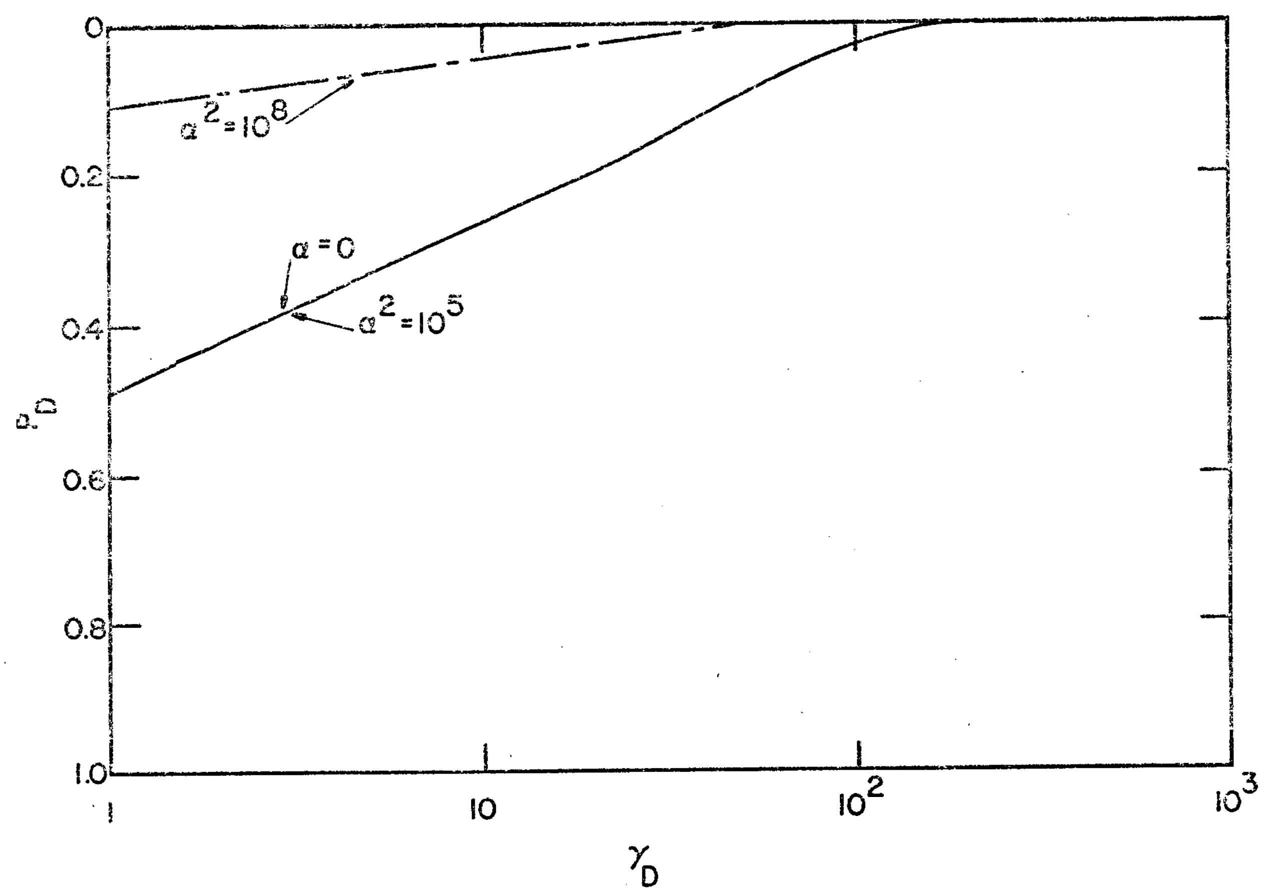

FIG. 32: EFFECT OF α ON PRESSURE DISTRIBUTION INSIDE THE RESERVOIR AT $t_D = 3\times10^3$, FOR $C_D = 10^3$, AND $s = 0$

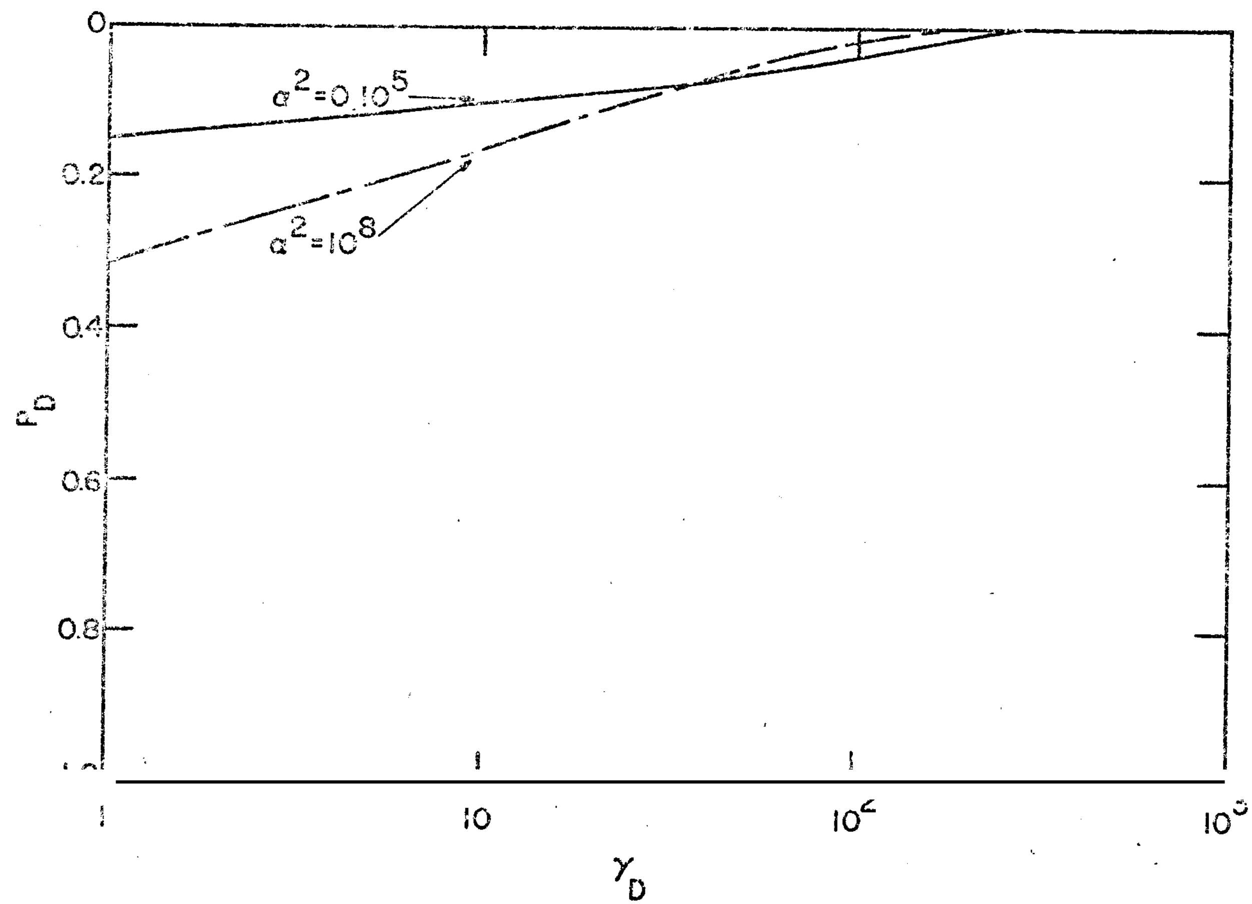

FIG. 33: EFFECT OF α ON PRESSURE DISTRIBUTION INSIDE THE RESERVOIR AT $t_D = 10^4$, FOR $C_D = 10^3$, AND s = 0

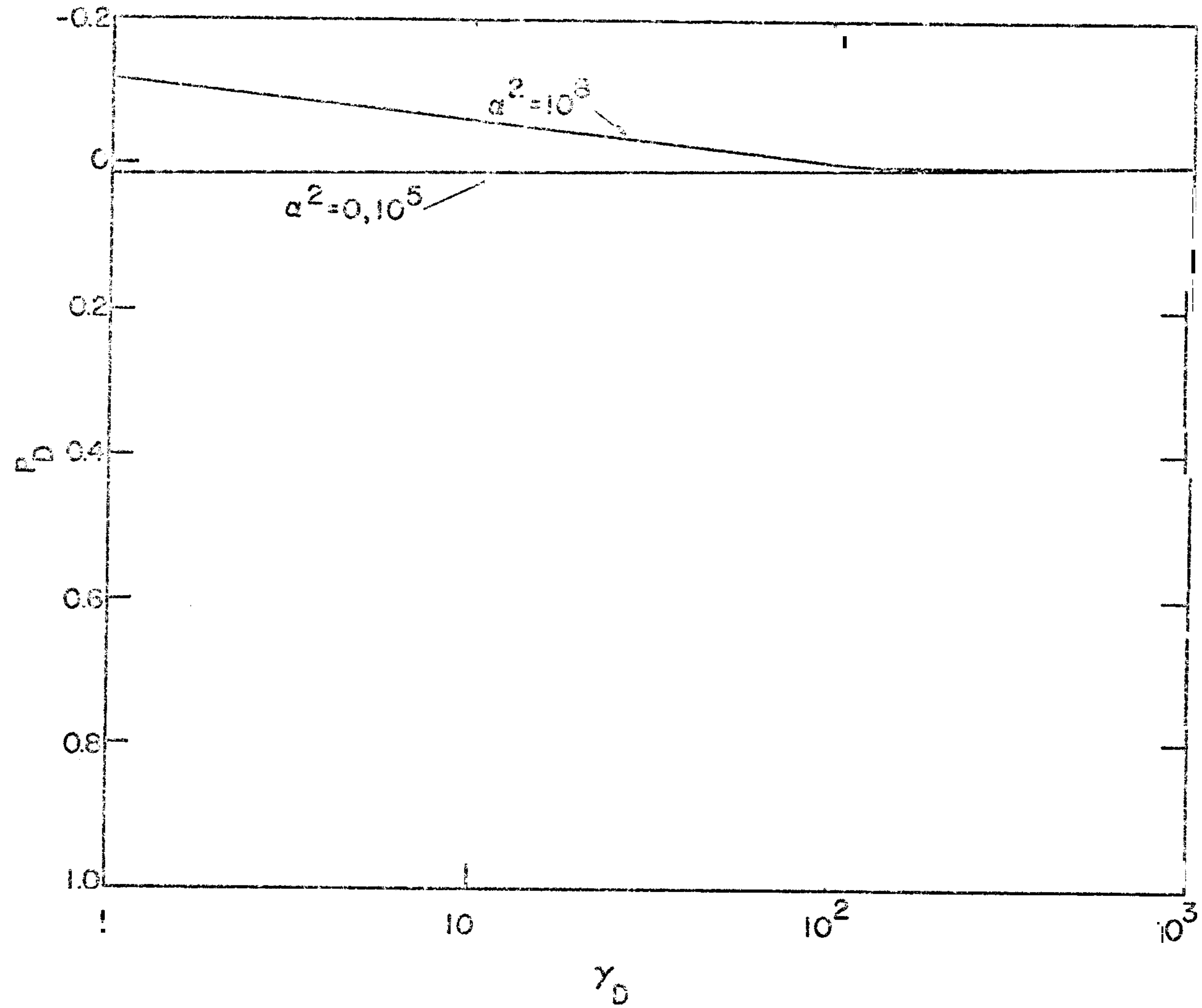

FIG. 34: EFFECT OF α ON PRESSURE DISTRIBUTION INSIDE THE RESERVOIR AT $t_D = 5 \times 10^{6}$, FOR $C_D = 10^3$ AND $s = 0$

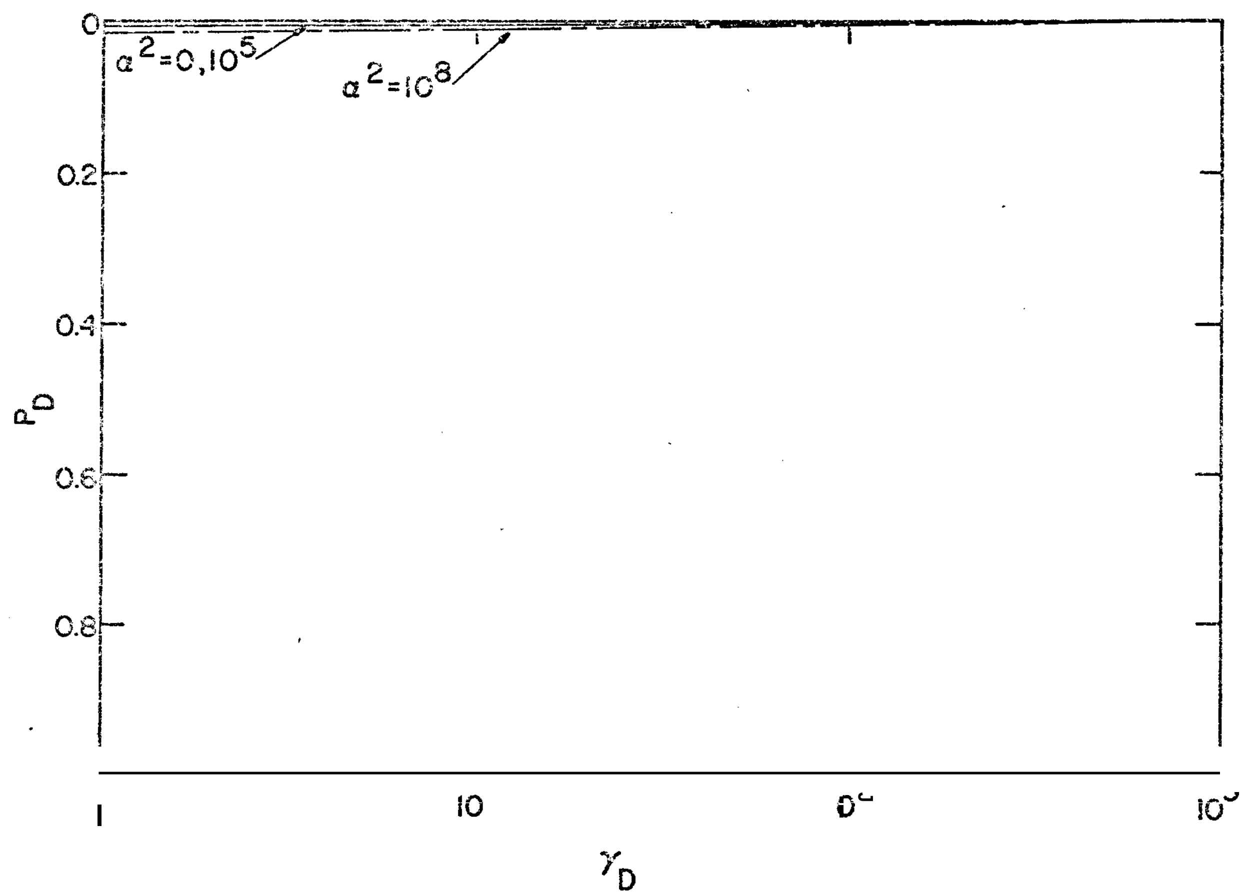

FIG. 35: EFFECT OF α ON PRESSURE DISTRIBUTION INSIDE THE RESERVOIR AT $t_D = 10^5$ F $C_D = 10^3$ AND $s = 0$

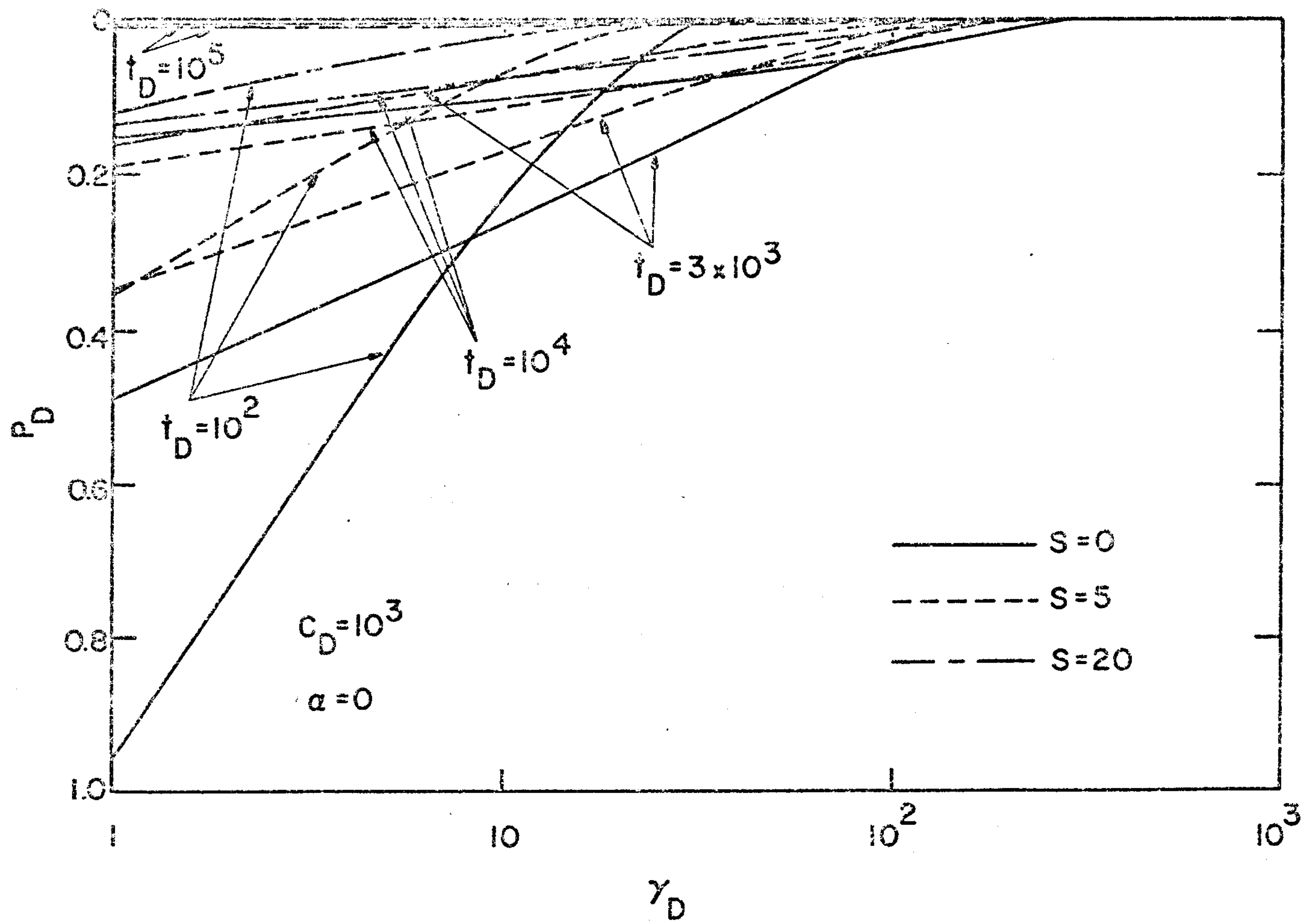

FIG. 36: EFFECT OF SKIN FACTOR ON INVESTIGATION RADIUS

Figure 37 shows how the dimensionless wellbore storage constant, C_D, affects the investigation radius for the $\alpha = s = 0$ case. We can prepare similar figures for different α and s values. The characteristics of these figures are the same. The greater the dimensionless wellbore storage constant, the deeper the investigation radius. If we define the investigation radius as the deepest point where p_D is 0.05, from Fig. 37 the magnitude of the investigation radii for the dimensionless wellbore storage constant $C_D = 10^3$, 10^4, and 10^5, among which actual field data are likely to fall, are about 100, 300, and 800, respectively.

As a summary of this section, the investigation radius depends on the dimensionless wellbore storage constant, C_D, and is not affected by the dimensionless number, α, or the skin factor, s, as much. The main pressure drops often lie in the region less than 100 r_w distant from the well produced.

2-2-4.5 Batch Injections

The solution presented in this study is not only for drawdown cases, but also applies for sudden batch injection cases. From the definition of the dimensionless liquid level in the wellbore, x_D, the fact that the initial dimensionless liquid level in the wellbore, $x_D(0)$, is always -1, as shown in Section 2-1, is also true for injection tests. However, the actual initial liquid level in the wellbore, $x(0)$, is negative for the drawdown case and is positive for the injection case.

2-2-4.6 Application of Solutions

Using the effective wellbore radius, $r_w' = r_w e^{-s}$, and a new coordinate t_D/C_D, we can shift all of the solutions to the same domain on a

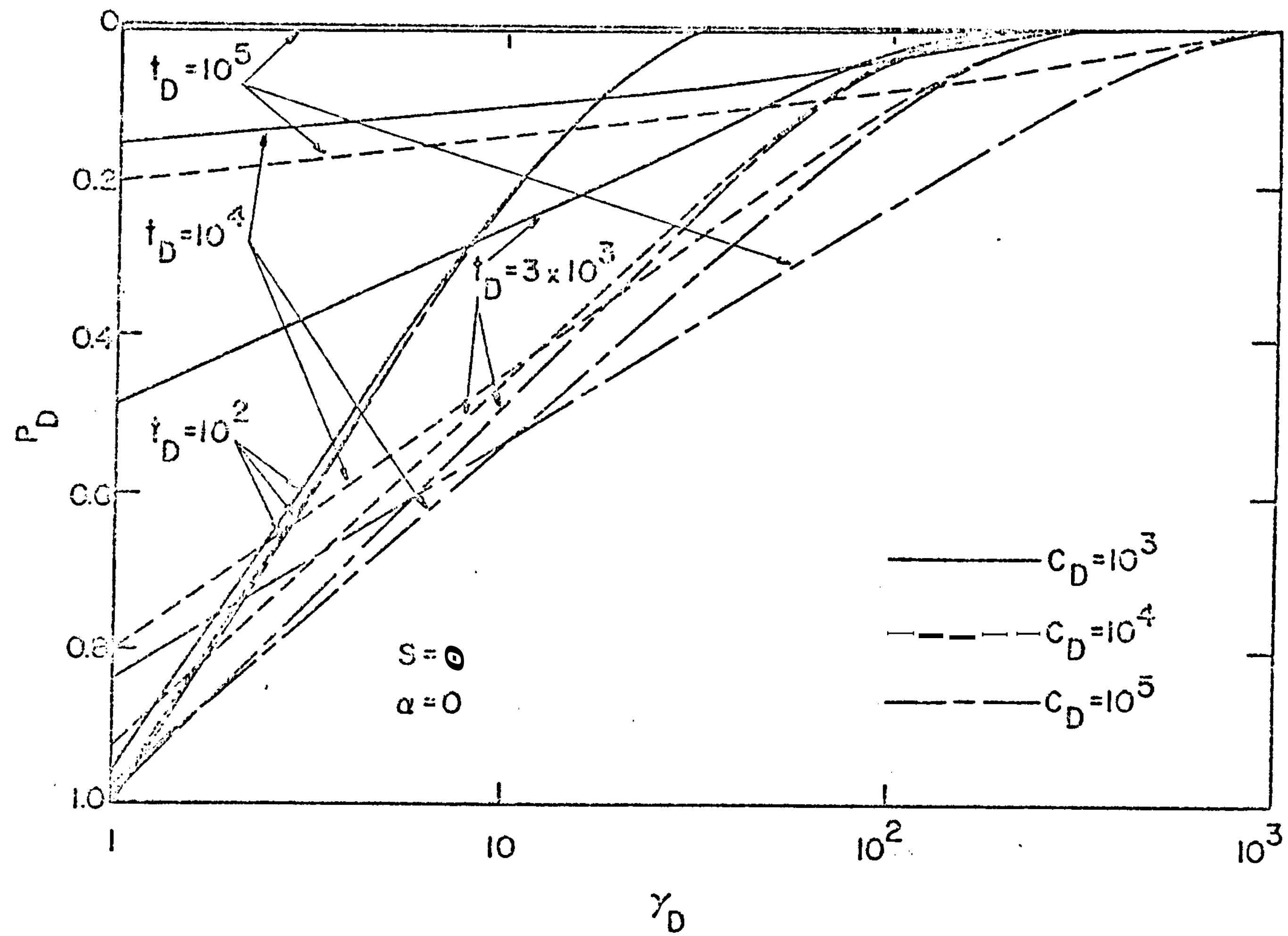

FIG. 37: EFFECT OF DIMENSIONLESS WELLBORE STORAGE CONSTANT ON INVESTIGATION RADIUS

graph. This has been done by Earlougher and Kersch[34] for conventional well test data analysis in 1973, and by Ramey et al.[13] for conventional slug test solutions, which do not include the inertial effect, as an apprcxi-mation in 1975. In our solutions we have one more parameter αe^{2s} besides C_De^{2s}, and the coordinate is the same, t_D/C_D. Tables 8 and 9 show the accuracy of this approximation for the example cases when the product, $C_De^{2s} = 10^4$ and $C_De^{2s} = 10^5$ for different α values. Since the detailed discussion of this approximation was given in Ramey et al.,[13] it is not repeated here. This approximation appears good enough for a practical range of C_De^{2s} and αe^{2s}. Figures 38 through 47 show the resulting solu-tion curves for the slug test including the inertial effect of the liquid in the wellbore with respect to the wellbore pressure, and Figs. 48 through 57 show the same results with respect to the liquid level in the wellbore. Although these figures are in reduced sizes, full-size figures are avail-able. We might be able to obtain the matched points for t_D/C_D, C_De^{2s} and αe^{2s} theoretically from these solution curves. However, as can be seen, it is practically impossible to select a unique curve matched to the actual field data, because there are so many similar curves caused by the new parameter αe^{2s}.

There are two ways to utilize the solutions proposed in this study to obtain some information for reservoirs (the main purpose is to determine the value of permeability). One way is to check the possibility that the inertia of the liquid in the wellbore will affect field performance. This procedure should be adopted when the effect of the inertia of the liquid in the wellbore on the field data is not clear; otherwise we should go directly to the second usage of the solutions which will be explained later.

TABLE 8: DIMENSI[illegible]SS WELLBORE PRESSURE VERSUS t_D C_D FOR $C_De^{2s} = 10^{[illegible]}$

t_D/C_D	$\alpha^2e^{2s} = 10^{[illegible]}$ s = 0	$\alpha^2e^{2s} = 10^{[illegible]}$ s = 1 151	$\alpha^2e^{2s} = 10^7$ s = 0	$\alpha^2e^{2s} = 10^7$ s = 1 151	$\alpha^2e^{2s} = 10^{10}$ s = 0	$\alpha^2e^{2s} = 10^{10}$ s = 1 151
0.10000D-3	0 486ɐ75c7c0	0 7ɐƎ28ƎɐƎ37	0 00058ɐƎ9Zɐ	0.0013660550	0 000000586Ǝ	0 000001Ǝ6ɐ9
0.20000D-3	(-1 ɐ01682ƎɐZ0)	0 98ccZ07cc0	(-0 0015760119)	0.0028872779	(-0 0000015759)	0 0000028911
0.30000D-3	1 1Z51583525	1 0Z87T8110Ǝ	0 00259c5Ǝɐ8	0.0044979246	0 0000025ƎɐƎ	0 00000c5072
0.40000D-3	1 161c91663c	1 0Z98503cƎ6	0 00381c6106	0.0061753522	0 000003819ɐ	0 0000061927
0.50000D-3	1 12ZƎ62Z953	1 0Z37ɐƎ2231	0 0051305115	0.0079067725	0 0000051397	0 0000079351
0.60000D-3	1 0720398138	1 0183c53193	0 0065Zc9100	0.0096839513	0 000006Ǝ399	0 000009726Ǝ
0.70000D-3	1 035ƎɐƎ1158	1 01cɐ078751	0 0079857713	0.0115026378	0 000008008c	0 000011Ǝ62Z
0.80000D-3	1 0159317515	1 011ɐƎ288c5	0 00950cZ113	0.0133456184	0 0000095ƎɐƎ	0 000013cZƎɐ
0.90000D-3	1 007923Z58T	1 0090709300	0 0110733799	0.0151999452	0 0000111175	0 000015303б
0.10000D-2	1 0059c85005	1 0129c735ɐ1	0 01268T8195	0.0172426583	0 00001ZTc61	0 00001737c9
0.20000D-2	1 00c05Z8338	(-0 Z259718293)	0 030ɐ0ɐƎ180	(0.0068801909)	0 0000309ɐ02	(0 000007Z606)
0.30000D-2	1 0009ɐƎ0858	1 00092Z520Z	0 0505559ɐɐ8	0.0589387833	0 000051550ɐ	0 0000ɐ0c970
0.40000D-2	0 999T905c9c	0 999801ɐ130	0 071ɐ76Z7cc	0.0812439819	0 0000737259	0 00008cZ33c
0.50000D-2	0.99895096ɐ8	0 999015210c	0 09352ɐ80ɐc	0.1039868609	0 000097036c	0 0001089cZ1
0.60000D-2	0.9982709632	0 99838ɐ088c	0 11583cƎɐ76	0.1269669416	0 000121cZ75	0 00013cc516
0.70000D-2	0 99Tɐ9373Ǝɐ	0 9978cɐ094Z	0.1384113785	0.1500432351	0 0001c65ɐ2c	0 0001606c35
0.80000D-2	0 99718cc518	0 997Ǝɐ2Zɐcc	0 1ɐ11Z07ɐ8c	0.1731110614	0 0001723885	0 000187c307
0.90000D-2	0 99ɐ720Ǝɐc3	0 9Ǝɐ91ɐƎ995	0 18Ǝ8580689	0.1960898419	0 0001988209	0 000Z1c7cɐ2
0.10000D-1	0 9Ǝɐ289T2cZ	0 9Ǝɐc977ɐƎ0	0 20ɐƎc1350Z	0.2189160414	0 000225T93c	0 0002cZ5Ǝɐ8
0.20000D-1	0 99ZT213281	0 9929714Ǝ21	0 cZ0c1690c3	0.4310746791	0 0005168883	0 00053Ǝ6809
0.30000D-1	0.9896465579	0 98990TTɐƎ6	0 597775c1ɐɐ	0.6045260270	0 00083Ǝ63c0	0 0008ɐ0c9T5
0.40000D-1	0 98677036Ǝ8	0 9870373T3Z	0 735cɐ2c379	0.7383173219	0 0011ɐ70789	0 001197062Z
0.50000D-1	0 98c01ɐ8532	0 98cZ8ɐ810T	0 837650Z7cɐ	0.8373770653	0 00151293бc	0 0015c5cɐɐƎ
0.60000D-1	0 9813511Z88	0 98162308Zc	0 910c788ɐɐ7	0.9080279482	0.0018686697	0 001903Ǝɐ10
0.70000D-1	0 9T875cZT1Z	0 9790ZT6711	0 9ɐ01ɐ1T86Ǝ	0.9564144587	0 00223Z5975	0 00226Ǝ1ɐƎ0
0.80000D-1	0 9T621c021c	0 976c882718	0 9922c88282	0.9879178230	0 002ɐ035214	0 002ɐc17593
0.90000D-1	0 9T3T2189cZ	0 97399ɐɐƎɐc	1 011380ZTT8	1.0069871590	0 00Z9805c35	0 0030Z0Z787
0.10000D 0	0 Ǝ71Z71783c	0 97154ɐɐƎ67	1 0212677028	1.0171581523	0 003Ǝɐ2965ɐ	0 003c0c0ɐ11
0.20000D 0	0 9c8Ǝɐc5ZƎɐ	0 9c86353T05	0 981ɐ2cZ35c	0.9816919156	0 00T3Ǝ67T61	0 00Tcc7Z1c7
0.30000D 0	0.9273406829	0.9276033926	0.9459102853	0.9462697549	0.0116737711	0.0117298401

TABLE 8. CONTINUED

t_D/C_D	$\alpha^2 e^4 s = 10^4$ s = 0	$\alpha^2 e^4 s = 10^4$ s = 1 151	$\alpha^2 e^4 s = 10^7$ s = 0	$\alpha^2 e^4 s = 10^7$ s = 1 151	$\alpha^2 e^4 s = 10^{10}$ s = 0	$\alpha^2 e^4 s = 10^{10}$ s = 1 151
0.40000D 0	0.9075684479	0.9078220256	0.9218481922	0.9221142078	0.0161004287	0.0161604426
0.50000D 0	0.8887643128	0.8890083975	0.9007101809	0.9009590995	0.0206316410	0.0206946127
0.60000D 0	0.8707637591	0.8709983234	0.8810976856	0.8813434183	0.0252404141	0.0253056843
0.70000D 0	0.8534586314	0.8536838281	0.8626167636	0.8628557567	0.0299086058	0.0299757005
0.80000D 0	0.8367709599	0.8369870974	0.8450358986	0.8452652449	0.0346230908	0.0346916490
0.90000D 0	0.8206419166	0.8208091431	0.8281992581	0.8284181133	0.0393738675	0.0394436055
0.10000D 1	0.8050248559	0.8052234084	0.8120004904	0.8122091713	0.0441530222	0.0442237078
0.20000D 1	0.6708307377	0.6709567618	0.6747106998	0.6748414340	0.0924625515	0.0925354358
0.30000D 1	0.5657167805	0.5657903680	0.5681775330	0.5682546385	0.1399053435	0.1399739948
0.40000D 1	0.4810322827	0.4810691733	0.4826490298	0.4826878121	0.1850609825	0.1851225542
0.50000D 1	0.4117563071	0.4117669941	0.4128244121	0.4128362693	0.2271062388	0.2271592536
0.60000D 1	0.3544978226	0.3544898914	0.3551943734	0.3551871353	0.2654868417	0.2655305642
0.70000D 1	0.3068010567	0.3067804765	0.3072410791	0.3072207611	0.2998136023	0.2998477922
0.80000D 1	0.2668168951	0.2667877819	0.2670780001	0.2670490421	0.3298168716	0.3298416140
0.90000D 1	0.2331164281	0.2330818759	0.2332526200	0.2332181243	0.3553221574	0.3553377842
0.10000D 2	0.2045765457	0.2043388945	0.2046260304	0.2045884052	0.3762355330	0.3762425655
0.20000D 2	0.0691596759	0.0691331845	0.0690685274	0.0690419692	0.3546739190	0.3546387913
0.30000D 2	0.0330239267	0.0330116446	0.0329849211	0.0329726237	0.0982130010	0.0981974049
0.40000D 2	0.0201563015	0.0201504687	0.0201417063	0.0201358566	-0.1005876331	-0.1005883316
0.50000D 2	0.0142949592	0.0142919105	0.0142892006	0.0142861289	-0.1099823492	-0.1099918961
0.60000D 2	0.0110673326	0.0110654684	0.0110647469	0.0110628856	-0.0288275825	-0.0288401446
0.70000D 2	0.0090381507	0.0090369275	0.0090368297	0.0090356183	0.0292450510	0.0292400291
0.80000D 2	0.0076435853	0.0076427278	0.0076428405	0.0076419730	0.0416834106	0.0416856260
0.90000D 2	0.0066247865	0.0066231551	0.0066243516	0.0066237129	0.0302010253	0.0302055635
0.10000D 2	0.0058473866	0.0058468732	0.0058471007	0.0058465813	0.0150177235	0.0150211876

TABLE 9: DIMENSIONLESS WELLBORE PRESSURE VERSUS t_D/C_D FOR $C_De^{2s} = 10^5$

t_D/C_D	$\alpha^2 e^{\sqsubset s} = 10^6$ s = 0	s = 2 303	$2_{a}4s = 10^9$ s =	s = Z 303	$Z_{a}{\sqsubset}s = 10^{12}$ s =	s = 2 303
0.10000D-3	0 81≤9822199	0.9356303719	0 001Z7⊏03⊏8	0 0025158655	0 00000127⊏≤	0 0000025189
0.20000D-3	1 1010159557	1.0115075660	0 00309Z⊏953	0 005182ZZ88	0 00000309≤1	0 0000051951
0.30000D-3	1 08Z785311Z	1.0117507323	0 0051⊏51073	0 0079330ʒØ1	0 0000051551	0 0000079≤32
0.40000D-3	1 037088⊏≤98	1.0087382139	0 0073519959	0 0107⊏5≤520	0 0000073728	0 0000108007
0.50000D-3	1 01≤3931535	1.0068122045	0 009≤735941	0 013≤0≤9877	0 0000097100	0 000013≤950
0.60000D-3	1 010Z98⊏9⊏⊏	1.0055746212	0 0120859922	0 01≤5087≤3⊏	0 0000121⊏33	0 00001≤≤38Z
0.70000D-3	1 008≤97⊏583	1.0047234318	0 01⊏5730928	0 019⊏⊏≤≤298	0 00001⊏≤570	0 000019≤2≤1
0.80000D-3	1 0078503131	1.0039239966	0 0171Z3Z833	0 022⊏0337⊏5	0 0000172399	0 000022≤⊏15
0.90000D-3	1 00≤95119⊏3	1.0031189193	0 0197Z77≤85	0 02536≤0793	0 0000198835	0 0000Z5≤71⊏
0.10000D-2	1 00≤008393≤	1.0047672423	0 0ZZ379≤⊏74	0 028510≤Z73	0 000022581Z	0 0000Z8894≤
0.20000D-2	1 0015≤≤2339	(0.5153275523)	0 050≤Z⊏1⊏58	(0 0290357≤9⊏)	0 000051≤987	(0 0000302997)
0.30000D-2	1 0003557⊏≤9	1.0001453101	0 08058029Z3	0 0910359≤33	0 0000833893	0 00009505⊏4
0.40000D-2	0 999≤⊏10⊏59	0.9995706607	0 111252⊏Z51	0 1Z2861338Z	0 00011≤7592	0 0001303087
0.50000D-2	0 999122≤7⊏8	0.9991279972	0 1⊏Z1483871	0 15⊏526ʒ959	0 0001513805	0 0001≤≤5346
0.60000D-2	0 99870130⊏0	0.9987505619	0 1729727575	0 185839861≤	0 0001870003	0 0002035≤06
0.70000D-2	0 99833⊏⊏8ZZ	0.9984113898	0 20353017≤1	0 Z1≤≤701395	0 0002Z3⊏510	0 000Z⊏12≤8Z
0.80000D-2	0 9980013357	0.9980971164	0 233≤840958	0 2⊏≤9Z≤9418	0 0002≤0≤134	0 000279570⊏
0.90000D-2	0 997≤90≤978	0.9977998928	0 Z≤33358933	0 Z7≤5452928	0 0002983981	0 000318⊏001
0.10000D-1	0 9973960⊏40	0.9975154145	0 2924130812	0 3054785≤15	0 0003367358	0 00035770⊏Z
0.20000D-1	0 99⊏8319≤40	0.9949922562	0 5⊏⊏ 089≤⊏3	0 553⊏882⊏08	0 0007⊏18ʒ88	0 0007≤99387
0.30000D-1	0 99Z53≤3790	0.9927105144	0 72≤1380550	0.7295498786	0 0011729122	0 0012057609
0.40000D-1	0 99035⊏5835	0.9905366947	0.8482898369	0 8⊏77≤0⊏⊏⊏5	0 001≤207388	0 001≤57Z418
0.50000D-1	0 988Z⊏⊏≤519	0.9884319704	0 92≤3959535	0 9Z3515⊏⊏39	0 00Z0809800	0 0021Z0⊏701
0.60000D-1	0 98≤1870034	0.9863781938	0 9735849Z17	0 9≤9≤⊏Z7937	0 00Z5510≤⊏5	0 0025930927
0.70000D-1	0 98417108Z0	0.9843652667	Ø 9999985220	Ø 99587Z1190	0 0030292907	0 0030735319
0 80000D-1	0 982189Z74Z	0.9823860714	1 01299≤Z111	1 009200Z990	0 00351⊏4⊏75	0 0035≤0≤545
0 90000D-1	0 98023715⊏8	0.9804359456	1 017685⊏55≤	1 01⊏4≤73≤10	0 00⊏005≤28Z	0 004053≤057

CONTINUED

TABLE 9, CONTINUED

t_L/C_D	$\alpha^2 e^{4s} = 10^6$, s = 0	$\alpha^2 e^{4s} = 10^6$, s = 2.303	$\alpha^2 e^{4s} = 10^9$, s = 0	$\alpha^2 e^{4s} = 10^9$, s = 2.303	$\alpha^2 e^{4s} = 10^{12}$, s = 0	$\alpha^2 e^{4s} = 10^{12}$, s = 2.303
0.10000D0	0.9783108252	0.9785113340	1.0174805389	1.0149126854	0.0045021279	0.0045517180
0.20000D0	0.9600458198	0.9602542708	0.9781414342	0.9783142230	0.0096715323	0.0097323403
0.30000D0	0.9429840778	0.9431937860	0.9548139839	0.9550103712	0.0150735709	0.0151413258
0.40000D0	0.9267396934	0.9269480827	0.9361683291	0.9363651665	0.0206139124	0.0206866753
0.50000D0	0.9111370704	0.9113433560	0.9191336527	0.9193379941	0.0262469939	0.0263236250
0.60000D0	0.8960740649	0.8962773219	0.9031130151	0.9033182276	0.0319454982	0.0320252350
0.70000D0	0.8814829353	0.8816828696	0.8878326531	0.8880352895	0.0376910372	0.0377733288
0.80000D0	0.8673150929	0.8675113667	0.8731364992	0.8733354185	0.0434702875	0.0435547113
0.90000D0	0.8535332695	0.8537258144	0.8589296691	0.8591246182	0.0492730794	0.0493593037
0.10000D1	0.8401082756	0.8402970360	0.8451500922	0.8453410793	0.0550913618	0.0551791108
0.20000D1	0.7215743670	0.7217243974	0.7246563850	0.7248091131	0.1130633883	0.1131576780
0.30000D1	0.6246560289	0.6247723692	0.6267808020	0.6268988413	0.1688148907	0.1689077155
0.40000D1	0.5436971627	0.5437856230	0.5452134269	0.5453032232	0.2209261299	0.2210136765
0.50000D1	0.4752938109	0.4753598196	0.4763877068	0.4764546791	0.2686409158	0.2686895085
0.60000D1	0.4170602457	0.4171081130	0.4178488064	0.4178973649	0.3113697538	0.3114411270
0.70000D1	0.3672047629	0.3672382916	0.3677678210	0.3678018576	0.3488946108	0.3489566085
0.80000D1	0.3243298269	0.3243518432	0.3247243943	0.3247467756	0.3810039796	0.3810563612
0.90000D1	0.2873183388	0.2873311767	0.2875864610	0.2875995120	0.4076227124	0.4076655658
0.10000D2	0.2552633011	0.2552690470	0.2554361633	0.2554420720	0.4287631458	0.4287968111
0.20000D2	0.0906710148	0.0906570814	0.0905959740	0.0905820193	0.3839687252	0.3839521472
0.30000D2	0.0415766318	0.0415672130	0.0415303628	0.0415209478	0.1093689915	0.1093677789
0.40000D2	0.0237962901	0.0237910255	0.0237756603	0.0237703721	-0.0852636114	-0.0852533302
0.50000D2	0.0160325352	0.0160295857	0.0160237271	0.0160207403	-0.0985937464	-0.0985994957
0.60000D2	0.0120094624	0.0120076818	0.0120055276	0.0120037480	-0.0309014136	-0.0309182275
0.70000D2	0.0096115322	0.0096103976	0.0096096106	0.0096084523	0.0200702584	0.0200578124
0.80000D2	0.0080257268	0.0080248993	0.0080246909	0.0080238397	0.0340855248	0.0340821294
0.90000D2	0.0068967200	0.0068961943	0.0068961196	0.0068955677	0.0272188800	0.0272213764
0.10000D2	0.0060502761	0.0060497848	0.0060498746	0.0060496526	0.0156060461	0.0156100708

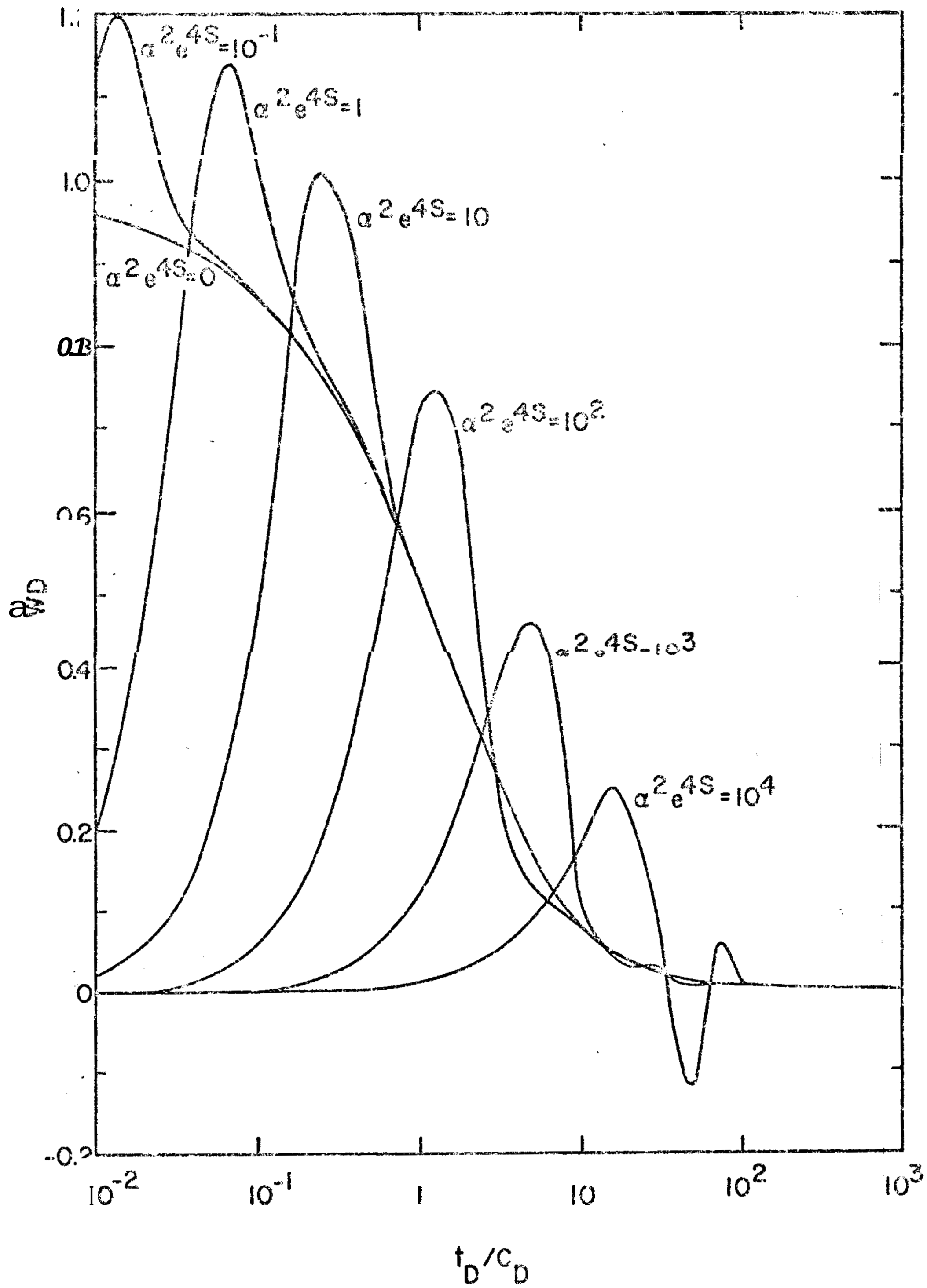

FIG. 38: DIMENSIONLESS WELLBORE PRESSURE VS t_D/C_D for $C_De^{2S} = 10$

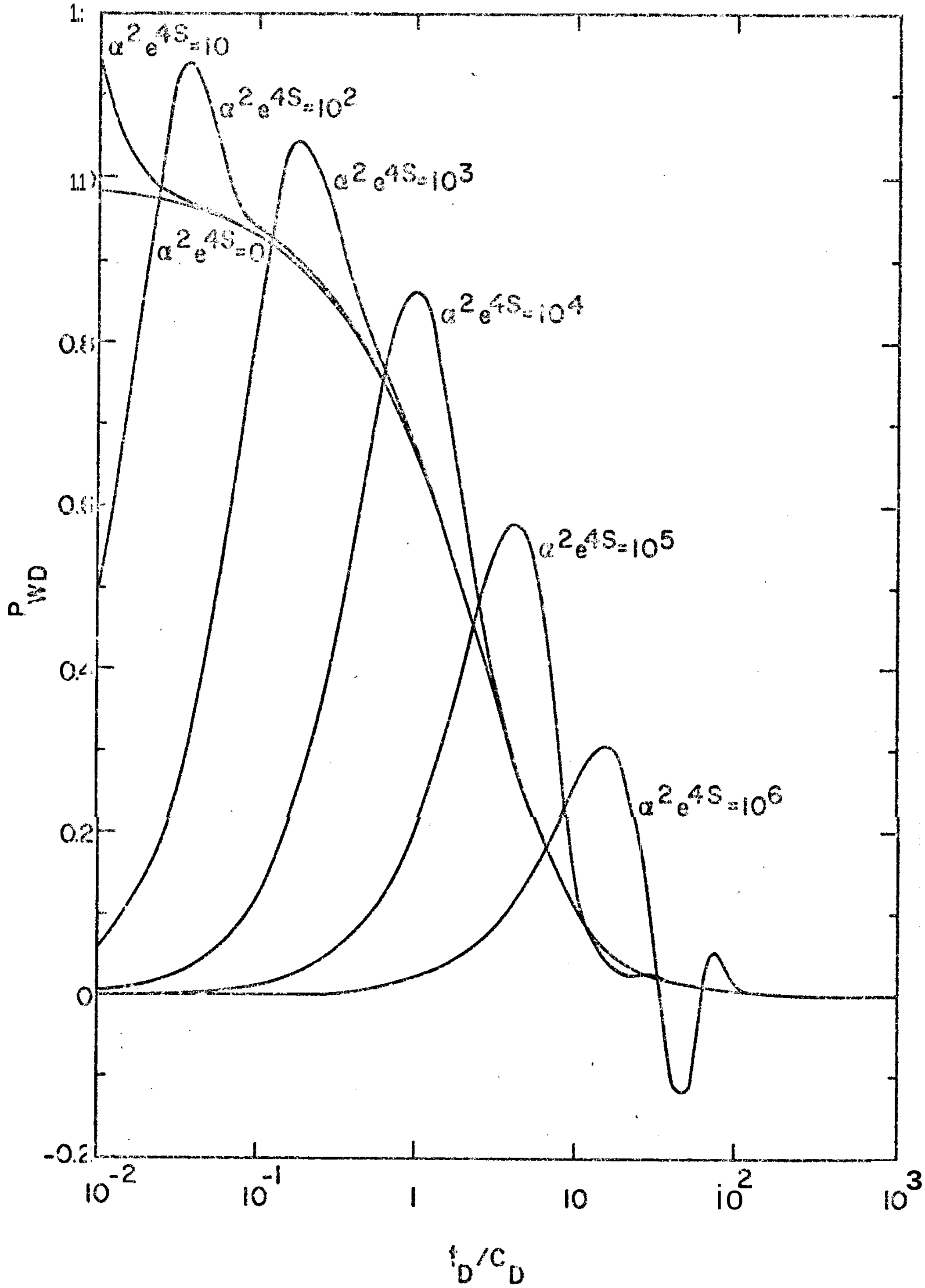

FIG. 39: DIMENSIONLESS WELLBORE PRESSURE VS t_D/C_D FOR $C_De^{2s} = 10^2$

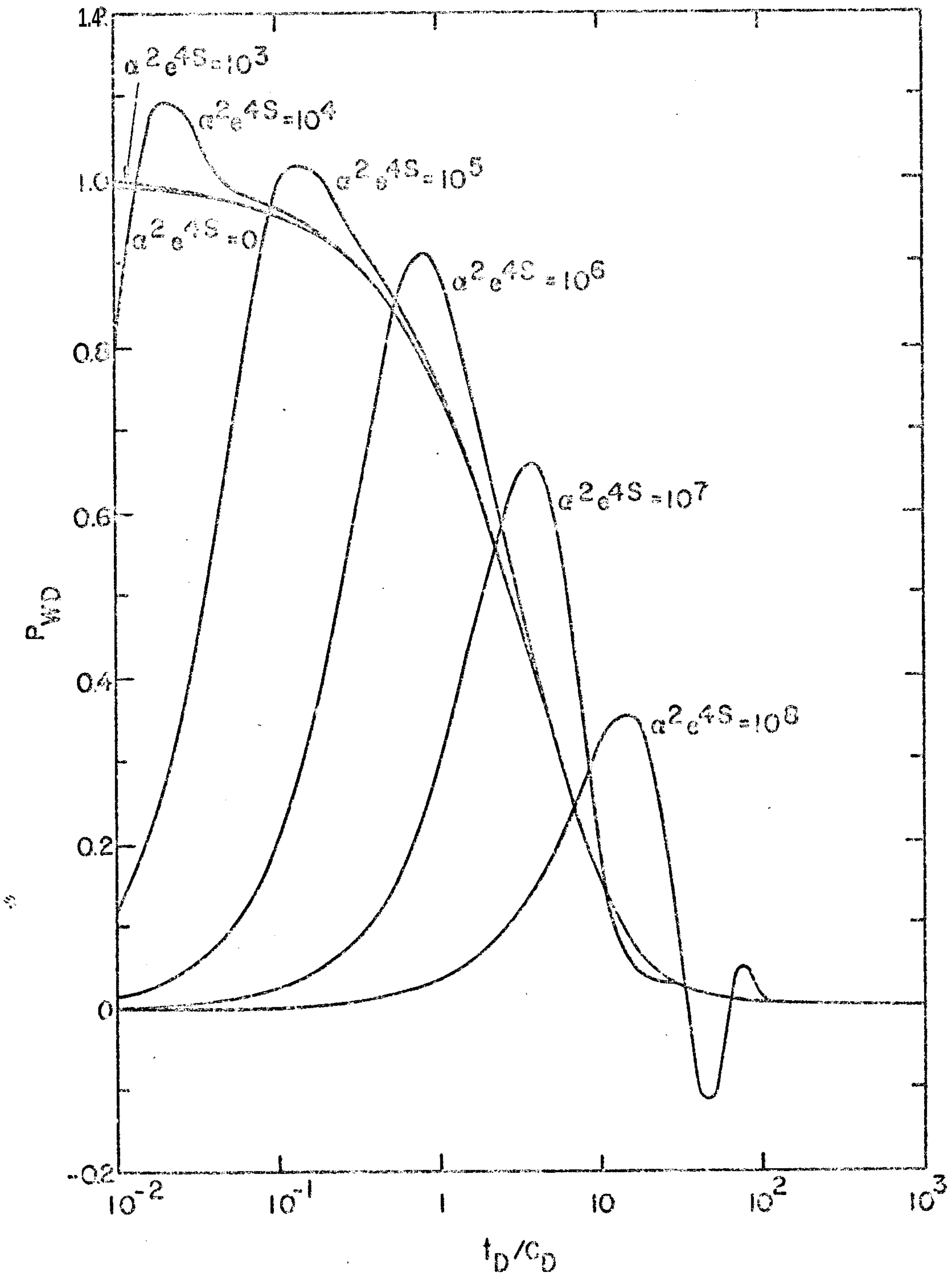

FIG. *40:* DIMENSIONLESS WELLBORE PRESSURE VS t_D/C_D FOR $C_De^{2s} = 10^3$

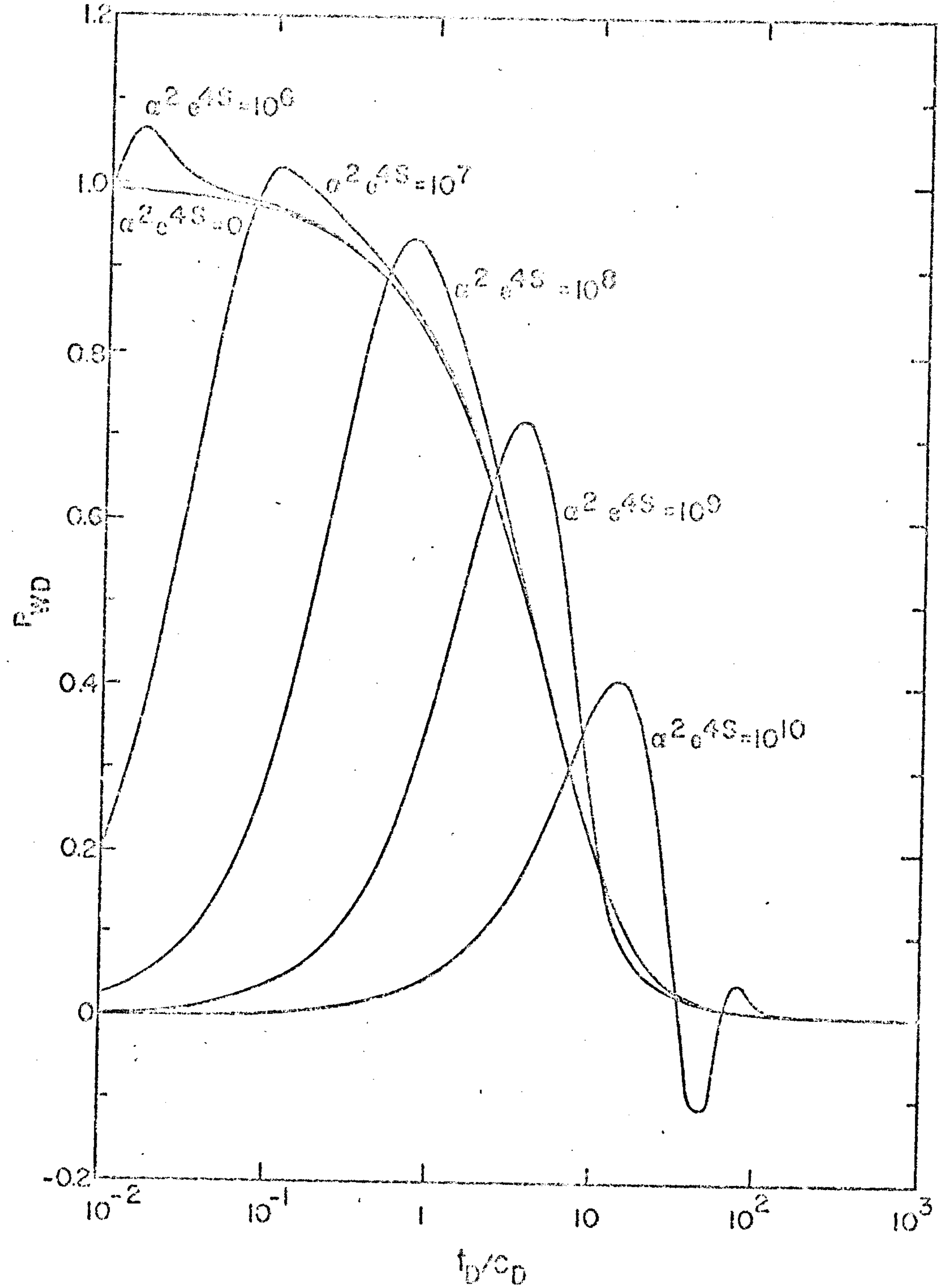

FIG. ***41:*** **DIMENSIONLESS WELLBORE PRESSURE VS t_D/C_D FOR C_De^{2s} = I.4**

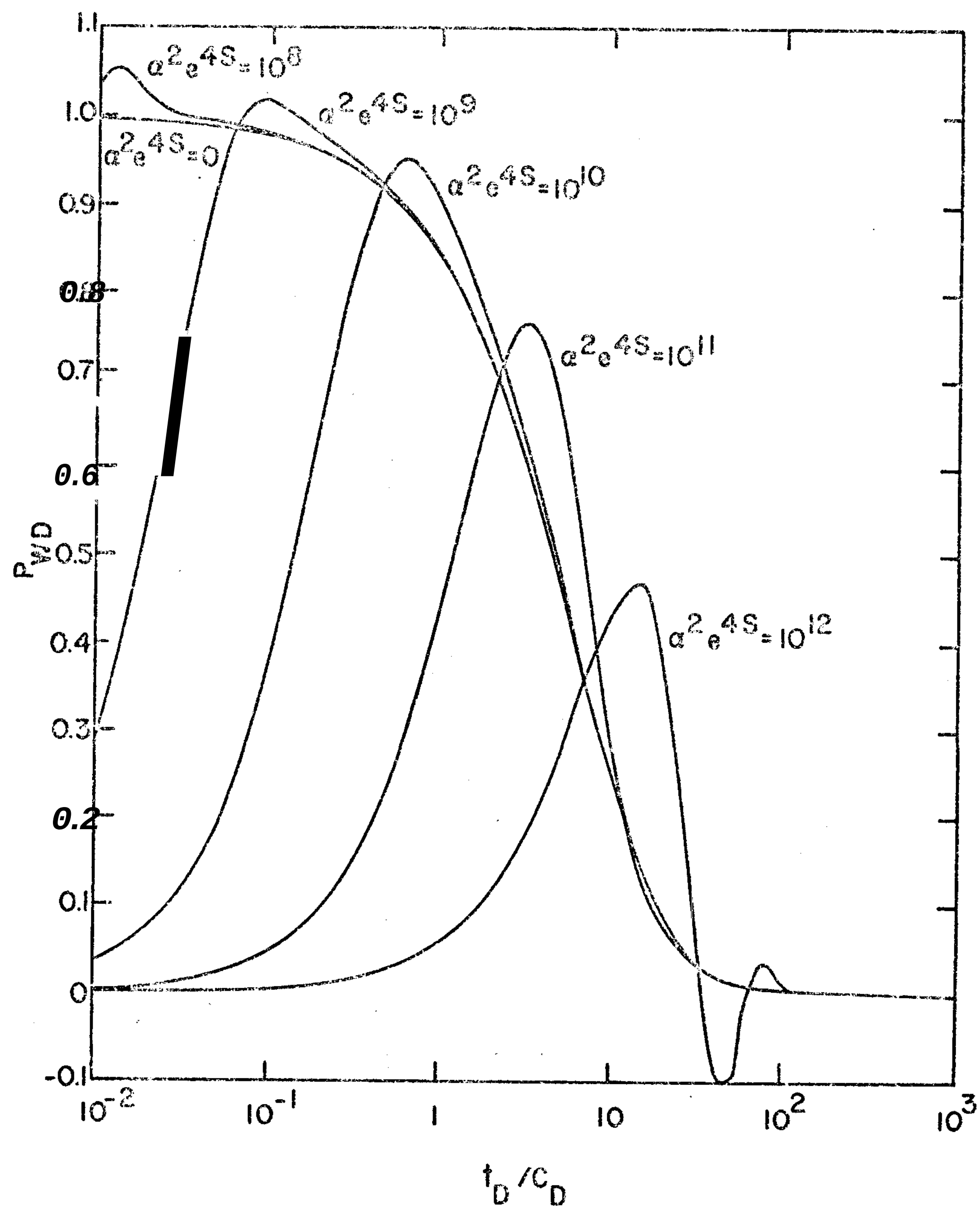

FIG. *42:* **DIMENSIONLESS WELLBORE PRESSURE VS t_D/C_D FOR $C_D e^{2s} = 10^5$**

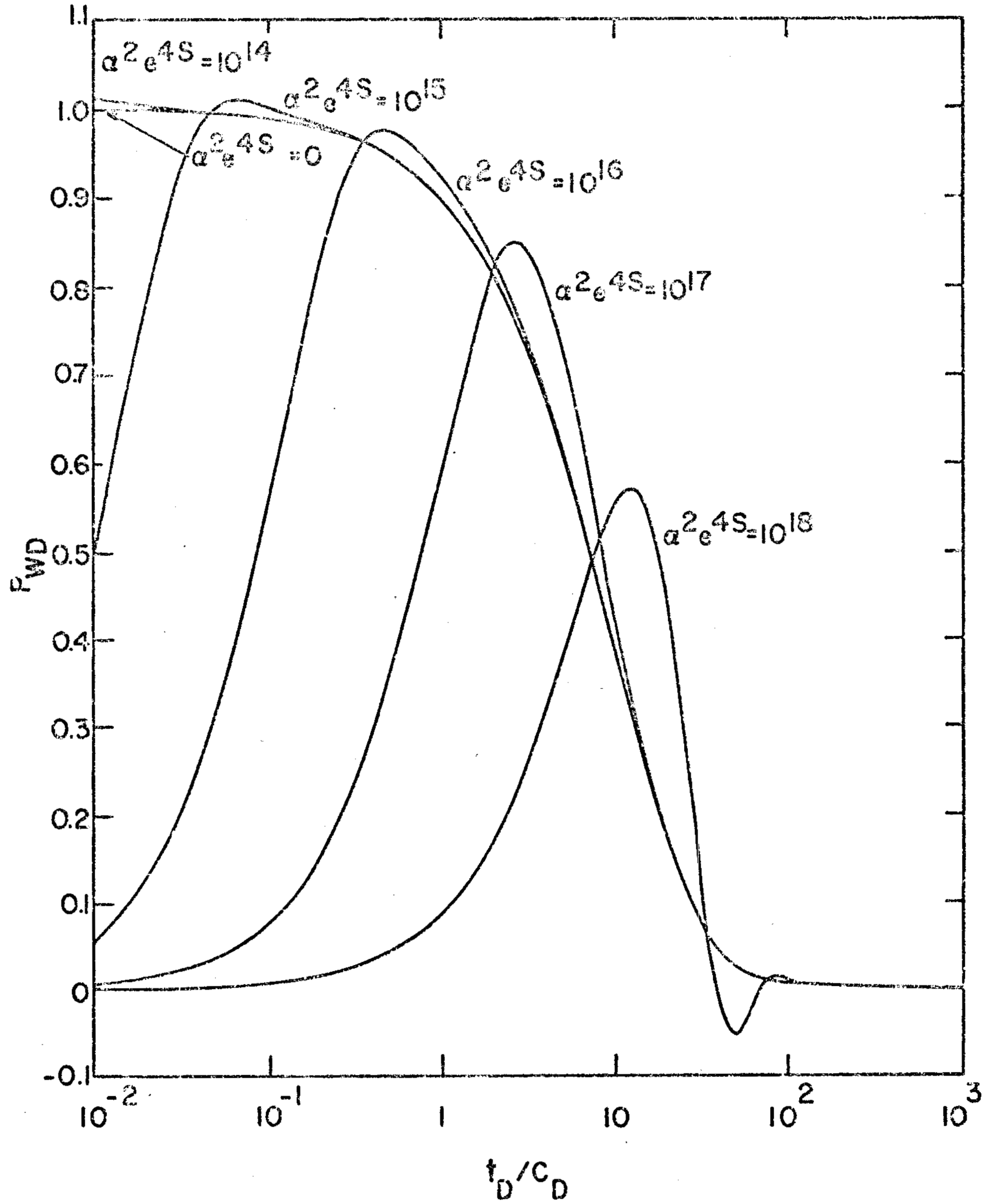

FIG. 43: DIMENSIONLESS WELLBORE PRESSURE VS t_D/C_D FOR $C_De^{2s} = 10^8$

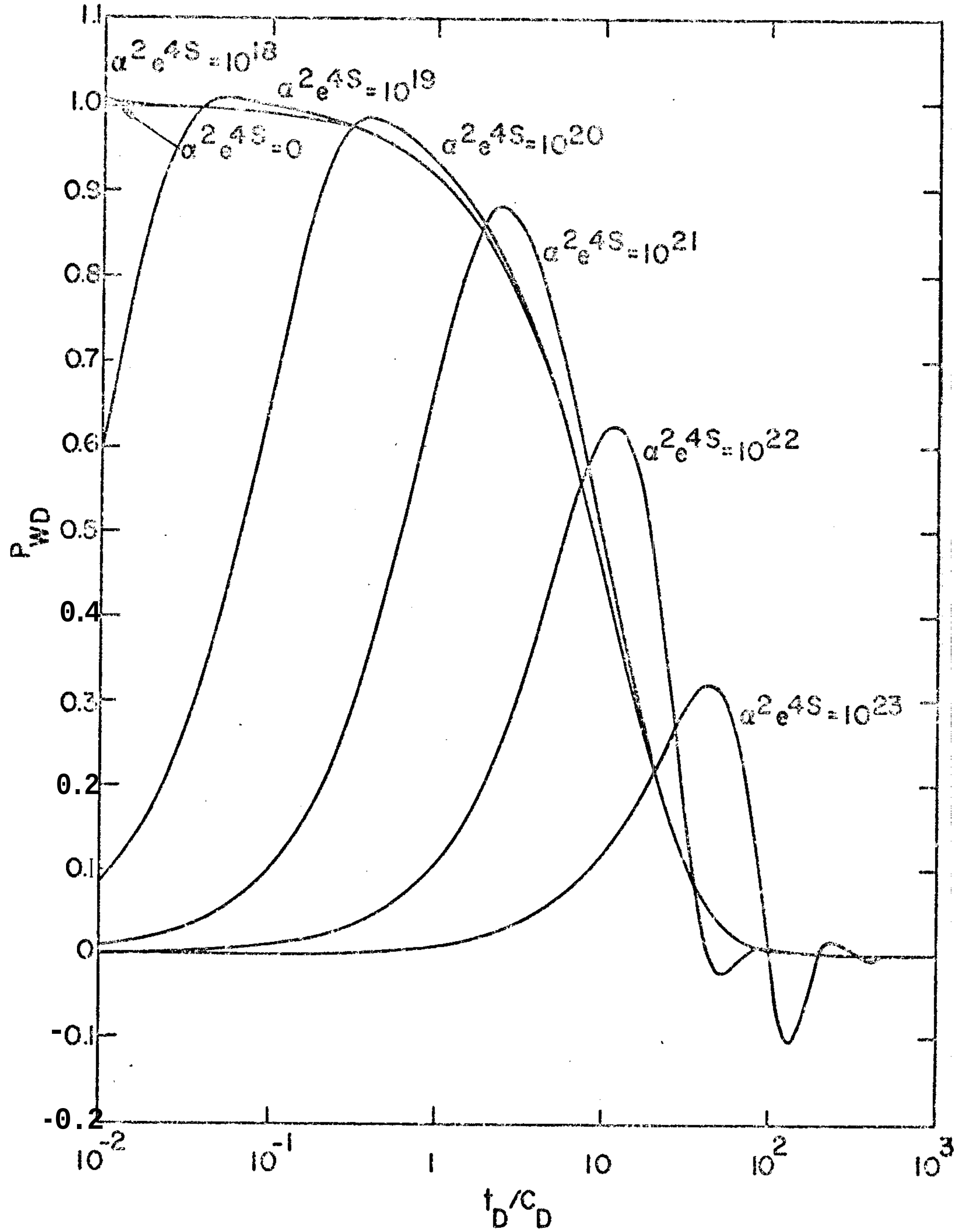

FIG. *44:* **DIMENSIONLESS WELLBORE PRESSURE VS** t_D/C_D FOR $C_D e^{25} = 10^{10}$

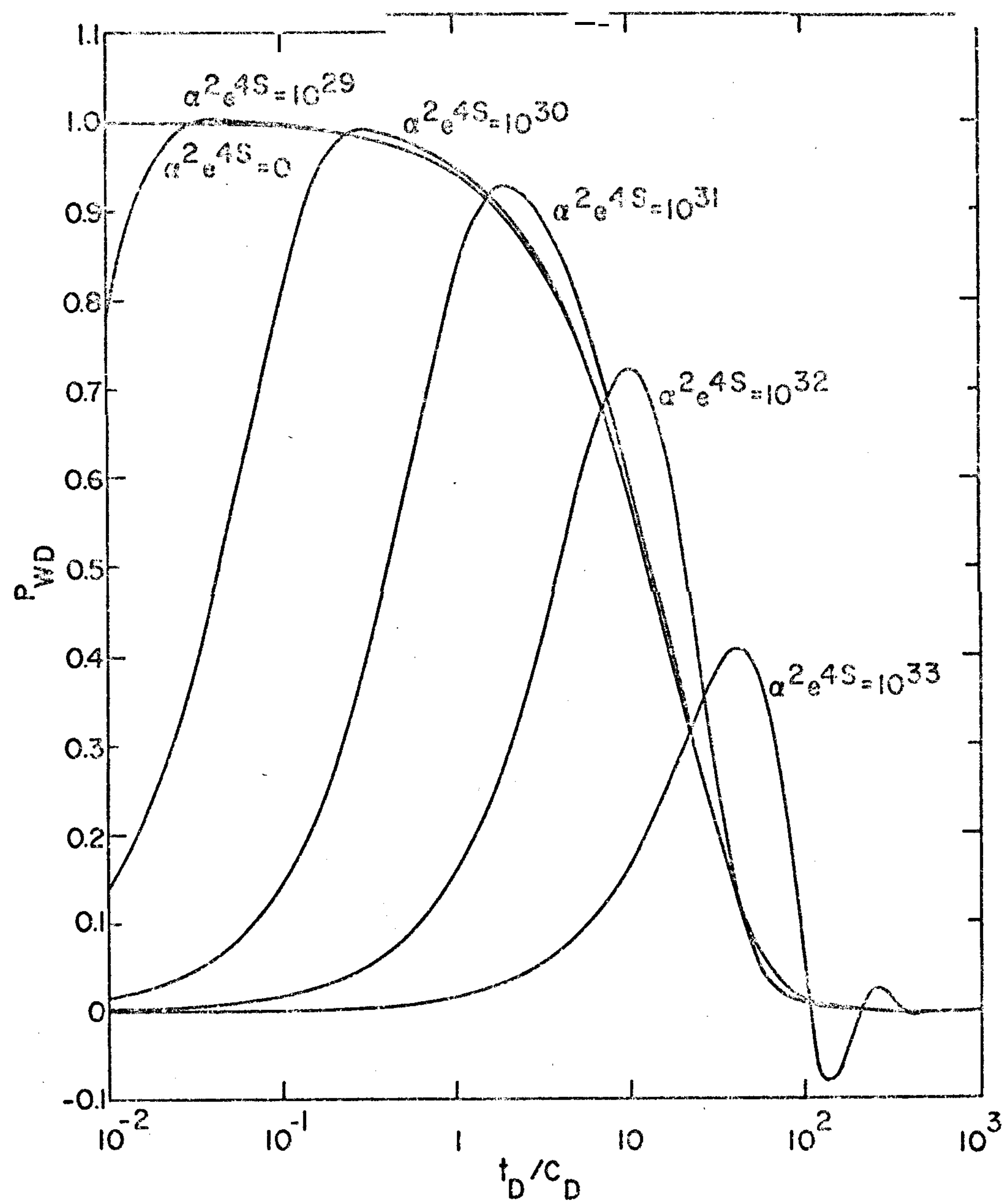

FIG. *45:* **DIMENSIONLESS WELLBORE PRESSURE VS t_D/C_D FOR $C_De^{2s} = 10^{15}$**

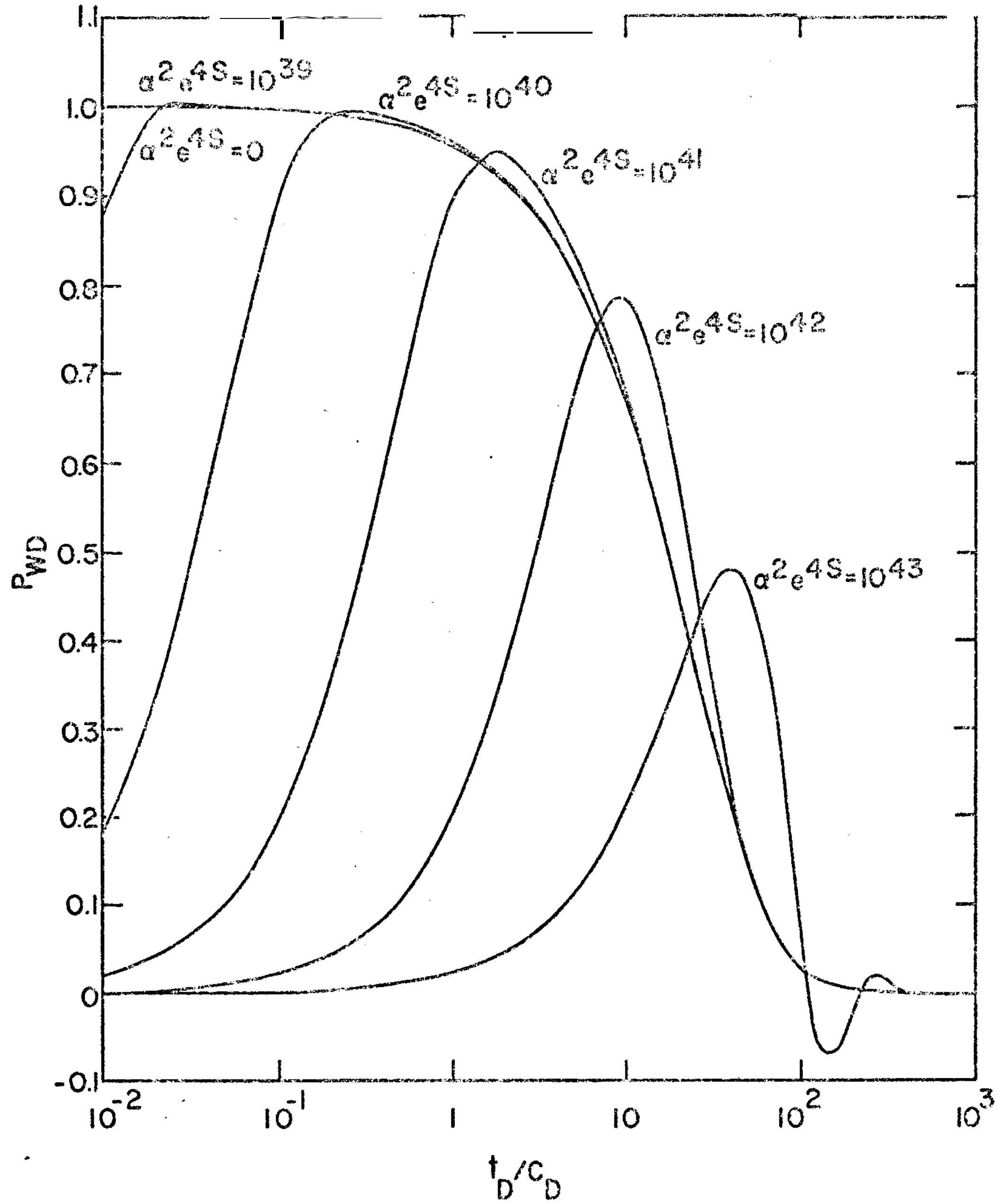

FIG. *46:* **DIMENSIONLESS WELLBORE PRESSURE VS** t_D/C_D **FOR** $C_De^{2s} = 10^{20}$

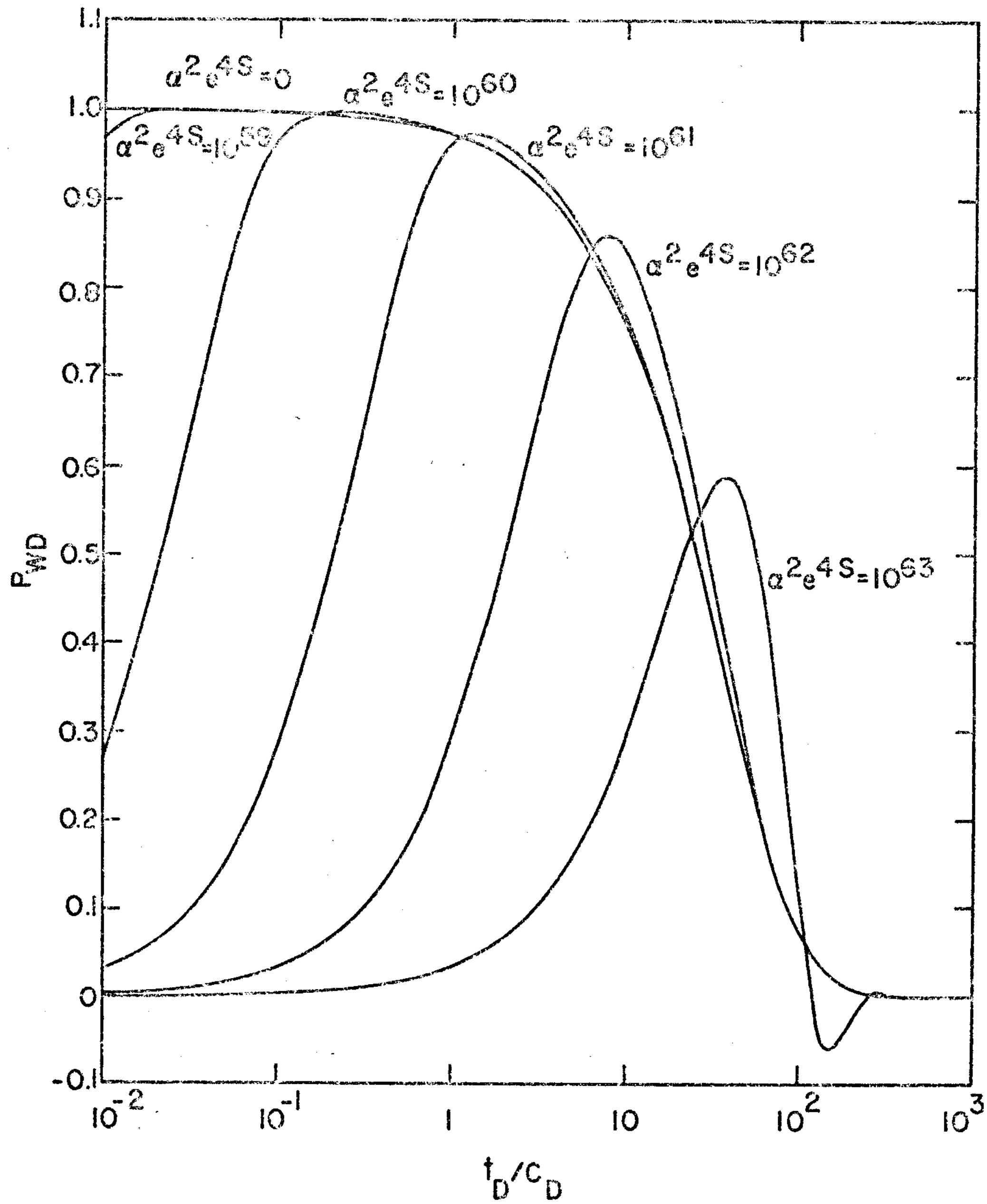

FIG. 47: **DIMENSIONLESS** WELLBORE **PRESSURE VS** t_D/C_D **FOR** C_De^{2s} = 1030

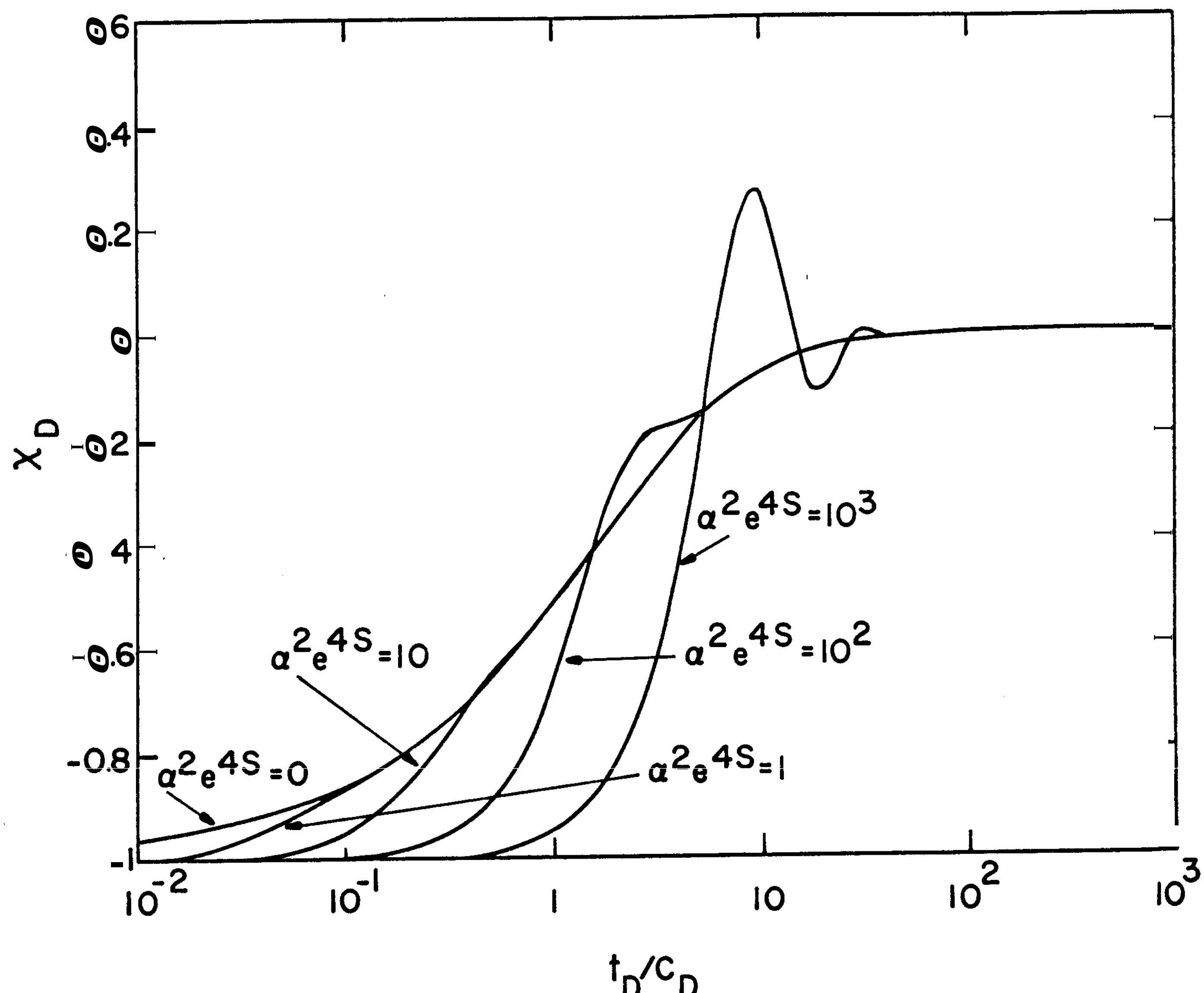

FIG. 48: DIMENSIONLESS LIQUID LEVEL IN THE WELLBORE VS t_D/C_D FOR C_De^{2s} = 10

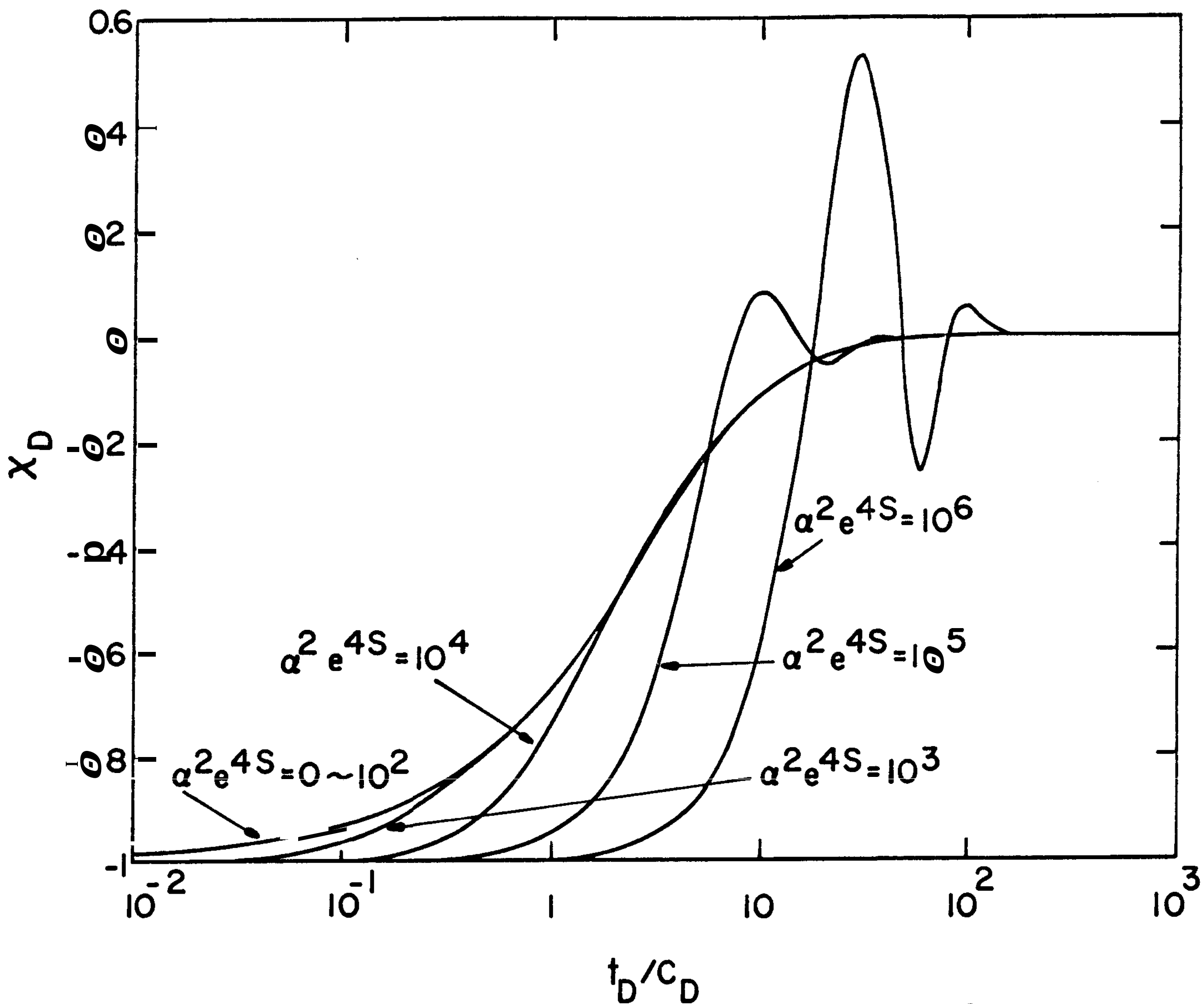

FIG. 49: DIMENSIONLESS LIQUID LEVEL IN THE WELLBORE VS t_D/C_D FOR $C_De^{2s} = 10^2$

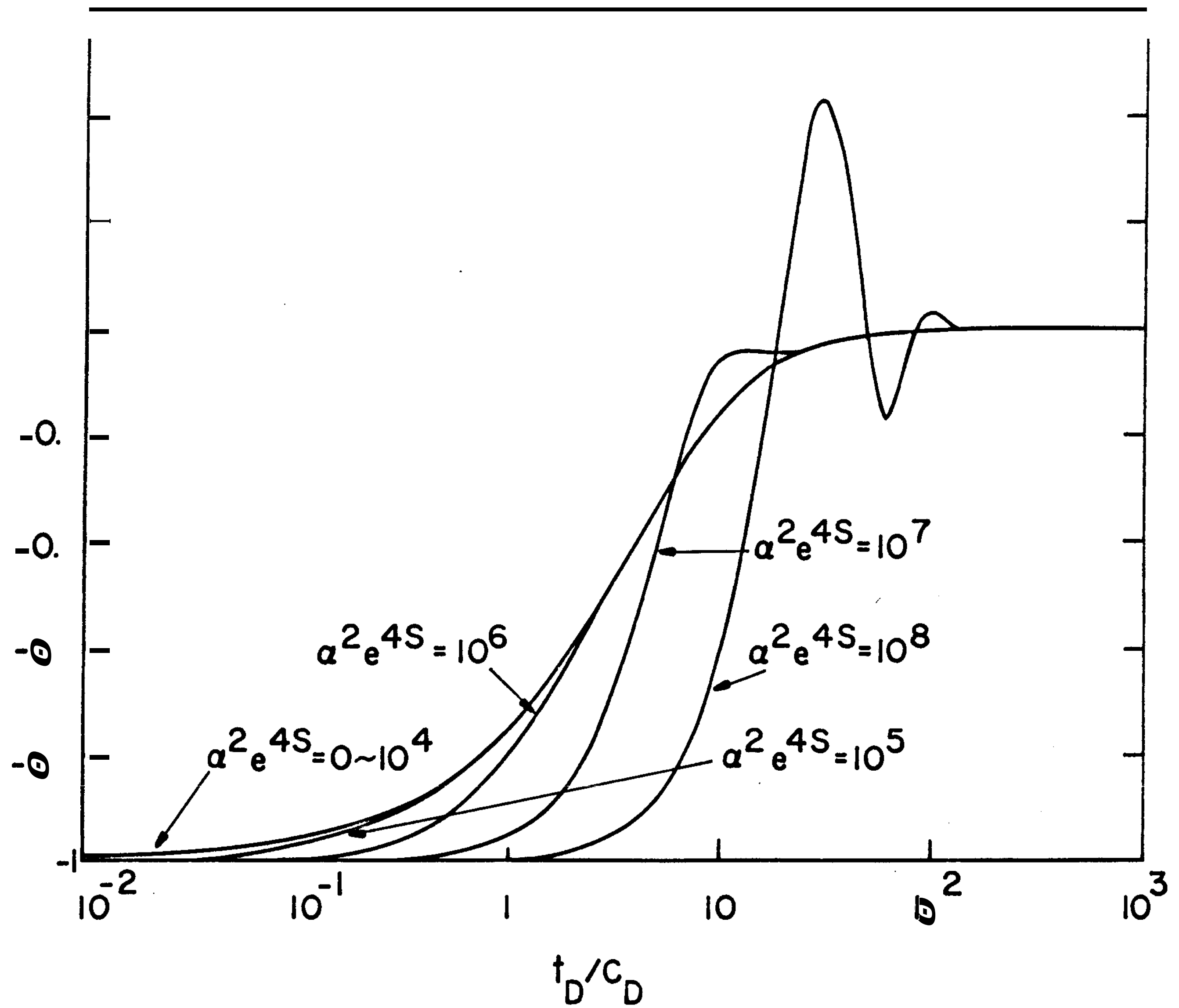

FIG. 50: DIMENSIONLESS LIQUID LEVEL IN THE WELLBORE VS t_D/C_D FOR $C_D e^{2s} = 10^3$

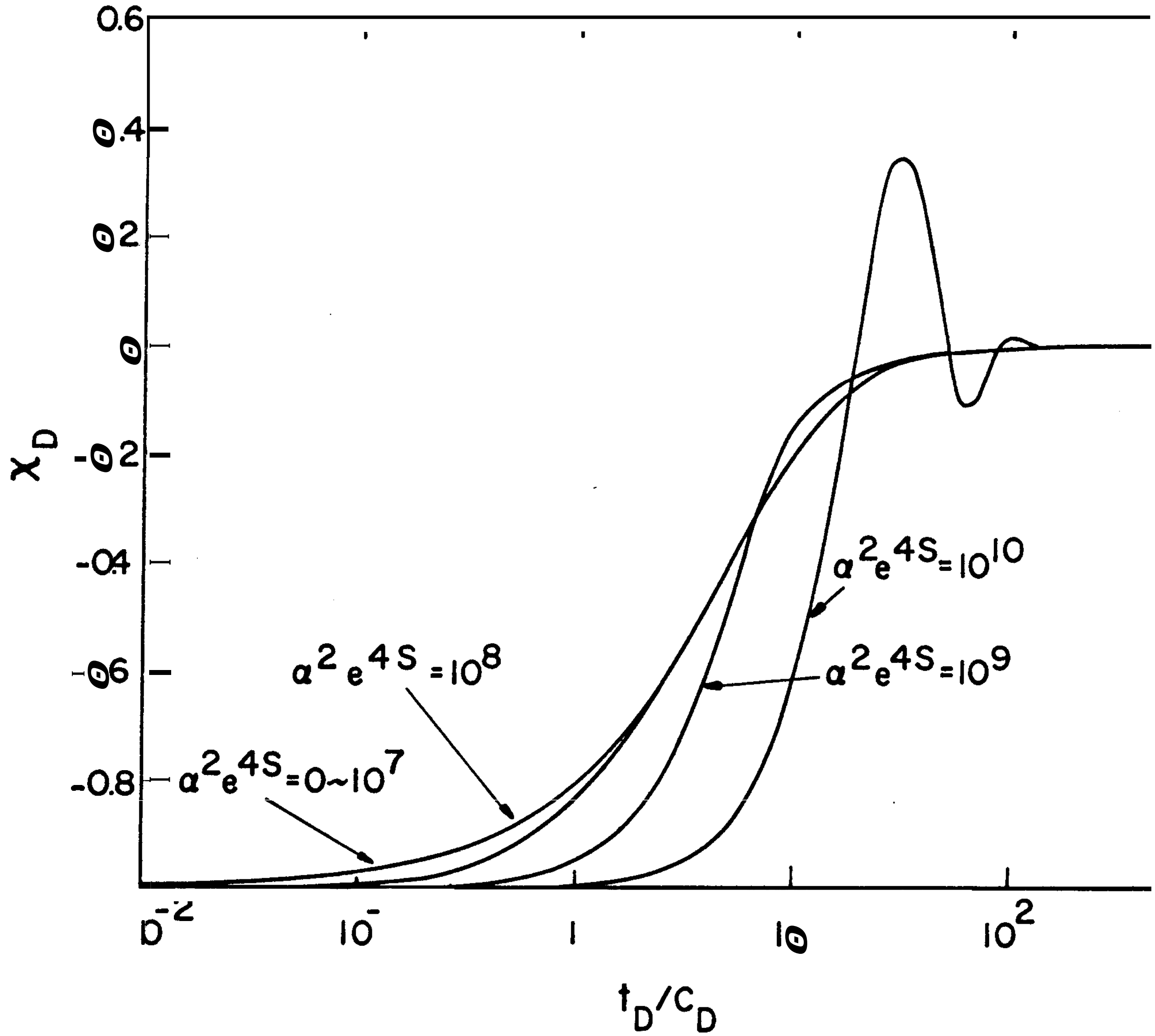

FIG. 51: DIMENSIONLESS LIQUID LEVEL IN THE WELLBORE VS t_D/C_D FOR $C_De^{2s} = 10^4$

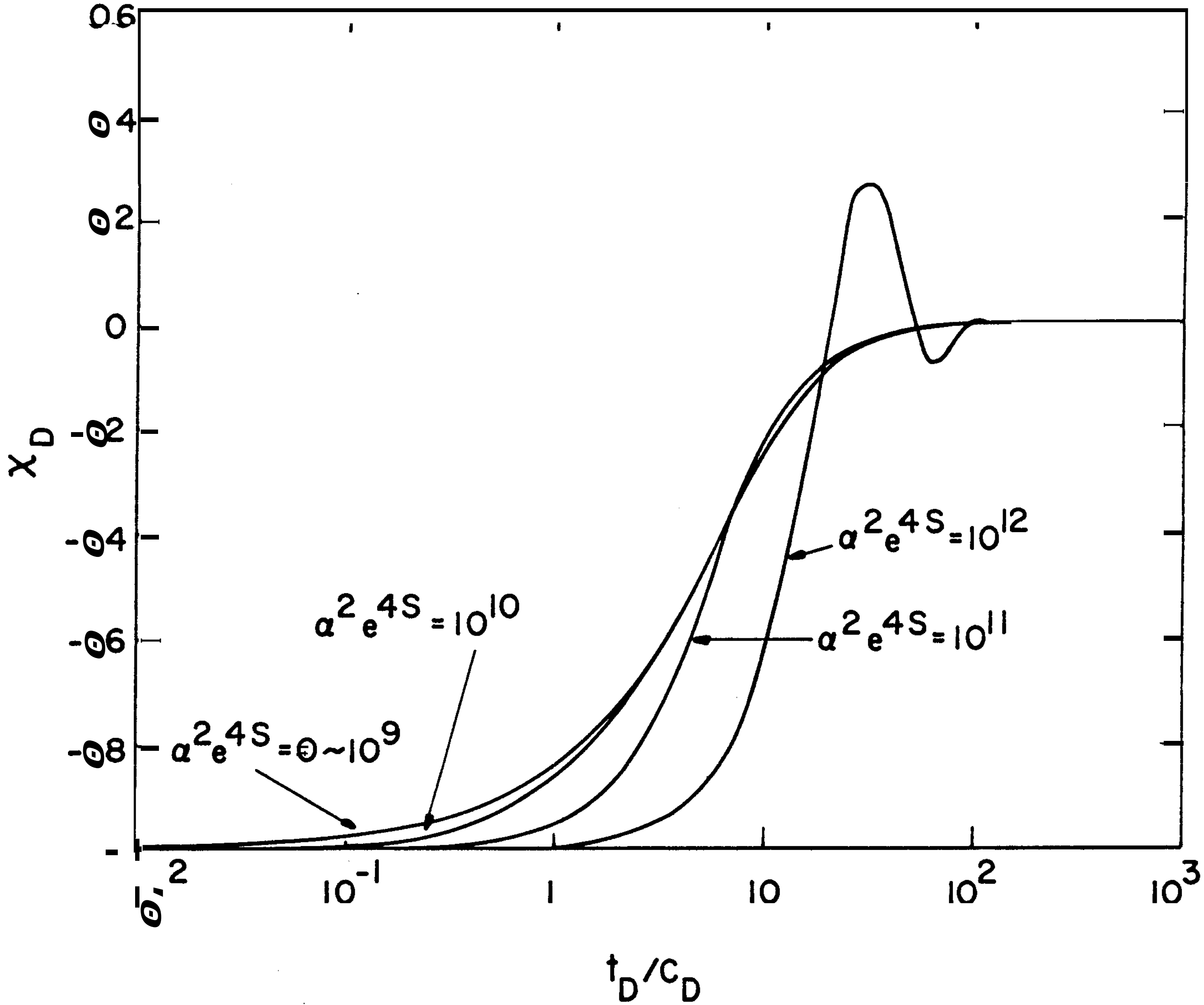

FIG. 52: DIMENSIONLESS LIQUID LEVEL IN THE WELLBORE VS t_D/C_D FOR $C_d e^{2s} = 10^5$

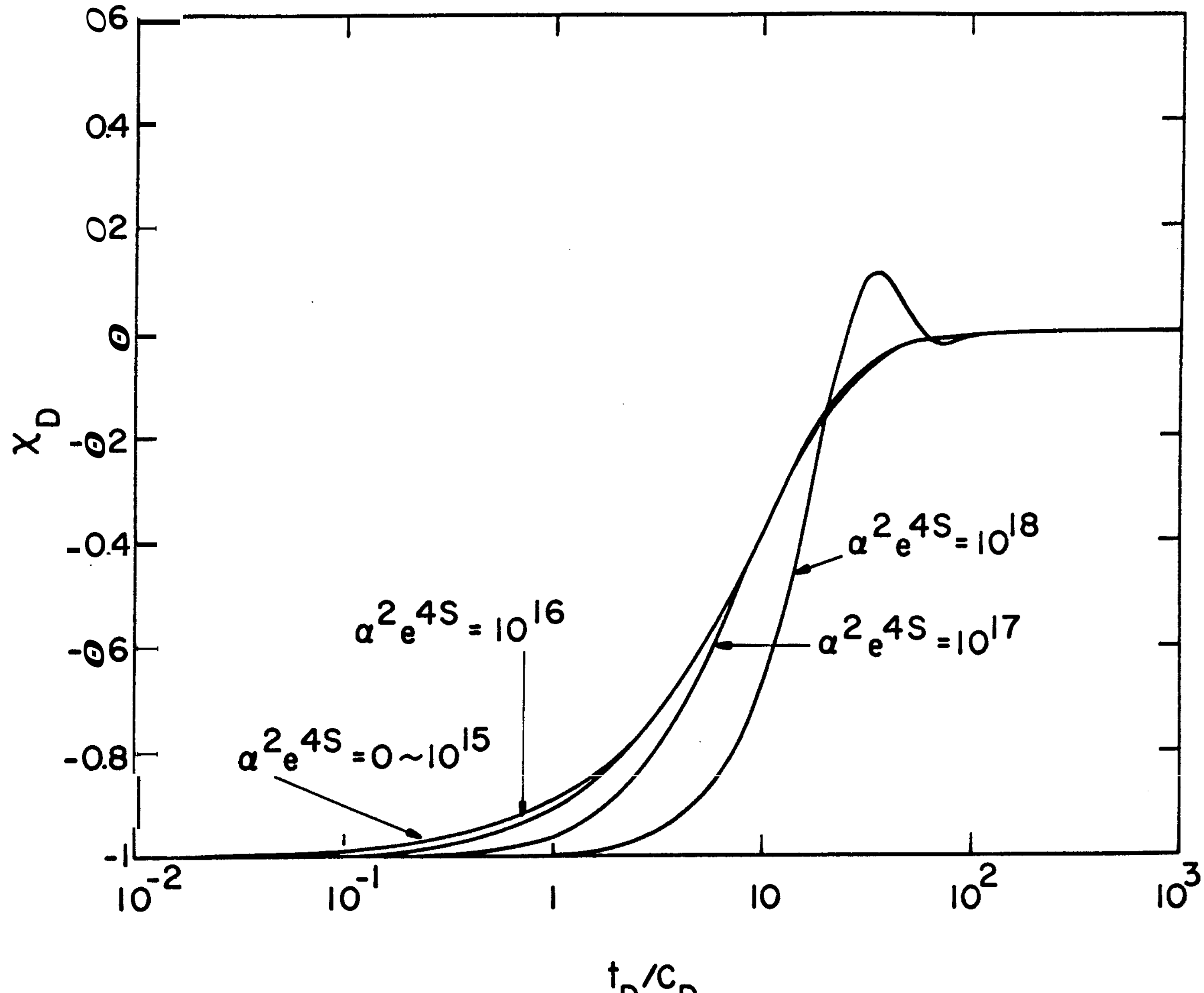

FIG. 53: DIMENSIONLESS LIQUID LEVEL IN THE WELLBORE VS t_D/C_D FOR $C_D e^{2s} = 10^8$

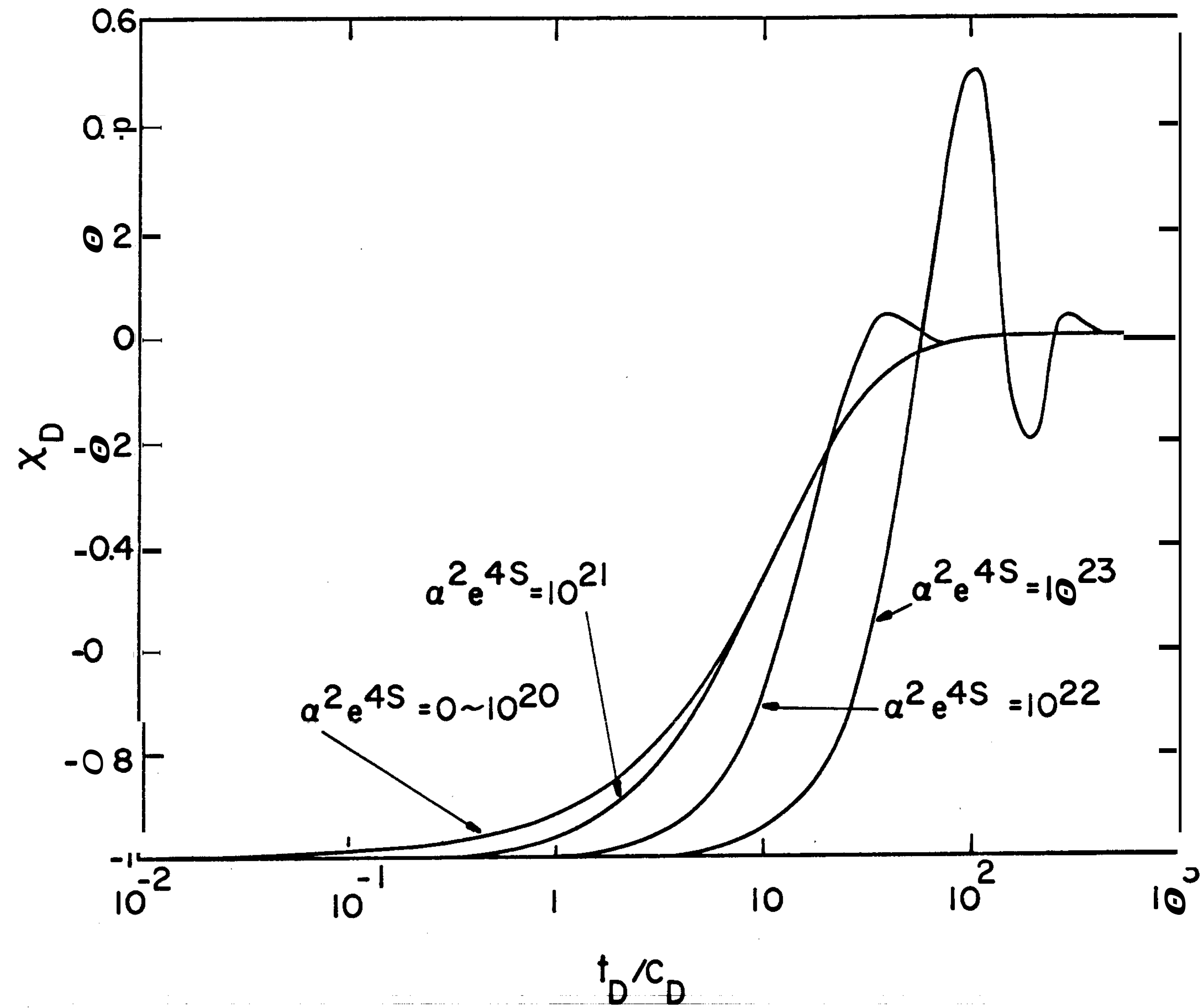

FIG. 54: DIMENSIONLESS LIQUID LEVEL IN THE WELLBORE VS t_D/C_D FOR $C_D e^{2s} = 10^{10}$

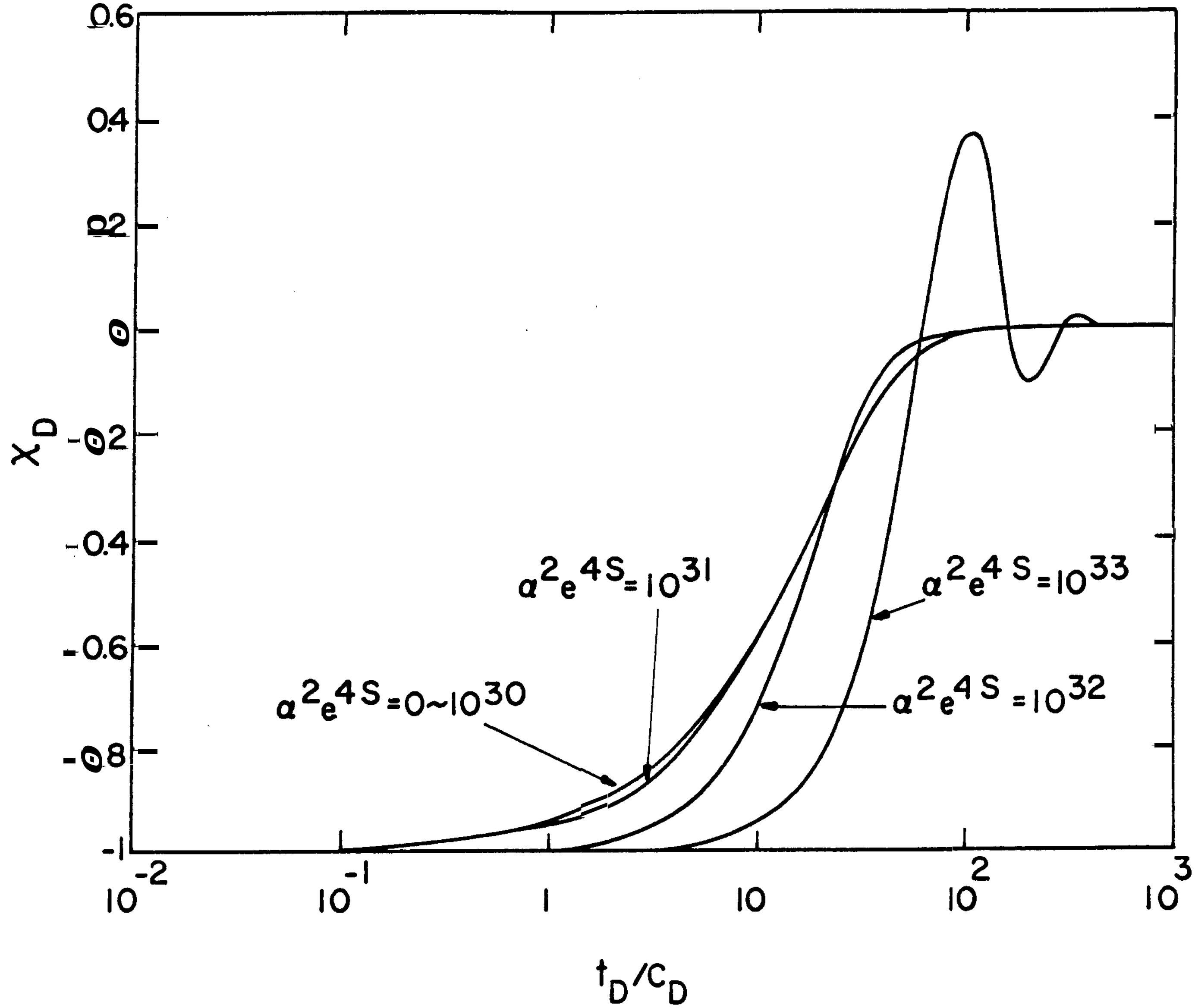

FIG. 55: DIMENSIONLESS LIQUID LEVEL IN THE WELLBORE VS t_D/C_D FOR $C_De^{2s} = 10^{15}$

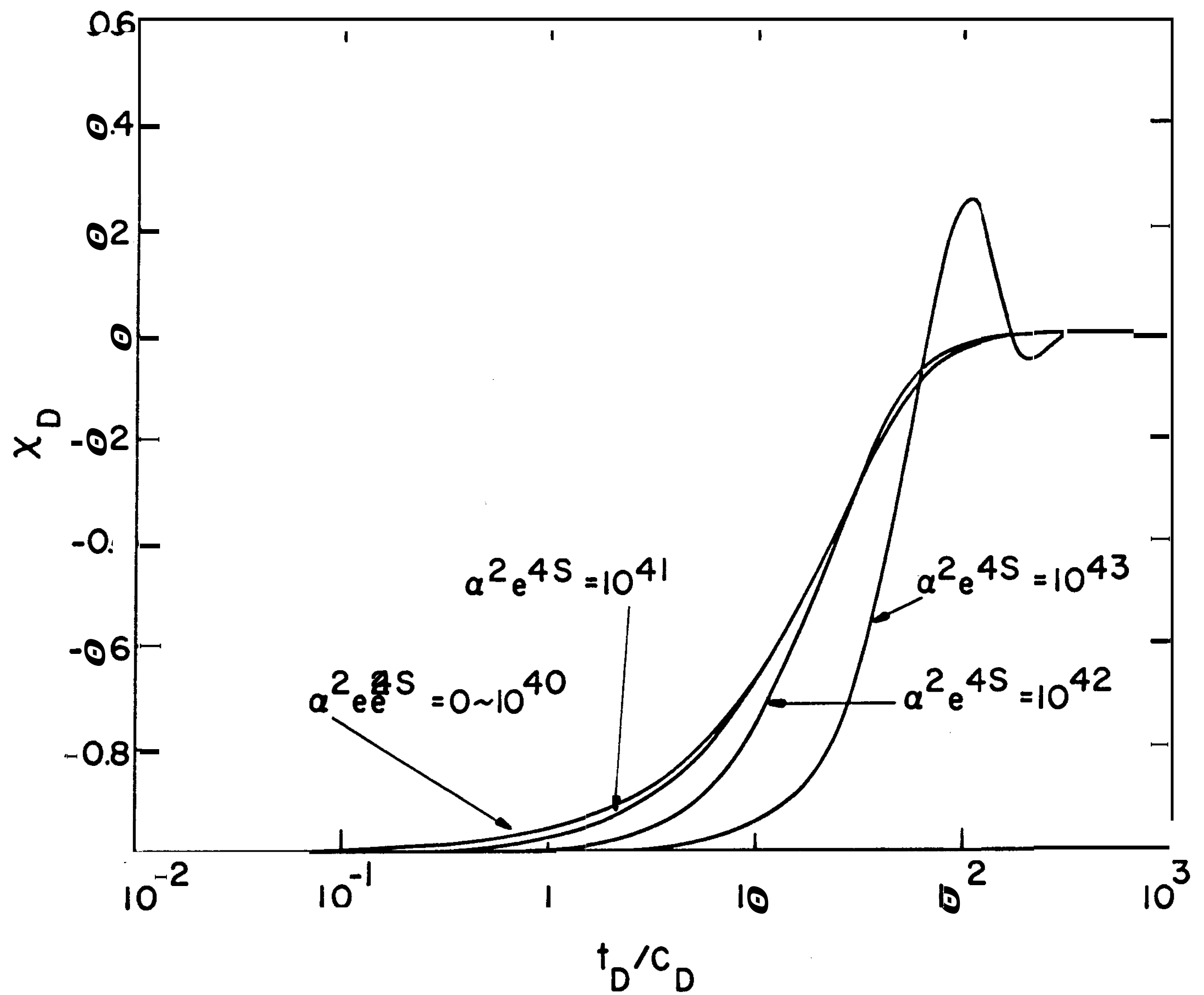

FIG 56: DIMENSIONLESS LIQUID LEVEL IN THE WELLBORE VS t_D/C_D FOR $C_D e^{2s} = 10^{20}$

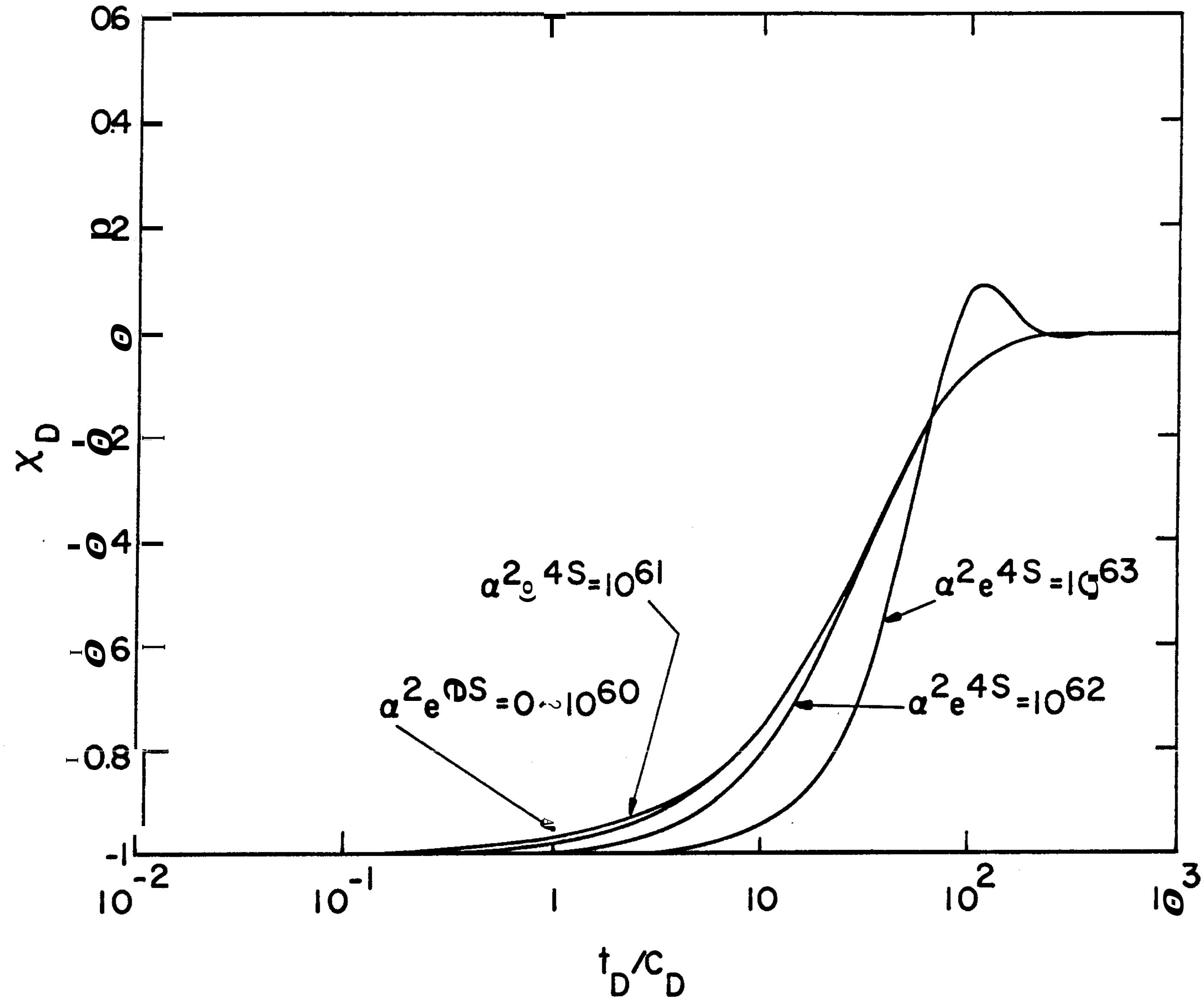

FIG. 57: DIMENSIONLESS LIQUID LEVEL IN THE WELLBORE VS t_D/C_D FOR $C_De^{2s} = 10^{30}$

First, we apply conventional slug test type-curves[13] to the field data. When there is a curve which matches the field data very well for the entire time range, we should calculate the skin factor and permeability from the matched points of C_De^{2s} and t_D/C_D. Using these values of skin factor and permeability, the α value and α_1 value can be obtained. If the α value is smaller than the α_1 value, the obtained permeability and skin factor are reliable, and this is the end of the slug test data analysis for this case. If the α value is greater than the α_1 value, we should proceed to the second usage of the solutions. When we cannot find a well-matched curve in the conventional slug test type-curves at the beginning, we have to go to the second usage of the solutions also.

One more way to utilize the solutions presented in this study is to use the solution curves in Fig. 38 through 57 as type-curves. This procedure may be adopted when the inertial effect of the liquid in the wellbore on the slug test data is not negligible, and therefore the conventional slug test data analysis cannot be applied. Thus far there is no method to analyze these data.

As mentioned before, it is practically impossible to select the suitable parameter values as C_De^{2s} by matching without knowing the skin factor, s, unfortunately. Therefore, we have to assume that the skin factor may be obtained by other methods, such as buildup test analysis. Then, we can choose the proper set of solution curves for a certain C_De^{2s} value from Figs. 38 through 57, or we can prepare the solution curves for this C_De^{2s} value using the computer program in Appendix E. Applying these solution curves to field data, the matched points of αe^{2s} and t_D/C_D can be obtained and the permeability can be calculated from either the matched α value or the matched t_D/C_D value. The methods presented herein can be applied to the analysis of both the wellbore pressure and the liquid level in the wellbore.

2-3 Field Data Examples

In order to investigate the slug test and check the validity of the solution obtained in this study, available field data were investigated using the solution. A few typical examples are shown and discussed in this section. The example 1 in Section 2-3-1 and the example 2 in Section 2-3-2 were published before as examples of slug test data. The example 3 has different results for the slug test analysis and the buildup test analysis. The reason for this difference is investigated in Section 2-3-3. The example 4 in Section 2-3-4 shows oscillations of the liquid level in the wellbore.

2-3-1 Example 1 (Typical DST Flow Period Data)

To use the slug test solutions presented in Figs. 38 through 47, it is necessary to know the correct value of the cushion liquid head; in other words, the pressure equivalent to the cushion liquid head, p_o. One should measure p_o before opening the tester valve. This pressure should not be replaced by the minimum wellbore pressure measured because it is shown in this study that the minimum measured wellbore pressure is not always equal to $(p_o + p_{atm})$. When the cushion liquid head is not known, a logarithmic coordinate for p_{wD} should be used in slug test type-curve matching to avoid the error caused by the incorrect cushion liquid head.

This example shows how field data can be misinterpreted because of an incorrect value of p_o. The data for this example were published by

Ramey et al.,[13] and reviewed in a previous paper.[33] The actual reservoir data and measured pressures are in Table C-1 in Appendix C. Figure 58 shows wellbore pressure versus time. There is a bend in the curve at early times. In the Ramey et al.[13] paper, the pressure measured at $t = 0$, 643 psig (4.53×10^6 p_a) was used as p_o. In a previous paper,[33] the extrapolated straight line at $t = 0$ in Fig. 58, 560 psig (3.96×10^6 p_a), was used as p_o. The former obtained kh = 698 md-ft (2.10×10^{-13} m^2-m) and s = 6.55, and the latter obtained kh = 763 md-ft (2.30×10^{-13} m^2-m) and s = 6.55. On the other hand, values of kh = 377 md-ft (1.13×10^{-13} m^2-m) and s = 0.80 were obtained from the buildup test analysis.[13]

Assuming that the initial cushion liquid head is not known, the log-log scale type-curves presented by Ramey et al.[13] were used in this study. It was found that the $C_De^{2s} = 10^5$ curve matches the field data best. However, it was almost impossible to select the best matched log-log type-curve without information from the buildup test analysis, because of the lack of data at late flow times. It is recommended that one should measure p_o before the test starts and obtain flow data at late times (for instance, until $p_{wD} \cong 0.01$) in a slug test. Figure 59 shows the matching result. From the matched points, kh = 420 md-ft (1.28×10^{-13} m^2-m) and s = 0.79 were obtained. These results are closer to results of the buildup test analysis than the previously reported results of slug test analysis.

The first two data points at early times in Fig. 59 appear to result from inertial effect. The same characteristics can be seen in the early time data in Fig. 58. However, this is not true. If the two early points in Fig. 59 show the effect of inertia, this means that α is about 1.4×10^4 and the permeability of the reservoir is about sixty times greater

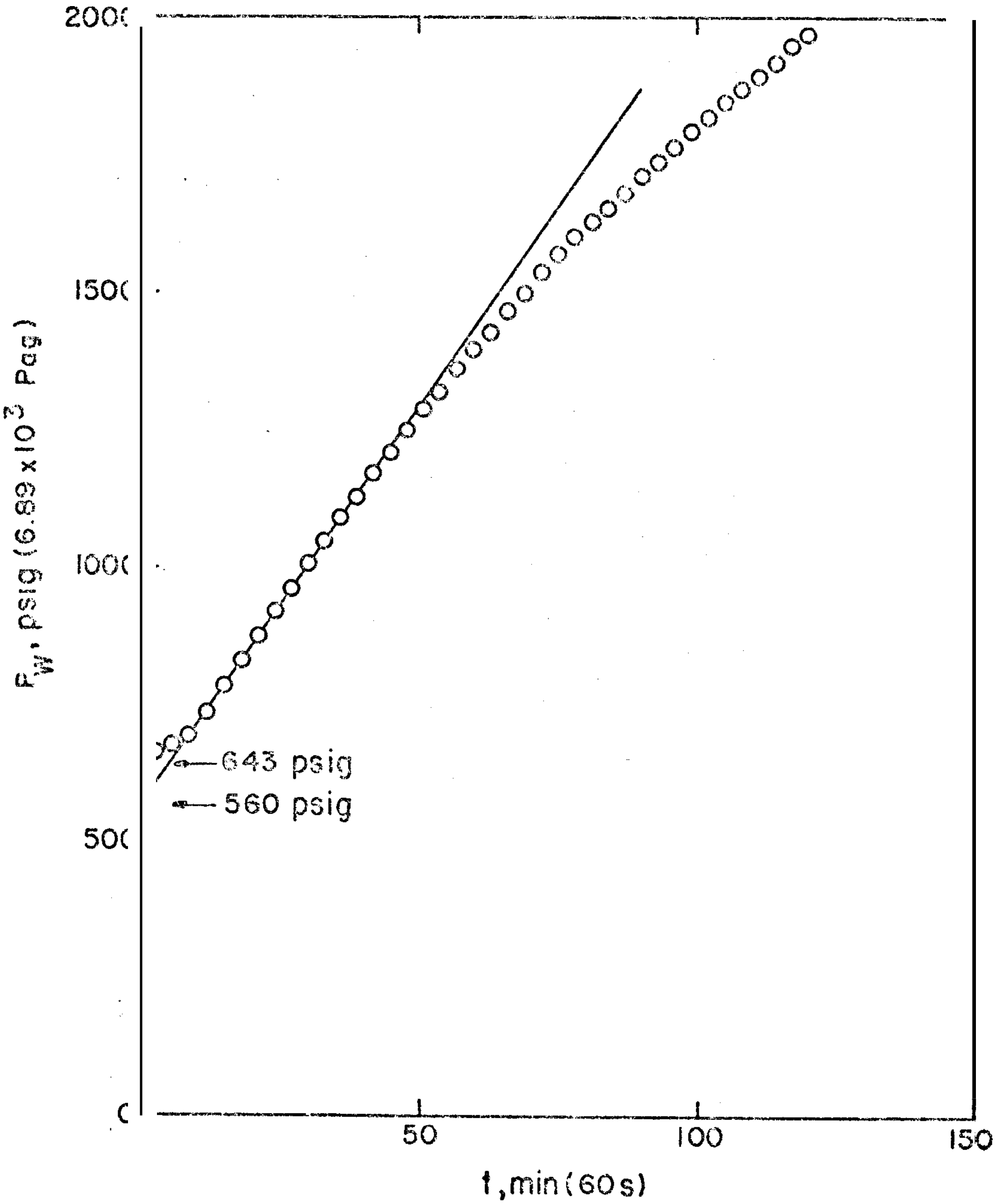

FIG. 58: FIELD DATA IN EXAMPLE 1

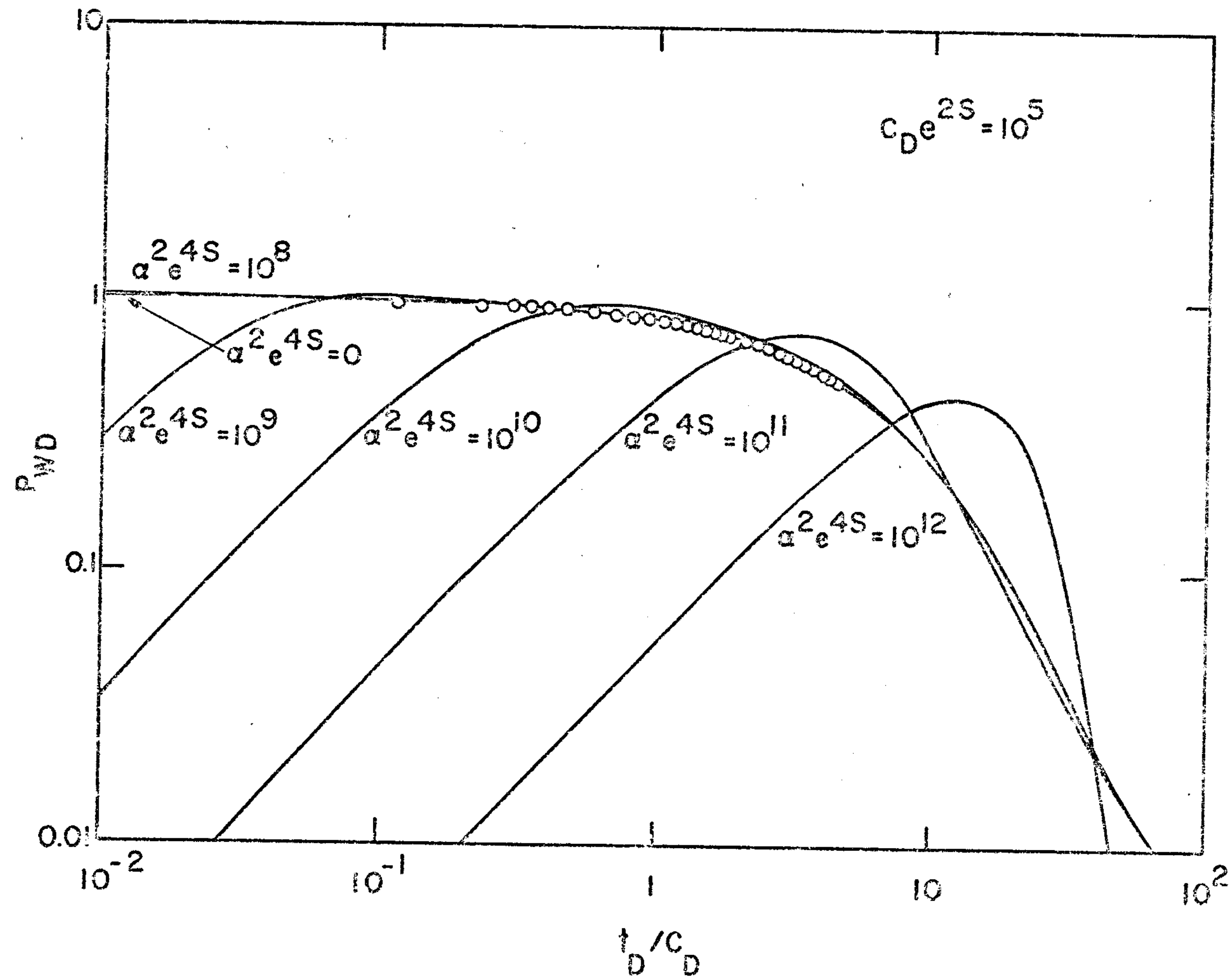

FIG. 59: RESULT OF MATCHING IN THE LOG-LOG SCALE IN EXAMPLE 1

than that obtained from the buildup test analysis. This is not likely, because we believe at least the order of magnitude of the result of the buildup test analysis. Therefore, we conclude that the first three points of the field data were not caused by the inertia of the liquid in the wellbore.

In order to make certain that we can neglect the inertial effect of the liquid in the wellbore on the field data, the dimensionless number α_1 was calculated using Eq. 72:

$$\alpha_1 = 5.81 \times 10^3$$

Using the result of slug test data analysis in this study:

$$\alpha = 2.73 \times 10^2$$

Since the field example α value is less than α_1, it can be said that the inertial effect is negligible for this slug test analysis.

The apparent constant flowrate period at early times which appeared in this example cannot be explained by the large skin effect proposed in this study. This might be caused by critical flow somewhere in the wellbore, as suggested by Ramey et al.[13] and reviewed by Earlougher.[14]

Finally, in order to check whether the assumption that the friction loss in the wellbore is negligible is reasonable or not, the actual pressure drop by friction in the wellbore was calculated in Appendix C. The magnitude of the pressure drop by friction is very small even though the flow is turbulent. The neglect of friction appears to be reasonable for this example.

2-3-2 Example 2 (Understanding Field Data)

This field example was first presented by Kohlhaas[6] and was used as an example of the flow period data interpretation. Later this example was investigated further by Ramey et al.,[13] and by a previous paper.[33] The actual data are shown in Table C-2 in Appendix C. Figure 60 shows the interpretation of these data in the previous study.[33] The initial portion of the pressure-time curve is linear (dashed line). The bend in the data is caused by a change in diameter from the drill collar (2.5 in. [6.35×10^{-2} m] ID) to the drill pipe (3.8 in. [9.65×10^{-2} m] ID). The second portion of the pressure-time curve is linear again. However, this interpretation of the data might not be correct. Figure 61 shows the slug test solution in dimensionless form for this example based on the results of the buildup test data analysis, $C_D = 1.77 \times 10^4$, k = 56.7 md (5.60×10^{-14} m^2), s = 44.6, and $\alpha = 5.99 \times 10^2$. The straight portion of the line at early times can be seen because of the large skin factor. Figure 62 shows a comparison between the field data and the calculated results. The calculated results based on the actual p_o = 161 psig (1.21×10^6 p_a) agree with the field data (except for some early time points) better than the calculated results based on an adjusted p_o = 205 psig (1.51×10^6 p_a) do. This means that the first interpretation of the data is wrong if we believe that the results of the buildup test data analysis are reliable. The reason for the overshooting at early times is not clear, even though this phenomenon looks similar to the result of wellbore phase redistribution on buildup tests reported by Fair.[35]

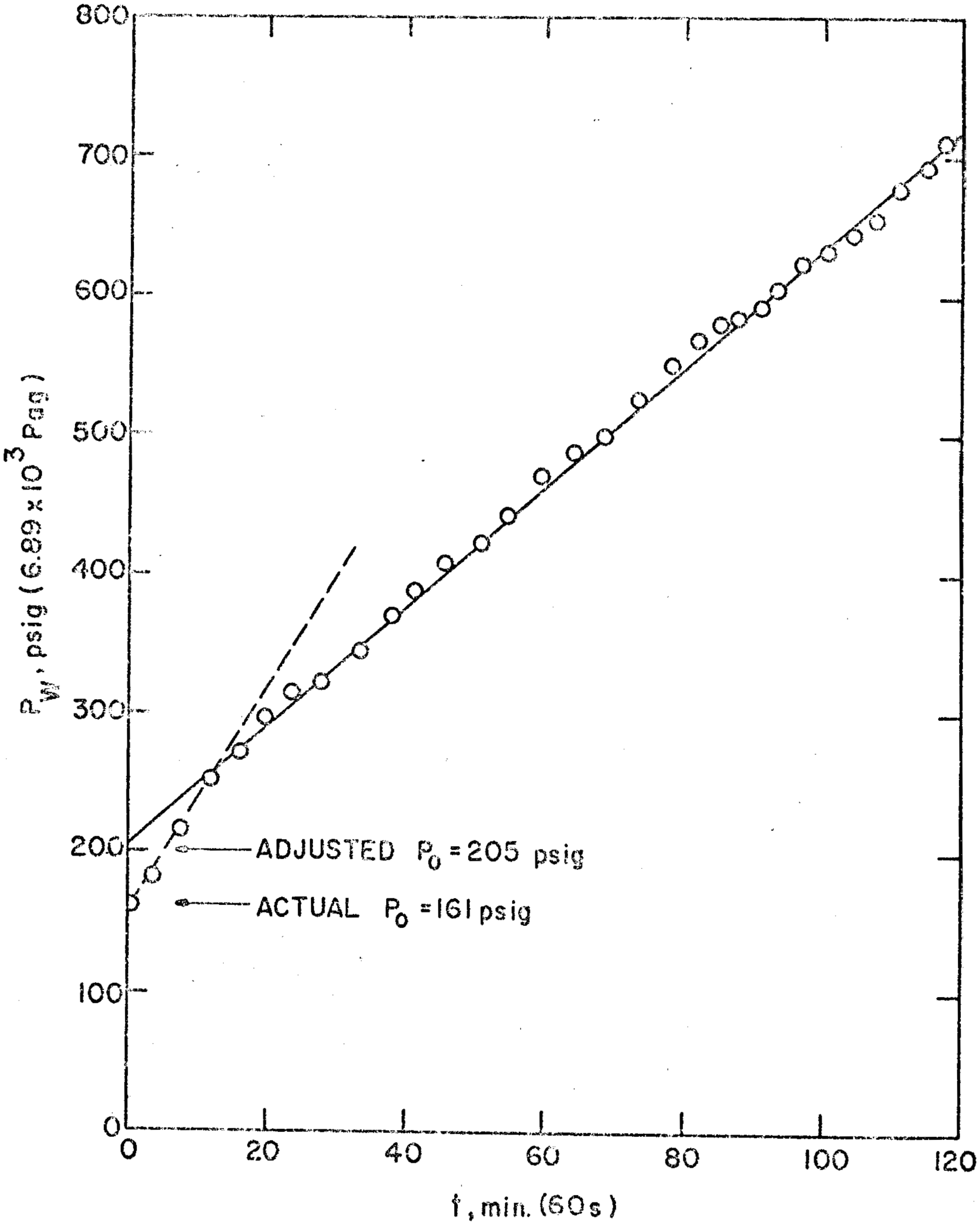

FIG. 60: FIRST INTERPRETATION OF THE DATA IN EXAMPLE 2

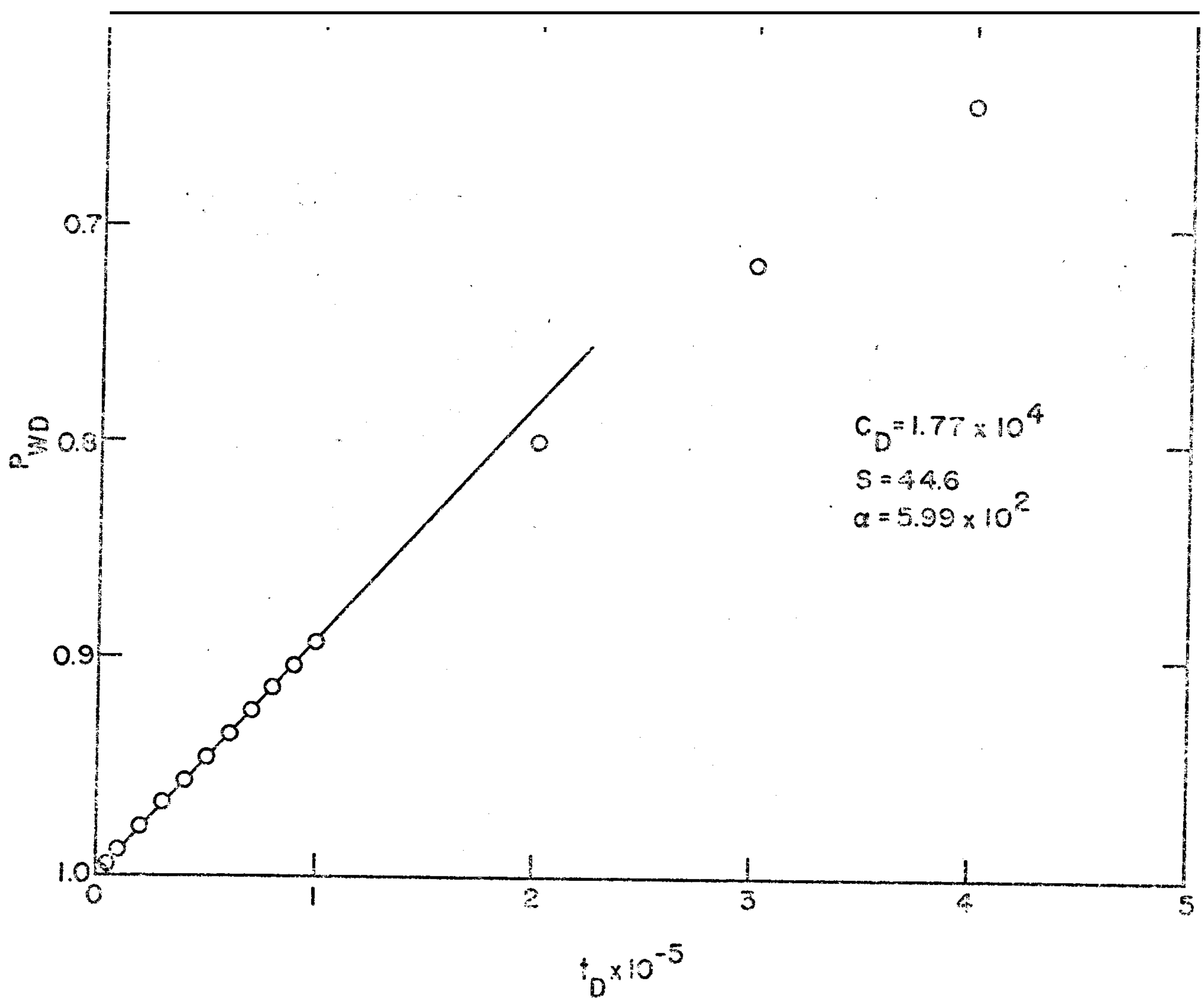

FIG E1: SLUG TEST SOLUTION IN DIMENSIONLESS FORM IN EXAMPLE 2

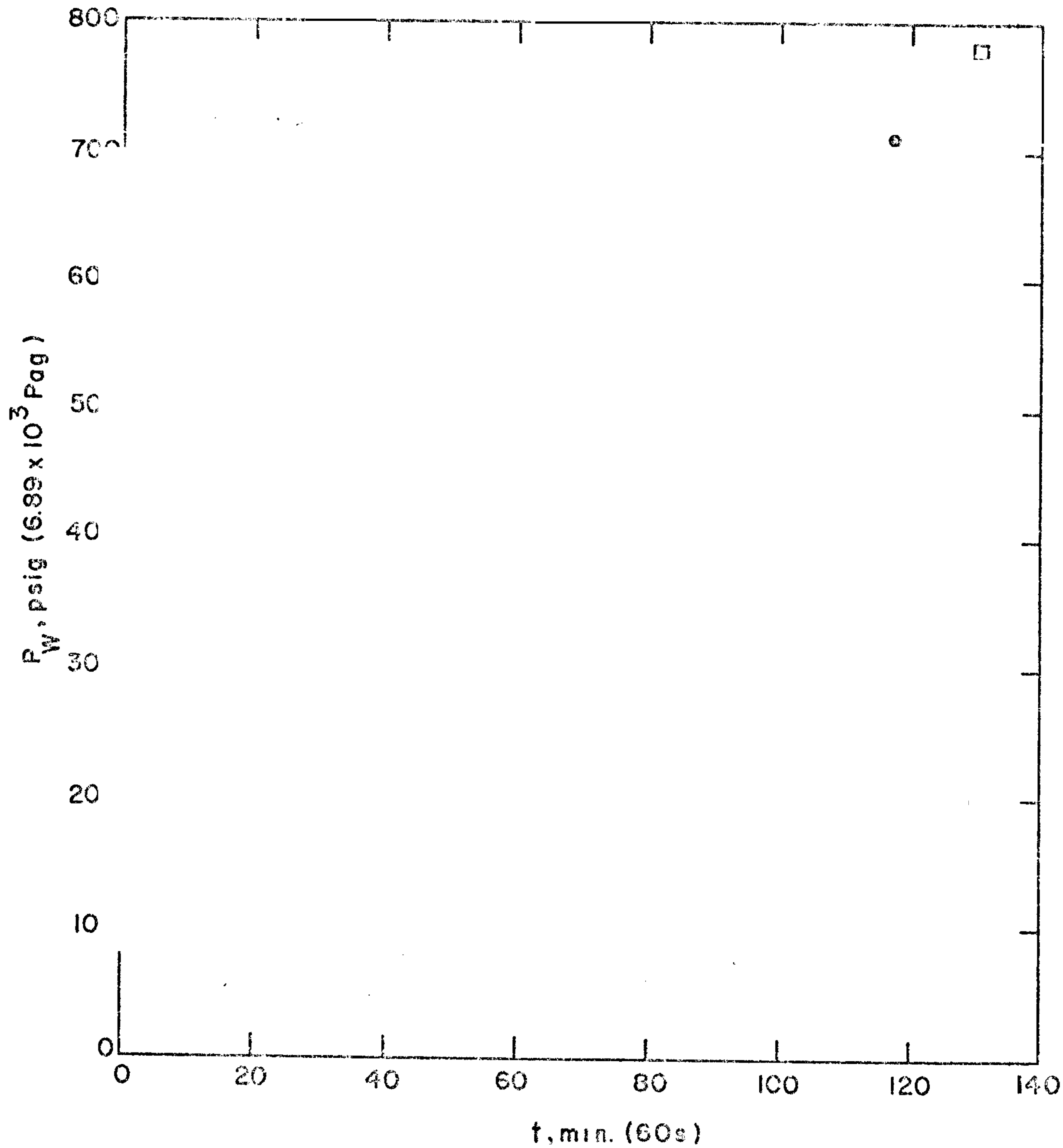

FIG. 62: COMPARISON OF ACTUAL DATA AND CALCULATED RESULTS IN EXAMPLE 2

2–3–3 Example 3 (Comparison of Results of Slug Test Analysis and Buildup Test Analysis)

The data in this example were presented in a previous study.[33] The reservoir data and the measured pressure are shown in Table C–3 in Appendix C. Not only the flow period data, but also the buildup data are available. It is reported that there is a significant difference between the result from the slug test analysis and that from the buildup test analysis, and th t such a difference is often observed. Also, it is suggested that the result from the buildup test analysis is more reliable than that from the slug test analysis by several investigators,[6,13,33] because it is difficult to match the data for large values of C_De^{2s} uniquely in the slug test analysis. According to the slug test analysis, **k** = 2,452 md (2.42×10^{-12} m^2) and **s** = 24.3. These results agree well with those from log–log type–curve matching in slug test analysis. This means that the measured p_o is reliable. On the other hand, following the buildup test analysis, **k** = 4,321 md (4.26×10^{-2} m^2) and s = 33.4. The dimensionless wellbore storage constant, C_D, is 8.64x103. Similar to Example 1, if the results from the slug test analysis are used, $\alpha = 3.46 \times 10^2$ and $\alpha_1 = 1.14 \times 10^4$. Since $\alpha < \alpha_1$, the result obtained by using the conventional slug test solution is reliable. If the results from the buildup test are used, $a = 6.12 \times 10^2$. Using the solutions in this study based on these data, the flow period data were calculated. Figure 63 shows the result. The calculated points based on the slug test analysis agree with the field flow period data very well; however, the calculated results based on the buildup test analysis do not agree with the field flow period data. In order to investigate the reason for this difference, the buildup was simulated by the finite difference solution which is explained in Appendix D, and

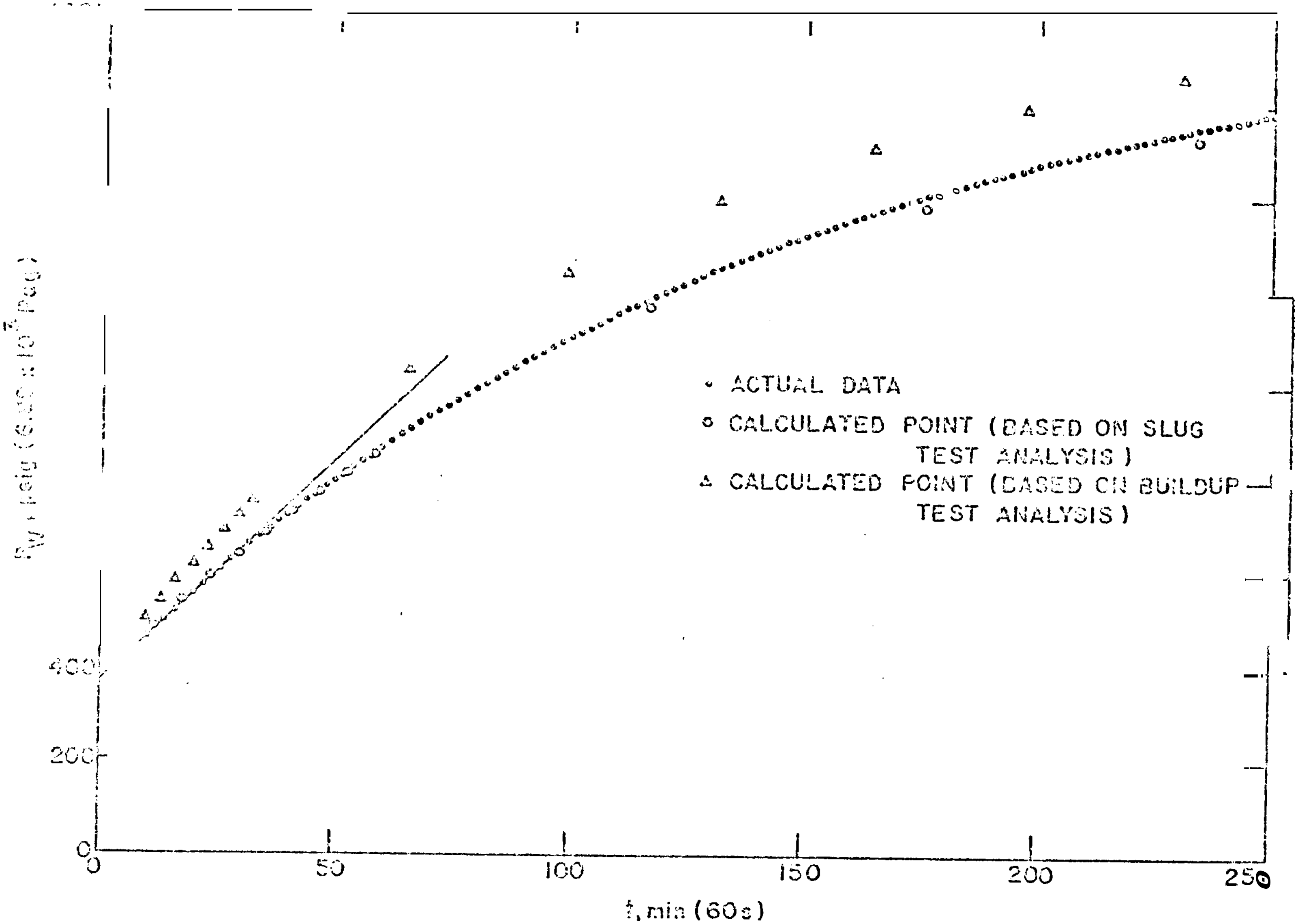

FIG. 63: COMPARISON OF ACTUAL DATA AND CALCULATED RESULTS IN EXAMPLE 3

whose computer program is in Appendix E. Figures 64 and 65 show the simulation results based on the slug test analysis and the buildup test analysis, respectively. It appears that the depth of investigation is almost the same for both the slug test and the buildup test. Figure 66 shows the field data and the calculated points on a Horner buildup graph. Since we do not know the external radius of the reservoir, we assumed that the reservoir is almost infinitely large by setting $r_{D_e} = 10^5$ in the simulation. This is one of the reasons why there is some difference between field data and the calculated values. However, since $p_w = p_i - p_{wD} \{ p_i - (p_o + p_{atm}) \}$, we can shift the calculated points up and down in parallel by changing the initial formation pressure, p_i. Then this difference has no significance. Our interest is in the slope of the line. The slope of the line of calculated points based on the slug test analysis is about 12.5 psi/cycle (8.62×10^4 Pa/cycle), as shown as slope 1 in Fig. 66. This slope corresponds exactly to the permeability which is obtained from the slug test analysis and used to calculate the dimensionless numbers. The slope of the line of calculated points based on the buildup test analysis is about 7 psi/cycle (4.83×10^4 Pa/cycle), as shown as slope 2 in Fig. 66. Again, this slope corresponds to the permeability obtained from the buildup test analysis based on the final flowrate. We can find a line which has a slope the same as the slope 1 and passes through some field data points at early times, and a line whose slope is the same as the slope 2 and connects field data points mainly at late times, as shown in Fig. 66. This means that the result of slug test analysis corresponds to the buildup test data at early times, and the result of the buildup test analysis corresponds to the buildup data at late times. On the other hand, judging from the result of the buildup simulation, only one semilog

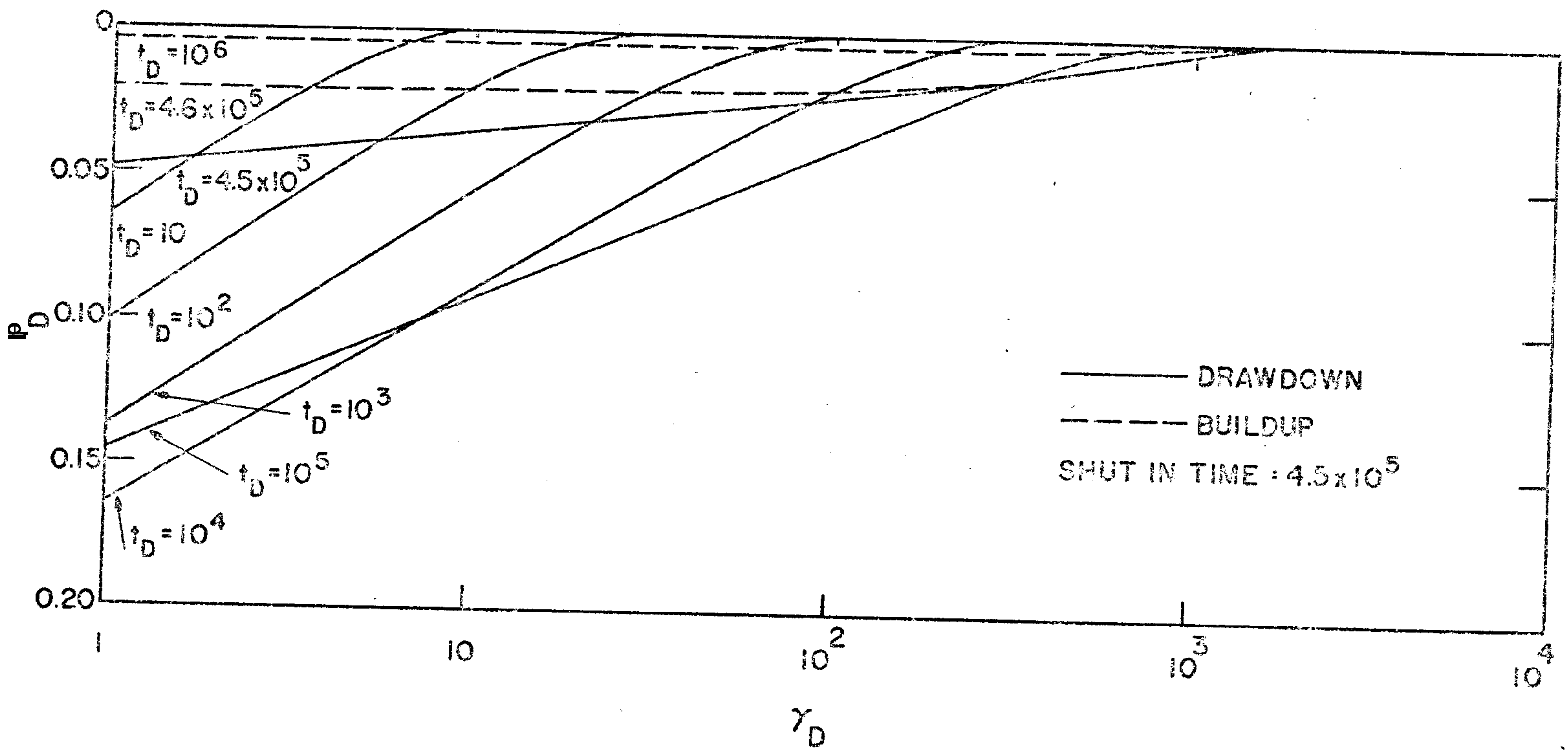

FIG. 64: PRESSURE DISTRIBUTION INSIDE THE RESERVOIR BASED ON SLUG TEST ANALYSIS IN EXAMPLE 3

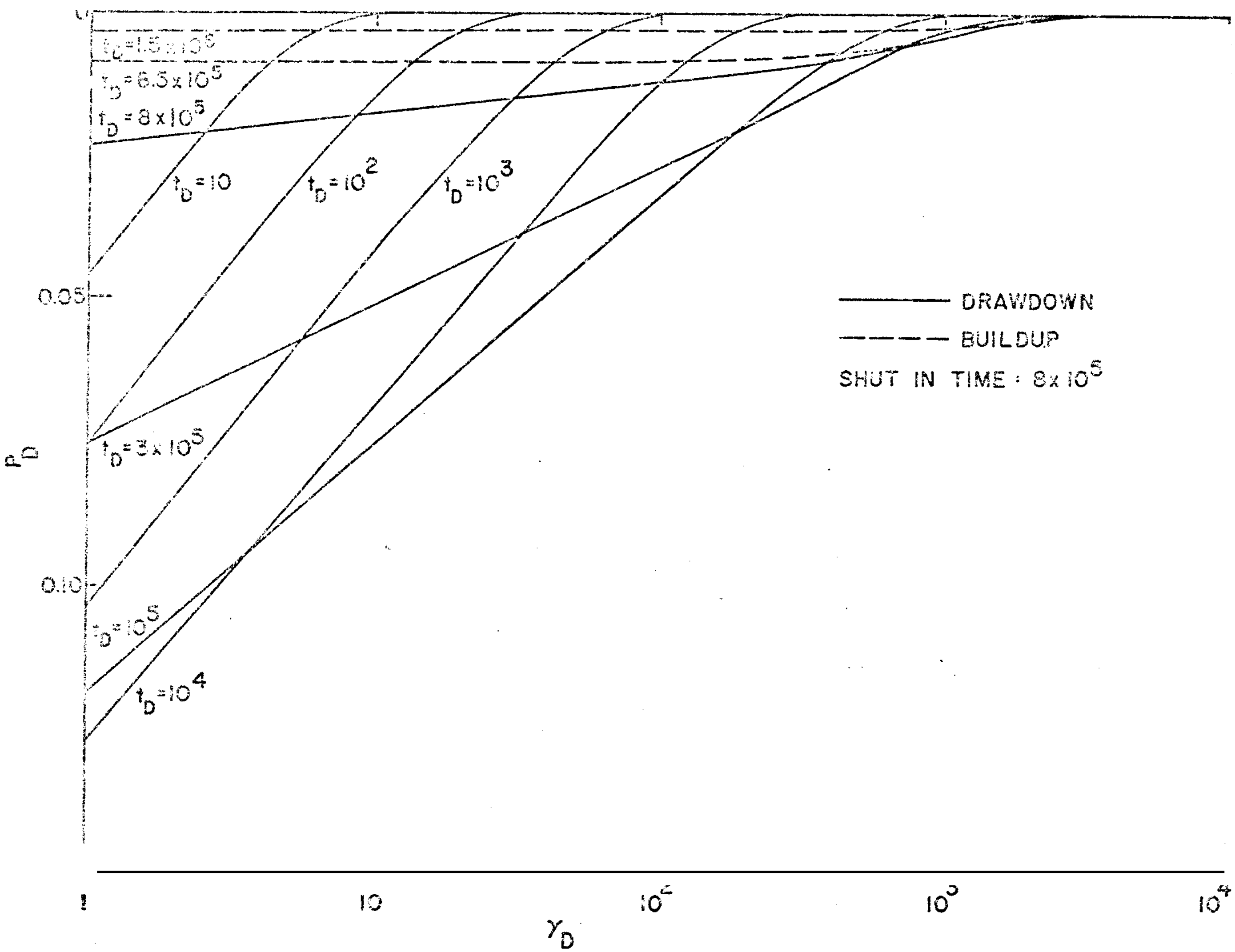

FIG. 65: PRESSURE DISTRIBUTION INSIDE THE RESERVOIR BASED ON BUILDUP TEST ANALYSIS IN EXAMPLE 3

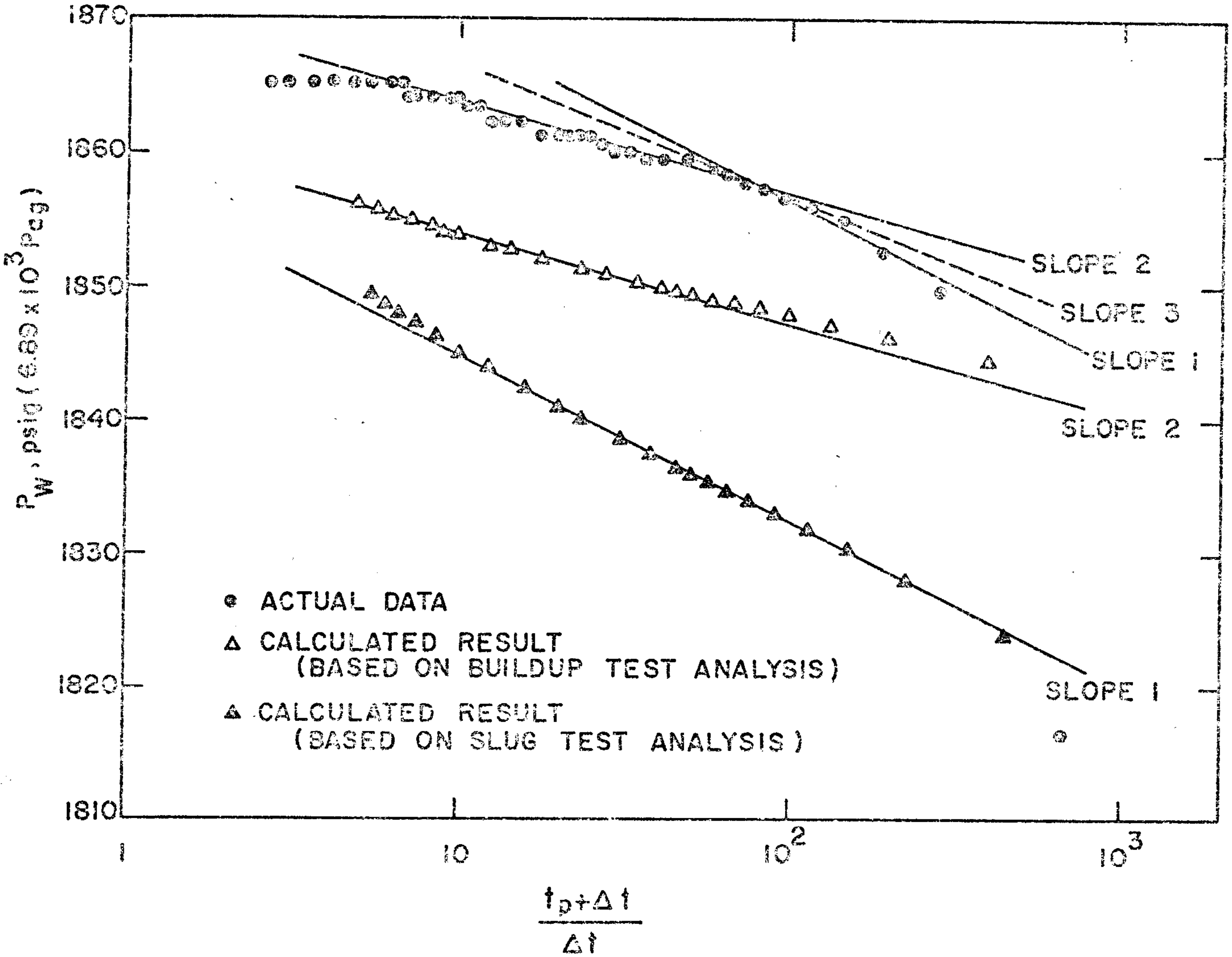

FIG. 66: COMPARISON OF ACTUAL DATA AND CALCULATED BUILDUP RESULTS FOR EXAMPLE 3

straight portion should be apparent on the Horner graph as long as the assumption that the reservoir is homogeneous holds. Therefore, it appears likely that this reservoir is not homogeneous, and this has been recently reported in another study,[36] in which the dashed line with the slope 3 in Fig. 66 was used for the buildup analysis. This heterogeneity explains why there is a bending of the line at late times, as shown in Fig. 66, which looks like the effect of a boundary, although there is little possibility that the boundary is apparent in short-time well tests. This heterogeneity appears to be the main reason why the different results were obtained by the slug test analysis and by the buildup test analysis. In summary, the slug test analysis gives some reasonable results, as does the buildup test analysis, and if there is a significant difference between the results of the two, we should search for the reason. This should increase understanding of the reservoir.

The slopes of the lines of calculated results based on both test analyses seem to become larger at long buildup times. The reason for this is not clear, although it is probably caused by the pressure gradient inside the reservoir at the shut-in time. This gradient, reflects the declining flowrates during production, and has a convex portion in the reservoir. How long the semilog straight portion in the Horner graph appears in the buildup data after a short-time production is beyond the range of this study. Buildup behavior in DST analysis deserves further attention. It is noteworthy that Fenske[37] reported recently that pressure buildup data for a well produced for a short time should follow the slug test typecurves. Thio observation means that the slug test solution should be proper for at least the initial cleanup buildup data, as well as for the flow period data. Buildup analysis after short-time production should be studied in the near future.

Similar to Example 1, the pressure drop caused by friction in the wellbore was calculated for this example in Appendix C. The order of magnitude of the friction loss was still small, even though not as small as that for Example 1. The assumption of negligible friction seems to hold for this example case also.

2-3-4 Example 4 (Oscillation Case)

The data for this example are from a water well test, and were presented by van der Kamp.[16] The solid lines in Figs. 67 and 68 show the measured liquid level in the wellbore for a well called 2-C and another well called 9-A, at New Brunswick, Canada, respectively. The liquid level read from these graphs are in Table C-4 in Appendix C. The liquid level in the wellbore of the well 2-C shows an oscillation, and the liquid level in the wellbore of the well 9-A shows no oscillation. The properties of the well-aquifer system were given in ground water hydrology symbols. The correspondence between the symbols used in ground water hydrology and those used in petroleum engineering were reported by Ramey et al.[11] Table 10 shows this correspondence, including the new dimensionless number, α, proposed in this study. In van der Kamp,[16] different values were reported as the properties of the well-aquifer system as the results of the pump test and the response test. We selected values which yield better results in the simulation. Table 11 summarizes the values used. Figure 67 shows a comparison between the field data and the calculated results for the well 2-C using the slug test solution presented in this study. The calculated results based on the transmissivity, $T = 0.0061\ m^2/s$, shows better agreement with the field data than does the calculated results based

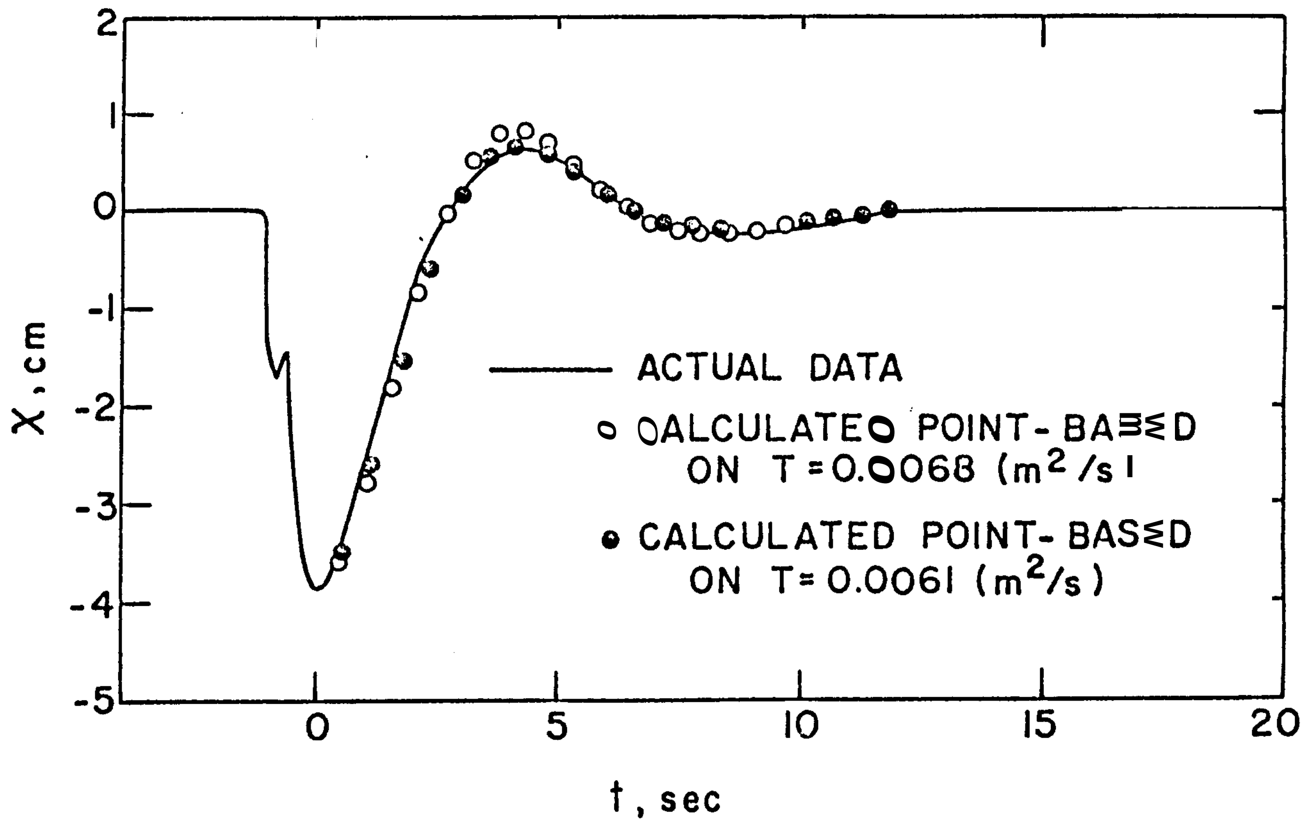

FIG. 67: LIQUID LEVEL IN THE WELLBORE FOR 2-C WELL

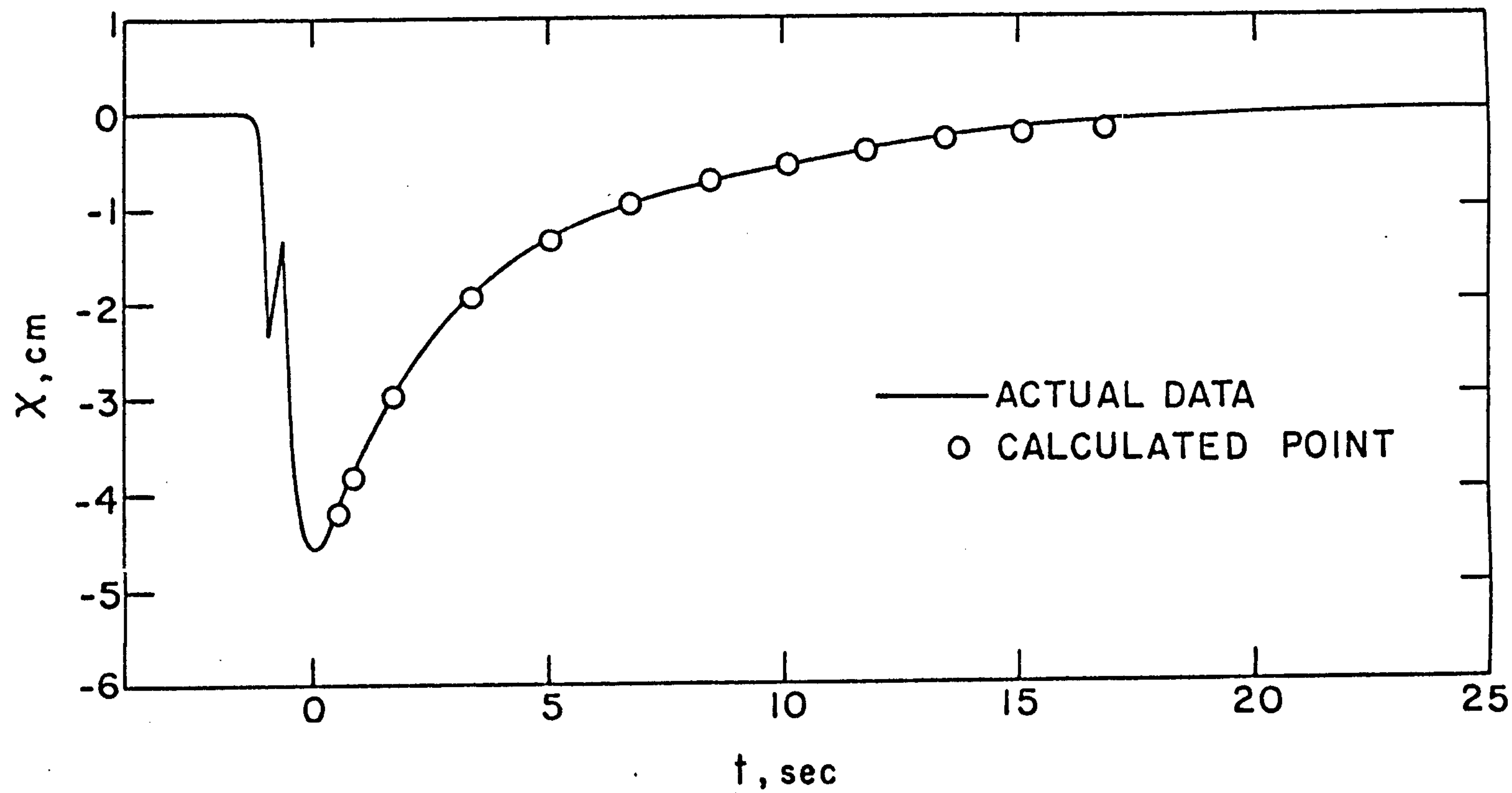

FIG. 68: LIQUID LEVEL IN THE WELLBORE FOR 9-A WELL

TABLE 10: CORRESPONDENCE BETWEEN THE SYMBOLS USED IN PETROLEUM ENGINEERING AND THOSE IN GROUND WATER HYDROLOGY

Petroleum Engineering	Ground Water Hydrology
C_D	$\left(\frac{r_c^2}{r_s^2}\right) \cdot \frac{1}{2S}$
t_D	$\frac{T \cdot t}{S \cdot r_s^2}$
α	$\sqrt{\frac{L}{g}}\left(\frac{T}{S \cdot r_s^2}\right)$

TABLE 11: ADJUSTED PROPERTIES OF WELL-AQUIFER SYSTEMS REPORTED BY VAN DER KAMP[16]

SYMBOLS OF GROUND WATER HYDROLOGY	WELL 2c	WELL 9A
Effective length of fluid column, L(m)	16	11
Transmissivity, T (m^2/s)	0.0068	0.0017
Coefficient of elastic storage, S	1.4×10^{-4}	1.1×10^{-4}
Radius of well filter, r_f (m)	0.051	0.051
Radius of well casing, r_c (m)	0.051	0.051
SYMBOLS OF PETROLEUM ENGINEERING		
Dimensionless wellbore storage constant, C_D	3.57×10^{3}	4.55×10^{3}
Dimensionless time, t_D	1.68×10^{4} t(-sec)	5.94×10^{3} t(-sec)
Skin factor, s (assumption)	0	0
Dimensionless number, a	2.39×10^{4}	6.29×10^{3}

on the transmissivity, T = 0.0068 m^2/s, which was reported by van der Kamp. The transmissivity of 0.0061 m^2/s is believed to be closer to the true value than is the transmissivity of 0.0068 m^2/s. Figure 68 presents the same comparison for the well 9-A. The calculated results based on the well-aquifer properties reported by van der Kamp agree very well with the actual data. The transmissivity of 0.0017 m^2/s is reliable for this aquifer.

In the case of shallow water wells producing from high permeability formations, the skin factor, s, is often nearly zero. Then, knowing the dimensionless wellbore storage constant, C_D (or the coefficient of elastic storage, S), we can prepare type-curves for various values of the dimensionless number, α, using the slug test solution presented in this study, and can obtain the permeability, k (or the transmissivity, T), from the matched α value. This example in which we could determine a better transmissivity shows how this type-curve matching method works.

Finally, the spike, which appears before the zero time (as seen in Figs. 67 and 68), can be seen in all test results reported by van der Kamp. This phenomenon might be caused by the way the test was performed, because a float was suddenly removed from the wellbore to give the initial condition of the test. This procedure causes a strange initial water surface. The first drop probably projects toward the liquid level at the bottom of the float. However, the water in the annulus between the float and the casing suddenly drops into the float cavity causing the spike and a new liquid level above the float bottom at the instant of withdrawal.

3. ANALYSIS OF FLOW PERIOD DATA IN CLOSED CHAMBER TESTS

A closed chamber test is a variation of a conventional drill stem test (DST) and is used for safety or for pollution protection. In closed chamber tests,[17,18] the well is shut in at the surface or at the top of the closed chamber when the fluid is being produced. The well may be open at the surface or at the top of the closed chamber, although in some cases kept closed in to maintain the pressure in the wellbore when the tester valve is closed. These operations are done to prevent the reservoir fluid from flowing out at the surface, which may cause pollution problems and perhaps danger, especially for offshore wells. Figure 69 shows a schematic diagram of a closed chamber test.

Usually the wellbore pressure data for the flow period have been discarded, and a method to analyze these data has not been presented thus far (to our knowledge). Section **3-1** presents the mathematical formulation of this problem, and the solution is investigated in Section **3-2.**

3-1 Mathematical Formulation

Since the pressure of the trapped gas in the closed chamber, p_{ch}, resists the movement of the reservoir liquid, p_{ch} should be used instead of the atmospheric pressure, p_{atm}, in the momentum balance equation in the wellbore (see Eq. **1).** The momentum balance equation in the wellbore for the closed chamber test becomes:

$$L \cdot \frac{d^2x}{dt^2} + gx = - \frac{p_i - p_w}{\rho_f} - \frac{p_{ch} - p_{atm}}{\rho_f} \tag{77}$$

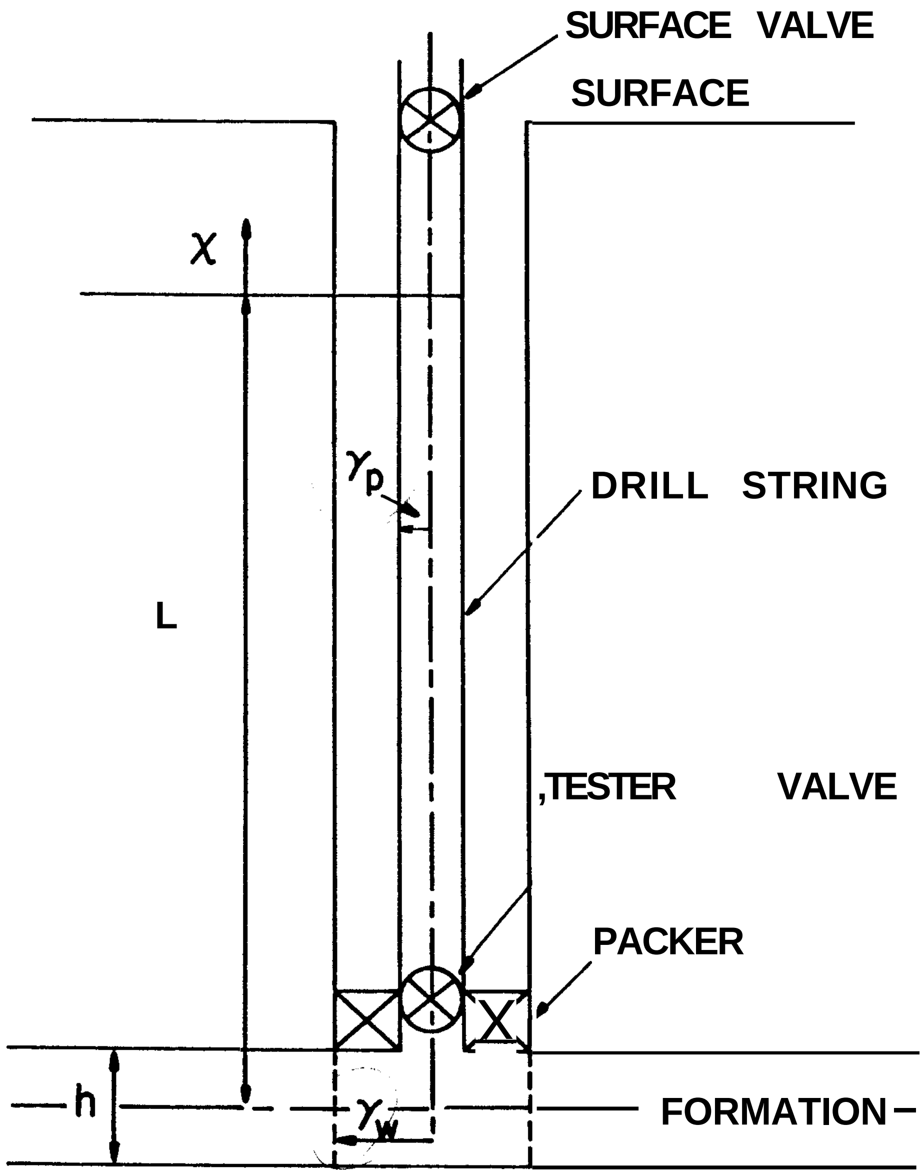

FIG. 69: SCHEMATIC DIAGRAM OF A CLOSED CHAMBER TEST

The definition of the variables and constants are the same as in Eq. 1.

From the gas equation:

$$p_{ch} = \frac{[L_i - x(0)]z}{(L_i - x)z_i} \; p_{ch,i} \tag{78}$$

L_i is the length of closed chamber, x is the liquid level in the wellbore, x(0) is the liquid level in the wellbore at zero time, z is the compressibility factor of the gas in the closed chamber, z_i is the initial compressibility factor of the gas in the closed chamber, and $p_{ch,i}$ is the initial pressure of the closed chamber.

Then:

$$\frac{d^2x}{dt^2} + \frac{g}{L}x = -\frac{p_i - p_w}{\rho_f L} - \frac{\cdot}{\rho_f L}\left\{\frac{[L_i - x(0)]z}{(L_i - x)z_i}\,p_{ch,i} - p_{atm}\right\} \tag{79}$$

In order to obtain a dimensionless form of this equation, we will use the dimensionless variables x_D, t_D, and p_{wD} defined in Eqs. 11, 9, and 12, and the dimensionless number a defined in Eq. 16. In addition to these dimensionless variables and number groups, the following dimensionless groups are introduced:

$$p_{Datm} = \frac{p_{atm}}{p_i - (p_o + p_{atm})} \tag{80}$$

$$L_{D_i} = \frac{\rho_f g L_i}{p_i - (p_o + p_{atm})} \tag{81}$$

$$\beta = \frac{p_{ch,i}}{p_i - (p_o + p_{atm})} \tag{82}$$

The dimensionless value, $p_{D_{atm}}$, represents the dimensionless atmospheric pressure. The dimensionless groups β and L_{D_i} represent the effect of the initial pressure of the closed chamber and the volume of the closed chamber on the closed chamber test solution, respectively. Then, Eq. 79 becomes:

$$\alpha^2 \cdot \frac{d^2 x_D}{dt_D^2} + x_D = - p_{wD} - \beta \left\{ \frac{[L_{D_i} - x_D(0)]z}{(L_{D_i} - x_D)z_i} - \frac{p_{D_{atm}}}{p} \right\} \tag{83}$$

If the initial closed chamber pressure, $p_{ch,i}$, is atmospheric, which is often true, Eq. 83 becomes:

$$\alpha^2 \cdot \frac{d^2 x_D}{dt_D^2} + x_D = - p_{wD} - \beta \left\{ \frac{[L_{D_i} - x_D(0)]z}{(L_i - x_D)z_i} - 1 \right\} \tag{84}$$

Since Eqs. 83 and 84 are nonlinear because of the last term, the solution was obtained using a finite difference solution which is explained in Appendix D. Appendix E shows the computer program for this finite difference solution. In order to see the dimensionless wellbore pressure within the same range, the following new dimensionless variable, p^*_{wD}, is introduced:

$$p^*_{wD} = \frac{p_i - p_w}{p_i - (p_o + p_{ch,i})} \tag{85}$$

The variable p^*_{wD} represents the dimensionless wellbore pressure based on the sum of the liquid cushion head, p_o, and the initial closed chamber pressure, $p_{ch,i}$, as an equivalent cushion head, which has the following relation with p_{wD} defined previously:

$$p^*_{wD} = \frac{p_{wD}}{1-\beta+p_{D_{atm}}} \tag{86}$$

The results, to be discussed in the next section, are presented in terms of the dimensionless wellbore pressure, p^*_{wD}.

3-2 Results and Discussion

In order to investigate the closed chamber test solution and the parameters which affect the solution, the case for $C_D = 10^3$ and $s = 0$ was again selected as a typical example. The solutions for some parameter values were obtained for this problem using the finite difference solution explained in Appendix D. To determine typical order of magnitudes of parameter values, let us consider the following example case. Suppose the initial formation pressure, p_i, is 3,000 psia ($2.07\text{x}10^7$ Pa); the liquid cushion head, p_o, is 2,000 psia ($1.38\text{x}10^7$ Pa); the atmospheric pressure, p_{atm}, is 14.7 psia ($1.01\text{x}10^5$ Pa); the initial pressure of the closed chamber, $p_{ch,i}$, is 14.7 psia ($1.01\text{x}10^5$ Pa), which is likely; the length of the closed chamber, L_i, is 2,000 ft (610 m); and the liquid density, ρ_f, is 0.8 ($8.0\text{x}10^2$ kg/m^3) (to water). Then the dimensionless number $p_{D_{atm}}$ is 0.015, β is 0.015, and L_{D_i} is 0.70. Therefore, as a typical example, we select 0.01 as $p_{D_{atm}}$ and β, and 1 as L_{D_i}. In addition to this combination of dimensionless numbers, we will consider the case when $\beta = 0.1$ and $L_{D_i} = 1$, as the high initial closed chamber pressure case, and $\beta = 0.1$ and $L_{D_i} = 0.01$ as the high initial closed chamber pressure and small closed chamber volume case.

Figure 70 presents the dimensionless wellbore pressure, p^*_{wD}, versus dimensionless time, t_D, and Fig. 71 shows the dimensionless liquid level

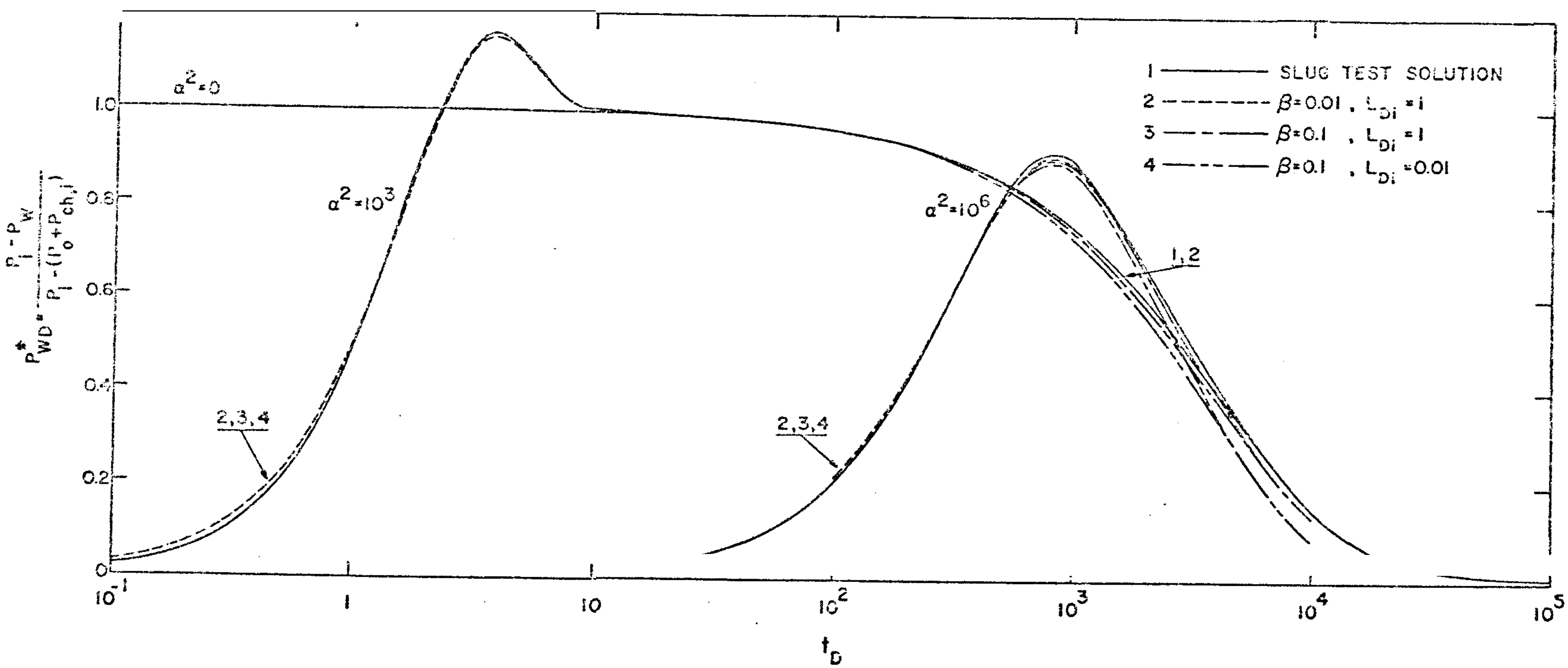

FIG. 70: DIMENSIONLESS WELLBORE PRESSURE p^*_{wD} VS DIMENSIONLESS TIME FOR CLOSED CHAMBER TESTS WHEN $C_D = 10^3$ AND $s = 0$

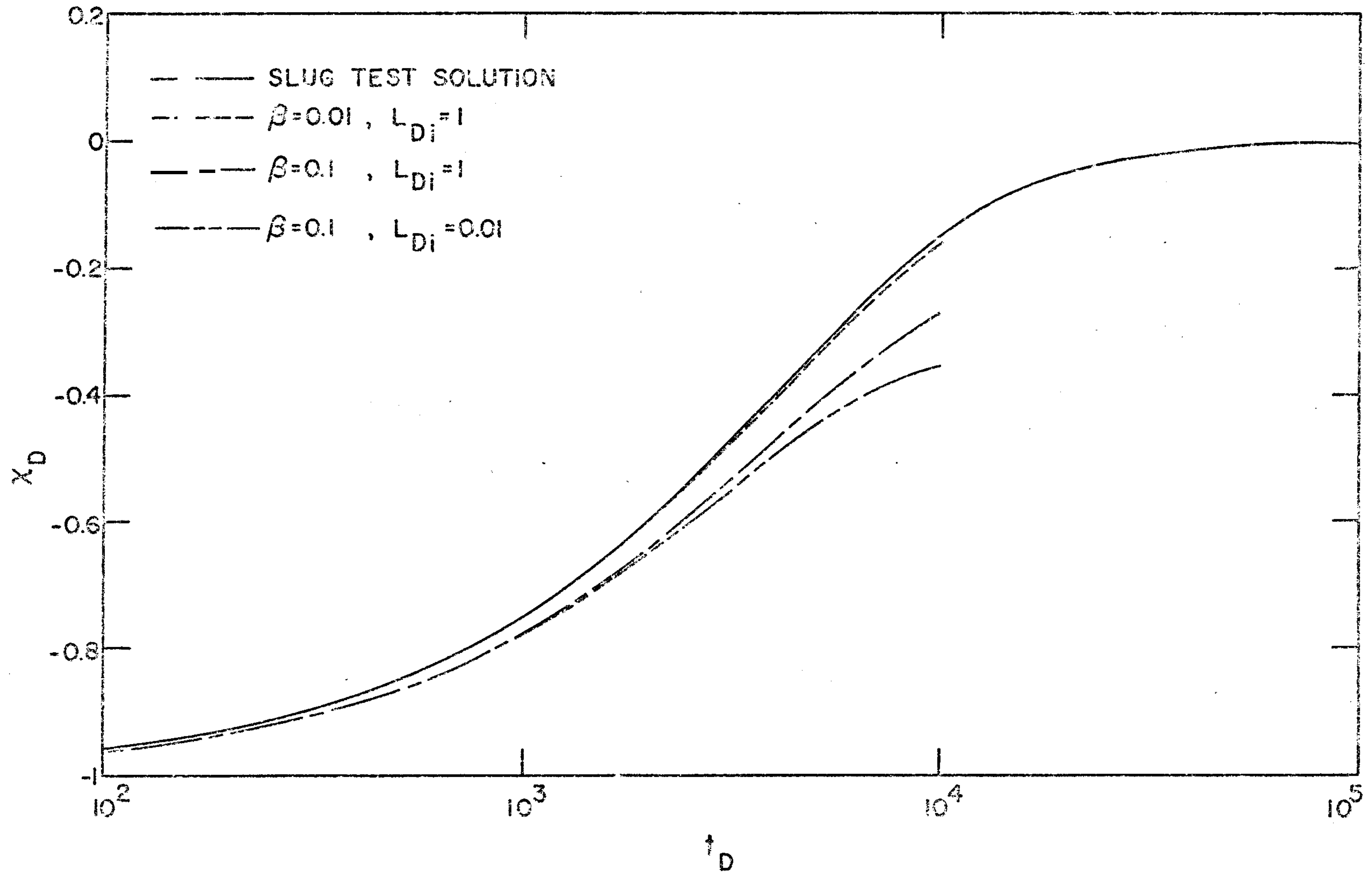

FIG 71: DIMENSIONLESS LIQUID LEVEL IN THE WELLBORE VS DIMENSIONLESS TIME FOR CLOSED CHAMBER TESTS WHEN $C_D = 10^3$, $s = 0$, and $\alpha = 0$

in the wellbore, x_D, versus t_D for these parameter values. It was assumed that the gas compressibility factor is 1. As we can see, there are larger differences between the x_D solutions than between the p^*_{wD} solutions for these example cases. This is because the dimensionless wellbore pressure, p^*_{wD}, is based on the sum of the liquid cushion head, p_o, and the initial closed chamber pressure, $p_{ch,i}$. If we use the dimensionless wellbore pressure, p_{wD}, we will see the same order of difference in the solutions as that in the x_D solutions. Then, the dimensionless wellbore pressure, p^*_{wD}, is a useful dimensionless variable to handle the closed chamber test solution; from now on, we will discuss the p^*_{wD} solutions.

For the typical case (β = 0.01, L_{D_i} = 1) and for practical purposes, there is no difference between the slug test solution and the closed chamber test solution in terms of the p^*_{wD} solutions, as seen in Fig. 70. We can say that the slug test solution can be applied to analyze the flow period data of the closed chamber test for this typical case using the dimensionless wellbore pressure, p^*_{wD}. The other two cases are unlikely in field testing; however, these two cases were studied in order to investigate the effect of the dimensionless numbers β and L_{D_i} on the solutions.

The first example, β = 0.1 and L_{D_i} = 1, represents the case when the pressure of the closed chamber is increased before the test starts. The second example, β = 0.1 and L_{D_i} = 0.01, represents the case when the closed chamber is pressurized before the test starts and the volume of the closed chamber is very small. The solutions for these cases are different from the slug test solution, especially at late times. Then, strictly speaking, the slug test solution cannot be used to analyze the flow period data from a closed chamber test for these cases. If the slug test solution were used, there would be some error in the results. However, it should be remembered that these two examples are not likely in actual testing. If $p_i - (p_o + p_{atm})$ is smaller than this example, the dimensionless numbers β and L_{D_i} become larger. Then, the effect of the dimensionless number β on the solution increases. On the other hand, the effect of the dimensionless number L_{D_i} decreases. However, as long as the initial pressure of the closed chamber is atmospheric, it is unlikely that the dimensionless number β will become greater than 0.1 in a closed chamber test. If the dimensionless number β is less than 0.1, the difference between the slug test solution and the closed chamber test solution is not large for practical purposes, as long as the volume of the closed chamber is not too small, as shown in Fig. 70. Therefore, our discussion on the effect of the dimensionless numbers β and L_{D_i} on the solution holds generally.

As a summary of this section, the slug test solution can be applied to analyze the flow period data from a closed chamber test except for the case when the initial pressure of the closed chamber is very high compared to the atmospheric pressure, or the volume of the closed chamber is very small. For these special cases, solutions should be obtained using the finite difference solution in Appendix D to analyze the flow period data from the closed chamber test. Phase change is not considered in this analysis.

4. CONCLUSIONS

The effect of the inertia of the liquid in the wellbore on the slug test solution was investigated. A new dimensionless number, *a*, which corresponds to Froude's number, was defined to determine how the inertia of the liquid in the wellbore affects a slug test solution. The effects of wellbore storage and the skin factor on the slug test solution were discussed, and the investigation radius of a slug test was studied. Some field data from slug tests were analyzed. The solution for the flow period data analysis in closed chamber tests was studied as an extension of the general slug test solution.

As a result of this study, the following conclusions appear warranted.

1. Solutions for the slug test fneluding the inertial effect of the liquid in the wellbore depend on a dimensionless number, *a*, defined in this study.

2. Approximately, the inertial effect of the liquid in the wellbore is negligible for practical purposes if a is less than α_1, defined by Eqs. 70 and 72.

3. Approximately, the oscillation of the liquid level in the wellbore may happen when a is greater than a_2, defined by Eqs. 71 and 73. The van der Kamp parameter d is approximately 0.5 for critical damping.

4. Increased wellbore storage increases the range of a wherein the inertial effect of the liquid in the wellbore is negligible, and decreases the tendency for the liquid level in the wellbore to oscillate.

5. Increased skin factor (wellbore damage) increases the range of a wherein the inertial effect of the liquid in the wellbore is negligible,

and decreases the tendency for the liquid level in the wellbore to oscillate. Negative skin factor makes the inertial effect of the liquid in the wellbore more significant, and increases the tendency of the liquid level in the wellbore to oscillate. Positive skin factor decreases the overshooting of p_{wD} at early times for small α values.

6. How the wellbore storage and skin factor force the slug test solution to shift on the time axis can be estimated by Eq. 76.

7. Generally speaking, the higher the initial formation pressure and permeability, and the lower the liquid viscosity, the drill string radius and the skin factor are, the more the inertia of the liquid in the wellbore affects the slug test solution.

8. A large skin factor may be one reason for apparent linearity between the wellbore pressure and time often observed in DST flow period data at the beginning of a flow period.

9. The investigation radius for a slug test depends on the dimensionless wellbore storage constant, C_D. The larger the dimensionless wellbore storage constant is, the deeper the investigation radius is. The skin factor, s, and the dimensionless number α do not affect the investigation radius as much. The depth of investigation for the buildup test and the slug test are almost the same if the shutdown is done at late time. The depth of investigation is on the order of hundreds of wellbore radii, in many cases.

10. The solution presented in this study is applicable not only to production, but also to batch injection.

11. There are two ways to utilize the solution obtained in this study in interpretation of field data. One way is to use the solution as a type-

curve when the skin factor, s, is known by other means, such as buildup test analysis. Permeability can be obtained from the matched α value or the matched t_D/C_D value. This type-curve can be used for large α value cases for which the conventional inertia-less slug test type-curves cannot be applied. The other way to use the solution is to check whether the result obtained by the conventional slug test analysis is reliable or not. After the conventional slug test analysis, a_1 should be calculated. If a is less than a_1, the result of conventional slug test analysis should be reasonable.

12. It is important to measure the cushion liquid head accurately before opening the tester valve and to obtain enough data at late times in the slug test. When the cushion liquid head is not known, the solution in log-log scale should be used to match the slug test data.

13. Several investigators have concluded that slug test results are not as reliable as buildup test results. This observation appears based on difficulty in type-curve matching. The results of this study indicate slug test results should be reliable and agree with buildup test results.

14. Further work is necessary to understand the buildup data after a short-time production. The Fenske[37] observation that buildup following a short production test may be analyzed as a slug test seems to be a very important idea.

15. The deviation of closed chamber solutionfrom the slug test solution depends upon the initial pressure of the closed chamber and the volume of the closed chamber. As long as the initial pressure of the closed chamber is nearly atmospheric, and the volume of the closed chamber is not too small, the slug test solution can be applied to analyze the flow period data of the closed chamber test.

5. NOMENCLATURE

a = positive number greater than the real part of the singularities of function; a constant defined in Eq. D-3, in Appendix D

A = arbitrary constant; coefficient of the equation which relate C_D and a_1

B = arbitrary constant; coefficient of the equation which relates C_D and a_2

C = wellbore storage, L^4T^2/M

C_D = dimensionless wellbore storage constant

c_f = compressibility of the liquid in the wellbore, LT^2/M

c_t = total system compressibility, LT^2/M

d = parameter which controls the critical damping condition

D = diameter of the pipe, L

E = exponent of C_D

f = Moody friction factor

g = gravitational acceleration, L/T^2

h = thickness of the formation, L

I_0 = modified Bessel function of the first kind, order zero

J_0 = Bessel function of the first kind, order zero

= Bessel function of the first kind, order unity

k = permeability, L^2

K_0 = modified Bessel function of the second kind, order zero

K_1 = modified Bessel function of the second kind, order unity

ℓ = variable of Laplace transform

L = liquid length whose head is equivalent to the initial formation pressure minus atmospheric pressure, L; liquid length in the wellbore in Appendix C, L

L_i = length of closed chamber, L

L_{D_i} = dimensionless length of closed chamber

M = number of nodes

N = number of terms

N_{Re} = Reynold's number

p = pressure at the point in the reservoir, M/LT^2

p_{atm} = atmospheric pressure, M/LT^2

p_{ch} = pressure of closed chamber, M/LT^2

$p_{ch,i}$ = initial pressure of closed chamber, M/LT^2

p_D = dimensionless pressure

$\overline{p}_D$ = Laplace transform of p_D

$p_{D_{atm}}$ = dimensionless atmospheric pressure

$p^n_{D_i}$ = dimensionless pressure at the node i at the time step n

p_i = initial formation pressure, M/LT^2

p_o = pressure equivalent to the cushion liquid head, M/LT^2

p_w = wellbore pressure, M/LT^2

p_{wD} = dimensionless wellbore pressure

$\overline{p}_{wD}$ = Laplace transform of p_{wD}

p^*_{wD} = dimensionless wellbore pressure based on the initial closed chamber pressure

p_{wf} = flowing wellbore pressure, M/LT^2

q = production flowrate, L^3/T

r = radial distance from the axis of the well, L

r_c = radius of casing, L

r_D = dimensionless radial distance from the axis of the well

r_{D_e} = dimensionless external radius

r_{D_i} = dimensionless radial distance at node i

Δr_{Di} = increment of dimensionless radial distance at node i

r_e = external radius, L

r_p = radius of pipe, L

r_s = radius of sandface, L

r_w = wellbore radius, L

r'_w = effective wellbore radius, L

R_e = residue

$Re\{\ \}$ = real part of $\{\ \}$

s = skin factor

S = coefficient of elastic storage

t = time, T

At = shut-in time, T

t_D = dimensionless time

= increment of dimensionless time

t_{D_1} = dimensionless time at which p_{wD} becomes 0.9 for $\alpha = 0$

t_p = production time, T

T = upper time limit for numerical Laplace transform inversion methods; transmissivity, L^2/T

u = variable in Appendix A; velocity of liquid column in the wellbore in Appendix C, L/T

x = liquid level in the wellbore, L

$x(t=0)$ = initial liquid level in the wellbore, L

x_D = dimensionless liquid level in the wellbore

$x_D(t_D=0)$ = initial dimensionless liquid level in the wellbore

$x'_D(t_D=0)$ = initial velocity of the dimensionless liquid level in the wellbore

$\overline{x}_D$ = Laplace transform of x_D

Y_0 = Bessel function of the second kind, order zero

Y_1 = Bessel function of the second kind, order unity

z = compressibility factor of the gas in the closed chamber; complex variable in Appendix A

z_i = initial compressibility factor of the gas in the closed chamber

GREEK NOMENCLATURE

α = dimensionless number defined in Eq. 16

α_1 = value of α below which p_{wD} becomes the same as the $\alpha = 0$ case solution when p_{wD} becomes 0.9.

α_2 = value of α beyond which the liquid level in the wellbore oscillates

β = dimensionless number defined in Eq. 80; complex variable in Appendix A

γ = Euler's constant

λ = variable in Appendix A

ρ_f = density of the liquid in the wellbore, M/L^3

ϕ = porosity

Knowles

6. REFERENCES

1. Ferris, J.G., and Knowels, D.B.: "The Slug Test for Estimating Transmissibility," U.S. Geol. Survey Ground Water Note 26 (1954), 1-7.

2. Beck, A., Jaeger, J.C., and Newstead, G.: "The Measurement of the Thermal Conductivities of Rocks by Observations in Boreholes," Aust. J. Phys. (1956), 9, 286.

3. Cooper, H.H., Jr., Bredehoeft, J.D., and Papadopulos, I.S.: "Response of a Finite-Diameter Well to an Instantaneous Charge of Water," Water Resources Research (1967), 3, No. 1, 263-269.

4. Maier, L.F.: "DST Interpretation Calculations for. Water Reservoirs," Halliburton Services Limited Report, Calgary, Alberta, Jan. 2, 1970.

5. van Poollen, H.K., and Weber, J.D.: "Data Analysis for High Influx Wells," Paper SPE 3017, presented at the 45th Annual Fall Meeting, SPE of AIME, Houston, Oct. 4-7, 1970.

6. Kohlhaas, C.A.: "A Method for Analyzing Pressures; Measured During Drillstem-Test Flow Periods," J. Pet. Tech. (Oct. 1972), 1278.

7. Jaeger, J.C.: "Conduction of Heat in an Infinite Region Bounded Internally by a Circular Cylinder of a Perfect Conductor," Aust. J. Phys. (1956), 9, No. 2, 167.

8. van Everdingen, A.F.: "The Skin Effect and Its Influence on the Productive Capacity of a Well," Trans., AIME (1953), ~~198~~, 171-176.

9. Hurst, W.: "Establishment of the Skin Effect and Its Impediment to Fluid-Flow Into a Well Bore," Pet. Eng. (Oct. 1953), 25, B-6.

10. Agarwal, R.G., Al-Hussainy, R., and Ramey, H.J., Jr.: "An Investigation of Wellbore Storage and Skin Effect in Unsteady Liquid Flow: I. Analytical Treatment," Soc. Pet. Eng. J. (Sept. 1970), 279.

11. Ramey, H.J., Jr., and Agarwal, R.G.: "Annulus Unloading Rates as Influenced by Wellbore Storage and Skin Effect," Soc. Pet. Eng. J. (Oct. 1972), 453.

12. Papadopulos, I.S., Bredehoeft, J.D., and Cooper, H.H., Jr.: "On the Analysis of 'Slug Test' Data," Water Resources Research (Aug. 1973), 9, No. 4, 1087.

13. Ramey, H.J., Jr., Agarwal, R.G., and Martin, I.: "Analysis of 'Slug Test' or DST Flow Period Data," J. Can. Pet. Tech. (July-Sept. 1975), 1-11.

14. Earlougher, R.C., Jr.: "Advances in Well Test Analysis," Monograph 5, SPE, Dallas, Texas (1977), 96-101.

15. Bredehoeft, J.D., Cooper, H.H., Jr., and Papadopulos, I.S.: "Inertial and Storage Effects in Well-Aquifer Systems: An Analog Investigation," Water Resources Research (1966), 2, No. 4, 697-7017.

16. van der Kamp, G.: "Determining Aquifer Transmissivity by Means of Well Response Tests: The Underdamped Case," Water Resources Research (Feb. 1976), 12, No. 1, 71-77.

17. Alexander, L.G.: "Theory and Practice of the Closed-Chamber Drillstem Test Method," J. Pet. Tech. (Dec. 1977), 1539-1544.

18. Marshal, G.R.: "Practical Aspect of Closed-Chamber Testing," 3. Can. Pet. Tech. (July-Sept. 1978), 82-85.

19. Matthews, C.S., and Russell, D.G.: "Pressure Buildup and Flow Tests in Wells," Monograph 1, SPE, Dallas, Texas (1967), 4-7.

20. Binder, R.C.: Fluid Mechanics, Prentice-Hall (1949), 82-83.

21. van Everdingen, A.F., and Hurst, W.: "The Application of the Laplace Transformation to Flow Problems," Trans., AIME (1949). 186, 305-324.

22. Karman, V.T., and Biot, M.A.: Mathematical Methods in Engineering, McGraw-Hill (1940), 61-63,

23, David, P.J., and Rabinowitz, P.: Numerical Integration, Blaisdell Publishing Co., Waltham, Mass. (1967), 166.

24. Watson, G.W.: A Treatise on the Theory of Bessel Functions, Cambridge Univ. Press (1944), 202.

25. Churchill, R.V.: Operational Mathematics, McGraw-Hill (1972), 459.

26. Carslaw, H.S., and Jaeger, J.C.: Operational Methods in Applied Mathematics, Oxford Univ. Press (1963), 248-249.

27. Stehfest, H.: "Numerical Inversion of Laplace Transforms," Communication of the ACM (Jan. 1970), 13, No. 1, 47-49.

28. Gaver, D.P.: "Observing Stochastic Process and Approximate Transform Inversion," Oper. Res. (1966), 14, No. 3, 445-459.

29, Veillon, F.: "Numerical Inversion of Laplace Transform," Communication of the ACM (Oct. 1974), 17, No, 10, 587-589.

30. Dubner, H., and Abate, J.: "Numerical Inversion of Laplace Transform and the Finite Fourier Transform," J. ACM (Jan, 1968), 15, No. 1, 115-123.

31. Albrecht, P., and Honig, G.: "Numerical Inversion der Laplace Transformierten," Angewandte Informstik (1977), 8, 336-345.

32. Abramowitz, M., and Stegun, I.A.: Handbook of Mathematical Functions with Formulas, Graphs, and Mathematical Tables, U.S. Dept. of Commerce, A.M.S. 55 (1964), 378–379.

33. Shinohara, K., and Ramey, H.J., Jr.: "Analysis of 'Slug Test' DST Flow Period Data with Critical Flow," Paper SPE 7981, presented at the 49th Annual California Regional Meeting, SPE of AIME, Yentura, Apr. 18–20, 1979.

34. Earlougher, R.C., Jr., and Kersh, K.M.: "Analysis of Short-Time Transient Test Data by Type-Curve Matching," J. Pet. Tech. (July 1974), 793-800.

35. Fair, W.B., Jr.: "Pressure Buildup Analysis with Wellbore Phase Redistribution," Paper SPE 8206, presented at the 54th Annual Fall Meeting;, SPE of AIME, Las Vegas, Sept. 23–26, 1979.

36. Stright, D.H., Jr.: "DST Analysis with Pressure Dependent Rock and Fluid Properties," Paper SPE 8352, presented at the 54th Annual Fall Meeting, SPE of AIME, Las Vegas, Sept. 23–26, 1979.

37. Fenske, P.R.: "Type Curves for Recovery of a Discharging Well with Storage," J. Hydrol. (1977), 33, 341-348.

38. Carslaw, H.S., and Jaeger, J.C.: op. cit., 71.

39. Churchill, R.V.: op. cit., 177–178.

40. Churchill, R.V.: op. cit., 170.

41. Carslaw, H.S., and Jaeger, J.C.: op. cit., 76.

42. Carslaw, H.S., and Jaeger, J.C.: op. cit., 173.

43. Frick, T.C.: Petroleum Production Handbook, Vol. 11, McGraw-Hill Book Co., New York (1962), 31–34.

44. Wylie, C.R.: Advanced Engineering Mathematics, McGraw-Hill (1975), 402–403.

45. Wylie, C.R.: op. cit., 315.

7. APPENDICES

A. INVESTIGATION OF THE ANALYTICAL LAPLACE TRANSFORM INVERSION OF EQ. 40

Applying the Mellin Inversion Formula[38] to Eq. 40:

$$x_D = \frac{1}{2\pi i}\int_{a-i\infty}^{a+i\infty} \frac{\{(\alpha^2\lambda+C_D s)\sqrt{\lambda}K_1(\sqrt{\lambda})+C_D K_0(\sqrt{\lambda})\}x_D(t_D=0)+\alpha^2\sqrt{\lambda}K_1(\sqrt{\lambda})x_D'(t_D=0)}{(\alpha^2\lambda^2+C_D s\lambda+1)\sqrt{\lambda}K_1(\sqrt{\lambda})+C_D\lambda K_0(\sqrt{\lambda})} e^{\lambda t_D} d\lambda \tag{A-1}$$

Since the integrand has a branch because of $\sqrt{\lambda}$,[39] we have to choose an integration path which does not contain the origin in evaluating Eq. A-1, as shown in Fig. A-1.

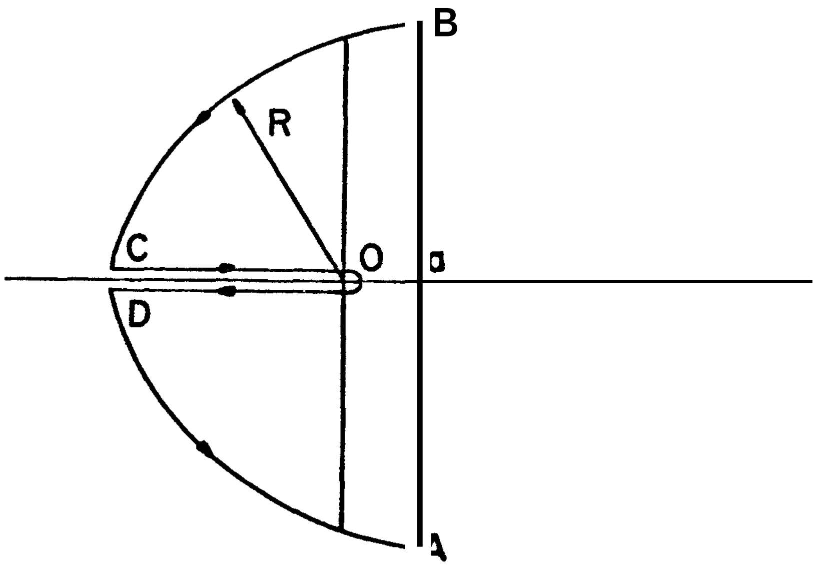

FIG. A-1: INTEGRATION PATH

From the Chauchy integral theorem:[40]

$$\int_A^B = \int_A^D + \int_D^0 + \int_0^C + \int_C^B + 2\pi i \sum \mathrm{Re} \tag{A-2}$$

Re are the residues of this function.

From Carslaw and Jaeger,[41] if $R \to \infty$:

$$\int_A^D = \int_C^B = 0 \tag{A-3}$$

Then:

$$\frac{1}{2\pi i}\int_A^B = \frac{1}{2\pi i}\left\{\int_D^0 + \int_0^C\right\} + \sum \mathrm{Re} \tag{A-4}$$

We can evaluate the integration $\int_0^C$ by replacing λ by u2eia. Substituting $\lambda = u^2 e^{i\pi}$ into Eq. A-1:

$$\frac{1}{2\pi i}\int_0^C$$

$$= \frac{1}{2\pi i}\int_0^\infty \frac{\left\{(\alpha^2 u^2 e^{i\pi} + C_D s)\, ue^{\frac{i\pi}{2}} K_1(ue^{\frac{i\pi}{2}}) + C_D K_0(ue^{\frac{i\pi}{2}})\right\} x_D(t_D=0) + \alpha^2 ue^{\frac{i\pi}{2}} K_1(ue^{\frac{i\pi}{2}})\, x_D'(t_D=0)}{(\alpha^2 u^4 e^{2i\pi} + C_D s u^2 e^{i\pi} + 1)\, ue^{\frac{i\pi}{2}} K_1(ue^{\frac{i\pi}{2}}) + C_D u^2 e^{i\pi} K_0(ue^{\frac{i\pi}{2}})}\, e^{u^2 e^{i\pi} t_D} \cdot 2ue^{i\pi}\, du \tag{A-5}$$

Since:[26]

$$K_0\left(ue^{\pm\frac{i\pi}{2}}\right) = \mp\frac{i\pi}{2}\left\{J_0(u) \mp iY_0(u)\right\} \tag{A-6}$$

$$K_1\left(ue^{\pm\frac{i\pi}{2}}\right) = -\frac{\pi}{2}\left\{J_1(u) \mp iY_1(u)\right\} \tag{A-7}$$

$$\frac{1}{2\pi i}\int_0^C$$

$$= \frac{1}{2\pi i}\int_0^\infty \left[\frac{-\{(\alpha^2u^3x_D(t_D=0) - C_Dsux_D(t_D=0) - \alpha^2ux_D'(t_D=0)\}\,J_1(u) - C_Dx_D(t_D=0)\,J_0(u)]}{\{(\alpha^2u^4-C_Dsu^2+1)\,J_1(u) - C_DuJ_0(u)\} - i\{(\alpha^2u^4-C_Dsu^2+1)\,Y_1(u) - C_DuY_0(u)\}}\right.$$
$$\left.+\frac{i[\{\alpha^2u^3x_D(t_D=0) - C_Dsux_D(t_D=0) - \alpha^2ux_D'(t_D=0)\}\,Y_1(u) - C_Dx_D(t_D=0)\,Y_0(u)]}{\{(\alpha^2u^4-C_Dsu^2+1)\,J_1(u) - C_DuJ_0(u)\} - i\{(\alpha^2u^4-C_Dsu^2+1)\,Y_1(u) - C_DuY_0(u)\}}\right] e^{-u^2t_D}\,du \tag{A-8}$$

Substituting Eqs. 44 through 47 into Eq. A-8:

$$\frac{1}{2\pi i}\int_0^C = \frac{i}{\pi}\int_0^\infty \frac{-\Delta_3(u)+i\Delta_4(u)}{\Delta_1(u)-i\Delta_2(u)}\, e^{-u^2t_D}\,du$$

$$= \frac{1}{\pi}\int_0^\infty \frac{\{\Delta_3(u)\Delta_2(u)-\Delta_4(u)\Delta_1(u)\}-i\{\Delta_3(u)\Delta_1(u)+\Delta_4(u)\Delta_2(u)\}}{\Delta_1(u)^2+\Delta_2(u)^2}\, e^{-u^2t_D}\,du \tag{A-9}$$

Similarly, we can obtain the integration $\int_D^0$ by setting $\lambda = u^2e^{-i\pi}$.

$$\frac{1}{2\pi i}\int_D^0 = \frac{1}{\pi}\int_0^\infty \frac{\{\Delta_3(u)\Delta_2(u)-\Delta_4(u)\Delta_1(u)\}+i\{\Delta_3(u)\Delta_1(u)+\Delta_4(u)\Delta_2(u)\}}{\Delta_1(u)^2+\Delta_2(u)2}\, e^{-u^2t_D}\,du \tag{A-10}$$

From Eqs. A-4, A-9, and A-10:

$$\frac{1}{2\pi i}\int_A^B = \frac{2}{\pi}\int_0^\infty \frac{\Delta_3(u)\Delta_2(u)-\Delta_4(u)\Delta_1(u)}{\Delta_1(u)^2+\Delta_2(u)^2}\, e^{-u^2t_D}\,du + \sum \mathrm{Re} \tag{A-11}$$

Next we will evaluate the residues of the function. First, consider the residue at the branch point. For small z:[26]

$$K_0(z) \cong -\left\{ \ell n\left(\frac{z}{2}\right) + \gamma \right\} \qquad (A-12)$$

$$K_1(z) \cong \frac{1}{z} \qquad (A-13)$$

Then the residue at $\lambda = 0$ becomes:

$$\lim_{\lambda \to 0} \frac{\lambda\left[\left\{(\alpha^2\lambda + C_D s) - \frac{C_D}{2}\,\ell n\,\lambda + C_D(\ell n\,2-\gamma)\right\}x_D(t_D=0) + \alpha^2 x_D'(t_D=0)\right]}{(\alpha^2\lambda^2 + C_D s\lambda + 1) - \frac{C_D}{2}\lambda\,\ell n\,\lambda + C_D\lambda(\ell n\,2-\gamma)}\; e^{\lambda t_D}$$

(A-14)

Since $\lim_{\lambda \to 0} \lambda\,\ell n\,\lambda = 0$, the residue at $\lambda = 0 = 0$.

In order to find the other poles, set $\lambda = -\beta^2$, as done by Carslaw and Jaeger.[42] The dennminator of the integrand in Eq. A-1 becomes:

$$\beta\{(\alpha^2\beta^4 - C_D s\beta^2 + 1)(\pm i)K_1(\pm i\beta) - C_D\beta K_0(\pm i\beta)\} \qquad (A-15)$$

Since:[26]

$$K_0(\pm iz) = \pm\frac{i\pi}{2}\left\{-J_0(z) \pm iY_0(z)\right\} \qquad (A-16)$$

$$K_1(\pm iz) = \frac{\pi}{2}\left\{-J_1(z) \pm iY_1(z)\right\} \qquad (A-17)$$

Equation **A-15** becomes:

$$\mp\frac{i\pi\beta}{2}\left[\{(\alpha^2\beta^4 - C_D s\beta^2 + 1)J_1(\beta) - C_D\beta J_0(\beta)\} \mp i\{(\alpha^2\beta^4 - C_D s\beta^2 + 1)\,Y_1(\beta) - C_D\beta Y_0(\beta)\}\right]$$

(A-18)

Then the poles have to satisfy the following equations:

$$(\alpha^2\beta^4 - C_D s\beta^2 + 1)\ J_1(\beta) - C_D\beta J_0(\beta) = 0 \tag{A-19}$$

$$(\alpha^2\beta^4 - C_D s\beta^2 + 1)\ Y_1(\beta) - C_D\beta Y_0(\beta) = 0 \tag{A-20}$$

However, it was not possible to find the values of β which satisfy these two equations analytically.

As a result:

$$x_D = \frac{2}{\pi}\int_0^\infty \frac{\Delta_3(u)\Delta_2(u) - \Delta_4(u)\Delta_1(u)}{\Delta_1(u)^2 + \Delta_2(u)^2}\, e^{-u^2 t_D}\, du + \overline{\geq}\ \mathrm{Re} \tag{A-21}$$

The sum of the residues of the function remains unknown.

APPENDIX B: SEPARATION OF REAL AND IMAGINARY PARTS OF EQ. 48 AND EQ. 49

Since we cannot obtain $\frac{K_0(\sqrt{\ell})}{K_1(\sqrt{\ell})}$ as an explicit function of ℓ in a simple form, the early time and the late time approximations for the modified Bessel function are adopted. Then, for the early times we should handle Eqs. 51 and 53, and for the late times we should handle Eqs. 59 and 61.

In order to obtain the real part and the imaginary part of the functions separately, set:

$$\ell \equiv a + ib \equiv re^{i\theta} \qquad \text{(B-1)}$$

Since we consider $\ell = a + i \cdot \frac{k\pi}{T}$ for $k = 1, 2, \ldots, \infty$, and a is positive and greater than the real parts of the singularities of the function,

$$0 \leq \theta \leq \frac{\pi}{2} \qquad \text{(B-2)}$$

Then:

$$\ell^2 = (a^2-b^2) + i(2ab) \qquad \text{(B-3)}$$

$$\sqrt{\ell} = \sqrt{\frac{r+a}{2}} + i\sqrt{\frac{r-a}{2}} \qquad \text{(B-4)}$$

$$\frac{1}{\ell} = \frac{a}{r^2} - i \cdot \frac{b}{r^2} \qquad \text{(B-5)}$$

B-1: FOR EARLY TIMES

Substituting Eqs. from B-1 to B-5 into Eq. 51:

$$\bar{x}_D = x_D(t_D=0)\left\{\frac{a}{r^2} - i\cdot\frac{b}{r^2}\right\} + \left\{a^2 x'_D(t_D=0) - \frac{a}{r^2}x_D(t_D=0) + i\cdot\frac{b}{r^2}x_D(t_D=0)\right\}$$

$$\cdot\frac{1}{\alpha^2\{(a^2-b^2)+i(2ab)\} + C_D s(a+ib) + C_D\left\{\sqrt{\frac{r+a}{2}} + i\sqrt{\frac{r-a}{2}}\right\} + 1} \qquad \text{(B-6)}$$

Define the following variables:

$$A \equiv \alpha^2(a^2-b^2) + C_D sa + C_D\sqrt{\frac{r+a}{2}} + 1 \qquad \text{(B-7)}$$

$$B \equiv 2\alpha^2 ab + C_D sb + C_D\sqrt{\frac{r-a}{2}} \qquad \text{(B-8)}$$

$$D \equiv \sqrt{A^2+B^2} \qquad \text{(B-9)}$$

$$E \equiv \alpha^2 x'_D(t_D=0) - \frac{a}{r^2}x_D(t_D=0) \qquad \text{(B-10)}$$

$$F \equiv \frac{b}{r^2}x_D(t_D=0) \qquad \text{(B-11)}$$

Then:

$$\bar{x}_D = \left\{-E + \alpha^2 x'_D(t_D=0) - iF\right\} + \frac{E+iF}{A+iB}$$

$$= \left\{\alpha^2 x'_D(t_D=0) - E + \frac{AE+BF}{D^2}\right\} + i\left\{-F + \frac{AF-BE}{D^2}\right\} \qquad \text{(B-12)}$$

Similarly, from Eqs. 53, and B-1 through B-11:

$$\bar{p}_{wD} = C_D(E+iF) \times \frac{s(a+ib) + \sqrt{\frac{r+a}{2}} + i\sqrt{\frac{r-a}{2}}}{A+iB}$$

$$- \frac{C_D\left[(AE+BF)\left\{sa + \sqrt{\frac{r+a}{2}}\right\} - (AF-BE)\left\{sb + \sqrt{\frac{r-a}{2}}\right\}\right]}{D^2}$$

$$+ i\,\frac{C_D\left[(AE+BF)\left(sb + \sqrt{\frac{r-a}{2}}\right\} + (AF-BE)\left\{sa + \sqrt{\frac{r+a}{2}}\right\}\right]}{D^2} \qquad \text{(B-13)}$$

B-2: FOR LATE TIMES

Substituting Eqs. B-1 through B-11 into Eq. 59:

$$\bar{x}_D = \left(a^2 x'_D(t_D=0) - E - iF\right\}$$

$$+ \frac{E+iF}{\bar{a}^2\{(a^2-b^2)+i(2ab)\}+C_D s(a+ib)+1-C_D(a+ib)\{\frac{1}{2}\ln r+\gamma-\ln 2+i\cdot\frac{\theta}{2}\}} \qquad \textit{(B-14)}$$

Define the following variables:

$$G \equiv a^2(a^2-b^2) + C_D sa + 1 - C_D a\left(\frac{1}{2}\ln r + \gamma - \ln 2\right) + C_D b \cdot \frac{\theta}{2} \qquad \textbf{(B-15)}$$

$$H \equiv 2\alpha^2 ab + C_D sb - C_D b\left(\frac{1}{2}\ln r + \gamma - \ln 2\right) - C_D a \cdot \frac{\theta}{2} \qquad \textbf{(B-17)}$$

$$I \equiv \sqrt{G^2+H^2} \qquad \textbf{(B-17)}$$

Then, Eq. B-14 becomes:

$$\bar{x}_D = \left\{ \alpha^2 x'_D(t_D=0) - E - iF \right\} + \frac{E+iF}{G+iH}$$

$$= \left\{ \alpha^2 x'_D(t_D=0) - E + \frac{GE+HF}{I^2} \right\} + i \left\{ -F + \frac{GF-HE}{I^2} \right] \tag{B-18}$$

Similarly, from Eqs. 61, B-1 through B-11, and B-15 to B-17:

$$\bar{p}_{wD} = C_D(E+iF) \times \frac{s(a+ib)-(a+ib)\{\frac{1}{2}\ln r + i \cdot \frac{\theta}{2} + \gamma - \ln 2\}}{G+iH}$$

$$- \frac{C_D(E+iF)(G-iH)\left[sa - a(\frac{1}{2}\ln r + \gamma - \ln 2) + b\frac{\theta}{2} + i\{sb - b(\frac{1}{2}\ln r + \gamma - \ln 2) - a\frac{\theta}{2}\}\right]}{I^2} \tag{B-19}$$

Define the following variables:

$$J \equiv a \left\{ s - \frac{1}{2}\ln r - \gamma + \ln 2 \right\} + \frac{b\theta}{2} \tag{B-20}$$

$$K \equiv b \left\{ s - \frac{1}{2}\ln r - \gamma + \ln 2 \right\} - \frac{a\theta}{2} \tag{B-21}$$

Then:

$$\bar{p}_{wD} = \frac{C_D\{(GE+HF)+i(GF-HE)\}(J+iK)}{I^2}$$

$$- \frac{C_D\{(GE+HF)J-(GF-HE)K\}}{I^2}$$

$$+ i \frac{C_D\{(GE+HF)K+(GF-HE)J\}}{I^2} \tag{B-22}$$

APPENDIX C: FIELD DATA EXAMPLE

C-1: WELL. RESERVOIR DATA. AND MEASURED PRESSURES

Four field examples are considered in Section 2. The following summarized the field data necessary for these examples.

TABLE C-1: WELL, RESERVOIR DATA AND MEASURED PRESSURE IN EXAMPLE 1

Well and Reservoir Data

Formation thickness, h	17 feet: (5.2 m)
Porosity, ϕ	16 percent
Viscosity, μ	1.0 cp ($1\text{x}10^{-3}$ Pa·s)
Compressibility, c_t	$8\text{x}10^{-6}$ 1/psi ($1.16\text{x}10^{-9}$ 1/Pa)
Fluid density, ρ_f	0.8458 ($8.458\text{x}10^{2}$ kg/m^3)
Formation temperature	168°F (349°K)
Dimensionless wellbore storage constant, C_D	$2.48\text{x}10^{4}$
Test interval	7782–7796 feet (2372–2376 m)
Test recovery	180 ft mud (55 m) 4060 ft. gassy oil (1237 m) 880 ft salt water (268 m)
Drill-pipe radius, r_P	2.25 inches ($5.72\text{x}10^{-2}$ m)
Hole-size radius, r_w	3.94 inches ($1.00\text{x}10^{-1}$ m)
Initial pressure, p_i	3475 psig ($2.396\text{x}10^{7}$ Pa g)

CONTINUED

TABLE C-1, CONTINUED

t (min) (60 s)	p_{wf} psig (6.89×10^3 Pa g)	p_i-p_{wf} psi (6.89×10^3 Pa)	t (min) (60 s)	p_{wf} psig (6.89×10^3 Pa g)	p_i-p_{wf} psi (6.89×10^3 Pa)
0	560 (643)	2915 (2832)	63	1430	2045
3	600 (665)	2875 (2816)	66	1467	2008
6	645 (672)	2830 (2803)	69	1499	1976
9	692	2783	72	1536	1939
12	737	2738	75	1570	1905
15	786	2684	78	1602	1873
18	832	2643	81	1628	1847
21	874	2601	84	1655	1820
24	919	2556	87	1683	1792
27	962	2513	90	1713	1762
30	1005	2470	93	1737	1738
33	1046	2429	96	1767	1708
36	1085	2390	99	1794	1681
39	1128	2347	102	1819	1656
42	1170	2305	105	1845	1630
45	1208	2267	108	1869	1606
48	1248	2227	111	1894	1581
51	1289	2186	114	1917	1558
54	1318	2157	117	1948	1527
57	1361	2114	120	1969	1506
60	1395	2080			

TABLE C-2: WELL, RESERVOIR DATA AND MEASURED PRESSURE IN EXAMPLE 2

Well and Reservoir Data

Formation thickness, h	9 ft (2.74 m)
Porosity, ϕ	0.15
Viscosity, μ	0.39 cp (3.9×10^{-4} Pa s)
Compressibility, c_t	14×10^{-6} 1/psi (2.03×10^{-9} 1/Pa)
Fluid density, ρ_f	0.65 (6.5×10^{2} kg/m3)
Drill pipe radius, r_p	1.9 in (4.83×10^{-2} m)
Hole-size radius, r_w	4 3/8 in (1.11×10^{-1} m)
Initial pressure, p_i	2240 psig (1.555×10^{7} Pa)

Slug Test Data

t (min)(60 s)	p_w (psig)(6.89×10^{3} Pa g)	p_{wD}
0.0	161	1.0000
3.29	181	0.9904
7.26	215	0.9740
11.52	251	0.9567
15.83	272	0.9466
19.70	298	0.9341
23.52	315	0.9259
27.38	322	0.9226
33.20	345	0.9115
37.99	370	0.8995
41.04	388	0.8937
45.79	407	0.8817
50.77	423	0.8740
54.74	443	0.8644
59.68	471	0.8509
64.03	486	0.8437
68.49	500	0.8369
73.42	525	0.8249
78.07	551	0.8124
81.94	569	0.8038
85.14	580	0.7985
87.65	585	0.7961
90.80	593	0.7922
93.07	605	0.7864
96.80	624	0.7773
100.33	632	0.7734
103.96	645	0.7720
107.40	655	0.7624
110.98	677	0.7518
114.90	694	0.7436
117.37	701	0.7403

TABLE C-3: WELL, RESERVOIR DATA AND MEASURED PRESSURE IN EXAMPLE 3

Well and Reservoir Data

Formation thickness, h	70 ft (2.13x10 m)
Porosity, ϕ	≈ 4% BV
Viscosity, μ_o	156.3 cp (1.56×10^{-1} Pa s)
Compressibility, c_t	6×10^{-6} psi-1 (8.70×10^{-10} Pa^{-1})
Wellbore oil density, ρ_f	0.925 gm/cc (9.25×10^{2} kg/m^3)
Formation temperature	87°F (304°K)
Test interval	4,374 ft to 4,444 ft (1333 m to 1355 m)
Drill pipe ID	3.34 in (8.48×10^{-2} m)
Hold radius, r_w	4.375 in (1.11×10^{-1} m)
Recovery	41.8 bbl (6.65 m^3) (3,853 ft oil) (1174 m)
Drill collar	630 ft (192 m) 2.25 in ID (5.72×10^{-2} m)
Oil formation volume factor	0.999
First flow period	15 min (900s)
Initial formation pressure, p_i	1865 psig (1.286×10^{7} Pa g)

Slug Test Data

t (min)(60 s)	p_{wf} (psig) (6.89×10^{3} Pa g)	p_{wD}
0	371.4	1
2	384.0	0.992
4	404.6	0.978
6	422.4	0.966
8	441.3	0.953
10	459.1	0.941
12	478.0	0.929
14	496.3	0.916
16	514.6	0.904
18	534.1	3.891
20	552.5	0.879
22	571.9	0.866
24	590.8	0.853
26	607.5	0.842
28	625.2	0.830
30	641.8	0.819

CONTINUED

TABLE C-3, CONTINUED

t (min)(60 s)	p_{wf} (psig) (6.89×10^3 Pa g)	p_{wD}
32	659.0	0.807
34	675.1	0.797
36	691.1	0.786
38	707.7	0.775
40	721.5	0.766
42	737.5	0.755
44	753.0	0.745
46	767.9	0.735
48	782.2	0.725
50	795.4	0.716
52	810.9	0.706
54	825.2	0.696
56	838.0	0.688
58	852.7	0.678
60	865.9	0.669
62	880.2	0.659
64	892.8	0.651
66	906.0	0.642
68	918.6	0.634
70	930.6	0.626
72	943.2	0.617
74	955.3	0.609
76	967.3	0.601
78	979.3	0.593
80	992.5	0.584
82	1002.3	0.578
84	1014.3	0.570
86	1025.8	0.562
88	1036.6	0.555
90	1049.2	0.546
92	1058.4	0,540
94	1069.9	0.532
96	1079.6	0.526
98	1089.9	0.519
100	1101.4	0.511
102	1110.0	0.505
104	1120.3	0.499
106	1129.5	0.492
108	1139.2	0.486
110	1150.7	0.478
112	1158.7	0.473
114	1167.9	0.467
116	1177.0	0.461
118	1186.8	0.454
120	1197.1	0.447
122	1204.5	0.442
124	1213.1	0.436
126	1222.3	0.430

CONTINUED

TABLE C-3, CONTINUED

t (min)(60 s)	p_{wf} (psig) ($6.89x10^3$ Pa g)	p_{wD}
128	1230.3	0.425
130	1240.1	0.418
132	1247.5	0.413
134	1256.1	0.408
136	1263.5	0.403
138	1272.1	0.397
140	1280.7	0.391
142	1287.6	0.387
144	1295.6	0.381
146	1303.1	0.376
148	1310.5	0.371
150	1319.1	0.365
152	1325.4	0.361
154	1332.9	0.356
156	1339.8	0.352
158	1347.2	0.347
160	1355.2	0.341
162	1360.4	0.338
164	1367.8	0.333
166	1374.1	0.329
168	1380.4	0.324
170	1387.9	0.319
172	1393.6	0.316
174	1399.3	0.312
176	1405.7	0.308
178	1411.4	0.304
180	1418.8	0.299
182	1423.4	0.296
184	1429.7	0.291
186	1435.4	0.288
188	1441.2	0.284
190	1448.1	0.279
192	1452.1	0.276
194	1457.2	0.273
196	1463.0	0.269
198	1468.1	0.266
200	1474.4	0.262
202	1478.4	0.259
204	1484.2	0.255
206	1488.7	0.252
208	1493.9	0.248
210	1499.6	0.245
212	1503.6	0.242
214	1508.8	0.238
216	1513.4	0.235
218	1518.5	0.232
220	1522.5	0.229

CONTINUED

TABLE C-3, CONTINUED

t (min) (60 s)	p_{wf} (psig) (6.89×10^3 Pa g)	p_{wD}
222	1527.1	0.226
224	1531.7	0.223
226	1536.3	0.220
228	1540.9	0.217
230	1545.5	0.214
232	1548.9	0.212
234	1552.9	0.209
236	1556.9	0.206
238	1560.9	0.204
240	1566.7	0.200
242	1569.5	0.198
244	1573.5	0.195
246	1577.6	0.192
248	1581.6	0.190
250	1586.1	0.187
252	1589.6	0.184
254	1592.4	0.183
256	1596.5	0.180
258	1600.5	0.177
260	1603.9	0.175
262	1607.3	0.173

Buildup Test Data

$t_p = 569.4$ min (3.416×10^4 s)

Δt (min) (60 s)	$\frac{t_p+\Delta t}{\Delta t}$	p_{ws} (psig) (6.89×10^3 Pa g)	Δt (min) (60 s)	$\frac{t_p+\Delta t}{\Delta t}$	p_{ws} (psig) (6.89×10^3 Pa g)
0		1607.3	22	26.88	1860.6
1	570.4	1816.5	24	24.73	1861.2
2	285.7	1849.7	26	22.90	1861.2
3	190.8	1852.6	28	21.34	1861.2
4	143.4	1854.9	30	19.98	1861.2
5	114.9	1856.0	35	17.27	1861.2
6	95.90	1856.6	40	15.24	1862.3
7	82.34	1857.2	45	13.65	1862.3
8	72.18	1857.7	50	12.39	1862.3
9	64.27	1858.3	55	11.35	1863.5
10	57.94	1858.9	60	10.49	1863.5
12	48.45	1859.5	65	9.76	1864.1
14	41.67	1859.5	70	9.13	1864.1
16	36.59	1859.5	75	8.59	1864.1
18	32.63	1860.0	80	8.19	1864.1
20	29.47	1860.0	85	7.70	1864.1

CONTINUED

TABLE C-3, CONTINUED

Δt (min) (60 s)	$\frac{t_p+\Delta t}{\Delta t}$	p_{ws} (psig) ($6.89x10^3$ Pa g)	Δt (min) (60 s)	$\frac{t_p+\Delta t}{\Delta t}$	p_{ws} (psig) ($6.89x10^3$ Pa g)
90	7.33	1864.1	155	4.67	1865.2
95	6.99	1864.6	160	4.56	1865.2
100	6.69	1865.2	180	4.16	1865.2
105	6.42	1865.2	200	3.85	1865.2
110	6.18	1865.2	220	3.59	1865.2
115	5.95	1865.2	240	3.31	1865.2
120	5.75	1865.2	260	3.19	1865.2
125	5.56	1865.2	280	3.03	1865.2
130	5.38	1865.2	300	2.90	1865.2
135	5.22	1865.2	320	2.78	1865.2
140	5.07	1865.2	340	2.68	1865.2
145	4.93	1865.2	355	2.60	1865.2
150	4.80	1865.2			

TABLE C-4: MEASURED LIQUID LEVEL (TAKEN FROM GRAPHS IN VAN DER KAMP[16])

Time, t (s)	Liquid Level, x (cm) 2-C Well	9-A Well
0	-3.87	-4.60
1	-2.65	-3.61
2	-0.76	-2.72
3	0.18	-2.10
4	0.60	-1.66
5	0.50	-1.32
6	0.17	-1.08
7	-0.13	-0.85
8	-0.23	-0.79
9	-0.24	-0.66
10	-0.20	-0.57
11	-0.11	-0.49
12	-0.02	-0.39
13	0	-0.30
14	-	-0.23
15	-	-0.20
16	-	-0.13
17	-	-0.11
18	-	-0.09
19	-	-0.06
20	-	-0.02
21	-	0

C-2: PRESSURE DROP CAUSED BY FRICTION

C-2.1 Example 1

We will consider the pressure drop by friction at the end of the apparent constant flowrate period at early times (i.e., t = 40 min, in this example), which is close to the maximum value. From Fig. 58 we can obtain the actual flowrate, q, for the apparent constant flowrate period.

$$q = \frac{\pi r_p^2}{\rho_f \cdot g} \cdot \frac{dp_{wf}}{dt}$$

$$= \frac{\pi \left(\frac{2.25}{12}\right)^2}{(0.8458)(62.4)(32.2)} \quad \frac{1732-712}{70}$$

(ft2) (ft3/lbm) (sec2/ft) (psi/min)

$$= 1126.1 \text{ bbl/day } (2.072\text{x}10^{-3} \text{ m}^3/\text{s})$$

Then the velocity of the liquid in the wellbore, u, becomes:

$$u = \frac{q}{\pi r_p^2}$$

$$= \frac{1126.1}{\pi\left(\frac{2.25}{12}\right)} = 10{,}196 \text{ (bbl/day) } (1/\text{ft}^2)$$

$$= 0.663 \text{ ft/s } (0.202 \text{ m/s})$$

Thus:

$$\text{Reynolds Number} = \frac{\rho_f u D}{\mu}$$

$$= \frac{(0.8458)\,(62.4)\,(0.663)\left(\frac{2.25\text{x}2}{12}\right)}{(1)(2.09\text{x}10^{-5})\,(32.2)}$$

$$= 19{,}500$$

Therefore the flow is turbulent.

From the Moody diagram[43] (assuming $\varepsilon/D = 0.01$), the friction factor, f, is about 0.04. The liquid length in the wellbore, L at t = 40 min ($2.4\text{x}10^3$ s) becomes (considering the cushion liquid):

$$L = (0.663)\ \ (40\text{x}60) + \frac{(560)\,(144)}{(0.8458)\,(62.4)}$$

$$= 3120 \text{ ft } (951 \text{ m})$$

Then the pressure drop caused by friction in the well-bore becomes:

$$\Delta p = f \cdot \frac{L}{D} \cdot \frac{\rho u^2}{2}$$

$$= (0.04) \cdot \frac{(3120)}{\frac{2\text{x}2.25}{12}} \cdot \frac{(0.8458)\,(62.4)\,(0.663)^2}{2}$$

$$(\text{ft})\ (1/\text{ft})\ (\ell\text{bm}/\text{ft}^3)\ (\text{ft}^2/\text{sec}^2)$$

$$= 0.83 \text{ psi } (5.72\text{x}10^3 \text{ Pa})$$

C-2.2: Example 3

Similar to Example 1, we will consider the pressure drop caused by friction at the end of the apparent constant flowrate period (i.e., t = 30 min, in this example).

Then:

$$q = 363.4 \text{ bbl/day } (6.687 \times 10^{-4} \text{ m}^3/\text{s})$$

$$u = 0.388 \text{ ft/s } (0.118 \text{ m/s})$$

$$\text{Reynolds Number} = 59.3$$

Thus the flow is laminar and the friction factor, f, becomes:

$$f = \frac{64}{N_{Re}} = 1.08$$

Similar to Example 1:

$$L = 1625 \text{ ft } (495 \text{ m})$$

Then:

$$\Delta p = 5.9 \text{ psi } (4.07 \times 10^4 \text{ Pa})$$

APPENDIX D: DERIVATION OF FINITE DIFFERENCE SOLUTIONS

D-1: Closed Chamber Test

From Eq. 14:

$$p_{D_{i-1}}^{n+1} - \left\{ 2 + \frac{a\left(r_{D_{i+\frac{1}{2}}}^{2} - r_{D_{i-\frac{1}{2}}}^{2} \right)}{2\Delta t_D} \right\} p_{D_i}^{n+1}$$

$$+ p_{D_{i+1}}^{n+1} = - \frac{a\left(r_{D_{i+\frac{1}{2}}}^{2} - r_{D_{i-\frac{1}{2}}}^{2} \right)}{2\Delta t_D} p_{D_i}^{n} \qquad \text{(D-1)}$$

where:

$$r_{D_i} = (r_{D_e})^{\frac{i-1}{M-1}} \qquad \text{(D-2)}$$

$$a = \frac{1}{M-1} \ln r_{D_e} \qquad \text{(D-3)}$$

r_{D_i} is the dimensionless radial distance at node i, r_{D_e} is the dimensionless external radius of the reservoir, and M is the number of nodes.

From Eq. 83:

$$\alpha^2 \cdot \frac{x_D^{n+1} - 2x_D^{n} + x_D^{n-1}}{(\Delta t_D)^2} + \frac{1}{2}\left(x_D^{n+1} + x_D^{n}\right)$$

$$\left({}_{wD}^{n+1} \quad p_{wD}^{n} \right) \qquad \left| \frac{L_D - x_D(0) \qquad p_{D_{atm}}}{L_D - x_D^{n}} \right|$$

(D-4)

From Eq. 27:

$$p_{wD}^{n+1} = p_{D_1}^{n+1} - \frac{s}{a}\left(p_{D_2} - p_{D_1}\right) \tag{D-5}$$

From Eq. *24:*

$$\frac{x_D^{n+1} - x_D^{n}}{\Delta t_D} = -\frac{1}{C_D}\,\frac{p_{D_2}^{n+1} - p_{D_1}^{n+1}}{a} \tag{D-6}$$

Then the system of equations becomes as follows:

When $s \neq 0$:

$$\begin{pmatrix} b(1) & c(1) & 0 & 0 & 0 & & \\ \frac{sC_D}{\Delta t_D} & -1 & 1 & 0 & 0 & 0 & \\ 0 & 1 & -\left(\frac{s}{a}+1\right) & \frac{s}{a} & 0 & & \\ 0 & 0 & 1 & E(2) & 1 & & \\ & & & \ddots & & \ddots & \\ & 0 & & 1 & E(M-1) & 1 & \\ & & & 0 & 1 & E(M)+ & \end{pmatrix} \begin{Vmatrix} x_D^{n+1} \\ p_{wD}^{n+1} \\ p_{D_1}^{n+1} \\ p_{D_2}^{n+1} \\ \vdots \\ p_{D_{M-1}}^{n+1} \\ p_{D_M}^{n+1} \end{Vmatrix} = \begin{pmatrix} A'' \\ \frac{sC_D}{\Delta t_D} x_D^n \\ 0 \\ [E(2)+2]p_{D_2}^n \\ \vdots \\ \vdots \\ [E(M)+2]p_{D_M}^n \end{pmatrix} \tag{D-7}$$

Where :

$$E(i) = - \left| 2 + \frac{a\left(\gamma_i^2 + \frac{1}{2} - \gamma_i^2 - \frac{1}{2}\right)}{2} \right| \qquad \text{(D-8)}$$

$$b(1) = \begin{cases} 1 + \dfrac{(\Delta t_D)^2}{2\alpha^2} & \text{for } \alpha \neq 0 \\ 1 & \text{for } \alpha = 0 \end{cases} \qquad \text{(D-9)}$$

$$c(1) = \begin{cases} \dfrac{(\Delta t_D)^2}{2\alpha^2} & \text{for } a \neq 0 \\ 1 & \text{for } a = 0 \end{cases} \qquad \text{(D-10)}$$

$$A^n = \begin{cases} \left\{2 - \dfrac{(\Delta t_D)^2}{2\alpha^2}\right\} x_D^n - x_D^{n-1} - \dfrac{(\Delta t_D)^2}{2a^2} p_{wD}^n \\ \quad - \beta \dfrac{(\Delta t_D)^2}{a^2} \left| \dfrac{L_{D_i} - x_D(0)}{L_{D_i} - x_D^n} - \dfrac{p_{D_{atm}}}{\beta} \right\} & \text{for } \alpha \neq 0 \qquad \text{(D-11)} \\ - \beta \left| \dfrac{L_{D_i} - x_D(0)}{L_{D_i} - x_D^n} - \dfrac{p_{D_{atm}}}{P} \right| & \text{for } a = 0 \qquad \text{(D-11)} \end{cases}$$

When $s = 0$:

$$\begin{pmatrix} b(1) & c(1) & & & & \\ 1 & -\frac{\Delta t_D}{C_D a} & \frac{\Delta t_D}{C_D a} & & 0 & \\ 0 & 1 & E(2) & 1 & & \\ & \cdot & & \ddots & & \\ & & \cdot & & \ddots & \\ 0 & & 1 & E(M-1) & 1 & \\ & & & 1 & E(M)+1 & \end{pmatrix} \begin{pmatrix} x_D^{n+1} \\ p_{D_1}^{n+1} \\ p_{D_2}^{n+1} \\ \vdots \\ p_{D_{M-1}}^{n+1} \\ p_{D_M}^{n+1} \end{pmatrix} = \begin{pmatrix} A^n \\ x_D^n \\ [E(2)+2]p_{D_2} \\ \\ \\ [E(M)+2]p_{D_M}^n \end{pmatrix} \qquad \text{(D-12)}$$

$E(i)$, $b(1)$, $c(1)$, and A^n are the same as defined in Eqs. **D-8** through D-11.

D-2: <u>Slug Test</u>

From Eq. 18:

$$\alpha^2 \cdot \frac{x_D^{n+1} - 2x_D^n + x_D^{n-1}}{(\Delta t_D)^2} + \frac{1}{2}(x_D^{n+1} + x_D^n) = -\frac{1}{2}(p_{wD}^{n+1} + p_{wI}^n) \qquad \text{(D-13)}$$

This equation should be used instead of Eq. *D-4*. Then, **Eq,** D-11 should be changed as follows:

$$A^n = \begin{cases} \left\{2 - \frac{(\Delta t_D)^2}{2\alpha^2}\right\} x_D^n - x_D^{n-1} - \frac{(\Delta t_D)^2}{2\alpha^2} p_{wD}^n & \text{for } \alpha \neq 0 \\ 0 & \text{for } \alpha = 0 \end{cases} \qquad \text{(D-14)}$$

The other equations are the same as those in the closed chamber test.

D-3: Buildup Test

After the shut-in, we will consider th pressure change only inside the reservoir, Then we can use Eq. D-1 for this case. Assuming the following equations to be the boundary conditions:

$$p_{D_1} = p_{D_2}$$
$$p_{D_{M-1}} = p_{D_M} \qquad \text{(D-15)}$$

the system of equations becomes as follows:

$$\begin{vmatrix} E(1)+1 & 1 & & & & \\ 1 & E(2) & 1 & & 0 & \\ & 1 & E(3) & 1 & & \\ & & \ddots & \ddots & \ddots & \\ & & & 1 & E(M-1) & 1 \\ 0 & & & & 1 & E(M)+ \end{vmatrix} \begin{vmatrix} p_{D_1}^{n+1} \\ p_{D_2}^{n+1} \\ p_{D_3}^{n+1} \\ \vdots \\ p_{D_{M-1}}^{n+1} \\ p_{D_M}^{n+1} \end{vmatrix} = \begin{vmatrix} [E(1)+2]p_{D_1}^{n} \\ [E(2)+2]p_{D_2}^{n} \\ [E(3)+2]p_{D_3}^{n} \\ \vdots \\ [E(M-1)+2]p_{D_{M-}}^{n} \\ [E(M)+2]p_{D_m}^{n} \end{vmatrix}$$

(D-16)

APPENDIX E: COMPUTER PROGRAM

The four computer programs are shown here. The first one is the program of the Stehfest method to obtain the Laplace transform inversion for the subject function. The second is the program of the Albrecht-Honig method for the same purpose. The third is the program to obtain the pressure distribution inside the reservoir. The last is the program to simulate a closed chanber test, slug test, and buildup test. The program of the Veillon method is not shown here. One can find the logic in the original paper.[28]

E-1 STEHFEST METHOD

```
C       LAPLACE INVERSION BY STEHFEST
C       ALF            SQUARE OF DIMENSIONLESS NUMBER ALFA
C       CD             DIMENSIONLESS WELLBORE STORAGE CONSTANT
C       DX0            INITIAL VALUE OF DIMENSIONLESS LIQUID LEVEL
C       DXD0           INITIAL VALUE OF VELOCITY OF DIMENSIONLESS LIQUID LEVEL
C       DT             INCREMENT OF DIMENSIONLESS TIME
C       DPW            DIMENSIONLESS WELLBORE PRESSURE
C       DX             DIMENSIONLESS LIQUID LEVEL
C       M              NUMBER OF TIME INCREMENT
C       N              NUMBER OF TERM IN STEHFEST ALGORITHM
C       NI             INITIAL VALUE OF EXPONENT TO GIVE ALF VALUE
C       NTIME          LAST VALUE OF EXPONENT TO GIVE ALF VALUE
C       SKIN           SKIN FACTOR
C       TD             DIMENSIONLESS TIME
        IMPLICIT REAL*8 (A-H,O-Z)
        DIMENSION TD(200),DX(200),DPW(200),A(200),V(50),G(50),H(50),GZ(2)
        SF=0.D0
        SF2=0.D0
        SKIN=0.D0
        CD=1.D3
        DX0=-1.D0
        DXD0=0.D0
        M=80
        N=16
        NI=1
        NTIME=10
        DLOGTW=.6931471805599453D0
        G(1)=1.D0
        NH=N/2
        DO 5 I=2,N
      5 G(I)=G(I-1)*I
        H(1)=2./G(NH-1)
        DO 10 I=2,NH
        FI=I
        IF(I.EQ.NH) GO TO 8
        H(I)=FI**NH*G(2*I)/(G(NH-I)*G(I)*G(I-1))
        GO TO 10
      8 H(I)=FI**NH*G(2*I)/(G(I)*G(I-1))
     10 CONTINUE
        SN=2*(NH-NH/2*2)-1
        DO 50 I=1,N
        V(I)=0.
        K1=(I+1)/2
        K2=I
        IF(K2.GT.NH) K2=NH
        DO 40 K=K1,K2
        IF(2*K-I.EQ.0) GO TO 37
        IF(I.EQ.K) GO TO 38
        V(I)=V(I)+H(K)/(G(I-K)*G(2*K-I))
        GO TO 40
     37 V(I)=V(I)+H(K)/(G(I-K))
        GO TO 40
     38 V(I)=V(I)+H(K)/G(2*K-I)
     40 CONTINUE
        V(I)=SN*V(I)
        SN=-SN
     50 CONTINUE
        DO 100 I=1,100
        TD(I)=0.
        DX(I)=0.
```

```
      DPW(I)=0.
      A(I)=0.
  100 CONTINUE
      DO 150 K=NI,NTIME
      IF(K.EQ.NI) GO TO 101
      ALF=10.**(K-1)
      GO TO 102
  101 ALF=0.
  102 CONTINUE
      WRITE(6,151) ALF
  151 FORMAT(1H1,D30.10)
      TT=0.D0
      DT=1.D-2
      DO 200 I=1,M
      TT=TT+DT
      IF(TT.GE.9.99D-5) DT=1.D-4
      IF(TT.GE.9.99D-4) DT=1.D-3
      IF(TT.GE.9.99D-3) DT=1.D-2
      IF(TT.GE.9.99D-2) DT=1.D-1
      IF(TT.GE.9.99D-1) DT=1.D0
      IF(TT.GE.9.99D0) DT=1.D1
      IF(TT.GE.9.99D1) DT=1.D2
      IF(TT.GE.9.99D2) DT=1.D3
      IF(TT.GE.9.99D3) DT=1.D4
      IF(TT.GE.9.99D4) DT=1.D5
      IF(TT.GE.9.99D5) DT=1.D6
      IF(TT.GE.9.99D6) DT=1.D7
      IF(TT.GE.9.99D7) DT=1.D8
      IF(TT.GE.9.99D8) DT=1.D9
      IF(TT.GE.9.99D9) DT=1.D10
      IF(TT.GE.9.99D10) DT=1.D11
      IF(TT.GE.9.99D11) DT=1.D12
      IF(TT.GE.9.99D12) DT=1.D13
      IF(TT.GE.9.99D13) DT=1.D14
      IF(TT.GE.9.99D14) DT=1.D15
      TD(I)=TT
      DO 300 J=1,N
      CC=2.
      CO=DLOG(CC)/TD(I)
      SS=CO*DFLOAT(J)
      RSS=DSQRT(SS)
      FA=ALF*SS+SKIN*CD
      A1=BK0(RSS)/BK1(RSS)
      F1=DX0/SS+(ALF*DXD0-DX0/SS)/(ALF*SS*SS+CD*SKIN*SS+1.
     $   +CD*RSS*A1)
      F2=CD*(ALF*DXD0-DX0/SS)*(SKIN*SS+RSS*A1)/(ALF*SS*SS
     $   +CD*SKIN*SS+1.+CD*RSS*A1)
      DF1=V(J)*F1
      DF2=V(J)*F2
      SF=SF+DF1
      SF2=SF2+DF2
  300 CONTINUE
      DX(I)=SF*CO
      SF=0.
      DPW(I)=SF2*CO
      SF2=0.
  200 CONTINUE
      WRITE(6,401) (TD(I),DX(I),DPW(I),I=1,M)
  150 CONTINUE
```

```
      STOP
      END
      FUNCTION BK0(X)
      IMPLICIT REAL*8 (A-H,O-Z)
      IF(X.GT.2.) GO TO 700
      T=X/2.
      A1=-DLOG(T)*BI0(X)-.57721566+.4227842*T**2+.23069756*T**4
      A2=.0348859*T**6+.00262698*T**8+.0001075*T**10+.0000074*T**12
      BK0=A1+A2
      GO TO 701
  700 IF(X.GT.1.74D2) GO TO 702
      T=2./X
      A3=1.25331414-.07832358*T+.02189568*T**2-.01062446*T**3
      A4=.00587872*T**4-.0025154*T**5+.00053208*T**6
      BK0=(A3+A4)/(DSQRT(X)*DEXP(X))
      GO TO 701
  702 BK0=1.D-70
  701 RETURN
      END
      FUNCTION BK1(X)
      IMPLICIT REAL*8 (A-H,O-Z)
      IF(X.GT.2.) GO TO 710
      T=X/2.
      A1=X*DLOG(T)*BI1(X)+1.+.15443144*T**2-.67278579*T**4
      A2=-.18156897*T**6-.01919402*T**8-.00110404*T**10-.00004686*T**12
      BK1=(A1+A2)/X
      GO TO 711
  710 IF(X.GT.1.74D2) GO TO 712
      T=2./X
      A3=1.25331414+.23498619*T-.0365562*T**2+.01504268*T**3
      A4=-.00780353*T**4+.00325614*T**5-.00068245*T**6
      BK1=(A3+A4)/(DSQRT(X)*DEXP(X))
      GO TO 711
  712 BK1=1.D-70
  711 RETURN
      END
      FUNCTION BI0(X)
      IMPLICIT REAL*8 (A-H,O-Z)
      IF(X.GT.3.75)  GO TO 720
      T=X/3.75
      A1=1.+3.5156229*T**2+3.0899424*T**4+1.2067492*T**6
      A2=.2659732*T**8+.0360768*T**10+.0045813*T**12
      BI0=A1+A2
      GO TO 721
  720 IF(X.GT.1.74D2) GO TO 722
      T=3.75/X
      A3=.39894228+.01328592*T+.00225319*T**2-.00157565*T**3+.00916281*T**4
      A4=-.02057706*T**5+.02635537*T**6-.01647633*T**7+.00392377*T**8
      BI0=(A3+A4)/(DSQRT(X)*DEXP(-X))
      GO TO 721
  722 BI0=1.D70
  721 RETURN
      END
      FUNCTION BI1(X)
      IMPLICIT REAL*8 (A-H,O-Z)
      IF(X.GT.3.75)  GO TO 730
      T=X/3.75
      A1=.5+.87890594*T**2+.51498869*T**4+.1508493*T**6+.02658733*T**8
      A2=.00301532*T**10+.00032411*T**12
      BI1=(A1+A2)*X
```

```
      GO TO 731
  730 IF(X.GT.1.74D2) GO TO 732
      T=3.75/X
      A3=.39894228-.03988024*T-.00362018*T**2+.00163801*T**3-.01031555*T**4
      A4=.02282967*T**5-.02895312*T**6+.01787654*T**7-.00420059*T**8
      BI1=(A3+A4)/(DSQRT(X)*DEXP(-X))
      GO TO 731
  732 BI1=1.D70
  731 RETURN
      END
CDATA
$STOP
//
```

E-2 ALBRECHT-HONIG METHOD

```
C      LAPLACE INVERSION BY ALBRECHT-HONIG
C      ALF                SQUARE OF DIMENSIONLESS NUMBER
C      ARI=1              DETERMINE EXTREME VALUE
C         =OTHERWISE      OPTIONAL
C      CON                VARIABLE TO DETERMINE MAXIMUM DESCRETIZATION ERROR
C      CD                 DIMENSIONLESS WELLBORE STORAGE CONSTANT
C      DX0                INITIAL VALUE OF DIMENSIONLESS LIQUID LEVEL
C      DXDO               INITIAL VALUE OF VELOCITY OF DIMENSIONLESS LIQUID LEVEL
       F                  EXTERNAL FUNCTION
C      M1N1               NUMBER OF FUNCTION VALUE TO BE COPIPUTED IN (T1,TN)
C      NN                 NUMBER OF EXTREME VALUE
C      NS1                NUMBER OF FUNCTION VALUE REQUIRED FOR CALCULATING INVERSION
C      NS2                NUMBER OF FUNCTION VALUE REQUIRED FOR CALCULATING CORRECTION TE
C      SKIN               SKIN FACTOR
C      Tl                 LOWER INTERVAL BOUNDARY OF TIME
C      TN                 UPPER INTERNAL BOUNDARY OF TIME
       IMPLICIT REAL*8 (A-H,O-Z)
       REAL*8 H(2,1000),TT(1000),E(1000)
       COMMON MM(2,1000)
       INTEGER*4 MM,ART,RICHT
       COMPLEX*16 F,S
       EXTERNAL F
       T1=0.
       TN=100.
       N1M1=9
       NS1=20
       NS2=20
       CON=5
       NN=8
       ART=1
       CALL LAPIN(F,T1,TN,N1M1,H,TT,NS1,NS2,CON,NN,MM,ART,E,IER)
       WRITE(6,1000) IER
 1000  FORMAT(I10)
       WRITE(6,2000)(TT(J),H(2,J),J=1,N1M1)
 2000  FORMAT(D20.5,F15.10)
       STOP
       END
       SUBROUTINE LAPIN(F,T1,TN,N1M1,H,TT,NS1,NS2,CON,NN,MM,ART,E,IER)
C
C      MINIMUM MAXIMUM ORRECTIVE TERM PASSES
C       (NUMERICAL INVERSION EINEP LAPLACE TRANSFORMATION F(S)
C
       IMPLICIT REAL*8(A-H,O-Z)
       REAL*8 E(NS1),H(2,N1M1),KOR,TT(N1M1),FAKT
       INTEGER*4 MM(2,N1M1),ART,RICHT
       COMPLEX*16  F,S
       EXTERNAL F
       IER=0
       IF(TN.LE.T1) IER=1
       IF(N1M1.LT.1) IER=IER+10
       IF(NS1.LT.1. OR. NS2.LT.1) IER=IER+100
       IF(NN.LT.1) IER=IER+1000
       IF(IER.GT.0) GO TO 250
       IF(NN.GT.NS1) NN=NS1
       IF(NN.GT.NS2) NN=NS2
       PI=4.D0*DATAN(1.D0)
       N1=N1M1+1
       DELTA=(TN-T1)/DFLOAT(N1)
       I=1
       K2=1
```

```
      NSUM=NS1
C
C     CALCULATION OF THE VALUE OF T IN (T1-TN)
C
   20 DO 100 K1=1,N1M1
      N=NN
      K=I*K1+1
      T=DFLOAT(K1*I)*DELTA+T1*I
      V=CON/T
      RAL=-0.5D0*DREAL(F(DCMPLX(V,0.D0)))
      SURE=0.D0
      PITE=PI/T
      EINS=1.DO
C
C     CALCULATION OF THE APPROXIMATE VALUE E(L) TO BE USED
C     AS AN INVERSE L=1,2,.....NSUM TO BE CALCULATED BY
C     THE METHOD OF DURBAN
C
      DO 30 L=1,NSUM
      W=DFLOAT(L-1)*PITE
      SURE=SURE+DREAL(F(DCMPLX(V,W)))*EINS
      EINS=-EINS
   30 E(L)=DEXP(V*T)/T*(RAL+SURE)
C
      IF(ART.NE.1) GO TO 50
C
C     NN SEEKING FOR THE EXTREME VALUES
C
      RICHT=-1
      IF(E(NSUM).GT.E(NSUM-1)) RICHT=1
      NSUMP1=NSUM+1
      J1=NSUMP1
      J2=NSUM
   42 RICHT=-RICHT
      J1=J1-1
      E(J1)=E(J2)
   44 IF(J2.GT.2) GO TO 46
      J1=J1-1
      E(J1)=E(1)
      N=NSUMP1-J1
      GO TO 50
   46 IF(NSUMP1-J1.EQ.N) GO TO 50
      J2=J2-1
      IF(E(J2)-E(J2-1)) 48,44,47
   47 IF(RICHT.EQ.-1) GO TO 44
      GO TO 42
   48 IF(RICHT.EQ.1)  GO TO 44
      GO TO 42
C
C     INTERPOLATION AND MID POINT DETERMINATIOM
C
   50 IF(N-3) 52,54,56
   52 H(K2,K1)=E(NSUM)
      GO TO 59
   54 H(K2,K1)=(E(NSUM-2)+E(NSUM))/4.D0+E(NSUM-1)/2.D0
      GO TO 59
   56 SUM=(E(NSUM)+E(NSUM-N+1))*0.25D0+(E(NSUM-1)+E(NSUM-N+2))*0.75D0
      IF(N.EQ.4) GO TO 58
      J1=NSUM-N+3
      J2=NSUM-2
```

```
      DO 57 J=J1,J2
   57 SUM=SUM+E(J)
   58 H(K2,K1)=SUM/DFLOAT(N-2)
   59 MM(K2,K1)=N
  100 CONTINUE
      IF(I.EQ.3) GO TO 150
      1=3
      K2=2
      NSUM=NS2
      GO TO 20
C
C     CALCULATION OF THE CORRECTED TERM AND CORRECTION TERM OF
C     OF THE 'MINIMAX'-WEPTE
C
  150 FAKT=-DEXP(-2.D0*CON)
      DO 200 K=1,N1M1
      H(2,K)=H(1,K)+FAKT*H(2,K)
      TT(K)=DFLOAT(K)*DELTA+T1
  200 CONTINUE
  250 RETURN
      END
      FUNCTION F(S)
      COMPLEX*16 F,S,BK0,BK1,Q,RS
      CD=10.**3
      ALF=10.**3
      SKIN=0.
      DX0=-1.
      DXD0=0.
      RS=CDSQRT(S)
      Q=(ALF*S*S+1.)*RS/(SKIN*RS+BK0(RS)/BK1(RS))
      F=CD*(-DX0+ALF*S*DXD0)/(CD*S+Q)
      RETURN
      END
      FUNCTION BK0(X)
      IMPLICIT REAL*8 (A-H,O-Z)
      COMPLEX*16 BK0,X,T,BI0,A1,A2,A3,A4
      IF(CDABS(X).GT.2.) GO TO 700
      T=X/2.
      A1=-CDLOG(T)*BI0(X)-.57721566+.4227842*T**2+.23069756*T**4
      A2=.0348859*T**6+.00262698*T**8+.0001075*T**10+.0000074*T**12
      BK0=A1+A2
      GO TO 701
  700 IF(X.GT.1.74D2) GO TO 702
      T=2./X
      A3=1.25331414-.07832358*T+.02189568*T**2-.01062446*T**3
      A4=.00587872*T**4-.0025154*T**5+.00053208*T**6
      BK0=(A3+A4)/(CDSQRT(X)*CDEXP(X))
      GO TO 701
  702 BK0=1.D-70
  701 RETURN
      END
      FUNCTION BK1(X)
      IMPLICIT REAL*8 (A-H,O-Z)
      COMPLEX*16 BK1,X,T,BI1,A1,A,A3,A4
      IF(CDABS(X).GT.2.) GO TO 710
      T=X/2.
      A1=X*CDLOG(T)*BI1(X)+1.+.15443144*T**2-.67278579*T**4
      A2=-.18156897*T**6-.01919402*T**8-.00110404*T**10-.00004686*T**12
      BK1=(A1+A2)/X
      GO TO 711
```

```
710 IF(X.GT.1.74D2) GO TO 712
    T=2./X
    A3=1.25331414+.23498619*T-.0365562*T**2+.01504268*T**3
    A4=-.00780353*T**4+.00325614*T**5-.00068245*T**6
    BK1=(A3+A4)/(CDSQRT(X)*CDEXP(X))
    GO TO 711
712 BK1=1.D-70
711 RETURN
    END
    FUNCTION BI0(X)
    IMPLICIT REAL*8 (A-H,O-Z)
    COMPLEX*16 BI0,X,T,A1,A2,A3,A4
    IF(CDABS(X).GT.3.75) GO TO 720
    T=X/3.75
    A1=1.+3.5156229*T**2+3.0899424*T**4+1.2067492*T**6
    A2=.2659732*T**8+.0360768*T**10+.0045813*T**12
    BI0=A1+A2
    GO TO 721
720 IF(X.GT.1.74D2) GO TO 722
    T=3.75/X
    A3=.39894228+.01328592*T+.00225319*T**2-.00157565*T**3+.00916281*T**4
    A4=-.02057706*T**5+.02635537*T**6-.01647633*T**7+.00392377*T**8
    BI0=(A3+A4)/(CDSQRT(X)*CDEXP(-X))
    GO TO 721
722 BI0=1.D70
721 RETURN
    END
    FUNCTION BI1(X)
    IMPLICIT REAL*8 (A-H,O-Z)
    COMPLEX*16 BI1,X,T,A1,A2,A3,A4
    IF(CDABS(X).GT.3.75) GO TO 730
    T=X/3.75
    A1=.5+.87890594*T**2+.51498869*T**4+.1508493*T**6+.02658733*T**8
    A2=.00301532*T**10+.00032411*T**12
    BI1=(A1+A2)*X
    GO TO 731
730 IF(X.GT.1.74D2) GO TO 732
    T=3.75/X
    A3=.39894228-.03988024*T-.00362018*T**2+.00163801*T**3-.01031555*T**4
    A4=.02282967*T**5-.02895312*T**6+.01787654*T**7-.00420059*T**8
    BI1=(A3+A4)/(CDSQRT(X)*CDEXP(-X))
    GO TO 731
732 BI1=1.D70
731 RETURN
    END
$DATA
$STOP
//
```

E-3 COMPUTER PROGRAM TO CALCULATE THE PRESSURE DISTRIBUTIONS INSIDE THE RESERVOIR

```
C     LAPLACE INVERSION BY STEHFEST FOR RADIUS OF INVESTIGATION
C     ALF                 SQUARE OF DIMENSIONLESS NUMBER ALFA
C     CD                  DIMENSIONLESS WELLBORE STORAGE CONSTANT
C     DX0                 INITIAL VALUE OF DIMENSIONLESS LIQUID LEVEL
C     DXD0                INITIAL VALUE OF VELOCITY OF DIMENSIONLESS LIQUID LEVEL
C     DT                  INCREMENT OF DIMENSIONLESS TIME
C     DPW                 DIMENSIONLESS WELLBORE PRESSURE
C     DPI(I=1,2,   )      DIMENSIONLESS PRESSURE AT POINT I
C     M                   NUMBER OF TIME INCREMENT
C     N                   NUMBER OF TERM IN STEHFEST ALGORITHM
C     NI                  INITIAL VALUE OF EXPONENT TO GIVE ALF VALUE
C     NTIME               LAST VALUE OF EXPONENT TO GIVE ALF VALUE
C     RADI(I=1,2, )       DIMENSIONLESS RADIAL DISTANCE AT POINT I
C     SKIN                SKIN FACTOR
C     TD                  DIMENSIONLESS TIME
      IMPLICIT REAL*8 (A-H,O-Z)
      DIMENSION TD(200),DX(200),DPW(200),A(200),V(50),G(50),H(50),GZ(2)
      DIMENSION DP1(200),DP2(200),DP3(200),DP4(200),DP5(200),
     $            DP6(200),DP7(200),DP8(200),DP9(200),DP10(200),
     $            DP11(200),DP12(200),DP13(200),DP14(200),DP15(200),
     $            DP16(200),DP17(200),DP18(200)
      SF1=0.D0
      SF2=0.D0
      SF3=0.D0
      SF4=0.D0
      SF5=0.D0
      SF6=0.D0
      SF7=0.D0
      SF8=0.D0
      SF9=0.D0
      SF10=0.D0
      SF11=0.D0
      SF12=0.D0
      SF13=0.D0
      SF14=0.D0
      SF15=0.D0
      SF16=0.D0
      SF17=0.D0
      SF18=0.D0
      SF19=0.D0
      SF20=0.D0
      SKIN=0.D0
      CD=1.D3
      DX0=-1.D0
      DXD0=0.D0
      RAD1=1.
      RAD2=3.D0
      RAD3=5.D0
      RAD4=7.D0
      RAD5=1.D1
      RAD6=3.D1
      RAD7=5.D1
      RAD8=7.D1
      RAD9=1.D2
      RAD10=3.D2
      RAD11=5.D2
      RAD12=7.D2
      RAD13=1.D3
      RAD14=3.D3
      RAD15=5.D3
```

```
      RAD16=7.D3
      RAD17=1.D4
      RAD18=3.D4
      M=30
      N=16
      NI=1
      NTIME=10
      DLOGTW=.69314718055994530D0
      G(1)=1.D0
      NH=N/2
      DO 5 I=2,N
    5 G(I)=G(I-1)*I
      H(1)=2./G(NH-1)
      DO 10 I=2,NH
      FI=I
      IF(I.EQ.NH) GO TO 8
      H(I)=FI**NH*G(2*I)/(G(NH-I)*G(I)*G(I-1))
      GO TO 10
    8 H(I)=FI**NH*G(2*I)/(G(I)*G(I-1))
   10 CONTINUE
      SN=2*(NH-NH/2*2)-1
      DO 50 I=1,N
      V(I)=0.
      K1=(I+1)/2
      K2=I
      IF(K2.GT.NH) K2=NH
      DO 40 K=K1,K2
      IF(2*K-I.EQ.0) GO TO 37
      IF(I.EQ.K) GO TO 38
      V(I)=V(I)+H(K)/(G(I-K)*G(2*K-I))
      GO TO 40
   37 V(I)=V(I)+H(K)/(G(I-K))
      GO TO 40
   38 V(I)=V(I)+H(K)/G(2*K-I)
   40 CONTINUE
      V(I)=SN*V(I)
      SN=-SN
   50 CONTINUE
      DO 100 I=1,200
      TD(I)=0.D0
      DX(I)=0.D0
      DPW(I)=0.D0
      A(I)=0.DO
      DP1(I)=0.D0
      DP2(I)=0.D0
      DP3(I)=0.D0
      DP4(I)=0.D0
      DP5(I)=0.D0
      DP6(I)=0.D0
      DP7(I)=0.D0
      DP8(I)=0.D0
      DP9(I)=0.D0
      DP10(I)=0.D0
      DP11(I)=0.D0
      DP12(I)=0.D0
      DP13(I)=0.D0
      DP14(I)=0.D0
      DP15(I)=0.D0
      DP16(I)=0.D0
      DP17(I)=0.D0
```

```
      DP18(I)=0.D0
  100 CONTINUE
      DO 150 K=NI,NTIME
      IF(K.EQ.NI) GO TO 101
      ALF=10.**(K-1)
      GO TO 102
  101 ALF=0.
  102 CONTINUE
      WRITE(6,151) ALF
  151 FORMAT(1H1,D30.10)
      TT=0.D0
      DT=1.D3
      DO 200 I=1,M
      TT=TT+DT
      IF(TT.GE.9.99D-2) DT=1.D-1
      IF(TT.GE.9.99D-1) DT=1.D0
      IF(TT.GE.9.99D0) DT=1.D1
      IF(TT.GE.9.99D1) DT=1.D2
      IF(TT.GE.9.99D2) DT=1.D3
      IF(TT.GE.9.99D3) DT=1.D4
      IF(TT.GE.9.99D4) DT=1.D5
      IF(TT.GE.9.99D5) DT=1.D6
      IF(TT.GE.9.99D6) DT=1.D7
      IF(TT.GE.9.99D7) DT=1.D8
      TD(I)=TT
      DO 300 J=1,N
      CC=2.
      CO=DLOG(CC)/TD(I)
      SS=CO*DFLOAT(J)
      RSS=DSQRT(SS)
      RSS1=RAD1*RSS
      RSS2=RAD2*RSS
      RSS3=RAD3*RSS
      RSS4=RAD4*RSS
      RSS5=RAD5*RSS
      RSS6=RAD6*RSS
      RSS7=RAD7*RSS
      RSS8=RAD8*RSS
      RSS9=RAD9*RSS
      RSS10=RAD10*RSS
      RSS11=RAD11*RSS
      RSS12=RAD12*RSS
      RSS13=RAD13*RSS
      RSS14=RAD14*RSS
      RSS15=RAD15*RSS
      RSS16=RAD16*RSS
      RSS17=RAD17*RSS
      RSS18=RAD18*RSS
      FA=ALF*SS*SS+CD*SKIN*SS+1.
      A1=BK0(RSS)/BK1(RSS)
      A21=BK1(RSS)/BK0(RSS1)
      A22=BK1(RSS)/BK0(RSS2)
      A23=BK1(RSS)/BK0(RSS3)
      A24=BK1(RSS)/BK0(RSS4)
      A25=BK1(RSS)/BK0(RSS5)
      A26=BK1(RSS)/BK0(RSS6)
      A27=BK1(RSS)/BK0(RSS7)
      A28=BK1(RSS)/BK0(RSS8)
      A29=BK1(RSS)/BK0(RSS9)
      A210=BK1(RSS)/BK0(RSS10)
```

```
A211=BK1(RSS)/BK0(RSS11)
A212=BK1(RSS)/BK0(RSS12)
A213=BK1(RSS)/BK0(RSS13)
A31=A1*A21
A32=A1*A22
A33=A1*A23
A34=A1*A24
A35=A1*A25
A36=A1*A26
A37=A1*A27
A38=A1*A28
A39=A1*A29
A310=A1*A210
A311=A1*A211
A312=A1*A212
A313=A1*A213
F1=DX0/SS+(ALF*DXD0-DX0/SS)/(FA+CD*RSS*A1)
F2=CD*(ALF*DXD0-DX0/SS)*(SKIN*SS+RSS*A1)/(FA+CD*RSS*A1)
F3=(ALF*DXD0-DX0/SS)*CD/(FA*A21/RSS+CD*A31)
F4=(ALF*DXD0-DX0/SS)*CD/(FA*A22/RSS+CD*A32)
F5=(ALF*DXD0-DX0/SS)*CD/(FA*A23/RSS+CD*A33)
F6=(ALF*DXD0-DX0/SS)*CD/(FA*A24/RSS+CD*A34)
F7=(ALF*DXD0-DX0/SS)*CD/(FA*A25/RSS+CD*A35)
F8=(ALF*DXD0-DX0/SS)*CD/(FA*A26/RSS+CD*A36)
F9=(ALF*DXD0-DX0/SS)*CD/(FA*A27/RSS+CD*A37)
F10=(ALF*DXD0-DX0/SS)*CD/(FA*A28/RSS+CD*A38)
F11=(ALF*DXD0-DX0/SS)*CD/(FA*A29/RSS+CD*A39)
F12=(ALF*DXD0-DX0/SS)*CD/(FA*A210/RSS+CD*A310)
F13=(ALF*DXD0-DX0/SS)*CD/(FA*A211/RSS+CD*A311)
F14=(ALF*DXD0-DX0/SS)*CD/(FA*A212/RSS+CD*A312)
F15=(ALF*DXD0-DX0/SS)*CD/(FA*A213/RSS+CD*A313)
DF1=V(J)*F1
DF2=V(J)*F2
DF3=V(J)*F3
DF4=V(J)*F4
DF5=V(J)*F5
DF6=V(J)*F6
DF7=V(J)*F7
DF8=V(J)*F8
DF9=V(J)*F9
DF10=V(J)*F10
DF11=V(J)*F11
DF12=V(J)*F12
DF13=V(J)*F13
DF14=V(J)*F14
DF15=V(J)*F15
SF1=SF1+DF1
SF2=SF2+DF2
SF3=SF3+DF3
SF4=SF4+DF4
SF5=SF5+DF5
SF6=SF6+DF6
SF7=SF7+DF7
SF8=SF8+DF8
SF9=SF9+DF9
SF10=SF10+DF10
SF11=SF11+DF11
SF12=SF12+DF12
SF13=SF13+DF13
SF14=SF14+DF14
```

```
      SF15=SF15+DF15
  300 CONTINUE
      DX(I)=SF1*CO
      SF1=0.D0
      DPW(I)=SF2*CO
      SF2=0.D0
      DP1(I)=SF3*CO
      SF3=0.D0
      DP2(I)=SF4*CO
      SF4=0.D0
      DP3(I)=SF5*CO
      SF5=0.D0
      DP4(I)=SF6*CO
      SF6=0.D0
      DP5(I)=SF7*CO
      SF7=0.D0
      DP6(I)=SF8*CO
      SF8=0.D0
      DP7(I)=SF9*CO
      SF9=0.D0
      DP8(I)=SF10*CO
      SF10=0.D0
      DP9(I)=SF11*CO
      SF11=0.D0
      DP10(I)=SF12*CO
      SF12=0.D0
      DP11(I)=SF13*CO
      SF13=0.D0
      DP12(I)=SF14*CO
      SF14=0.D0
      DP13(I)=SF15*CO
      SF15=0.D0
  200 CONTINUE
      DO 1000 I=1,M
      WRITE(6,1001) TD(I)
 1001 FORMAT(D20.5)
      WRITE(6,1002) DX(I),DPW(I),DP1(I),DP2(I),DP3(I)
 1002 FORMAT(5F20.10)
      WRITE(6,1003) DP4(I),DP5(I),DP6(I),DP7(I),DP8(I)
 1003 FORMAT(5F20.10)
      WRITE(6,1004) DP9(I),DP10(I),DP11(I),DP12(I),DP13(I)
 1004 FORMAT(5F20.10)
      WRITE(6,1005) DP14(I),DP15(I),DP16(I),DP17(I),DP18(I)
 1005 FORMAT(5F20.10)
 1000 CONTINUE
  150 CONTINUE
      STOP
      END
      FUNCTION BK0(X)
      IMPLICIT REAL*8 (A-H,O-Z)
      IF(X.GT.2.) GO TO 700
      T=X/2.
      A1=-DLOG(T)*BI0(X)-.57721566+.4227842*T**2+.23069756*T**4
      A2=.0348859*T**6+.00262698*T**8+.0001075*T**10+.0000074*T**12
      BK0=A1+A2
      GO TO 701
  700 IF(X.GT.1.74D2) GO TO 702
      T=2./X
      A3=1.25331414-.07832358*T+.02189568*T**2-.01062446*T**3
      A4=.00587872*T**4-.0025154*T**5+.00053208*T**6
```

```
      BK0=(A3+A4)/(DSQRT(X)*DEXP(X))
      GO TO 701
  702 BK0=1.D-70
  701 RETURN
      END
      FUNCTION BK1(X)
      IMPLICIT REAL*8 (A-H,O-Z)
      IF(X.GT.2.) GO TO 710
      T=X/2.
      A1=X*DLOG(T)*BI1(X)+1.+.15443144*T**2-.67278579*T**4
      A2=-.18156897*T**6-.01919402*T**8-.00110404*T**10-.00004686*T**12
      BK1=(A1+A2)/X
      GO TO 711
  710 IF(X.GT.1.74D2) GO TO 712
      T=2./X
      A3=1.25331414+.23498619*T-.0365562*T**2+.01504268*T**3
      A4=-.00780353*T**4+.00325614*T**5-.00068245*T**6
      BK1=(A3+A4)/(DSQRT(X)*DEXP(X))
      GO TO 711
  712 BK1=1.D-70
  711 RETURN
      END
      FUNCTION BI0(X)
      IMPLICIT REAL*8 (A-H,O-Z)
      IF(X.GT.3.75) GO TO 720
      T=X/3.75
      A1=1.+3.5156229*T**2+3.0899424*T**4+1.2067492*T**6
      A2=.2659732*T**8+.0360768*T**10+.0045813*T**12
      BI0=A1+A2
      GO TO 721
  720 IF(X.GT.1.74D2) GO TO 722
      T=3.75/X
      A3=.39894228+.01328592*T+.00225319*T**2-.00157565*T**3+.00916281*T**4
      A4=-.02057706*T**5+.02635537*T**6-.01647633*T**7+.00392377*T**8
      BI0=(A3+A4)/(DSQRT(X)*DEXP(-X))
      GO TO 721
  722 BI0=1.D70
  721 RETURN
      END
      FUNCTION BI1(X)
      IMPLICIT REAL*8 (A-H,O-Z)
      IF(X.GT.3.75) GO TO 730
      T=X/3.75
      A1=.5+.87890594*T**2+.51498869*T**4+.1508493*T**6+.02658733*T**8
      A2=.00301532*T**10+.00032411*T**12
      BI1=(A1+A2)*X
      GO TO 731
  730 IF(X.GT.1.74D2) GO TO 732
      T=3.75/X
COLLECT 372.1
      GO TO 731
  732 BI1=1.D70
      A3=.39894228-.03988024*T-.00362018*T**2+.00163801*T**3-.01031555*T**4
      A4=.02282967*T**5-.02895312*T**6+.01787654*T**7-.00420059*T**8
      BI1=(A3+A4)/(DSQRT(X)*DEXP(-X))
  731 RETURN
      END
$DATA
$STOP
//
```

E-4 COMPUTER PROGRAM TO SIMULATE CLOSED CHAMBER TEST, SLUG TEST, AND BUILDUP TEST

```
C     CALCULATION OF PRESSURE OF CLOSED CHAMBER TEST
C     NOMENCLATURE
C     P(1)        LIQUID LEVEL
C     P(2)        WELLBORE PRESSURE
C     P(I)        PRESSURE AT NODE I
C     R           RADIAL DISTANCE
C     RE          RADIUS OF OIJETR BOUNDARY
C     DRL         INCREMENT OF RADIAL DISTANCE IN LOG SCALE
C     SA(I)       ELEMENT OF TRIDIAGONAL MATRIX
C     SB(I)       ELEMENT OF TRIDIAGONAL MATRIX
C     SC(I)       ELEMENT OF TRIDIAGONAL MATRIX
C     DK(I)       ELEMENT OF RIGHT SIDE OF EQUATION
C     A(I)        COEFFICIENT OF THOMAS
C     B(I)        COEFFICIENT OF THOMAS
C     CD          DIMENSIONLESS WELLBORE STORAGE
C     SKIN        SKIN FACTOR
C     M           NUMBER OF NODE
C     N           NUMBER OF TIME INCREMENT
C     DL          DIMENSIONLESS LENGTH OF CLOSED CHAMBER
C     DRO         INCREMENT OF RADIUS AT FIRST NODE
      IMPLICIT REAL*8 (A-H,O-Z)
      DIMENSION P(510),SA(510),SB(510),SC(510),A(510),B(510),DK(510)
C
C     INITIAL SET
C
      DO 100 I=1,510
      P(I)=0.
      SA(I)=0.
      SB(I)=0.
      SC(I)=0.
      A(I)=0.
      B(I)=0.
      DK(I)=0.
  100 CONTINUE
      CD=1.D3
      SKIN=0.DO
      N=100
      M=202
      TT=0.DO
      DX0=-1.
      ALF=1.D6
      BETA=1.D-2
      DL=1.
      DATM=1.D-2
      RE=1.D5
      DT0=1.D2
      DT=1.D2
      M1=M-1
      M2=M-2
      M3=M-3
      M4=M-4
      DRL=DLOG(RE)/M3
      DD=RE**(1./DFLOAT(M3))
C
C     CALCULATION OF P
C
      DO 1000 I=1,N
      IF (I.GT.1) GO TO 200
      TT=TT+DT0
C
```

```
C     INITIAL VALUES
C
      IF(ALF.EQ.0.) GO TO 208
      DK(1)=(1.-DT**2/(2.*ALF))*DX0-(DT**2)*(BETA-DATM)/ALF
      GO TO 209
  208 CONTINUE
      DK(1)=-BETA+DATM
  209 CONTINUE
      IF(SKIN.EQ.0.) GO TO 206
      DK(2)=SKIN*CD*DX0/DT
      GO TO 207 .
  206 DK(2)=DX0
  207 CONTINUE
      DO 201 J=3,M
      DK(J)=0.
  201 CONTINUE
      GO TO 300
C
C     CALCULATION OF DK
C
  200 CONTINUE
      IF(TT.EQ.10000.)  DT=1000.
      TT=TT+DT
      IF(ALF.EQ.0.) GO TO 210
      DK(1)=(2.-DT**2/(2.*ALF))*P(1)-PP1-(DT**2)*P(2)/(2.*ALF)
     $      -(DT**2)*((DL-DX0)*BETA/(DL-P(1))-DATM)/ALF
      GO TO 211
  210 CONTINUE
      DK(1)=-BETA*(DL-DX0)/(DL-P(1))+DATM
  211 CONTINUE
      IF(SKIN.EQ.0.) GO TO 203
      DK(2)=SKIN*CD*P(1)/DT
      DK(3)=0.
      DO 202 J=2,M2
      AJ=DFLOAT(J)
      DK(J+2)=-DRL*((DD**(AJ-1.+0.5))**2-(DD**(AJ-1.-0.5))**2)
     $         *P(J+2)/(2.*DT)
  202 CONTINUE
      GO TO 204
  203 CONTINUE
      DK(2)=P(1)
      DO 205 J=2,M2
      AJ=DFLOAT(J)
      DK(J+1)=-DRL*((DD**(AJ-1.+0.5))**2-(DD**(AJ-1.-0.5))**2)
     $         *P(J+1)/(2.*DT)
  205 CONTINUE
  204 CONTINUE
C
C     CALCULATION OF SA,SB,SC
C
  300 CONTINUE
      IF(ALF.EQ.0.) GO TO 306
      SB(1)=1.+DT**2/(2.*ALF)
      SC(1)=DT**2/(2.*ALF)
      GO TO 307
  306 CONTINUE
      SB(1)=1
      SC(1)=1.
  307 CONTINUE
      IF(SKIN.EQ.0.) GO TO 302
```

```
      SA(2)=SKIN*CD/DT
      SB(2)=-1.
      SC(2)=1.
      SA(3)=1.
      DR1=DRL
      SB(3)=-(SKIN/DR1+1.)
      SC(3)=SKIN/DR1
      DO 301 J=2,M3
      AJ=DFLOAT(J)
      SA(J+2)=1.
      SB(J+2)=-(2.+DRL*((DD**(AJ-1.+0.5))**2
     $        -(DD**(AJ-1.-0.5))**2)/(2.*DT))
      SC(J+2)=1.
  301 CONTINUE
      SA(M)=2.
      AM=DFLOAT(M2)
      SB(M)=-(2.+DRL*((DD**(AM-1.+0.5))**2
     $      -(DD**(AM-1.-0.5))**2)/(2.*DT))
      GO TO 303
  302 CONTINUE
      DR1=DRL
      SA(2)=1.
      SB(2)=-DT/(CD*DR1)
      SC(2)=DT/(CD*DR1)
      DO 304 J=2,M3
      AJ=DFLOAT(J)
      SA(J+1)=1.
      SB(J+1)=-(2.+DRL*((DD**(AJ-1.+0.5))**2
     $        -(DD**(AJ-1.-0.5))**2)/(2.*DT))
      SC(J+1)=1.
  304 CONTINUE
      SA(M-1)=2.
      AM=DFLOAT(M2)
      SB(M-1)=-(2.+DRL*((DD**(AM-1.+0.5))**2
     $        -(DD**(AM-1.-0.5))**2)/(2.*DT))
  303 CONTINUE
C
C     CALCULATION OF A,B
C
      A(2)=-SC(1)/SB(1)
      B(2)=DK(1)/SB(1)
      IF(SKIN.EQ.0.) GO TO 401
      DO 400 J=2,M1
      A(J+1)=-SC(J)/(SA(J)*A(J)+SB(J))
      B(J+1)=(DK(J)-SA(J)*B(J))/(SA(J)*A(J)+SB(J))
      JJ=J+1
      IF(DABS(B(JJ)).LT.10.D-70 .AND. J.GT.4) GO TO 404
  400 CONTINUE
      GO TO 402
  404 CONTINUE
      DO 405 K=JJ,M1
      A(K+1)=-SC(K)/(SA(K)*A(K)+SB(K))
      B(K+1)=0.
  405 CONTINUE
      GO TO 402
  401 DO 403 J=2,M2
      A(J+1)=-SC(J)/(SA(J)*A(J)+SB(J))
      B(J+1)=(DK(J)-SA(J)*B(J))/(SA(J)*A(J)+SB(J))
      JJ=J+1
      IF(DABS(B(JJ)).LT.10.D-70 .AND. J.GT.3)  GO TO 406
```

```
  403 CONTINUE
      GO TO 402
  406 CONTINUE
      DO 407 K=JJ,M2
      A(K+1)=-SC(K)/(SA(K)*A(K)+SB(K))
      B(K+1)=0.
  407 CONTINUE
  402 CONTINUE
C
C     CALCULATION OF P
C
      IF(I.EQ.1) GO TO 501
      PP1=P(1)
      GO TO 502
  501 PP1=DX0
  502 CONTINUE
      IF(SKIN.EQ.0.) GO TO 503
      P(M)=(DK(M)-SA(M)*B(M))/(SA(M)*A(M)+SB(M))
      DO 500 J=1,M1
      J1=M-J
      P(J1)=A(J1+1)*P(J1+1)+B(J1+1)
  500 CONTINUE
      GO TO 504
  503 CONTINUE
      P(M-1)=(DK(M-1)-SA(M-1)*B(M-1))/(SA(M-1)*A(M-1)+SB(M-1))
      DO 505 J=2,M1
      J1=M-J
      P(J1)=A(J1+1)*P(J1+1)+B(J1+1)
  505 CONTINUE
  504 CONTINUE
C
C     OUTPUT
C
      P(2)=P(2)/(1.-BETA+DATM)
      WRITE(6,600) TT,P(1),P(2),P(M-1)
  600 FORMAT(D20.5,3F20.10)
      P(2)=(1.-BETA+DATM)*P(2)
C
 1000 CONTINUE
      STOP
      END
$DATA
$STOP
//
```